Hemodynamic Regulation of Blood-Brain Barrier Phenotype: A Cooperative Effort Linking Adherens and Tight Junction Complexes

A dissertation submitted for the degree of Ph.D by

Tony G. Walsh, B.Sc

Under the supervision of Dr. Philip M. Cummins

June 2010

Faculty of Science and Health, School of Biotechnology,
Dublin City University, Dublin 9, Ireland

Declaration:

I hereby certify that this material, which I now submit for assessment on the programme of study leading to the award of Doctor of Philosophy is entirely my own work, that I have exercised reasonable care to ensure that the work is original, and does not to the best of my knowledge breach any law of copyright, and has not been taken from the work of others save and to the extent that such work has been cited and acknowledged within the text of my work.

Signed: _____

(Candidate) ID No.: **51454404**

Date: _____

Acknowledgements

The depth of my gratitude for completion of this body of research spans a wide audience so I apologise in advance for any unintentional omissions

First and foremost, I would like to thank my supervisor, Dr. Philip Cummins for his invaluable guidance and encouragement over the years. It was a pleasure to work within your research facility and I wish the 'Endothelium Biology Group' the very best for the years ahead. I also want to extend my appreciation to Dr. Ronan Murphy for his sharp insightfulness and suggestions over the years. They were extremely useful and I wish him and his research group every success in the future.

I would also like to thank the many postgraduate students/friends who were extremely helpful during my keep in DCU and ensuring it was such an enjoyable one. Firstly, I would like to thank former colleagues of the EBG, Olga, Maria, Nick and Paul Fitz '1' who were extremely helpful during my induction into the lab. Within recent years, I have been blessed to work alongside a friendly and cheerful group of fellow students and in this regard I would like to thank: Paul Fitz '2' for lending his exceptional knowledge and incredible patience; Anthony for making sure none of us went thirsty (or sober); Mishan for some of the most random yet interesting conversations; Andrew for all the lifts out to tag rugby and Shaunta for putting up with the male dominance in the lab. I would like to take this opportunity to wish the new generation of postgraduate students, Keith, Fiona, Ciaran, Brian and Chan a memorable experience in DCU. Also, I want to express my profound appreciation to my girlfriend Sandra, whose friendship and support was invaluable during the final year of my PhD.

Last and by no means least, I'm greatful for the constant support and encouragement from my family, and for giving me the opportunity to pursue my professional ambitions.

Abstract

Intercellular adherens junction (AJ) and tight junction (TJ) proteins (e.g. VE-Cadherin, occludin, ZO-1, claudin-5) jointly consolidate the apical surface of adjacent brain microvascular endothelial cells (BBMvEC's) creating the blood-brain barrier (BBB), a critical regulator of CNS homeostasis. Junctional disassembly and barrier dysfunction are established features of cerebrovascular diseases (e.g. stroke) manifesting compromised blood flow, allowing us to hypothesize a pivotal regulatory link between BBB phenotype and flow-associated shear stress. In this regard, our research has demonstrated that exposure of BBMvEC's to physiological levels of shear stress *in vitro* can upregulate tight junction protein expression and enhance protein immunolocalization at the cell-cell border, in parallel with reduced paracellular solute flux.

For these studies, cultured bovine brain microvascular endothelial cells (BBMvEC's) were exposed to laminar shear stress (0-10 dynes/cm^2, 0-24 h) in conjunction with targeted inhibition strategies to delineate the intracellular signaling pathways mediating adaptation of BBB phenotype to fluid shear stress.

Initial findings showed that shear-dependent reduction in BBMvEC permeability was initially observed after 3-6 h of shear onset (10 dynes/cm^2), with more significant decreases observed after 12 and 24 h. These responses were temporally mirrored by BBMvEC morphological realignment, and were reversed by flow reduction (i.e. to 1 dynes/cm^2, 24 h), the latter flow reduction also attenuated the enhanced cell-cell border localization of ZO-1 and reduction in phosphotyrosine (pTyr)-occludin levels induced by high shear.

Furthermore, our studies show that Rac1 activation - possibly by triggering a significant reduction in pTyr-occludin levels - is essential to the shear-induced upregulation of BBB phenotype. Consistent with the critical nature of pTyr-occludin level, a tyrosine phosphatase inhibitor (dephostatin) was found to block shear-induced BBB upregulation. In subsequent experiments, the use of molecular strategies to functionally block either VE-Cadherin (VE-Cad ΔEXD) or Tiam1 (Tiam-C580), the latter a Rho guanine nucleotide exchange factor mediating Rac1 activation, attenuated shear-induced BBB upregulation and the associated reduction in pTyr-occludin levels, concomitant with a loss of cell-cell border localization of ZO-1 and claudin-5. We also observed that RhoA is crucial to the shear-induced regulation of BBB phenotype during the initial shear-onset phase, however Rac1 activity is more prominent with regards to maintaining shear-induced barrier enhancement in the chronic shear phase.

In conclusion, the adaptation of BBB phenotype to fluid shear stress is mediated through a VE-Cadherin/Tiam1/Rac1 signaling pathway. Collectively, these data confirm the existence of a highly novel functional "cross-talk" mechanism between adherens and tight junctions.

Abbreviations

ADP	Adenosine Diphosphate
AET	Active Efflux Transporter
AF-6	All-1 fusion partner from chromosome 6
APTS	8-Aminopyrene-1,3,6-trisulfonic acid trisodium salt
ARP	Actin Related Protein
ATP	Adenosine Triphosphate
BAEC	Bovine Aortic Endothelial Cell
BBB	Blood Brain Barrier
BBMvEC	Bovine Brain Microvascular Endothelial Cell
bFGF	basic Fibroblast Growth Factor
BSA	Bovine Serum Albumin
cAMP	cyclic Adenosine Monophosphate
CD5	Cadherin-5
cGMP	cyclic Guanosine Monophosphate
CNS	Central Nervous System
CSF	Cerebrospinal Fluid
CVD	Cardiovascular Disease
DAPI	4',6-diamidino-2-phenylindole
DEP-1	Density Enhanced-Phosphatase-1
DH	Dbl-Homology
DMEM	Dulbecco's Modified Eagle Medium
DMSO	Dimethyl Sulfoxide
DNA	Deoxyribonucleic Acid
EC	Endothelial Cell
EC	Extracellular
ECL	Extracellular Loop
ECM	Extracellular Matrix
EDD	Endothelium Dependent Dilation
EDHF	Endothelium Derived Hyperpolarizing Factor
EDTA	Ethylenediaminetetraacetic acid

E-face	Exo-cytoplasmic-face
EG	Endothelial Glycocalyx
eGFP	enhanced Green Fluorescent Protein
eNOS	endothelial Nitric Oxide Synthase
ERK	Extracellular Signal-Regulated Kinase
ET-1	Endothelin-1
FACS	Fluorescent Activating Cell Sorting
F-actin	Filamentous Actin
FAK	Focal Adhesion Kinase
FBS	Foetal Bovine Serum
FITC	Fluorescein Isothiocyanate
FRET	Fluorescence Resonance Energy Transfer
GAPDH	Glyceraldehyde 3-Phosphate Dehydrogenase
GDP	Guanosine Diphosphate
GPCR	G-Protein Coupled Receptor
GTP	Guanosine Triphosphate
GUK	Guanylate Kinase
HBMvEC	Human Brain Microvascular Endothelial Cell
HGF	Hepatocyte Growth Factor
HIV	Human Immunodeficiency Virus
HRP	Horse Radish Peroxidase
HUVEC	Human Umbilical Vein Endothelial Cell
IB	Immunoblot
ICAM	Intracellular Adhesion Molecule
IFNγ	Interferon Gamma
IgG	Immunoglobulin G
IL	Interleukin
IP	Immunoprecipitation
IPTG	iso-propyl-β-D-thiolgalactoside
IQGAP	IQ motif containing GTPase-activating protein 1
JAM	Junctional Adhesion Molecule

LB	Luria-Burtani
LDL	Low-Density Lipoprotein
LPS	Lipopolysaccharide
LSS	Laminar Shear Stress
mAb	Monoclonal Antibody
MAGUK	Membrane Associated Guanylate Kinase
MAPK	Mitogen-Activated Protein Kinase
MDCK	Madin Darby Canine Kidney
MI	Myocardial Infarction
MLC	Myosin Light Chain
MLCK	Myosin Light Chain Kinase
MMP	Matrix Metalloproteinases
mRNA	messenger Ribonucleic Acid
MS	Multiple Sclerosis
NO	Nitric Oxide
NVU	Neurovascular Unit
PAK	p21-activated Kinase
PBS	Phosphate Buffered Saline
PDGF	Platelet Derived Growth Factor
PECAM-1	Platelet Endothelial Cell Adhesion Molecule-1
P-face	Protoplasmic-face
P-gp	P-glycoprotein
PH	Pleckstrin Homology
PI	Propidium Iodide
PI3K	Phosphoinisotide 3-OH-Kinsae
PKA	Protein Kinase A
PKC	Protein Kinase C
PTK	Protein Tyrosine Kinase
PTP	Protein Tyrosine Phosphatase
PTPμ	Protein Tyrosine Phosphatase Receptor type M
pTyr	Phosphotyrosine

RhoGAP	RhoGTPase Activating Protein
RhoGDI	Rho Guanine Dissociation Inhibitors
RhoGEF	Rho Guanine Nucleotide Exchange Factor
ROCK	Rho-associated Kinase
ROS	Reactive Oxygen Species
RTK	Receptor Tyrosine Kinase
S1P	Sphingosine-1 Phosphate
SDS	Sodium doecyl sulphate
SDS PAGE	SDS Polyacrylamide gel electrophoresis
SEM	Standard Error of the Mean
SH2	Src Homology 2
SH3	Src-homology 3
SHP2	SH2 containing Phosphotyrosine Phosphatase
SSB	Sample Solubilization Buffer
SSRE	Shear Stress Response Element
TBS	Tris Buffered Saline
TEE	Transendothelial Exchange
TEER	Transendothelial Electrical Resistance
TNFα	Tumour Necrosis Factor Alpha
VCAM	Vascular Adhesion Molecule
VE-Cadherin	Vascular Endothelial Cadherin
VEGF	Vascular Endothelial Growth Factor
VEGFR2	Vascular Endothelial Growth Factor Receptor 2
VE-PTP	Vascular Endothelial Protein Tyrosine Phosphatase
VM	Vasculogenic Mimicry
VSMC	Vascular Smooth Muscle Cell
WASP	Wiskott-Aldrich Syndrome Protein
WAVE	WASP Verpolin Homologous
ZO-1	Zonula Occludens-1

Units

cm^2	Centimeter Squared
°	Degree Celsius
U	Enzyme Units
g	Grams
g/mol	Grams Per Mole
h	Hours
kDa	Kilo Daltons
kb	Kilobase
L	Liter
µg	Microgram
µl	Microlitre
µm	Micrometre
mA	Milliamps
mg	Milligrams
ml	Millilitre
mm^2	Millimetre Squared
mM	Millimolar
ms	Millisecond
min	Minutes
M	Molar
ng	Nanogram
nm	Nanometre
OD	Optical Density
rpm	Revolution Per Minute
sec	Seconds
V	Volts
v/v	Volume Per Volume
w/w	Weight Per Volume

Publications

Walsh T.G, Fitzpatrick P, Murphy A, Murphy RP, Cummins PM. Stabilization of brain microvascular endothelial barrier function by shear stress: Roles for VE-cadherin, Tiam1 and Rac1 signaling in the regulation of tight junction phenotype. *J Cell Sci* 2010; **[Submitted].**

Lieggi NT, **Walsh T.G,** Colgan OC, Murphy RP, Cahill PA, Cummins PM. Cyclic Strain-Induced Barrier Enhancement in Vascular Endothelial Cells Involves Activation of Gα-subunit, p38 MAPK, and Rac1 Signalling Mechanisms. *Am J Physiol Heart Circ Physiol* 2010; **[In Revision]**.

Fitzpatrick P, Britto M, **Walsh T.G**, Meade G, Cummins PM, Murphy RP. LASP-1 is an important regulator in the molecular complex controlling cell-cell and cell-matrix adhesion in the vasculature. *J Cell Biol* 2010; **[In Preparation]**.

Fitzpatrick PA, Guinan AF, **Walsh T.G**, Murphy RP, Killeen MT, Tobin NP, Pierotti AR, Cummins PM. Down-regulation of neprilysin expression in vascular endothelial cells by laminar shear stress involves NADPH oxidase-dependent ROS production. *Int J Biochem Cell Biol* 2009;41**:**2287-2294.

Presentations

Walsh T.G, Guinan A.F, Rochfort K.D, Cummins P.M: Stabilization of brain microvascular endothelial barrier function by shear stress involves a signaling pathway linking adherens and tight junctions via Rac1. *University Hospital Zurich, 13th International Symposium of the Blood Brain Barrier 2010;* Zurich, Switzerland, **[Abstract/Oral]**

Walsh T.G. Regulation of blood-brain barrier function by shear stress: Hemodynamic regulation of Blood Brain Barrier Phenotype: A Cooperative Effort Linking Adherens and Tight Junction Complexes. *School of Biotechnology: Research Day 2010*, Dublin City University. **[Abstract/Poster]**

Walsh T.G, Fitzpatrick P, Murphy RP, Cummins PM. Roles for VE-Cadherin, Rac1, and occludin signalling in the regulation of brain microvascular endothelial permeability by blood flow-associated shear stress. *University College London Symposium: Signalling in the blood-brain and blood-retinal barrier 2009;* London, England. **[Abstract/Poster]**

Walsh T.G. Regulation of blood-brain barrier function by shear stress: Role of Rac1-GTPase in tight junction assembly and function. *School of Biotechnology: Research Day 2009*, Dublin City University. **[Abstract/Oral]**

Walsh T.G, Fitzpatrick P, Murphy RP, Cummins PM. Regulation of blood brain barrier function by shear stress: role of Rho-GTPases in tight junction assembly and function. *North American Vascular Biology Organization (NAVBO) Workshop: Biology of Signaling in the Cardiovascular System 2008;* Hyannis MA, USA. **[Abstract/Poster]***

Fitzpatrick P, Britto M, **Walsh T.G**, Meade G, Cummins PM, Murphy RP. Cytoskeletal re-organization by mechano-transduced LASP-1 regulates cell-matrix and cell-cell adhesion through activation of Rac1. *North American Vascular Biology Organization (NAVBO) Workshop: Biology of Signaling in the Cardiovascular System 2008*; Hyannis MA, USA. **[Abstract/Poster]**

* NAVBO trainee award for best postgraduate abstract.

List of Figures

Chapter 1

Fig 1.1: Human blood vessel.

Fig. 1.2: Atherosclerotic plaque progression.

Fig. 1.3: Shear stress and cyclic strain.

Fig. 1.4: Endothelial mechanosensors.

Fig. 1.5: Physiological laminar shear vs. disturbed shear.

Fig. 1.6: Pathways at the blood brain barrier.

Fig. 1.7: The Neurovascular Unit at the blood brain barrier.

Fig. 1.8: Tight Proteins of the blood brain barrier.

Fig. 1.9: Schematic depiction of occludin structure and domains.

Fig. 1.10: Structure and binding partners of ZO-1.

Fig. 1.11: Schematic depiction of claudin structure.

Fig. 1.12: Endothelial adherens junction.

Fig. 1.13: Schematic of RhoGTPases.

Fig. 1.14: Regulation of barrier function by Rho and Rac.

Fig. 1.15: Schematic structure of Tiam1.

Fig. 1.16: RhoGTPase regulation by RhoGEF's, RhoGDI's and RhoGAP's.

Fig. 1.17: Schematic depiction of experimental approach.

Chapter 2

Fig. 2.1: The Haemocytometer

Fig. 2.2: ADAM counter microfluidic chip for viable cell counting.

Fig. 2.3: Orbital Rotation model used in laminar shear stress studies.

Fig. 2.4: IBIDI flow system for laminar shear studies.

Fig. 2.5: Transendothelial permeability assay.

Fig. 2.6: Amaxa nucleofection system.

Fig. 2.7: Microporation System.

Fig. 2.8: Wet transfer cassette assembly.

Fig. 2.9: G-LISA principle.

Chapter 3

Fig. 3.1: Characterization of BBMvEC's.

Fig. 3.2: Effect of laminar shear stress on BBMvEC and F-actin re-alignment.

Fig. 3.3: Magnitude-dependent effects of shear stress on BBMvEC permeability and morphological realignment.

Fig. 3.4: Time dependent effects of shear stress on BBMvEC permeability and morphological realignment.

Fig. 3.5: Effect of laminar shear stress on ZO-1 and Claudin-5 localization.

Fig. 3.6: Effect of laminar shear stress on occludin tyrosine phosphorylation.

Fig. 3.7: Effect of dephostatin on laminar shear-induced BBMvEC barrier enhancement.

Fig. 3.8: Effect of flow reduction on the barrier properties of shear-preconditioned BBMvEC's.

Fig. 3.9: Effect of shear stress on BBMvEC permeability using the "paracellular" marker, APTS-dextran.

Chapter 4

Fig. 4.1: Assessment of plasmid DNA transfection viability and efficiency via Amaxa nucleofection and microporation.

Fig. 4.2: Effect of laminar shear stress on Rac1 activation.

Fig. 4.3: Effect of Rac1 inhibition on laminar shear-induced BBMvEC morphological and F-actin realignment.

Fig. 4.4: Effect of Rac1 blockade on laminar shear-induced regulation of BBMvEC permeability.

Fig. 4.5: Effect of Rac1 blockade on laminar shear-induced localization of ZO-1.

Fig. 4.6: Effect of Rac1 inhibition on laminar shear stress-induced occludin tyrosine dephosphorylation.

Fig. 4.7: Effect of laminar shear stress on RhoA activation.

Fig. 4.8: Effect ROCK inhibition on shear-induced BBMvEC morphological and F-actin realignment.

Fig. 4.9: Effect of ROCK inhibition on shear-induced regulation of BBMvEC permeability.
Fig 4.10: Effect of Rho-associated kinase inhibition (ROCK) on shear-induced regulation of ZO-1 localization.

Chapter 5

Fig. 5.1: Illustration and overexpression of VE-Cad ΔEXD (VE-Cadherin Extracellular Domain Deletion) in BBMvEC's.
Fig. 5.2: Effect of VE-Cadherin inhibition on laminar shear induced-Rac1 activation.
Fig. 5.3: Effect of VE-Cadherin inhibition on laminar shear-induced regulation of BBMvEC permeability.
Fig. 5.4: Effect of VE-Cadherin inhibition on laminar shear-induced ZO-1 localization.
Fig. 5.5: Effect of VE-Cadherin inhibition on laminar shear-induced claudin-5 localization.
Fig. 5.6: Effect of VE-Cadherin inhibition on laminar shear-induced occludin tyrosine dephosphorylation.
Fig. 5.7: Illustration and overexpression of Tiam1 C580 (lacking PHn and DHR domains) in BBMvEC's.
Fig. 5.8: Effect of Tiam1 inhibition on laminar shear-induced Rac1 activation.
Fig. 5.9: Effect of Tiam1 inhibition on laminar shear-induced cellular realignment.
Fig. 5.10: Effect of Tiam1 inhibition on laminar shear-induced regulation of BBMvEC permeability.
Fig. 5.11: Effect of Tiam1 inhibition on laminar shear-induced ZO-1 localization.
Fig. 5.12: Effect of Tiam1 C580 inhibition on laminar shear-induced occludin tyrosine dephosphorylation.

Chapter 6

Fig. 6.1: Schematic depiction of experimental approach.
Fig. 6.2: Signaling mechanisms mediating the barrier-stabilizing influence of shear stress in BBMvEC's.
Fig. 6.3: DIV-BBB model and computer controlled TEER monitoring device.
Fig. 6.4: Effect of shear stress on HBMvEC re-alignment and ZO-1 localization.

List of Tables

Table 2.1: Antibiotic concentrations.

Table 2.2: SDS-PAGE resolving gel composition

Table 2.3: SDS-Page stacking gel components.

Table 2.4: Protein concentrations loaded.

Table 2.5: Western blot primary and secondary antibody dilutions.

Table 2.6: Immunocytochemistry primary antibody dilutions.

Title Page **I**
Declaration **II**
Acknowledgements **III**
Abstract **IV**
Abbreviations **V**
Units **IX**
Publications **X**
Presentations **XI**
List of Figures **XII**
List of Tables **XV**
Table of Contents **XVI**

Chapter 1: Introduction

1.1 ***Vascular Endothelium*** 2
1.1.1 Endothelial Dysfunction 4
1.1.2 Atherosclerosis 5
1.2 ***Hemodynamics*** 8
1.2.1 Hemodynamics and Vessel Remodeling 10
1.2.2 Mechanotransduction 11
1.2.2.1 Luminal Mechanosensors 11
1.2.2.2 Cell Adhesion Mechanosensors 13
1.2.2.3 Cytoskeleton 17
1.2.3 Mechanoregulation of Gene Expression 18
1.3 ***The Blood Brain Barrier*** 21
1.3.1 Blood Brain Barrier Permeability 22
1.3.1.1 Physical Barrier 22
1.3.1.2 Enzymatic Barrier 24
1.3.1.3 Efflux Barrier 24
1.3.2 Blood Brain Barrier Heterogeneity 24

1.3.3 The Neurovascular Unit 25
1.3.3.1 Astrocytes 26
1.3.3.2 Pericytes 27
1.3.3.3 Neurons 28
1.3.3.4 Extracellular Matrix 28
1.3.4 Blood Brain Barrier Disruption 29
1.3.5 Regulation of Cerebral Blood Flow 30
1.3.6 Shear Stress and the Blood Brain Barrier 31

1.4 ***Tight Junctions*** 32
1.4.1 Occludin 35
1.4.1.1 Occludin Function 37
1.4.1.2 Occludin Regulation 38
1.4.1.3 Occludin Clinical Implications 39
1.4.2 ZO-1 40
1.4.2.1 ZO-1 Function 42
1.4.2.2 ZO-1 Regulation 43
1.4.2.3 ZO-1 Clinical Implications 43
1.4.3 Claudin 45
1.4.3.1 Claudin-5 Function 45
1.4.3.2 Claudin-5 Regulation 47
1.4.3.3 Claudin-5 Clinical Implications 48

1.5 ***Adherens Junction*** 49
1.5.1 VE-Cadherin 50
1.5.2 VE-Cadherin Function 52
1.5.3 VE-Cadherin Regulation 53
1.5.4 VE-Cadherin Clinical Implications 55

1.6 ***Intracellular Signaling Mechanisms*** 57
1.6.1 RhoGTPases 57
1.6.2 RhoGTPase Function 59

1.6.2.1 RhoA 60
1.6.2.2 Rac1 and Cdc42 61
1.6.3 RhoGTPase Regulation 64
1.6.3.1 Rho Guanine Exchange Factors 65
1.6.3.2 Rho GTPase Activating Proteins 66
1.6.3.3 Rho Guanine Dissociation Inhibitors 67
1.6.4 Mechanoregulation of RhoGTPases 68

1.7 ***Final Summary and Study Rationale*** 71

1.8 ***Thesis Overview*** 72

Chapter 2: Materials and Methods

2.1 ***Materials*** 74

2.2 ***Cell Culture Methods***

2.2.1 Culture of BBMvEC's 78
2.2.2 Trypsinisation of BBMvEC's 78
2.2.3 Cryogenic Preservation and Recovery of BBMvEC's 79
2.2.4 Cell Counting
2.2.4.1 Haemocytometer 80
2.2.4.2 ADAM Counter 81
2.2.5 Laminar Shear Stress
2.2.5.1 Orbital Rotation 82
2.2.5.2 IBIDI Flow System 83
2.2.6 Transendothelial Permeability Assay
2.2.6.1 FITC Dextran 84
2.2.6.2 APTS-Dextran 84
2.2.7 Treatment with Pharmacological Inhibitors 85
2.2.8 FACS Analysis 86

2.3 ***Molecular Biology Techniques***

2.3.1 Plasmid DNA reconstitution 87

2.3.2 Transformation of Competent Cells 87
2.3.3 Purification of Plasmid DNA 88
2.3.4 Spectrometric Analysis of Plasmid DNA 89
2.3.5 Agarose Gel Electrophoresis 90

2.4 ***Transfections***

2.4.1 Plasmid DNA Nucleofection 91
2.4.2 Microporation 92

2.5 ***Immunodetection Techniques***

2.5.1 Western Blotting
2.5.1.1 Preparation of Whole Cell Lysate 93
2.5.1.2 BCA Assay 94
2.5.1.3 Immunoprecipitation 94
2.5.1.4 Protein Precipitation 95
2.5.1.5 SDS-PAGE 96
2.5.1.6 Transfer to Nitrocellulose Membrane 98
2.5.1.7 Blotting and Chemiluminescence detection 99
2.5.2 Immunocytochemistry 101

2.6 ***RhoGTPase GLISA® Activation Assays***

2.6.1 Lysate Preparation 102
2.6.2 GLISA Procedure and Immunodetection 102

2.7 ***Statistical Analysis*** 104

Chapter 3:

The effects of laminar shear stress and/or flow cessation on BBMvEC tight junction assembly and barrier function.

3.1 ***Introduction*** 106
3.2 ***Results*** 108
3.3 ***Discussion*** 122

Chapter 4:

The contribution of RhoGTPases, Rac1 and RhoA, to shear-induced adaptation of BBMvEC tight junction assembly and barrier function.

4.1 ***Introduction*** 128

4.2 ***Results*** 130

4.3 ***Discussion*** 144

Chapter 5:

The role of VE-Cadherin and Tiam1 in shear-induced upregulation of BBMvEC tight junction assembly and barrier function.

5.1 ***Introduction*** 151

5.2 ***Results*** 153

5.3 ***Discussion*** 165

Chapter 6: Final Summary 171

Bibliography 187

Chapter 1:

Introduction

1.1 The vascular endothelium

A basic understanding of the vascular system would describe a network of blood filled vessels (arteries, veins and capillaries) supplying oxygen and essential nutrients to every tissue throughout the body. Although completely accurate in summation, a more in depth understanding from a vascular biologist stand-point would describe a highly specialized layer of cells embedded within the lumen of blood vessels, namely the endothelium. Originally conceived to be an innate monolayer of cells, endothlelial cells (EC's) are now considered a highly specialized, metabolically active organ exerting multifunctional homeostatic effects on the vasculature and surrounding tissues. The term 'endothelium' was first coined in 1865 by a Swiss anatomist Wilhelm His, with a later definition limiting its presence to the inner cell layer of blood vessels and lymphatics. During the 1950's and 60's the discovery of the electron microscope proved to be an invaluable tool in the structural identification and characterization of EC's. However, the 1970's and 80's exposed a new era in cell biology with the first successful isolation of EC's in culture, allowing investigators to influence, in a controlled manner, the extracellular environment and thus study endothelial responses in greater detail (Aird, 2007). A recent search for the term 'vascular endothelium' on PubMed yielded 92,434 articles, which highlights the surge in research interests toward this exciting field of research since the advent of such technologies as cited above.

Endothelial cells display the same characteristics as other cells in the human body; organelles within a cytoplasm, surrounding a nucleus and contained within a cellular membrane (Esper et al., 2006). They arise from the mesoderm layer via the differentiation of hemangioblasts and or angioblasts (Coultas et al., 2005). Structurally, EC's are flat and realigned in the direction of blood flow with a thickness ranging from 0.1μm in capillaries to 1μm in the aorta. They typically exist in a quiescent state, i.e. non proliferating with an average lifespan of a year (Aird, 2007). The human blood vessel (arteries and veins) is depicted in figure 1.1 below

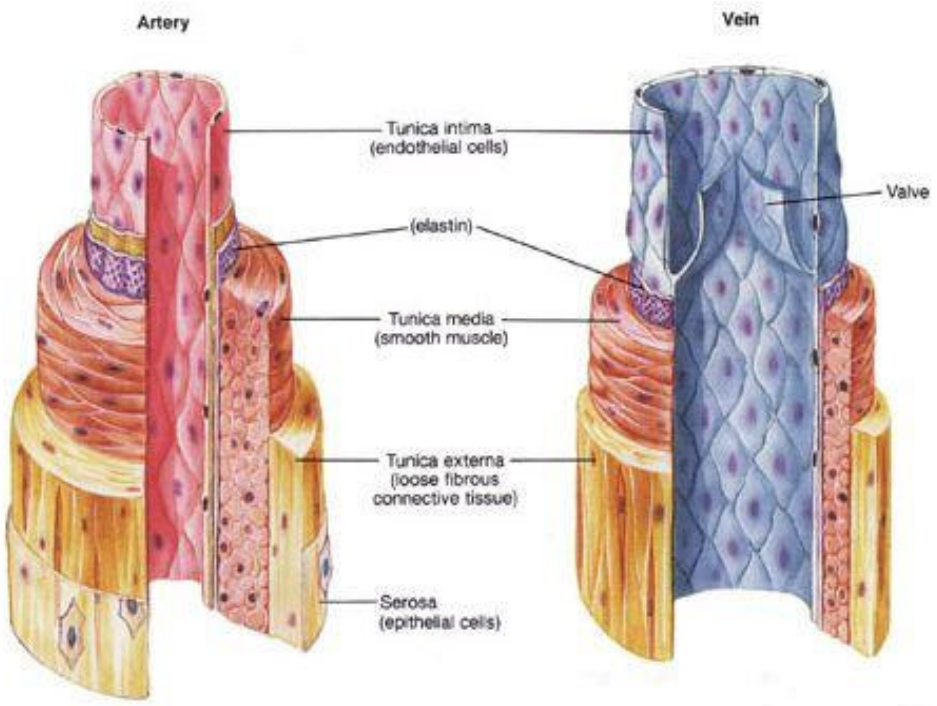

Fig. 1.1: Human blood vessel. This image displays the three main layers of a typical conduit vessel. EC's are anchored to a basement extracellular matrix (ECM), rich in collagenous and elastic fibers forming the tunica intima layer of the blood vessel. An internal elastic lamina separates the tuncia media, a layer composed primarily of vascular smooth muscle cells (VSMCs) and elastin collagen fibers. The external elastic lamina is separated from the outermost layer, the tunica externa, composed mainly of connective tissue attaching the vessel to the underlying tissues. (http://www.nicksnowden.net/images/artery-vein).

Primary functions of EC's include its regulatory effects on vascular tone, blood coagulation, wound healing, acute inflammation and leukocyte recruitment, all of which are pivotal to vascular homeostasis (Gerritsen, 1987). Maintenance of these functions under physiological conditions requires a complex interplay of various 'blood borne' biochemical and biomechanical stimuli, transduced by the EC, with consequences for various aspects of cell function, including proliferation, migration, apoptosis, gene expression and permeability. Under physiological conditions the endothelium acts to maintain homeostatic balance by presenting an anti-inflammatory, anti-thrombotic and anti-coagulative phenotype. The endothelium derived compound nitric oxide (NO) has

been one of the most extensively studied molecules with respect to vessel homeostasis. Indeed, a Nobel prize was awarded to Robert Furchgott's group in 1998 for describing the L-arginine – NO – cyclic guanosine monophosphate (cGMP) system as the major 'player' regulating endothelium-dependent dilation (EDD), which promotes vascular smooth muscle (VSMC) relaxation and resulting vessel dilation (Furchgott and Zawadzki, 1980). Apart from acting as a potent vasodilator, NO regulates vascular permeability, reduces monocyte adhesion, platelet aggregation, tissue oxidation, cytokine expression and favors fibrinolysis (Esper et al., 2006). All these factors decrease the risk of atherosclerosis, the most prevalent form of cardiovascular disease (CVD), and it is for this reason that NO is considered an anti-atherogenic molecule. Other important vasodilators such as prostacyclin, bradykinin and cytochrome P450 2C have also been described (Fleming, 2000, Giannotti and Landmesser, 2007). Hemodynamic forces are prime candidates involved in the regulation of NO, where healthy, atheroprotective laminar flow stimulates NO production (Harrison et al., 2006).

1.1.1 Endothelial dysfunction

Pathological conditioning of the endothelium, via altered hemodynamics or inflammatory cytokines are known to induce a state referred to as 'vascular dysfunction', which has the capacity to provoke unfavorable changes in endothelial specific functions, at the cell and molecular level with inevitable consequences for disease. It may even be argued that the endothelium plays a part in most if not all diseases, either as a primary determinant of pathophysiology or a 'victim of collateral damage' (Aird, 2005). CVD is a generic diagnostic for a range of diseases that affects the heart and blood vessels, and includes atherosclerosis, myocardial infarction (MI), stroke, hypertension, peripheral vascular disease, aneurysm and coronary artery disease. According to the respective Heart Foundations, it is estimated that CVD accounts for 36% (2005) of all deaths in Ireland and 34% (2006) in the United States. Atherosclerosis (arterial disease) is the most prevalent class of CVD that is diffusely localized throughout the vascular tree. As a prototypical model of endothelial dysfunction its pathophysiology is described in more detail below. It is a disease related to activation of the immunological system that responds to chronic levels of inflammation. The

'classical' risk factors for atherosclerosis include hyper-cholesterolemia, hypertension, diabetes, smoking and a sedentary lifestyle, while so called new risk factors include hyper-homocysteinemia, lipoprotein Lp(a), infections by *Chlamydia pneumonia* and *Helicobacter Pylori*, all of which contribute to an atherogenic cascade of cytokine/adhesion molecule production and ablation of NO production (Esper et al., 2006, Tobin et al., 2008).

Although the vasculature is exposed to various 'systemic' risk factors for disease, atherosclerotic plaques tend to form at hemodynamically vulnerable points within the vascular bed (curvatures or branch points), highlighting the importance of blood flow to endothelial health and disease. Shear stress hemodynamic forces (discussed properly in section 1.2) are imposed directly on the endothelium and modulate their structure and function through a series of mechanotransduction mechanisms. Low endothelial shear stress and/or oscillatory flow play a crucial role in the initiation of atherosclerosis (Chatzizisis et al., 2008, Cunningham and Gotlieb, 2005). A recent study by Chatzizisis *et al.*, demonstrated that low levels of shear stress (non-physiological levels) determines the location and complexity (high risk plaque content) of coronary atherosclerotic plaque development and progression (Chatzizisis et al., 2008). Indeed the earliest detectable manifest of atherosclerosis is a decreased NO response to hemodynamic stimuli or pharmacological stimulation (Hunt, 2002).

1.1.2 Atherosclerosis

Although multi-factorial in its progression, a brief synopsis of atherosclerosis development would describe a modulation of the mechanotransduction process leading to alterations in expression of inflammatory cytokines, tumor necrosis factor (TNF-α), interleukin-1 (IL-1), IL-6 and vascular adhesion molecules recruiting leukocytes (monocytes) to the endothelium, concomitant with a reduction in NO production (Esper et al., 2006). Migration of monocytes into the sub-endothelial layer ensues, leading to their activation and transformation into macrophages, which digest oxidized low-density lipoprotein (LDL-ox) cholesterol molecules forming foam cells. Foam cells, the principal component of 'fatty streaks' are the first step of atheromatous plaque

formation, which may undergo programmed death (apoptosis) releasing stored lipids, thus creating a lipid/necrotic core in the sub-endothelial layer of intima. As this lipid core expands, its thrombogenicity is enhanced and is separated only from the circulating blood by a fibrous cap, formed by an abundance of ECM proteins (collagen and laminin). These proteins are produced by VSMC's, which normally act to regulate vascular tone, but undergo phenotypic change, migrate to the intima and counteract the developing lipid core. To the detriment of VSMC's, inflammatory cytokines such as interferon gamma (IFN-γ) act to inhibit collagen synthesis and macrophages secrete matrix metalloproteinases (MMP's), which degrade components of the fibrous cap (Hunt, 2002). This plaque formation is associated with 'remodeling' of the vessel wall, and can have two possible fates;1): The plaques expands until it occludes the vessel, leading to irreversible ischemia or 2):The plaque ruptures, releasing its thrombotic content, and the resulting intravascular thrombosis could lead to MI or stroke. Figure 1.2 below shows the logical progression of atherosclerotic plaque formation within the vessel wall.

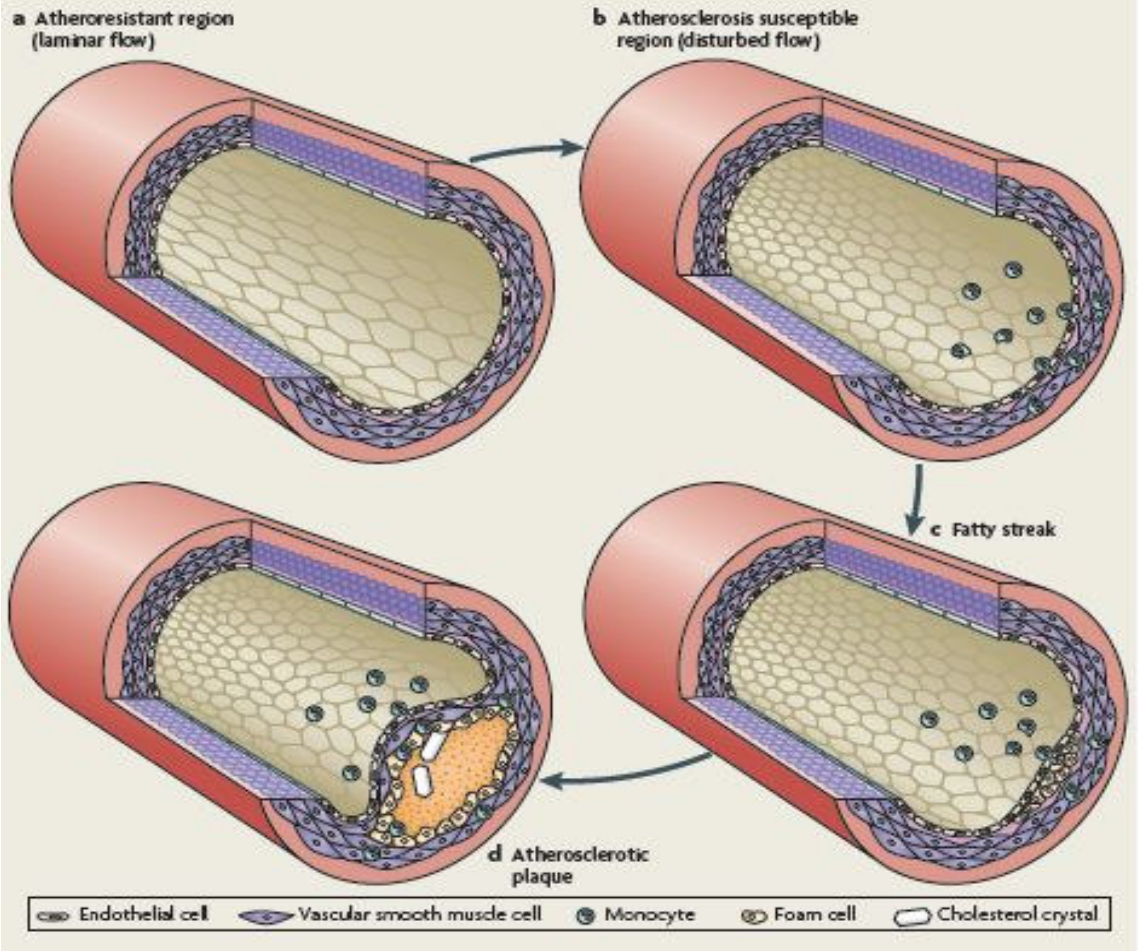

Fig. 1.2: Atherosclerotic plaque progression. (A) represents a healthy, atherosclerotic resistant area of the vasculature exposed to undisturbed laminar flow. (B-D) depicts the initiation of atherosclerotic plaque development, progression through to rupture in a branched area of the vasculature where flow patterns are disturbed (Hahn and Schwartz, 2009).

Physiological levels of shear stress are critical in maintaining vascular function, including thromboresistance, barrier function and vascular homeostasis. Continuous exposure to these forces, especially in straight sections of the arteries promotes the establishment of essential physiological characteristics of the vessel wall promoting an anti-atherogenic phenotype (Cunningham and Gotlieb, 2005). Thus, shear stress is critically vital in regulating the normal vessel physiology as-well as the pathobiology of vascular dysfunction through multifaceted mechanisms that promote atherogenesis. Crucially however, as alterations in blood flow (low/disturbed shear stress) are inevitable due to the complex spatial architecture of the vasculature, individuals with

elevated levels of CVD risk factors will be at a heightened risk for priming these 'hotspots' in the vasculature for endothelial cell activation, and thus initiate the atherosclerotic cascade described above.

1.2 Hemodynamics

With regards to extracellular stimuli regulating endothelial function, blood borne hemodynamic forces are of utmost importance and dramatically influence endothelial cell properties and function. These forces are fundamental to the development and physiology of the vasculature but a dysregulation significantly contributes to human disease. Two prominent hemodynamic forces exist, both of which exert physical (mechanical) stimulation of endothelial receptors (mechanosensors) with the ability to convert these stimuli into intracellular signalling cascades with downstream consequences for cellular functions (see figure 1.3). Cyclic strain is the circumferential force/wall tension generated by blood pressure causing a physical stretch in the vessel wall and is sensed by both endothelial and VSMC's (Lehoux et al., 2006). It is defined by Laplace's Law, which describes wall tension as a function of vessel radius and blood pressure (Laplace, 1899).

$$T = \frac{\mathrm{Pr}}{h}$$

Where T = wall tension (force per unit length of the vessel), P = blood pressure, r = vessel radius and h = thickness of the vascular wall. Cyclic strain is most prominent on the arterial side of the vasculature, in larger vessels such as the aorta, but less significant on the venous side. More importantly though, this hemodynamic force has the capacity to regulate a number of endothelial functions essential to vessel homeostasis, including permeability (Collins et al., 2006), migration (Von Offenberg Sweeney et al., 2005) and apoptosis (Haga et al., 2003).

Shear stress describes the frictional force of the blood against the vessel wall sensed principally by endothelial cells and is experienced more uniformly throughout the

vasculature. Laminar shear stress describes the undisturbed, unidirectional flow of blood in a vessel that is generally atheroprotective and essential for endothelial physiology. By comparison, disturbed/oscillatory shear, which predominates at complex vessel geometries in the vasculature promotes differential gene expression to induce a pro-atherogenic phenotype (Davies, 2009). Shear stress is proportional to the viscosity and velocity of blood flow and inversely proportional to the vessel radius.

$$\tau = \frac{4\mu Q}{\pi r^3}$$

Where, τ = shear stress (dynes/cm^2); μ = viscosity, Q = flow rate and R = vessel radius. (Lehoux and Tedgui, 2003). Physiological ranges of shear stress typically fluctuate between 10-20 dynes/cm^2 depending on the specific area within the vasculature (Deli et al., 2005). Not only is this force critical to controlling vascular physiology, it is also a key factor responsible for induction of the vascular plexus, and thus the cardiovascular system during embryonic development (Hahn and Schwartz, 2009).

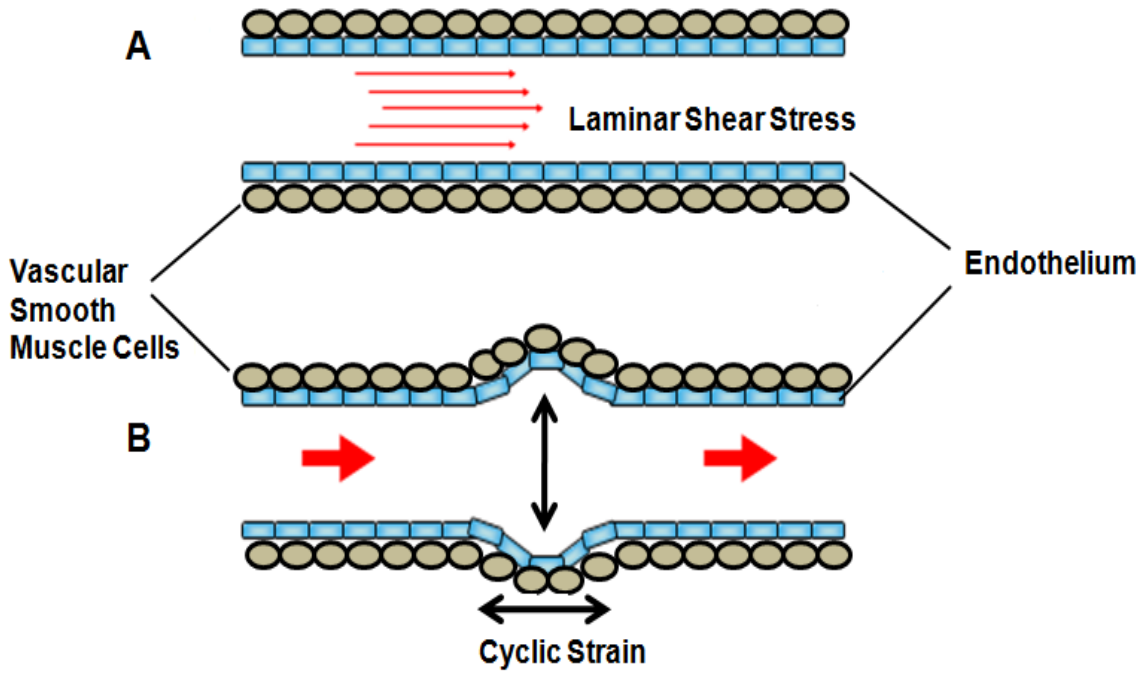

Fig. 1.3: Shear stress and cyclic strain. Schematic of hemodynamic forces within the vasculature; (A) laminar shear stress and (B) cyclic strain. Arrows in red indicate the direction of blood flow.

1.2.1 Hemodynamics and vessel remodeling

Blood vessels are highly dynamic, elastic structures that rapidly respond to changes in their internal environment, i.e. blood flow. Fluctuations in shear stress/cyclic strain evoke transient changes in vessel diameter to accommodate changes in blood flow and thus preserve the initial 'baseline' level of hemodynamic force. This response is mediated by endothelial release of potent vasodilators, such as NO, prostacyclin and endothelium-derived hyperpolarizing factor (EDHF) and arachidonic acid, which induce VSMC hyperpolarization and opening of potassium ion channels. This mechanism blocks the influx of calcium ions (Ca^{2+}) through voltage dependent calcium channels which naturally occurs in a depolarized state, thus inhibiting myosin mediated VSMC contraction, allowing the vessel to dilate (Vanhoutte et al., 1995, Haddy et al., 2006). This endothelial dependent response to blood flow occurs over seconds to minutes. On the contrary, sustained levels of aberrant hemodynamics (e.g. hypertension) have the ability to induce profound genotypic and phenotypic alterations in the vessel wall. This adaptive, structural process involves remodeling of VMSC's which causes thickening of the vasculature, allowing the vessel to resist these elevated forces. However over an extended period of time, this remodeling will ultimately compromise vessel elasticity and thus reduce the vessels ability to adapt to any further change in pressure (Hahn and Schwartz, 2009). Non-physiological conditioning of the vasculature as observed with hypertension can result in shearing rates greater than 40 dynes/cm^2 (Resnick et al., 2003). Wall stretch-associated hypertension, along with other aforementioned classical CV risk factors has been shown to enhance atherosclerotic plaque progression through the production of reactive oxygen species (ROS) and activation of pro-inflammatory genes (Chobanian and Alexander, 1996). Induction of vascular dysfunction is an early manifestation of CVD, defined as an impaired flow-mediated dilation through an artery bed. High resolution brachial artery ultrasound is a non invasive technique employed to assess endothelial dependent dilation in response to flow and thus used as an indicator of vascular function.

1.2.2 Mechanotransduction

Mechanotransduction describes the process by which EC's detect physical/mechanical stimuli generated by blood flow and transduce them into an intracellular signalling cascade(s) with downstream consequences for cellular functions. Differentiating between physiological or pathological hemodynamic stimuli is a host of membrane bound mechanosensors (receptors) which includes luminal based membrane proteins, cell-cell and cell-matrix adhesion proteins and the cytoskeleton (Deli et al., 2005, Tzima et al., 2005). Mechanotransduction of blood flow is a complex process that involves rapid and almost simultaneous activation of multiple mechanosensors on the luminal, lateral and subluminal surface of EC's. This suggests that a coordinated effort amongst receptors is fundamental to the initiation of cellular responses and that there is no single shear stress receptor. Shear stress is the principal hemodynamic stimulus influencing EC's at the blood brain barrier (BBB) and thus the responsivity of various mechanosensors will be discussed within this context (Desai et al., 2002). The mechanosensors discussed below are among the commonly studied receptors in vascular mechanobiology. A schematic representation is presented in figure 1.4

1.2.2.1 Luminal mechanosensors

Ion channels

Several ion channels have been identified in vascular EC's, of which some have been shown to shear responsive. They exist as membrane bound protein complexes that regulate ion transport across the membrane, establishing small voltage gradients. The P2X purinoceptors and transient receptor potential are shear-sensitive Ca^{2+}- permeable cation channels mediating Ca^{2+} influx. Intracellular Ca^{2+} rapidly increases within 1 min of shear application and subsides by 5 min (Ando et al., 1988). Significant to these responses, P2X4 (subtype of P2X) gene knock-out mouse models show a blunted vasodilatory response to increases in blood flow and have elevated blood pressure compared to wild type controls (Yamamoto et al., 2006) . Furthermore, studies have shown that shear stress activates an inward rectifying K^+ current, inducing hyperpolarization of the plasma membrane, compared to activation of chloride ion

channels, which cause membrane depolarization. Blockade of shear-induced K^+ current inhibited the induction of NO suggesting its importance in shear responsiveness and vascular function (Uematsu et al., 1995). Changes in membrane fluidity or tension under flow have been proposed as mechanisms facilitating regulation of these mechanosensitive channels as high plasma membrane levels of cholesterol inhibit their responses to flow (Fang et al., 2005).

G-proteins and G-protein coupled receptors

G-proteins are aptly named because of their ability to bind the guanine nucleotides, guanosine diphosphate (GDP) and guanosine triphosphate (GTP). They are heterotrimers consisting of Gα, Gβ and Gγ subunits and associate with transmembrane G-protein coupled receptors (GPCR). GPCR's contain extracellular loops facilitating ligand binding and a cytoplasmic tail which interacts with the heterotrimeric G-proteins. The Gα subunit sequesters GDP in its binding site, but upon ligand binding with the GPCR, an allosteric change takes place triggering GDP release and GTP binding to Gα. This promotes dissociation of Gα from $G_{\beta\gamma}$, both acting on specific downstream effectors (Wieland and Mittmann, 2003). Gudi *et al.*. showed that G-protein activation occurs 1 sec following shear onset, while inhibition of G-proteins using antisense Gαq oligonucleotides blocked shear induced Ras-GTPase activity (Gudi et al., 1996, Gudi et al., 2003). Furthermore pretreatment of EC's with pertussis toxin inhibited shear-mediated extracellular signal regulated kinases (ERK) 1/2 activation (Jo et al., 1997). However, the precise nature of shear-induced G-protein activation is contradictory. Reports from *in-vitro* studies seems to suggest ligand independence, as Frangos *et al.*. have shown that G-proteins reconstituted in liposome's are activated in response to shear (White and Frangos, 2007), while genetic deletion of kinin in mice (precursor of bradykinin) blocked responses to flow (Bergaya et al., 2001). Thus further clarification on the precise roles of G-proteins and GPCR's as mechanotransducers are required.

Endothelial glycocalyx

The luminal surface of EC's is coated with a dense layer of proteoglycan projections anchored to the plasma membrane, which constitute the endothelial glycocalyx (EG). The EG consists of heparan sulfate, chondroitin/dermatan sulfate and hyaluronic acid, all of which are modified by plasma proteins, enzymes, growth factors and cytokines (Weinbaum et al., 2007). More recent developments have suggested a role of the EG in force transmission of shear stress to the actin cytoskeleton, possibly through direct associations with the cytoskeleton or signalling molecules that dock with the core proteins of the glycocalyx (Ando and Yamamoto, 2009). Florian *et al.* using selective cleavage of heparin sulfate proteoglycans, was able to abrogate shear-induced NO production (Florian et al., 2003) and further work by Yao and colleagues identified a role for the proteoglycan in flow-induced EC realignment (Yao et al., 2007). Interestingly, cleavage of chondroitin with chondroitinase did not inhibit NO production in aortic EC's in response to flow. However, studies involving cleavage of glycocalyx proteoglycans may also affect the interaction of integrins with their cognate ECM ligand(s) along the basolateral surface; molecules which have also been strongly implicated in flow responses (see section 1.2.2.2), therefore calling into question the feasibility of the EG in apical mechanotransduction (Hahn and Schwartz, 2009). Further work is required to determine the precise contribution of the EG to mechanotransduction.

1.2.2.2 Cell adhesion mechanosensors

The sensing of hemodynamic forces by cell-cell and cell-matrix adhesion components has been well documented. Tzima *et al.* have previously characterized an intracellular mechanosensory complex consisting of 3 laterally located transmembrane receptors comprising the platelet endothelial cell adhesion molecule-1 (PECAM-1), vascular endothelial (VE)-Cadherin and vascular endothelial growth factor receptor 2 (VEGFR2). This complex was found to mediate a host of intracellular responses to flow but required

each receptor component to elicit a functional response. The proposed sequential participation of each receptor is discussed below (Tzima et al., 2005).

PECAM-1, a 130kDa glycoprotein abundantly expressed in EC's can also be found in circulating platelets and leukocytes. It contains 6 extracellular immunoglobulin (IgG) domain-like loops which participate in homophilic interaction with neighboring cells, an intracellular domain which interacts with the actin cytoskeleton, and is crucial to the transendothelial migration of leukocytes (Vaporciyan et al., 1993, Nakada et al., 2000). More recent investigations have shifted towards a putative role for this molecule in mechanosensing. Within seconds of flow onset, PECAM-1 is tyrosine phosphorylated, allowing the binding of the tyrosine phosphatase SHP-2. This association initiates a Ras GTPase signalling pathway which leads to ERK activation (Osawa et al., 2002), a response that appears to be independent of other early shear stress responses such as ion channels, as alterations in intracellular Ca^{2+} or K^{+} concentrations had no effects on PECAM-1 phosphorylation (Fujiwara, 2006). Furthermore, studies using magnetic beads coated with antibodies for different adhesion receptors have concluded that PECAM-1 is a direct mechanotransducer of mechanical force within this adhesion complex (Osawa et al., 2002, Tzima et al., 2005). Mechanical stimulation of PECAM-1 has been implicated in activating a Src family kinase, which is the earliest known intracellular signalling event in this particular pathway (Tzima et al., 2005).

Downstream of PECAM-1 activation, VE-cadherin (discussed in section 1.5) functions as an adaptor molecule within this mechanosensory complex. The adherens junction has previously been implicated in the adaptation of EC's to long term shear stress (Noria et al., 1999, Schnittler et al., 1997) but its role in mechanosensing was first elucidated by *Shay*-Salit *et.al.*(Shay-Salit et al., 2002) Following flow onset, a mutli-member complex is formed consisting of VE-Cadherin, β-catenin and VEFR2, which associates with the endothelial cytoskeleton. This complex is essential for shear-induced responses as EC's null for VE-Cadherin lacked the acute shear-mediated phosphorylation of Akt and p38, and more chronic induction of shear stress response element (SSRE) genes (Shay-Salit et al., 2002). It was suggested however that participation of VE-Cadherin in shear-

dependent signalling was shown to occur independently of cell-cell adhesion, as a blocking antibody of VE-Cadherin extracellular domains had no effect on flow stimulated WOW-1 binding, an active form of the shear responsive integrin αvβ3 (Tzima et al., 2005).

VEGFR2/Flk-1 is a receptor tyrosine kinase (RTK), for which its extracellular ligand VEGF is one of the main inducers of endothelial proliferation and permeability. Approximately 20 different RTK's have been identified, which exist as monomeric transmembrane receptors exhibiting a high affinity for many polypeptide growth factors, cytokines and hormones. Ligand binding triggers tyrosine phosphorylation, which creates binding sites for a Src Homology 2 (SH2) and phosphotyrosine binding domain-containing proteins to regulate effector proteins controlling various cellular activities (Pawson, 1994, Zwick et al., 2001). Shear stress and cyclic strain have also been implicated in their activation, as exposure to hemodynamic forces results in the activation and phosphorylation of the platelet-derived growth factor receptor-α (PDGF) (Hu et al., 1998). Moreover, VEGFR2 shows a rapid, Src-dependent, ligand-independent activation in response to flow facilitating the association of the adaptor protein Shc, a SH2 domain containing adaptor protein (Chen et al., 1999). Blocking Shc attenuates the shear-induced activation of ERK and c-Jun N-terminal kinase and the consequent gene transcription mediated by the binding of the transcription factor activator protein-1 to the 12-*O*-tetradecanoylphorbol-13-actetate responsive element (TRE). Shear-dependent activation of VEGFR2 in a ligand-independent manner causes the recruitment of phosphoinisotide 3-OH-kinsae (PI3K) and the consequent activation of Akt and endothelial nitric oxide synthase (eNOS) (Jin et al., 2003). Interestingly, flow-mediated activation of VEGFR2 was absent in PECAM -/- and VE-Cadherin -/- EC's, confirming its downstream role in signalling within this mechanosensory complex (Tzima et al., 2005).

To summarize the proposed signalling complex, following flow onset, PECAM-1 acting as a mechanotransducer is tyrosine phosphorylated which leads to the activation of Src. Through association with VE-Cadherin/β-catenin as an adaptor, VEGFR2 is brought

into proximity with PECAM-1 which facilitates its transactivation by Src to initiate cellular processes described above. Indeed, ectopic plasmid expression of PECAM-1, VE-Cadherin and VEGFR2 in COS-7 African monkey cells would only allow cellular alignment to flow when all 3 plasmids were present (Tzima et al., 2005).

Integrins

Integrins comprise a family of 20 transmembrane proteins, which exist as heterodimers consisting of α and β subunits. They are topically expressed on the basolateral surface of EC's where their extracellular domains mediate cell-matrix adhesion via specific ECM ligands such as fibronectin, vitronectin and collagen. The cytoplasmic domain associates with various molecules forming focal adhesions, comprising signalling molecules such as focal adhesion kinase (FAK), C-src, adaptor molecules Shc and Grb2, and actin binding proteins talin and α-actinin, thus establishing a link with the actin cytoskeleton (Sastry and Horwitz, 1993). Integrins are unique structures in the sense that they can mediate 'inside out' signalling, where intracellular signals affect their binding affinity to ECM ligands, and 'outside in' signalling whereby extracellular signals drive integrin-mediated intracellular signalling cascades. They are highly sensitive to hemodynamic force, and their subsequent activation has been shown to be essential to flow-mediated NO release (Muller et al., 1997), cellular realignment (Tzima et al., 2005), I-kappa-B (IkB) release (Bhullar et al., 1998) and ERK 1/2 activation (Takahashi and Berk, 1996). In the context of the mechanosensory complex described above, shear induced integrin activation was shown to occur downstream of VEGFR2-mediated PI3K activation. Wang *et al.* however has shown that shear induced VEGFR2 activation is attenuated by blockade of integrins; suggesting bi-directional signalling within this mechanosensing network (Wang et al., 2002). Interestingly the specificity of the integrin-matrix interaction is also an important determinant of the flow-mediated intracellular response. For example, flow triggers activation of the MAP kinase p38 on EC matrices coated with collagen and not fibronectin, whereas flow induces activation of the transcription regulator nuclear factor-kappa-B (NF-κB) on fibronectin but not collagen or laminin (Orr et al., 2005). Although discrepancies in the literature exist, the functional relevance

of integrins in shear-mediated cellular processes is undoubted, but requires a precise control over the extracellular environment these molecules are exposed to.

1.2.2.3 The cytoskeleton

The cytoskeleton describes a cellular scaffold that is essential to a number of cellular processes responding to spatially organised signalling mechanisms, which determines cell shape and mediates cell growth and differentiation. It consists of 3 types of protein filaments; actin microfilaments, vimentin intermediate filaments and tubulin microtubules. With a growing number of endothelial receptors implicated in shear-mediated signalling events, some of which are not directly exposed to flow, raised the possibility that a common structure could tie these receptors together. The endothelial cytoskeleton became the natural candidate, based on its ability to sense and transmit mechanical force and associate directly or indirectly to the mechanosensors described above (Helmke and Davies, 2002). Indeed spatio-temporal analysis of vimentin following flow onset shows a displacement of these structures to lateral and basal structures, suggesting transmission of force to these sites, therefore consistent with models of cell-cell or cell-matrix adhesion mediating mechanotransduction (Helmke et al., 2001). Furthermore disruption of the actin cytoskeleton by drugs was sufficient to abrogate shear stress mediated signalling and changes in gene expression (Malek et al., 1999, Hutcheson and Griffith, 1996, Imberti et al., 2000).

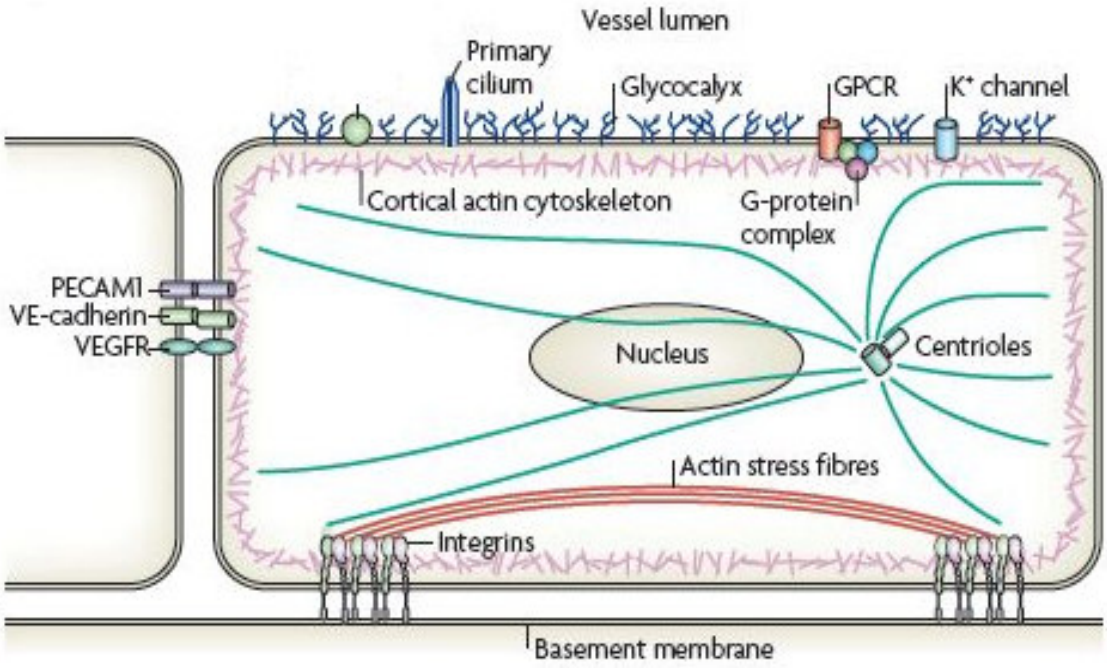

Fig. 1.4: Endothelial mechanosensors. This figure schematically shows the cellular localization of the aforementioned mechanosensors described in section 1.2.2 (Hahn and Schwartz, 2009).

1.2.3 Mechanoregulation of endothelial gene expression

Hemodynamic forces profoundly influence gene expression with the capacity to evoke phenotypic changes essential to physiology or pathophysiology. Based on a series of studies assessing shear-dependent changes in endothelial gene expression, the specificity of the response is highly dependent on the shear rate, location in the vasculature and the time course of exposure to shear stimulus. Shear-responsive genes possess a short nucleotide sequence termed shear stress response elements (SSRE), which, following transcriptional factor binding, activate/repress gene expression. The first of such SSRE was identified by Resnick *et al.* in the promoter region of the PDGF-B gene containing a nucleotide sequence of GAGACC, with a later study by Khachigian and colleagues attributing the NF-κB/p50-p65 heterodimer as the transcriptional factor regulating this response (Resnick et al., 1993, Khachigian et al., 1995). Through the exploitation of gene array technology, hundreds of genes have been shown to be regulated by laminar

shear stress and chronic exposure (24 h) of shear suppressed more genes than it induced (Resnick et al., 2003). The transcription factor kruppel-like factor 2 has been shown to regulate up to a third of shear-activated genes and has been suggested to underpin the molecular basis of the healthy state of flow exposed to EC's (Parmar et al., 2006, Garcia-Cardena and Gimbrone, 2006).

Interestingly, the early onset of physiological levels of laminar shear stress (0-60 min) triggers the activation of multiple signalling pathways, which favour the induction of genes consistent with a pro-inflammatory, pro-coagulant, atherosclerotic phenotype, thus transiently mimicking pathways evoked by turbulent/oscillatory shear flow patterns. Alteration in gene expression during this immediate laminar shear phase includes an upregulation of intracellular adhesion molecule (ICAM-1), vascular adhesion molecule (VCAM-1), and E-selectin concomitant with enhanced levels of monocyte adhesion (Walpola et al., 1995, Chappell et al., 1998), increase in ROS activity (McNally et al., 2003, De Keulenaer et al., 1998), while levels of eNOS are downregulated (Wilcox et al., 1997). However within 1-3 hr of exposure to laminar flow conditions, the activity of this pro-inflammatory cascade decreases substantially to below baseline levels, while induction is sustained under non-physiological flow conditions such as oscillatory flow. This suggests that the main difference between atheroprotective laminar flow and athero-promoting disturbed flow is the ability of EC's to temporally adapt to the laminar flow stimulus and downregulate relevant pathways influencing gene expression (see figure 1.5 below) (Hahn and Schwartz, 2009).

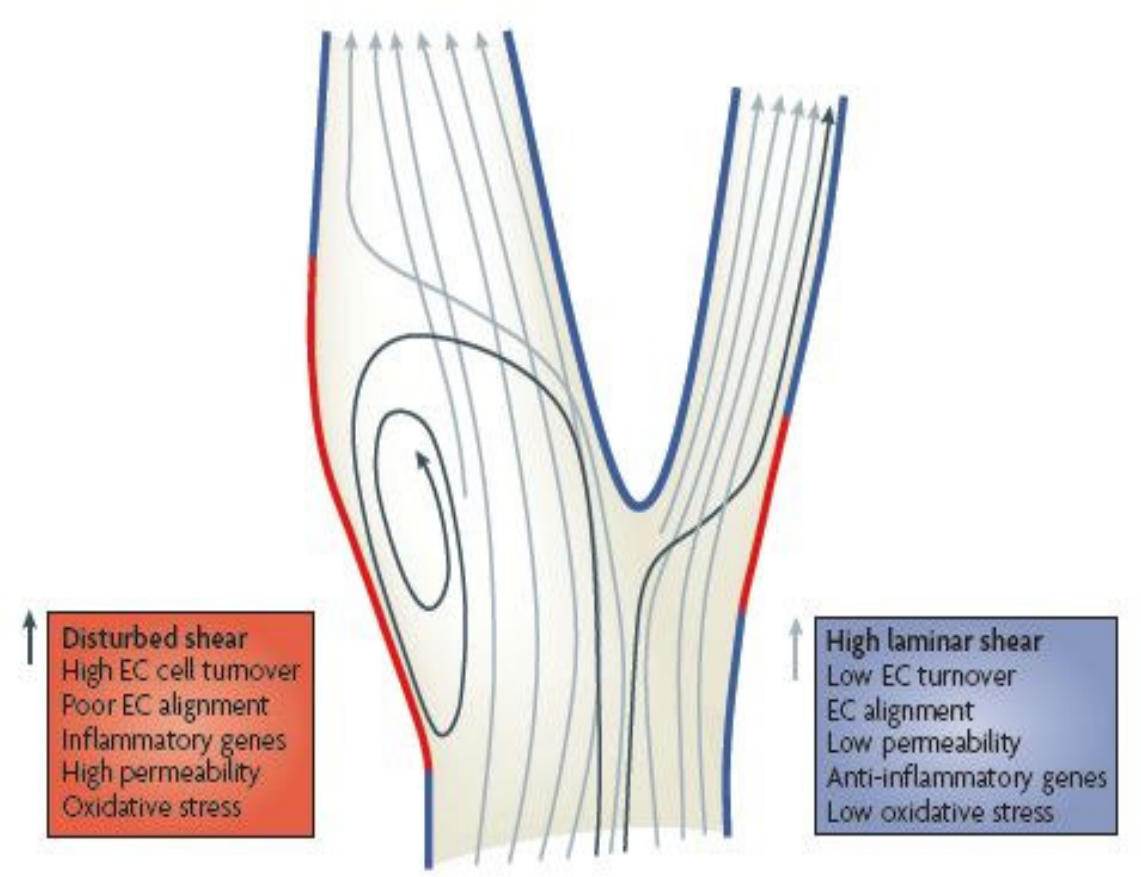

Fig. 1.5: Physiological laminar shear vs. disturbed shear. This figure depicts a branch point (bifurcation) in a blood vessel, which is a common site for atherosclerotic plaque progression. Possible endothelial cell fates at specific sites in the vessel are presented in two colour coded boxes (red/blue) depending on the hemodynamic stimuli experienced at this particular point (Hahn and Schwartz, 2009).

As described above, a wealth of knowledge exists about various mechanosensors implicated in coupling hemodynamic force to biochemical activity. The complexity of understanding these mechanisms is compounded by the fact that a great deal of interplay among mechanosensors seems to exist. Furthermore, adhesion sites and intercellular junctions are rich in various kinases, phosphatases and adaptor molecules necessary to elicit biochemical mechanotransduction processes. As such, the diversity of endothelial functions is reflected by this variety of mechanosensing mechanisms, suggesting that a single mechanism for coordinated mechanotransduction in EC's is unlikely.

1.3 The blood brain barrier

Despite the global localization of the EC's throughout the body, their specific function(s) can vary considerably depending on the specific vascular bed (Bouis et al., 2001). They are highly heterogeneous in nature, and thus have important implications for strategies in basic research, diagnostics and therapeutics. This premise certainly holds true for the dense network of EC's located within the cerebrovascular capillaries, which form the 'Blood-Brain-Barrier' (BBB). The BBB is an extremely selective barrier to the passage of blood-borne solutes to the central nervous system (CNS) by acting as a 'physical barrier' due to the presence of complex tight junction proteins between adjacent EC's regulating paracellular transport and specific transport systems on the luminal and abluminal membranes controlling transcellular traffic (Abbott et al., 2006).

The initial characterization of the BBB dates back to the 1880's as work by Paul Ehrlich found that cationic vital dyes were quickly taken up by all organs of the body following intravascular injection with the exception of the brain and spinal cord (Ehrlich, 1904). Although initially interpreted as a freak occurrence, work by Edwin E. Goldman showed soon after that intracranial injection of the very same dyes exclusively stained CNS tissue while all other organs remained unstained (Goldmann, 1913). The concept of the BBB was born, however the term 'BBB' was first coined by Lewandowsky who demonstrated that neurotoxic compounds only exerted aberrant effects on brain function following intracranial injection compared to intravenous administration. The precise location of the barrier remained unknown for 70 years, until Reese and co-workers using electron microscopy, tracked the barrier to be situated in the EC's of brain capillaries (Brightman and Reese, 1969, Reese and Karnovsky, 1967). Two other barriers within the CNS exist; the choroid plexus epithelium between blood and the ventricular cerebrospinal fluid (CSF), and the arachnoid epithelium between the blood and the subarachnoid CSF. However, individual neurons may be millimeters or centimeters from a CSF compartment whereas individual neurons are rarely more than 8-20μm from brain capillaries. Hence out of all the CNS barriers, the BBB exhibits the utmost control over the immediate microenvironment of the CNS (Schlageter et al., 1999).

1.3.1 Blood brain barrier permeability

As alluded to earlier, the endothelium performs a variety of functions central to homeostasis of the vessel wall and the underlying tissue. Specific to the BBB, regulation of vascular permeability is a dominant, non-stagnant function involving coordinated interaction of adjacent brain EC's and the surrounding neurovascular unit (NVU). Permeability can be described as the sum of many mechanisms that increase or decrease barrier function (Mehta and Malik, 2006). Different vascular beds have unique barrier characteristics which are essential to appropriate functioning of the underlying interstitium. The arteries and capillaries of the BBB elicit a relatively impermeable barrier, whereas regions within post-capillary venules are often cited as having 'leaky barriers' (Simionescu et al., 1975, Simionescu et al., 1976) and the adhesion of platelets and leukocytes is more probable here (del Zoppo, 2008). Brain capillary EC's are the primary constituent forming the BBB, which display barrier properties that significantly impede the movement of virtually all blood borne solutes to the brain, with the exception of those that are small and lipophilic. Three distinctive barrier functions within the BBB, have been described and their roles are categorized below (Pardridge, 2002).

1.3.1.1 Physical barrier

The flux of molecular traffic from blood to CNS occurs via two distinctive pathways. The transcellular pathway describes molecular movement through the cell membrane and is mediated by processes such as passive diffusion (O_2 and CO_2), active transport of glucose and various amino acids, and receptor/absorption mediated transport of larger molecules such as insulin or leptin (Ballabh et al., 2004). This transport mechanism is severely restrictive at the BBB as EC's display minimal pinocytosis to minimize non-specific transport into the CNS (Brightman, 1977). The paracellular pathway describes the movement of substances between adjacent endothlelial cells (gate function), a pathway within the BBB that is tightly controlled by a series of opposing tight and adherens junctional complexes limiting paracellular flux of ions, hydrophilic molecules

and hormones. Furthermore these tight junction protein complexes (see section 1.4) also have a valuable role (fence function) by separating the apical and basolateral domains of the cell membrane so the endothelium can take on the polarized (apical – basal) properties that are also common in certain epithelia (Abbott et al., 2006). The overall thickness of the brain endothlelial cell is about 200-300nm, but this extremely thin barrier has been described as having some of the most restrictive barrier properties of any biological membrane (Oldendorf, 1971). Figure 1.6 below highlights the different pathways present at the BBB.

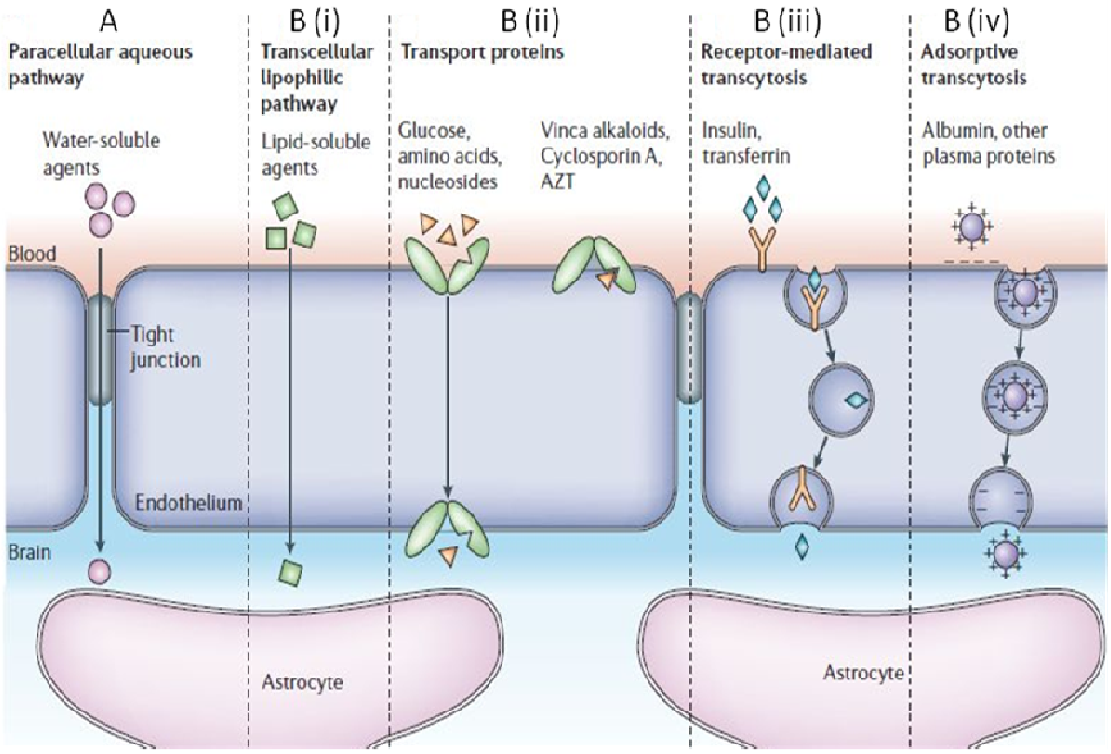

Fig. 1.6: Pathways at the blood brain barrier. A schematic representation of EC's at the BBB and the mechanisms of molecular traffic across the barrier. A) The paracellular pathway, regulated by tight junction proteins, which controls the penetration of water soluble molecules. B) The transcellular pathway regulates solute flux through B (i) the cell membrane, B (ii) active transporters, B (iii) receptor mediated endocytosis and B (iv) absorptive mediated transcytosis (Abbott et al., 2006).

1.3.1.2 Enzymatic/Metabolic barrier

The BBB possess a diverse range of enzymes capable of neutralizing many drugs or nutrients that attempt to pass the endothelial barrier. This includes a variety of ectoenzymes such as peptidases and nucleotidases capable of metabolizing peptides and ATP respectively, while intracellular enzymes such as monoamine oxidase and cytochrome P450 can block many neuroactive and toxic compounds (el-Bacha and Minn, 1999). These enzymes act in concert with the physical barrier properties of the tight junctions to restrict unwelcome entry of blood-borne solutes into the CNS. This enzymatic barrier also plays a role in regulating the polarity between the luminal and abluminal surfaces of brain endothelial cells that contribute to barrier function. Enzymes involved in establishing these properties are the γ-glutamyl transpeptidase and alkaline phosphatases on the luminal surface and the Na^+-K^+ ATPase and sodium-dependent neutral amino acid transporter associated with the subluminal surface (Abbott, 2005).

1.3.1.3 Efflux barrier

Another essential function of the BBB is the controlled removal of waste products and any potentially harmfully compounds from the brain into the blood stream. Even if certain drugs cross the endothelium via free diffusion and influx in the CNS, they can be followed by immediate active efflux back into the blood if the drug is a substrate for one of the many different active efflux transporters (AET). P-glycoprotein (P-gp) is the classic AET present at the BBB which has a broad substrate specificity for many xenobiotics compounds (Zhou, 2008). Multidrug resistance proteins (MRP-1), brain multidrug resistance protein (ABCG2/BCRP) and the organic anion-transporting polypeptide (OATP2) represent other commonly cited AET at the BBB (Deli et al., 2005).

1.3.2 Heterogeneity at the blood brain barrier

The microvasculature within the BBB shows the most extreme form of phenotypic differentiation of any vascular bed within the body, with an upregulation and/ or down regulation of certain factors that are poorly expressed or absent from peripheral

endothelium (Abbott, 2005). Examples of this include the lack of fenestrations in neuronal endothelium, which are small pores between EC's (common in capillaries of the glomerulus) and are replaced by tight junction complexes. These tight junctions are more complex and extensive in the brain and thus seal the intercellular cleft more effectively. The tightness of these junctions is such that they even restrict the movement of small ions such as Na^+ and Cl^- and exhibit transendothelial electrical resistance (TEER) values (an index of paracellular barrier integrity) between 1000-2000 ohm (Ω) cm^2 compared to 2-20 Ω cm^2 in peripheral capillaries (Rubin and Staddon, 1999, Abbott et al., 2006). It is believed that BBB EC's contain 5-6 times more mitochondria per capillary section compared to rat skeletal tissue, enhancing the energy potential required for the active transport of nutrients to the brain (Persidsky et al., 2006b). The anticoagulant factor thrombomodulin, which is expressed by vessels surrounding all organs with the exception of the brain (Ishii et al., 1986), as is the anticoagulant tissue factor pathway inhibitor predominantly expressed in microvascular endothelium but is lowest in the brain (Osterud et al., 1995). Even though there is a definite diversity of factors present at the BBB interface, EC's of this origin are not conformed to predetermined phenotype, but are induced by a variety of factors from the local environment. This local input from surrounding structures hold the key to this unique heterogeneity, as the endothelium is exposed to paracrine/endocrine influences from different cell types, along with varying degrees of biomechanical stresses.

1.3.3 The Neurovascular Unit

The NVU describes the interaction of microvascular endothelium with neural and glial tissue. Figure 1.7 below illustrates the close interactions of the four components of the NVU, namely astrocytes, pericytes, neurons and the basal lamina with their putative roles in establishing BBB characteristics as described.

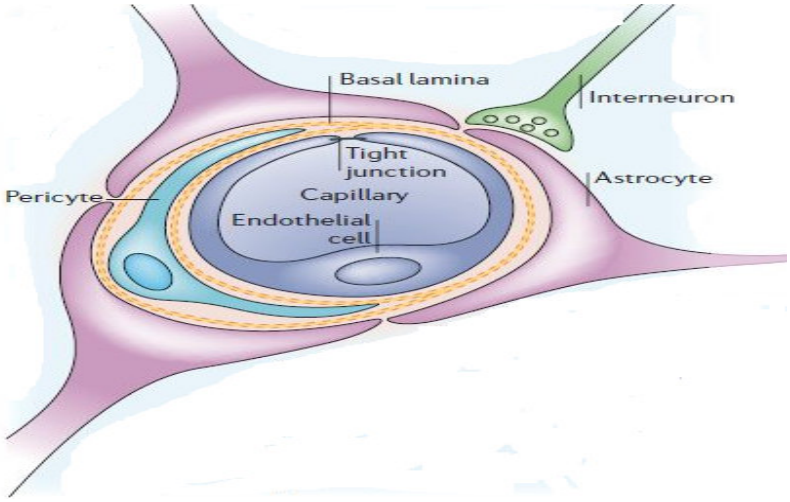

Fig. 1.7: The Neurovascular Unit at the Blood Brain Barrier. The BBB is formed by cerebral capillary endothelial cells, which are anchored to a basal lamina of ECM proteins and surrounded by astrocytic end feet processes. Pericytes are also in close proximity, while astrocytes provide the cellular link to neurons (Abbott et al., 2006).

1.3.3.1 Astrocytes

Astrocytes are a subtype of glial cells, i.e. non neuronal cells that comprise approximately 90% of brain mass and are categorized into divisions based on their structure and location. Fibrous astrocytes posses a star like morphology and are predominantly found in the white matter, while protoplasmic astrocytes reside in the grey matter containing a branched architecture enveloping neuronal processes. The third type, are the Bergmann glia, contained within the Purkinje layer of the cerebellar cortex containing two types of processes: thick processes which connect to Purkinje neurons and thin processes which project out of the cortex ultimately contacting blood vessels (Gee and Keller, 2005). One of the primary functions of astrocytes is to maintain extracellular K^+ ion levels as a result of their release from signalling neurons, and thus regulate an optimal environment for neuronal signalling (Ransom and Sontheimer, 1995). Importantly though, astrocytes envelop 99% of the BBB endothelium and this close cell-cell association led to the suggestion that they could mediate specific features of the BBB barrier phenotype. Indeed there is overwhelming evidence from *in-vitro* studies suggesting that the co-culture of brain EC's with astrocytes can induce/restore common BBB features, including tighter barriers as shown by increases in TEER (Colgan et al., 2008, Willis et al., 2004b, Willis et al., 2004a), the expression and

polarized localization of AET's including P-gp (Schinkel, 1999), and specialized enzymes systems (Haseloff et al., 2005). Astrocytes secrete a variety of chemical mediators which act in paracrine fashion to induce specific effects on the endothelium. These include transforming growth factor-β, glial derived neurotrophic factor, basic fibroblast growth factor (bFGF) and angiopoietin 1, which have been shown to induce an increased localization of Claudin-1 and ZO-1 to cell-cell junctions, key proteins involved in the regulation of paracellular permeability. Although astrocytes have been shown to induce a range of characteristics in brain endothlelial cells it is unlikely that they are sufficient to induce the broad spectrum of BBB properties seen as astrocytes are present in circumventricular organs where capillaries have leaky barriers (Engelhardt, 2005).

1.3.3.2 Perictyes

"Peri' meaning around and "cyto" cell reflects the anatomical description of the location of pericytes at the abluminal side of the microvessel. For the large part, they are separated from brain EC's by the basal lamina of ECM proteins, however cellular projections do invaginate through the lamina to cover approximately 20-30% of the microvascular circumference (Frank et al., 1987). Morphologically, pericytes contain a spherical cell body with a prominent nucleus and many cytoplasmic processes (Farrell et al., 1987). Pericytes have a close physical association with the endothelium as they share a common basal membrane and communication between them via gap junctions has been shown *in-vitro* (Lai and Kuo, 2005). Pericytes significantly contribute to the development, maintenance and regulation of the BBB and it has also been suggested that they help regulate the endothelial-astrocyte interaction (Ramsauer et al., 2002). As with astrocytes, co-culture models of brain EC's and pericytes have been shown to induce tighter paracellular barriers as monitored by TEER and water soluble fluorescein tracer studies (Deli et al., 2005). These finding may in part be reflected by the fact that pericyte derived angiopoietin-1 has been shown to enhance occludin gene expression in brain EC's, which would contribute to tight junction assembly at the paracellular junction (Hori et al., 2004). Furthermore under hypoxic conditions, an event associated

with BBB disruption, pericytes were shown to migrate away from the microvessel further implicating their role in barrier stabilization (Gonul et al., 2002).

1.3.3.3 Neurons

Whether or not neurons play a role in the development of the BBB phenotype is yet to be determined, however a wealth of evidence exists showing their critical importance in the regulation of cerebral blood flow and thus BBB function (Hawkins and Davis, 2005). Neuronal tissue exhibits a constant, dynamic demand on the local cerebral microvasculature to meet their metabolic needs, and this close relationship between brain activity and blood flow has been demonstrated by neuroimaging although the exact signalling mechanisms are unknown (Paemeleire, 2002). Brain EC's and/or associated astrocytes are innervated by a variety of neuronal projections, namely noradrenergic, serotonergic, cholinergic and GABA-ergic neurons (Persidsky et al., 2006b). Chemically induced loss of noradrenergic stimulation of the microvasculature was associated with an enhanced vulnerability of the BBB to hypertension (Ben-Menachem et al., 1982), as was a loss of cholinergic innervation (as observed in Alzheimer's) associated with impaired cerebrovascular function (Tong and Hamel, 1999). Moreover a study by Lee *et al.* showed a selective increase in BBB permeability rather than an anatomical disruption in response to intra-cerebral hemorrhage implying that communication between neurons and the vasculature may not just simply regulate cerebrovascular blood flow, but BBB permeability too (Lee et al., 1999).

1.3.3.4 Extracellular matrix (ECM)

The ECM through the expression of matrix proteins such as laminin, collagen IV and fibronectin serves as an anchor (basal lamina) for the endothelium and aforementioned members of the NVU. Brain endothelium expresses specific integrin and dystrogylcan receptor family members, which have been shown to be essential for organ development and physiological functioning of the CNS. For example deletion of the α6, αV or β6 integrin subunits results in embryonic or perinatal lethality or in the case of the latter two receptors, cerebral hemorrhage (Georges-Labouesse et al., 1996). These receptors

regulate cellular activities in a variety of ways including transducing extracellular stimuli to intracellular signals, forming a transmembrane link between the basal lamina and the cell cytoskeleton (Del Zoppo et al., 2006). With respect to BBB function, these matrices have been shown to influence the expression of tight junction proteins, suggesting a plausible role for the ECM in maintenance of paracellular permeability (Savettieri et al., 2000). A study by Rosenberg *et al.* was able to show that the ECM is strongly associated with the BBB permeability as a bacterial collagenase induced severe disruption of the basal lamina and opened the BBB (Rosenberg et al., 1993). Moreover Rascher and colleagues (2002) demonstrated that in response to a glioblastoma, BBB breakdown is reflected by changes in the molecular composition of both tight junction proteins and the basal lamina component agrin (Rascher et al., 2002).

This concept of the NVU provides a framework for understanding the development, physiology and pathology of the BBB. An understanding of these factors is therefore crucial to the design and undertaking of any *in-vitro* based systems to mimic the in situ microenvironment of the BBB. Recently a triple co-culture *in-vitro* model incorporating freshly isolated primary brain EC's, astrocytes and pericytes was established. This model elicited a characterizational profile of common BBB markers (Occludin, Claudin-5, ZO-1) with typical junctional localization and TEER values of approximately 400 Ωcm^2 (Nakagawa et al., 2009). Therefore, this *in-vitro* model represents an ideal candidate for research on BBB physiology and pathology, and to test novel compounds for CNS drug delivery.

1.3.4 Blood brain barrier disruption

As discussed earlier, under physiological conditions the BBB is relatively impermeable. Conversely BBB dysfunction is characterized by disassembly of intercellular junctional complexes and has been implicated in a number of neurological diseases, including inflammation (uncontrolled leukocyte extravasation and cytokine production), infection (meningitis), neoplasia (metastatic brain tumors) and neurodegeneration (multiple sclerosis and Alzheimer's Disease) (Weiss et al., 2008). In some incidences, the increase in BBB permeability can be a consequence of the pathology, as is the case with ischemic

stroke (Ilzecka, 1996) and a brain trauma (Morganti-Kossmann et al., 2002), whereas in the case of multiple sclerosis (MS), BBB opening is speculated to be the precipitating event (Hawkins and Davis, 2005). The vasoactive peptides bradykinin and histamine, along with the polyunsaturated fatty acid, arachidonic acid, and the neurotransmitter serotonin have been cited as classical inflammatory mediators of BBB permeability modulation (Abbott, 2000). Other humoral agents serving as permeabilizing factors include glutamate, aspartate, taurine, ATP, endothelin-1 (ET-1), TNF-α, IL-1 (Abbott, 2000, Abbott, 2004, Chen et al., 2000, Kustova et al., 1999, Magistretti et al., 1999). Interestingly, these BBB-modulating agents can be released by the endothelium itself, albeit in response to inflammatory cytokines, and thus in autocrine fashion act on associated endothlelial receptors, e.g. ET-1 acts on ETa receptors. Also, cells of the surrounding NVU can interact with activated macrophages, which amplify the inflammatory responses leading to BBB alterations (Persidsky et al., 1999) or enhanced monocyte transmigration (Persidsky et al., 2006a). Although two possible pathways of molecular flux across the BBB exist, alterations in the tight and adherens junction complexes regulating paracellular permeability mechanisms are continually associated with various CNS disorders (Huber et al., 2001). Moreover the BBB has often been described as the rate limiting step in the development of drugs targeting neurological disorders of the brain. Thus, understanding the assembly and interactions of these junctional complexes will provide valuable insights into possible mechanisms for treatment of such disorders.

1.3.5 Regulation of cerebral blood flow

Being such a dynamic, non-stagnant organ, the brain requires a continuous supply of blood to ensure essential neuronal function and eliminate any risk of irreversible damage to its constituents, as observed with flow cessation during cerebral ischemia. Organs such as the kidney or liver are more tolerant to ischemia whereas the brain must incorporate specific defence mechanisms to compensate and sustain appropriate levels of cerebral perfusion. An integrated effort between the NVU and cerebral blood vessels crucially regulate this process. Three lines of defence have been proposed.

1. Via neural influence over the cardiovascular system, the brain controls the distribution of blood flow. This hierarchical control can counteract any deficits in cerebral perfusion by redirecting blood flow from peripheral regions to the cerebral circulation.
2. In response to fluctuations in arterial blood pressure, cerebrovascular autoregulation ensues to stabilize the cerebral perfusion rate. Under low arterial pressure the cerebral arteries vasodilate, compared to vasoconstriction when the arterial pressure increases, both of which impact to maintain downstream flow rates within the cerebral capillaries and venules
3. The brain can also induce functional hyperaemia which causes an increase in blood flow to a specific region within the brain based on activity within that region, insuring adequate delivery of essential nutrients/gases to that area, but also removing any metabolic waste (Iadecola, 2004).

These defence mechanisms are essential to CNS homeostasis. Any aberrant conditioning of factors regulating these processes i.e. vascular dysfunction will therefore have detrimental consequences for the CNS.

1.3.6 Shear stress and the BBB

Vascular endothelial sensitivity to blood flow was first observed more than 150 years ago by the famous pathologist Virchow, who noted profound changes in endothelial morphology along the arterial tree, which correlated with flow patterns. Indeed the hallmark of the endothelial response to prolonged exposure of laminar shear stress results in their elongation and realignment in the direction of flow (Dewey et al., 1981, Galbraith et al., 1998). This is an important adaptive response which alters the way in which the shear acts on the endothelium (Hahn and Schwartz, 2009). Furthermore, physiological levels of laminar shear stress can suppress EC apoptosis (Dimmeler et al., 1997), decrease EC rates of proliferation (Akimoto et al., 2000), enhance levels of migration in response to wound healing (Sprague et al., 1997), regulate EC permeability (Siddharthan et al., 2007), repress anti-inflammatory mediators and activate various antioxidants to control ROS levels (Berk et al., 2001).

Rates of shear stress in the cerebral microvasculature range between 3-20 dynes/cm^2 (Desai et al., 2002). Interestingly, levels of cyclic strain are barely detectable in microvascular beds making shear stress the primary hemodynamic force influencing EC's at the BBB. Similar to EC's of non-neuronal origin, shear-induced stimulation of BBB endothelium can release a variety of protective vasoactive substances including NO, cyclooxygenase-2, adenosine and EDHF which induce vasodilation (Busse and Fleming, 2003).

Stannes and colleagues demonstrated that shear stress acting in tandem with glial-derived factors was essential for the induction and maintenance of the BBB (Stanness et al., 1997). Furthermore, recent experiments using the HCMEC/D3 cell line (human immortalized brain microvascular endothelial cell line) showed that physiological levels of flow maintained permeability characteristics of the BBB in the absence of co-culture with abluminal astrocytes, strengthening the functional relevance of physiological flow for BBB maintenance (Cucullo et al., 2008). Consistent with these findings, loss of flow alone (independent of hypoxia-hypoglycemia) contributed to BBB failure by enhancing leukocyte-mediated inflammatory mechanisms (Krizanac-Bengez et al., 2006). Moreover, Colgan *et al.* showed that biochemical changes in tight junction proteins were responsible for shear-induced upregulation of BBB function, thus offering a potential cellular mechanism for the physiological regulation of BBB function in response to flow (Colgan et al., 2007). Signalling mechanisms linking shear stress to changes in tight junction assembly at the BBB are notably lacking from literature, however could be of real therapeutic significance in pathologies eliciting compromised BBB function.

1.4 Tight junctions

A series of junctional complexes constitute most known barrier systems, namely tight junctions, adherens junctions, gap junctions and desmosomes. Out of all these junctions, endothelial tight junctions (zonula occludens) have been described as having the highest degree of complexity within the cardiovascular system (Nagy et al., 1984). By definition, tight junctions are domains of occluded intercellular clefts as first evidenced by initial studies using freeze fracture electron microscopy (Schulze and Firth, 1993,

Brightman and Reese, 1969). In general, tight junctions perform two distinctive functions; first they contribute to maintaining cell polarity and second, they seal adjacent EC's preventing uncontrolled molecular flux (Schnittler, 1998). The assembly of the tight junction barrier during morphogenesis/tissue repair is a multistage process, initially involving the establishment of cell-cell contact by adherens junctions, the lateral extension of these contacts and the subsequent recruitment of transmembrane tight junction proteins to the intercellular cleft, forming the paracellular barrier (Fanning and Anderson, 2009). A study by Gumbiner and Simons first supported this notion, as they found that blocking antibodies against E-Cadherin, an essential component of adherens junction in epithelial cells, was a prerequisite for tight junction formation (Gumbiner and Simons, 1986). As the strands of the tight junction proteins become longer and interconnected, i.e. complex, the outer leaflets of adjacent membranes within junctional contacts become fused, forming "membrane kisses" (Kniesel et al., 1996).

There are two key parameters that determine the functional quality of the tight junction: the intricacy of the strands and their association with the protoplasmic fracture face (P-face) of the plasma membrane or with the exo-cytoplasmic fracture face (E-face) (Wolburg and Lippoldt, 2002, Engelhardt, 2005). In non-neuronal EC's, tight junctions predominantly associate with the E-face of the plasma membrane, whereas P-face associations prevail at the BBB. This P-face association was considered to correlate with barrier function and become a morphological criterion of endothelial barrier properties in mammals and is hypothesized that this particle distribution is the result of cytoplasmic anchoring of tight junction proteins, which differs in BBB and non-BBB endothelia (Wolburg et al., 1994). The basic molecular equipment of the tight junction is similar to those found between epithelial cells, however components of the adherens and tight junction intermingle in endothlelial rather than epithelial cells (Schulze and Firth, 1993). Specific to the BBB, tight junctions are the rate limiting step in the paracellular flux of solutes between endothlelial cells and are the most apically located of the intercellular junctions (see figure 1.8) (Huber et al., 2001). Tight junctions are composed of an intricate series of transmembrane and cytoplasmic accessory proteins linked to the actin cytoskeleton that from the paracellular seal.

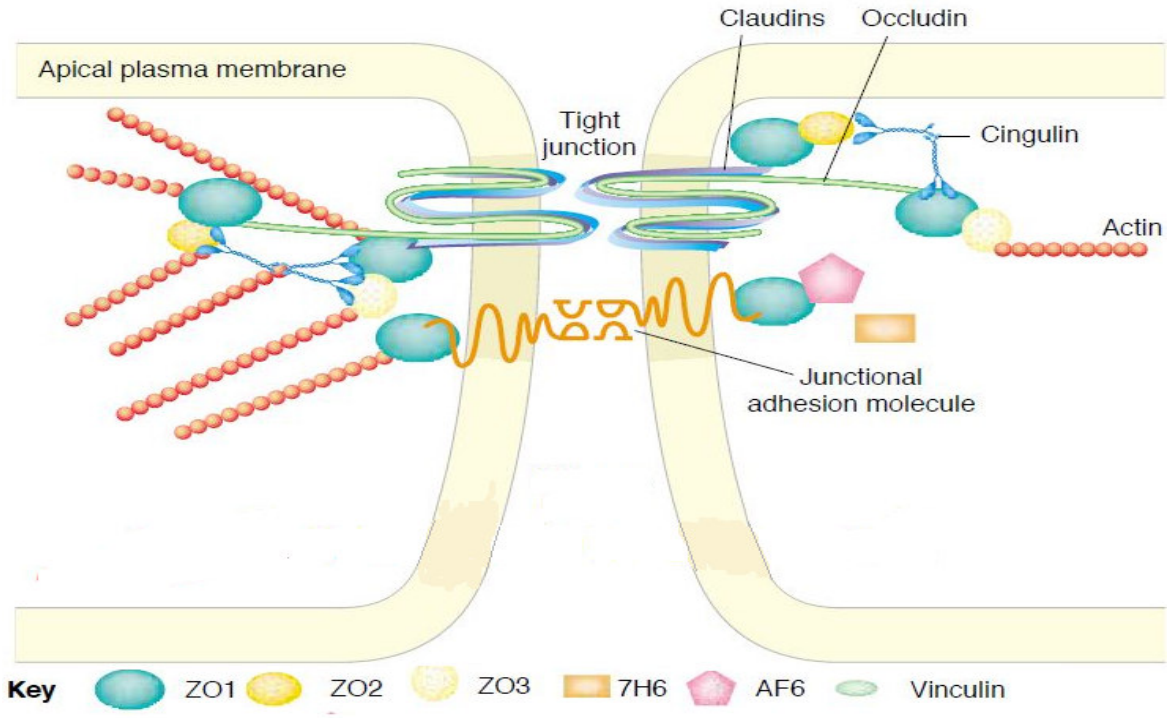

Fig. 1.8: Tight Proteins of the Blood Brain Barrier. Schematic figure of the proposed associations of the key, well known proteins of the tight junction complex at the BBB (Huber et al., 2001)).

As demonstrated in figure 1.8, there are three integral transmembrane proteins forming the tight junction complex. Occludin, a 60-65 kilodalton (kDa) protein was the first of these to be identified (Furuse et al., 1993), with a key role in the regulation of barrier tightness (discussed further in section 1.4.1). To date, 24 mammalian isoforms of the claudin family have been identified, with molecular weight ranges between 20-27 kDa and are vital in the assembly of junctional complex (discussed further in section 1.4.3) (Krause et al., 2008). The junctional adhesion molecules (JAM's) are members of the Immunoglobulin superfamily, of which 3 isoforms have been identified; JAM-A, JAM-B and JAM-C. Their predominant function besides tight junction maintenance is to facilitate leukocyte extravasation, in association with the platelet endothelial cellular adhesion molecule 1 (PECAM-1) (Huber et al., 2001). These transmembrane proteins are anchored to the actin cytoskeleton by a complex of cytoplasmic accessory proteins, which provide structural support adjacent to the junctional cell membrane. The zonula occludens proteins (ZO-1, ZO-2 and ZO-3) belong to family of proteins known as

MAGUKs (membrane-associated guanylate kinase like proteins), which serve as recognition sites for tight junction placement and a support structure for signal transduction proteins (discussed further in section 1.4.2) (Haskins et al., 1998). AF6 (All-1 fusion partner from chromosome 6) interacts with JAM via N-terminus interaction with ZO-1 and serves as a scaffold protein regulating cell-cell contacts (Yamamoto et al., 1997). Cingulin, a 140 kDa myosin-like protein, existing as a dimer intertwined in a "coiled-coil", has been shown to interact with ZO-1, -2, -3, myosin, JAM and AF6, and links the tight junction cytoplasmic accessory complex to the cytoskeleton (Cordenonsi et al., 1999). The 7H6 antigen is a phosphoprotein, which has been shown to play a role in the regulation of paracellular permeability to ions and macromolecules (Satoh et al., 1996). Vinculin is another actin binding phosphoprotein, which facilitates the interaction of the tight junction with the actin cytoskeleton, and its activation by specific kinases can trigger disassembly of the complex (Harhaj and Antonetti, 2004).

Many signalling pathways have been implicated in the regulation of permeability through modification of tight junctions, including G-proteins (Granderath et al., 1999), serine-, threonine-, tyrosine-kinases (Collins et al., 2006), cyclic adenosine monophosphate (cAMP) levels (Wolburg et al., 1994), aswell as proteases and cytokines (Adamson et al., 1999). These mediators can act at the level of the tight junction or through modulation of cytoskeletal elements. Furthermore, the importance of cytoskeletal integrity *in-vivo* was demonstrated by infusions of cytochalasin D, an inhibitor of actin polymerization, which led to increased blood brain barrier permeability (Nag, 1995).

1.4.1 Occludin

In 1993, Furuse *et al.* using chick liver raised 3 monoclonal antibodies specific for a 65 kDa protein in rats. It was assigned the name occludin derived from the Latin word "occlude" and became the first transmembrane tight junction protein to be identified. This anti-chick antibody failed to detect occludin in mammalian tissues and it wasn't until 1996 that the protein was first detected in humans (Ando-Akatsuka et al., 1996).

Based on amino acid sequencing, there is a 90% homology between human, murine and canine occludin, however only a 50% homology exists between avian and marsupial structures. Structurally occludin is a tetraspanning membrane protein, consequently possessing two extracellular loops that form homophilic interactions with occludin from adjacent EC's, a cytoplasmic COOH- and NH_2- terminus, and can be divided into 5 separate domains (A-E). The COOH terminus is strongly concentrated with charged amino acids and the extracellular (EC) domains are rich in tyrosine and glycine residues (see figure 1.9 below) (Feldman et al., 2005). The human occludin gene was mapped to chromosome band 5q.13.1, and the possibility of several alternatively spliced products was noted due to the existence of several occludin mRNA bands in Northern blots (Saitou et al., 1997). Mankertz *et al.* identified 4 alternately spliced mRNA transcripts, of which two expressed translated occludin proteins that resulted in altered distribution patterns of occludin and a loss of co-localization with ZO-1. These splice variants lacked the 4th transmembrane domain, thus highlighting the significance of the region in targeting occludin to the tight junction (Mankertz et al., 2002).

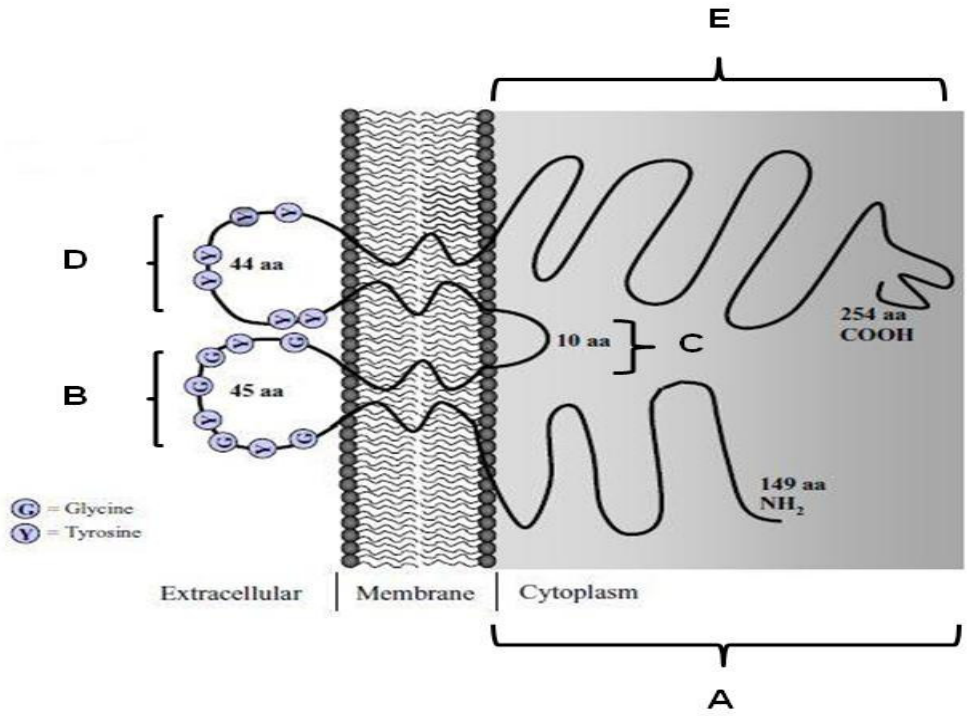

Fig. 1.9: Schematic depiction of occludin structure and domains. Adapted from (Feldman et al., 2005).

1.4.1.1 Occludin function

The function of occludin was initially investigated following transfection of chick occludin complementary DNA (cDNA) in Madin-Darby Canine Kidney (MDCK) cells using a Lac-inducible vector. Following induction of occludin expression by iso-propyl-β-D-thiolgalactoside (IPTG), TEER values across MDCK monolayers increased progressively and were 30-40% greater than control levels at 31 hours post induction (McCarthy et al., 1996). Expression of occludin correlates with barrier function, as arterial EC's express 18-fold greater occludin protein levels than venous EC's and form a tighter barrier (Kevil et al., 1998). Moreover occludin expression is most prominent at the BBB. The N-terminus of occludin (domain A) has been shown to be functionally relevant to the regulation of barrier function. Studies using NH_2 truncated mutants of occludin exhibited alterations in transendothelial electrical resistance (TEER) values and gaps were shown to appear in the P-face associated tight junction strands. It was postulated that the N-terminally truncated mutant was unable to oligomerize with other tight junction proteins, thus explaining the gaps between the strands (Bamforth et al., 1999). Wong and Gumbiner used peptide mimics of the two EC domains (B and D) of occludin, termed Occ-1 (corresponding to domain B) and Occ-2 (domain D) to decipher their roles in the junctional seal. Occ-2 appeared to have the most significant effect as it not only disrupted the integrity of the tight junction barrier, it also reduced the localization of occludin to the junction complex (Wong and Gumbiner, 1997). Subsequent work by Medina and colleagues confirmed these findings using truncated constructs of the relevant EC domains and found occludin present at the basolateral surface and not at the tight junction (Medina et al., 2000).

The COOH terminus is also believed to perform essential roles in correct tight junction assembly. This region binds with ZO-1 within its coiled-coil domain, although conflicting data concerning specific roles of the COOH terminus in trafficking of occludin to the junctional complex exist. Work by Furuse *et al.* showed that this region is required for ZO-1/ZO-2 binding, and that it is necessary for occludin to localize at the tight junction (Furuse et al., 1994). However experiments by Balda *et al.* using stable MDCK-II lines expressing either full-length or COOH terminally truncated chicken

occludin showed that the COOH-terminal cytoplasmic domain is not essential for trafficking of occludin to the tight junction. Both mutants did induce an increase in TEER, but overexpression of occludin also increased paracellular permeability (Balda et al., 1996). It was postulated that the interaction of occludin with ZO-1 is necessary for occludin to function with the junctional complex. With continued overexpression of occludin, saturation of the cellular pool of ZO-1 may of occurred, and the unbound occludin was able to form pores within the tight junction (McCarthy et al., 1996).

1.4.1.2 Regulation of occludin

A host of signal transduction pathways appear to be able to modulate occludin behavior and thus tight junction assembly. Phosphorylation seems to be the key mechanism, thus placing a great emphasis on the role of specific kinases and phosphatases regulating the functional activity of occludin. Work by Sakakibara and colleagues initially discovered that occludin was highly phosphorylated in MDCK cells exhibiting high levels of TEER, with phosphospecific sites identified to be predominantly on serine, and to a lesser extent threonine residues (Sakakibara et al., 1997). Moreover findings by Clarke *et al.* found an increase in permeability in LLC-PK_1 epithelial cells concomitant with a dephosphorylation of occludin threonine residues as a result of protein kinase C (PKC) activation (Clarke et al., 2000). PKC is a serine/threonine kinase, and the detection of dephosphorylated occludin at threonine residues would suggest PKC is not acting directly on occludin, but further upstream in a signalling cascade. The role of phosphorylation of tyrosine residues of occludin also appears crucial in regulating barrier function. Indeed published findings from our laboratory has shown the cyclic strain-induced tight junction organization of bovine aortic endothelial cells (BAEC's) involved a significant tyrosine dephosphorylation of occludin (Collins et al., 2006). Other investigations support this response, including work by Wachtel *et al.* who showed that inhibition of tyrosine phosphatases with phenylarsine oxide and pervanadate induced proteolysis of occludin in human umbilical vein endothelial cells (HUVEC's) (Wachtel et al., 1999). Furthermore oxidative stress-induced tyrosine phosphorylation of occludin disrupted the occludin-ZO-1 association at the tight junction complex (Rao et al., 2002). Consistent with this focal ischemia in cerebral

capillaries lead to an increase in occludin tyrosine phosphorylation levels via a Src dependent mechanism (Takenaga et al., 2009).

The coiled-coil domain is also believed to function as a target site that can interact with specific regulatory proteins, including c-Yes (non-receptor tyrosine kinase), the p85 regulatory subunit of PI3K, protein kinase C-ζ and the gap junction protein connexin 26 (Feldman et al., 2005). Some of the cell-signalling mediators identified in regulating occludin include members of the small GTPases, namely RhoA and Rac1,which through constitutively active mutants induced disorganization of occludin at the tight junction (Jou et al., 1998). The protease rMCP-II, which is a chymotrypsin like enzyme decreased immunostaining of occludin at the junction in MDCK monolayers (Scudamore et al., 1998). The cytokine hepatocyte growth factor (HGF), had been shown to decrease expressional levels of occludin in human vascular endothelial cells, concomitant with a decrease in TEER (Jiang et al., 1999). Low levels of the hemodynamic force, laminar shear stress was also shown to decrease both endothelial cell occludin mRNA and protein expression in porcine arterial endothelial cells (Conklin et al., 2002). Thus occludin can be regulated by a variety of extracellular and intracellular signalling mechanisms, and it appears that the downstream consequence of either serine/threonine phosphorylation and/or tyrosine dephosphorylation of occludin are critical to maintaining tight junction assembly. Moreover, it appears that various kinases and phosphatases work in a coordinate manner to regulate these post-translational changes.

1.4.1.3 Clinical implications

Disturbances in the physiological regulation of occludin, with respect to phosphorylation changes and altered distribution or expression patterns are often evident during early manifestations in human disease. Microvessels of human brain tumors are consistently known for their ability to down-regulate occludin levels, and the resulting tight junction ‘leakiness’ has been attributed to the formation of cerebral edema (Davies, 2002, Papadopoulos et al., 2001). Similarly, occludin localization patterns and expression are altered with increasing grades of prostate cancer, which was associated

with loss of cell polarity (Busch et al., 2002). With respect to diabetes, elevated levels of vascular endothelial growth factor (VEGF) in diabetic rats was believed to be the mechanism which significantly reduced occludin expression and altered the occludin phosphorylation state, a result which correlated with an increased permeability to macromolecules at the blood retinal barrier (Antonetti et al., 1998, Barber and Antonetti, 2003). Furthermore, alterations in the homeostatic occludin profile are observed in various disease conditions including inflammation (Burgel et al., 2002, Kucharzik et al., 2001), human immunodeficiency virus (HIV) encephalitis (Dallasta et al., 1999), MS (Minagar et al., 2003) and even aging (Mooradian et al., 2003). In summary occludin represents an excellent therapeutic strategy for controlling junctional barriers, but requires a more in-depth understanding about the specific cellular/molecular mechanisms regulating its role in disease/physiology.

1.4.2 Zonula Occludens

Tight junctions consist of several cytoplasmic accessory proteins, of which the zonula occludens 1 (ZO-1) protein has been the most extensively studied. ZO-1, with a molecular weight of 210-225 kDa was the first tight junction protein to be identified and was later found to co-precipitate with other polypeptides of this plaque, namely ZO-2 (160 kDa) and ZO-3 (130 kDa) (Stevenson et al., 1986, Jesaitis and Goodenough, 1994). ZO-1 is ubiquitously expressed at both the tight and adherens junctions of endothelial and epithelial cells, but can also be found in cells lacking tight junctions, such as fibroblasts and cardiac myocytes through its interactions with the cadherin superfamily (Itoh et al., 1993).

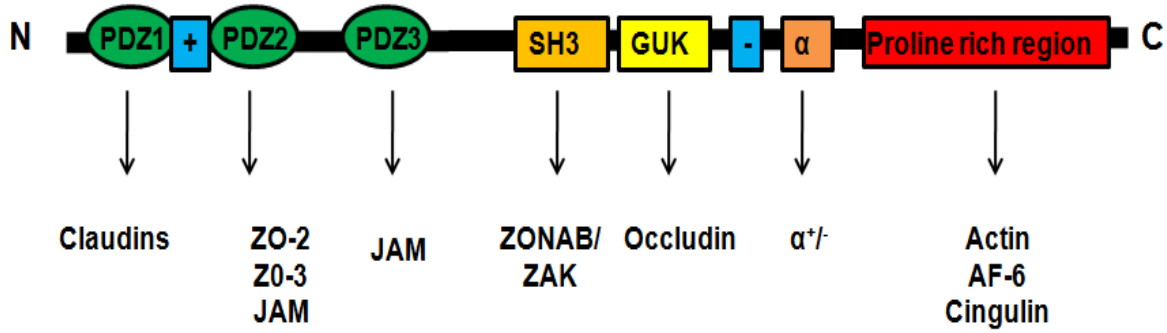

Fig. 1.10: Structure and binding partners of ZO-1. The N terminal portion of ZO-1 contains 3 PDZ domains, a basic domain (+), Src homology region 3(SH3), and a catalytically inactive guanylate kinase (GUK) homologue. The C-terminal half contains an acidic region (-), an alternatively spliced α motif and proline rich terminal domain (structure adapted from (Gonzalez-Mariscal et al., 2003).

When full length cDNA of ZO-1 was sequenced, the protein was identified as a member of the family of *membrane associated guanylate kinase* proteins, termed MAGUK, that shared sequence homology to the tumor suppressor protein disc large (Dlg) of septate junctions in Drosophila and the postsynaptic density protein PSD95/SAP-90 of synaptic densities in neurons (Willott et al., 1993). Proteins in this family are recognized by having structurally conserved PDZ, SH3 and GUK domains (see figure 1.10 above). ZO-1 contains 3 PDZ domains, which enable protein-protein interactions. These modules are approximately 80-90 amino acids long, enable protein-protein interactions via recognition of a short peptide motif in the target protein and play a crucial role in the spatial clustering and anchoring of transmembrane proteins within specific subcellular domains (Gonzalez-Mariscal et al., 2000). With ZO-1, PDZ1 at the COOH terminal binds with the transmembrane protein claudin, PDZ2 associates with ZO-2 and -3 through dimerization of their respective PDZ domains, while PDZ2 and 3 interacts with JAM (Gonzalez-Mariscal et al., 2003). The SH3 domain mediates interactions with cytoskeletal elements and signalling proteins such as the ZO-1 associated kinase (ZAK), which is a serine/threonine kinase that phosphorylates residues between the SH3 and GUK domain. Occludin lacks a PDZ binding consensus on its C-terminus and binds to ZO-1 via a portion of the GUK and acidic domain (Furuse et al., 1994, Fanning et al., 1998), a domain on occludin that has also has been implicated in its

trafficking to the tight junction. ZO-1 has a proline rich C-terminus which favors associations to actin binding proteins or the actin cytoskeleton. The C-terminus also contains a variably expressed α motif arising from post-transcriptional modifications due to alternative RNA splicing. This α^+ isoform (80 amino acid sequence) is predominantly expressed in epithelial cells, while the α^- isoform is more specific to endothelial cells (Willott et al., 1992).

1.4.2.1 ZO-1 function

Besides it role as a hub facilitating protein-protein interactions, ZO-1 is also crucial in the assembly of tight junction complexes via the trafficking of tight junction proteins to the apical sub-membrane domain and bridging their connection to the cortical based actin cytoskeleton (Fanning and Anderson, 2009). ZO-1 has also been implicated in the assembly of the adherens junction complex, a process mediating cell-cell adhesion, which occurs prior to the establishment of the tight junction complex. Studies have shown that ZO-1 co-localized with adherens junction proteins such as α-catenin, AVCRF (armadillo repeat member of the catenin family) and afadin before associating with the tight junction complex. (Kausalya et al., 2004, Yamamoto et al., 1997). The notion of ZO-1-mediated cell-cell adhesion also holds true for non endothelial/epithelial cells such as fibroblasts where ZO proteins are active components in adherens junction formation. Thus the accepted hypothesis is that ZO proteins use the direct interaction with adherens junction proteins as a positional signal during initial cell-cell adhesion and thus recruit tight junction proteins into an apical complex that becomes separated from the adherens junction (Fanning and Anderson, 2009).

With respect to functional consequences of ZO-1 exhaustion, work by Umeda and colleagues showed that depletion of ZO-1 and ZO-2 in a mammary epithelial cell line completely abrogated tight junction assembly and more recently work by Fanning *et al.* have revealed a novel role for the acidic/U6 motif in the correct cellular localization of tight junction proteins, as a mutant of ZO-1 (lacking the U6 motif) induced ectopic displacement of tight junctional proteins, ZO-1, occludin and claudin on the lateral cell membrane (Umeda et al., 2006, Fanning et al., 2007). Moreover, targeted disruption of

ZO-1 in mice results in embryonic lethality that is correlated with the disruption of the paracellular barrier and the structure of cell junctions (Katsuno et al., 2008). Besides junctional regulation, a role for ZO-1 in the regulation of cell-cell cycle has also been well documented (Gottardi et al., 1996, Balda and Matter, 2000). In sub-confluent epithelial cells, ZO-1 localizes in the nucleus, as compared to the edge of cells in wounded monolayers indicating its nuclear localization in relation to the immaturity of the cell contact. A Y-box transcription factor ZONAB binds with the SH3 domain of ZO-1, and co-localizes with it at the tight junction and the nucleus suggesting a role for ZO-1 in regulating gene expression. Thus, it is apparent that ZO-1 is a multifunctional protein involved in establishing and recruiting junctional components, but is also implicated in cell cycle progression.

1.4.2.2 ZO-1 regulation

Like occludin, ZO-1 is a phosphoprotein that can be subjected to post-translational modifications regulating its biological function. The effect of specific phosphorylation changes of ZO-1 on physiology of the tight junction remains somewhat controversial. For the main part, tyrosine phosphorylation of ZO-1 seems to be associated with a weakening of the junctional barrier, as treatment with the non-receptor tyrosine kinase Src (Takeda and Tsukita, 1995), vascular endothelial growth factor (VEGF) (Antonetti et al., 1999), and tyrosine phosphatase inhibitors (Staddon et al., 1995) significantly increased paracellular permeability. Interestingly though, during tight junction reassembly following ATP repletion, ZO-1, -2 and -3 become tyrosine phosphorylated, however only in the latter two were significant changes detected (Tsukamoto and Nigam, 1999). Inconsistencies in studies that assessed serine/threonine phosphorylation of ZO-1 in parallel with assays of permeability are also prevalent. Reports have shown that inhibition of serine/threonine phosphatases with okadaic acid reduced levels of TEER and immunostaining of ZO-1 at cell borders in mammary epithelial cells, which was consistent with the finding of Ward and colleagues using MDCK cells in response to epidermal growth factor treatment (Ward et al., 2002, Singer et al., 1994). Conversely, the activation of PKC (serine/threonine kinase) through the activator 1,2-dioctanoylglycerol induced the junctional localization of ZO-1 and development of

TEER, which were consistent with published findings from our laboratory by Collins *et al.* showing that cyclic strain-induced regulation of tight junction assembly and barrier function involves phosphorylation of ZO-1 on serine and threonine residues (Balda et al., 1993, Collins et al., 2006). Collectively, these results reveal that ZO phosphorylation plays a vital role in junctional remodeling and permeability regulation and differences in responses may be reflected due to variation in applied stimulants and differences in cell lines used.

1.4.2.3 ZO-1 clinical implications

Studies have shown that under inflammatory conditions such as those accompanied with MS, increases in the infiltration of leukocytes lead to the breakdown of ZO-1 and occludin, which is accompanied by re-organization of the actin cytoskeleton. The inflammatory cytokines TNF-α and IL-1 have been described as key inflammatory mediators of the alterations of BBB permeability in animal models of MS (Minagar and Alexander, 2003, Forster et al., 2007). Also, the pro-inflammatory transcription factor, nuclear factor-kappa B (NF-κB) has been shown to specifically down regulate ZO-1 gene expression and re-distribution of the protein away from the intercellular junctions, concomitant with an increase in Caco-2 tight junction permeability (Ma et al., 2004). Heightened levels of VEGF, as observed in diabetic retinopathy have been shown to regulate post-translational modifications of ZO-1 (and occludin), which as described in section (1.4.1.3) are capable of modulating paracellular permeability (Harhaj et al., 2006). The expression profile of ZO-1 also appears to be down-regulated/abnormal in liver metastases (Erin et al., 2009) and gastric carcinoma (Ohtani et al., 2009). Based on the information above, strategies targeting ZO-1 could potentially enhance tight junction assembly in disease states, possibly via restoration of its expression profile or re-localization to the junctional membrane but a greater understanding of the multitude of factors regulating ZO-1 is still required.

1.4.3 Claudin

Claudin is derived from the Latin *claudere,* meaning to close, thus alluding to a potential function for this pivotal tight junction protein. In 1998, work by Furuse and co-workers purified two peptides and sequenced full-length cDNAs from chick liver, revealing related proteins of 211 and 230 residues which were named claudin-1 and -2 (Furuse et al., 1998a). Currently 24 different isoforms of claudin have been identified in humans but they lack sequence homology to occludin (Krause et al., 2008). Like occludin, claudin possesses a tetraspan membrane topology, with two extracellular loops and a cytoplasmic C- and N- terminus (See figure 1.11 below).

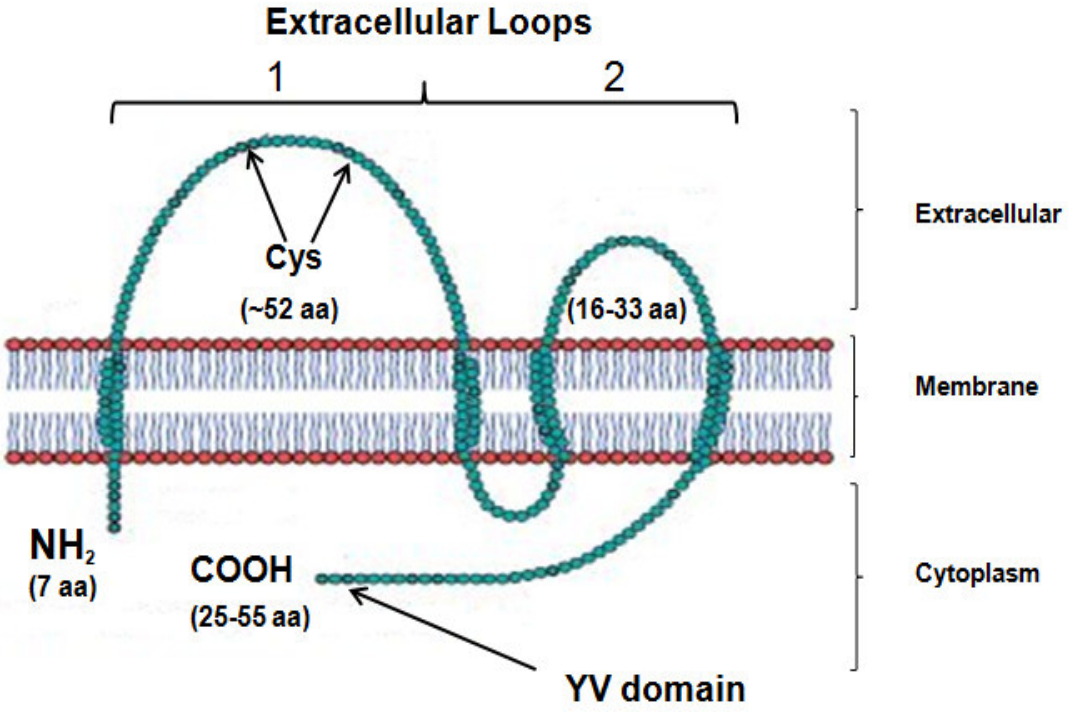

Fig. 1.11: Schematic depiction of claudin structure. The N-terminus and first EC loop are well conserved among claudins. The second EC loop is much shorter and less characterized while the C-terminus contains variable sequences amongst isoforms with the exception of the YV motif which is highly conserved. (structure adapted from (Turksen and Troy, 2004).

1.4.3.1 Claudin function

Interest in identifying other markers regulating paracellular barrier tightness stemmed from findings whereby tight junctions still formed in occludin knockout mice, although these mice did develop a variety of abnormalities in tissues requiring tight junctions

(Saitou et al., 1998). Experiments by Furuse and co-workers first established a functional role for claudins in tight junction formation. Transfection of claudins1-3 into mouse L fibroblasts (which don't express tight junctions) induced the establishment of intra-membranous strands as observed in freeze fracture replica's, findings which were similar to work by Morita and colleagues with claudin-5 performed shortly after (Furuse et al., 1998b, Morita et al., 1999). Not only are claudins pivotal to the formation of tight junctions, they also play an important role in maintaining the barrier properties of the cell-cell contact, thus sealing the intercellular cleft for solute flux. Work by Inai *et al*. showed that overexpression of claudin-1 in MDCK cells increased TEER values four fold, concomitant with a reduced flux of fluorescently labelled dextran versus control cells (Inai et al., 1999)

Claudin expression profile varies substantially within different tissues, thus highlighting potential divergence in the contribution of claudin isoforms to barrier properties. For example claudins-2, -7, -10, -15 and -16 have been described as 'pore' forming claudins regulating paracellular cation permeability whereas claudins -4, -5, -8, -11, -14 and -19 selectively inhibit cation flux through the tight junction (Krause et al., 2008). The first extracellular loop (ECL1) of claudin appears pivotal in determining the sealing and pore forming potential of the claudin strand, which is dependent on the specific charge present on amino acids residues. For example replacement of basic by acidic residues in claudin-4 ECL1 increases cation permeability (Hou et al., 2005). Less is known about the ECL2 but it is believed to be essential for claudin-claudin interactions between adjacent cells (Piontek et al., 2008). Moreover, Furuse *et al*. demonstrated that the introduction of claudin-2 into MDCK I cells (normally expressing claudin-1 and -4), decreased TEER values 20 fold to levels characteristic of those observed in MDCK II cells (normally expressing claudin-2), whereas introduction of claudin-3 into MCDK I cells showed no shift in TEER values (Furuse et al., 2001). This suggests that the co-existence of various isoforms in certain tissues determine the degree of barrier tightness within the tight junction. The cysteine residues contained within a signature motif in ECL1 are thought to form an intramolecular disulfide bond, thus stabilizing the conformation of the loop (Findley and Koval, 2009). The C-terminus contains a YV

motif which enable interactions with the PDZ1 domain of ZO-1, -2 and -3. Claudins can still however be targeted to the tight junction in the absence of this ZO binding motif, but it formed aberrant tight junction strands suggesting that the localization or retention of claudin at the apical tight junction requires interactions with ZO-1 (Kobayashi et al., 2002). To date, claudins-1, -3, -5 and -12 have been shown to be expressed in capillary EC's of the BBB, of which none are described as pore forming claudins, thus contributing to the stringent control over paracellular flux within the CNS.

1.4.3.2 Claudin regulation

Phosphorylation changes in claudin drastically regulate the barrier properties at the tight junction complex. A host of multiple kinases and phosphatases have been shown to regulate claudin. The serine/threonine phosphatase PP2A was shown to decrease claudin-1 phosphorylation in MDCK cells, an event which correlated with an increase in paracellular permeability (Nunbhakdi-Craig et al., 2002). Protein kinase A (PKA)-mediated threonine phosphorylation of claudin-3 in ovarian cancer cells was shown to induce its cytoplasmic localization and barrier dysfunction (D'Souza et al., 2005), whilst PKA was shown to be necessary for claudin-16 assembly and function in MDCK cells via serine phosphorylation. Palmitoylation on cysteine residues is another type of post-translational modification that increases the hydophobicity of claudin, and thus it's integration into the tight junction complex (Van Itallie et al., 2005). Specific to signalling at the BBB, the secondary messenger cAMP was shown to not only enhance claudin-5 expression, but also phosphorylate (via PKA) claudin-5 and enhance its immunoreactivity along cell borders, suggesting a promotional role in tight junction assembly (Ishizaki et al., 2003). Interestingly though, other PKC isoforms (PKC-α and ζ) have been shown to phosphorylate claudin-5 under inflammatory conditions, leading to the disappearance of claudin-5 from the cell membrane. PKC-α also induced an increase in paracellular permeability, a mechanism which was found to be dependent of RhoA (see section 1.6.2.1), a RhoGTPase known to drive actin based cell contractility (Stamatovic et al., 2006). For the most part, post-translational modifications at the cytoplasmic C-terminus of claudin are the dominant target sites for kinases/phosphatases, with the resulting effect on barrier function highly dependent on

the specific upstream signalling mediators and the specific residues phosphorylated (Fujibe et al., 2004, Yamauchi et al., 2004, Tanaka et al., 2005).

1.4.3.3 Claudin clinical implications

Several pathological conditions are capable of modulating tight junction assembly via alterations in claudin physiology. Bacterial toxins such as cytotoxic necrotizing factor-1, and the gram negative bacterium *Helicobacter pylori*, have both been shown to cause claudin internalization, with a resulting increase in epithelial permeability (Fedwick et al., 2005, Hopkins et al., 2003). *Clostridium perfringens* enterotoxin exposure was also shown to specifically interact with ECL2 of claudin-3 and -4, thus blocking tight junction reformation, in addition to its endocytotic capabilities (Fujita et al., 2000). Prasad and colleagues showed that the inflammatory cytokine TNF-α can downregulate claudin-2 and-3 expression in crypt epithelial cells with a resulting increase in paracellular permeability. Paradoxically in the same set of experiments, the cytokine interleukin (IL)-13 enhanced claudin-2 expression, but increased permeability suggesting a different mechanism of action to TNF-α (Prasad et al., 2005). Mutations in four claudin genes have also been reported, of which a mutation in the claudin-19 gene (highly expressed in the renal tubules and retina) has been linked to families affected by severe hypomagnesemia, renal failure and ocular abnormalities (Konrad et al., 2006). At the BBB, HIV infected cells are capable of modulating BBB structures via the release of the Tat protein, which has been shown to decrease expression of claudins-1 and -5, along with inducing the cellular redistribution of claudin-5 immunoreactivity (Andras et al., 2003). This mechanism could therefore facilitate HIV trafficking into the brain. Moreover, Wolburg and colleagues demonstrated that claudin-3 is a central component determining the integrity of the BBB in vivo, as its localization is selectively lost during pathological conditions such as tumors (glioblastoma multiforme) or during inflammation (autoimmune encephalomyelitis) (Wolburg et al., 2003). These findings make claudin an ideal target for therapy-based interventions, however a greater understanding of signalling mechanisms regulating claudin in physiology/pathophysiology need to be deciphered.

1.5 Adherens junctions

Adherens junctions are a dynamic complex present at cell-cell borders between adjacent endothelial and epithelial cells. In EC's they exist as intermingled complexes with tight junction proteins, compared to spatially distinctive complexes in epithelial monolayers. Unlike tight junction complexes, which are more renowned for their 'sealing properties', the associated proteins of the adherens junction have been implicated in a wide variety of cellular functions and changes in their composition or function can therefore have more complex effects on overall vascular homeostasis (Dejana et al., 2008). Adherens junction establishment has been shown to precede the development of tight junctions during initial cell-cell contact, which is followed by tight junction organization once the adherens junction has been stabilized (Dejana, 2004). Adherens junctions are formed by members of the cadherin superfamily of adhesion proteins, of which there are different subtypes. Most is known about the classic cadherins, of which epithelial (E) – cadherin (type I classical cadherin) is most commonly associated with epithelial cells whereas vascular endothelial (VE) – cadherin (type II classical cadherin) is a vascular specific cadherin. The cytoplasmic tail of VE-Cadherin (as with many other cadherins) interacts with other adherens junction proteins, namely the catenins, comprising p120-catenin, β-catenin, and α-catenin (see figure 1.12 below). Catenin is the Greek for 'link', and its members were named as such because of their roles in linking cadherins to the actin cytoskeleton (Gumbiner, 2005). Also important in adherens junction assembly is nectin, a cell-cell adhesion molecule of the IgG superfamily, which is recruited to the cell-cell complex through its interaction with the actin binding protein afadin, which has also been implicated in the organization of tight junctions through interactions with ZO-1 and JAM (Takahashi et al., 1999, Fukuhara et al., 2002).

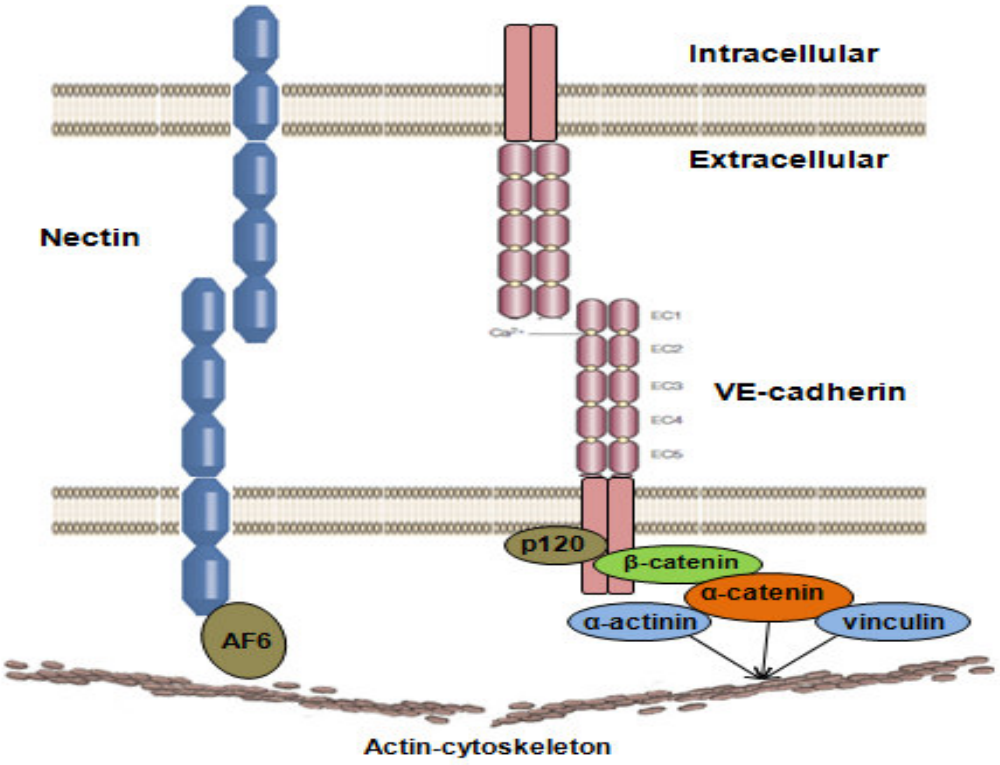

Fig. 1.12: Endothelial adherens junction. VE-Cadherin is presented as a cis homodimer exhibiting homophilic interaction with neighboring VE-Cadherin via extracellular (EC) domains. The core cadherin-catenin complex and its proposed mechanism of contact with the actin cytoskeleton are also presented. Nectin is linked to the actin cytoskeleton via afadin (AF6). Figure adapted from (Wallez and Huber, 2008, Gumbiner, 2005).

1.5.1 VE-Cadherin

In 1990 Heimark and colleagues produced a monoclonal antibody (mAb) (Ec6C10), which reacted with a specific cell surface antigen present in confluent monolayers of bovine aortic endothelial cells, and not MDCK monolayers. This molecule was found to mediate intercellular adhesion in a calcium-dependent manner, a feature which had already been shown to be a requirement of cadherin family cell adhesion molecules in certain epithelia (Heimark et al., 1990). The biological and biochemical characteristics of this novel endothelial-specific cadherin were further characterized in 1992 by Lampugnani and colleagues using the 7B4 mAb, who noted an exclusive staining pattern localized to cell borders of human endothelium in vitro and in situ, and found no cross reactivity with other cell types such as fibroblasts, SMC's or circulating blood

cells. The cDNA was sequenced and found to be identical to cadherin-5 (CD5), a recently characterized cadherin family member by Suzuki *et al.* CD5 displayed significant homology with previously described cadherin sequences including a highly conserved cytoplasmic tail (Suzuki et al., 1991, Lampugnani et al., 1992). It was subsequently renamed VE-Cadherin and may also be referred to as CDH5, CD144 or 7B4 (Breviario et al., 1995).

VE-Cadherin with a molecular weight of 140 kDa, is a single pass transmembrane protein exhibiting cis and trans homophilic interactions via five homologous extracellular domains (EC1-5) in a Ca^{2+}-dependent manner. Binding of Ca^{2+} is essential for the correct conformational organization of EC domains (Halbleib and Nelson, 2006). Dimerization/trimerization of VE-Cadherin in cis occurs through interactions of EC4, while VE-Cadherin dimers interact in trans through their EC1 domain (as shown in figure 1.12) (Hewat et al., 2007). Once homophilic engagement occurs, the EC domains develop additional forces, therefore tightening the adhesive contacts between adjacent cells. However this mechanism can also be dissociated in response to a shift in the cellular environment (Gavard, 2009). VE-Cadherin's cytoplasmic domains associate with the catenin family members of the adherens junction. Each catenin member has unique roles in stabilizing the association of VE-Cadherin between adjacent cells and with the actin cytoskeleton. The VE-Cadherin proximal cytoplasmic tail contains a binding site for p120 catenin, with a distal binding region for β-catenin towards the C-terminus. In contrast to this, α-catenin does not bind directly to VE-Cadherin, but binds to β-catenin and bridges the cadherin-catenin complex to the actin cytoskeleton either through direct binding to actin filaments or indirectly through actin binding proteins such as α-actinin or vinculin (Dejana et al., 2008, Vestweber, 2008). The exact molecular basis of this interaction is still a matter of debate as recent investigations showed that α-catenin cannot bind to both β-catenin and actin simultaneously with the binding preference appearing to be dependent on the oligomeric state of α-catenin as either a monomer or homodimer (Weis and Nelson, 2006). Furthermore, numerous protein kinases including Src, c-Src tyrosine kinase and proline rich tyrosine kinase 2, and phosphatases including vascular endothelial protein tyrosine phosphatase (VE-PTP),

protein tyrosine phosphatase receptor type M (PTPμ) and the density-enhanced phosphatase-1 (DEP1) may directly/indirectly associate with the adherens junction complex in response to various conditions suggesting their active participation in VE-Cadherin/catenin function and regulation.

1.5.2 VE-Cadherin-catenin function

The adherens junction complex performs multiple functions in endothelial biology. Based on its distinctive junctional localization within confluent endothelial monolayers it would be prudent to implicate its involvement in some aspect of barrier function. Indeed the first evidence for the role of VE-Cadherin *in-vivo* demonstrated its functional participation in the regulation of vascular permeability and leukocyte transmigration. Blocking antibodies targeting specific EC domains of VE-Cadherin were able to affect adhesion and clustering of the protein, inducing significant increases in vascular permeability (Gotsch et al., 1997). Mice deficient in VE-Cadherin die as a result of severe vascular defects, which are characterized by defective capacities in sprouting angiogenesis suggesting a putative role for VE-Cadherin in vascular morphogenesis (Gory-Faure et al., 1999). Carmeliet and colleagues further analyzed VE-Cadherin function using mice with partially truncated cytoplasmic VE-Cadherin at the β-catenin binding site. Interestingly, C-terminal truncation of VE-Cadherin reduced complex formation with the VEGFR-2, β-catenin and PI3K and abolished cell survival signals transmitted by VEGF-A to Akt (serine/threonine) kinase, thus unveiling VE-Cadherin as mediator of pro-survival signals (Carmeliet et al., 1999).

Moreover, VE-Cadherin has been determined to be an essential molecule in the contact inhibition of EC cell proliferation as a result of junctional stabilization (Caveda et al., 1996, Grazia Lampugnani et al., 2003). A number of possible mechanisms have been attributed to explain this phenomenon, with Pierce and colleagues suggesting that VE-Cadherin docking at the plasma membrane sequesters β-catenin at the cadherin-catenin complex, effectively blocking its capacity to translocate into the nucleus and regulate genes involved in cell proliferation via the Tcf/Lef transcription factor (Pierce et al.,

2003). Another explanation suggests that VE-Cadherin binding to VEFGR-2 provokes a dramatic tyrosine phosphorylation of VEGFR2, thereby attenuating mitogen-activated protein kinase (MAPK) activation and its subsequent role in cellular proliferation (Grazia Lampugnani et al., 2003). Furthermore, VE-Cadherin expression in VE-Cadherin null (-/-) EC's was found to augment the activation of Rac1, a small RhoGTPase family member, which had functional consequences for the organization of the actin cytoskeleton (Lampugnani et al., 2002). Dynamic remodeling of the actin cytoskeleton occurs under conditions of blood flow-associated shear stress, which profoundly influences EC realignment and elongation in the direction of flow (Masuda and Fujiwara, 1993, Colgan et al., 2007, Hahn and Schwartz, 2009). This effect is abrogated under flow conditions in COS-7 cells (VE-Cadherin -/- cell line) but can be restored following transfection of a plasmid encoding VE-Cadherin. In view of this, VE-Cadherin has been shown to be a crucial receptor in the mechanosensing of blood flow-associated shear stress within the vasculature, where it acts as an adaptor molecule in a mechanosensory complex with PECAM-1 and the VEGFR-2, regulating various intracellular signalling cascades (as discussed in section 1.2.2.2) (Tzima et al., 2005).

Finally, a significant role for VE-Cadherin in regulating expression of claudin-5 was recently demonstrated by Taddei and colleagues. This suggests a mechanism of "cross-talk" between adherens and tight junctions through which VE-Cadherin acts as a hierarchy in organization of cell-cell junctions, and thus may also further explain why VE-Cadherin inhibition induces increases in permeability (Taddei et al., 2008). Thus VE-Cadherin exhibits several essential functions in vascular homeostasis through its ability to develop and organize cellular junctions, control signal transduction pathways with implications for proliferation, cell survival and gene transcription, and regulate vascular permeability.

1.5.3 VE-Cadherin-catenin regulation

As described above, VE-Cadherin can act as a receptor mediating 'outside-in' signalling, a function analogous to integrins expressed basolaterally, which can drive various cellular processes. Interestingly, VE-Cadherin engagement upon cell-cell

contact also initiates a complex intracellular 'inside-out' signalling cascade that acts as a cue for regulating VE-Cadherin assembly. Studies using fluorescence resonance energy transfer (FRET) probes revealed that cell-cell contact is a prerequisite for activation of Rap1, a small GTPase belonging to the Ras family of proteins. Docking of the adaptor molecule MAGUK inverted domain structure (MAGI-1) with β-catenin following homophilic engagement has been shown to activate Rap1, which enhances cortical actin cytoskeleton accumulation at the cell borders, thereby stabilizing the adherens junction and reducing cell permeability (Sakurai et al., 2006, Mochizuki et al., 2001). Furthermore, p120 catenin has been shown to be of vital significance for VE-Cadherin retention at the adherens junction. Binding of p120 catenin within a highly conserved juxtamembrane domain of VE-Cadherin not only stabilizes its membrane insertion, but also prevents the cadherin from been internalized, degraded and may even facilitate the recycling of internalized cadherin back to the membrane (Xiao et al., 2003, Xiao et al., 2005).

Similar to tight junctions, phosphorylation of the adherens junction complex drastically influences complex integrity. A wealth of knowledge exist about multiple intracellular and extracellular signalling mediators that are directly or indirectly associated with VE-Cadherin, with the capacity to affect endothelial permeability. For the most part, *in-vitro* experiments have suggested that tyrosine phosphorylation of VE-Cadherin or catenin family members have detrimental consequences for barrier function. Exposure of endothelial monolayers to some of the classical permeability inducing agents such as TNF-α (Angelini et al., 2006), histamine (Andriopoulou et al., 1999) and VEGF (Esser et al., 1998) induce the tyrosine phosphorylation of VE-Cadherin, β-catenin and p120 catenin, causing cadherin-catenin dissociation and possible internalization. Common intracellular signalling mediators of such effects include the family members of the RhoGTPases, Rho or Rac, which may act indirectly, while the tyrosine kinase Src has been shown to interact directly with the cytoplasmic domain of VE-Cadherin (Wallez et al., 2007). Moreover, tyrosine phosphorylation of residue Y731 was identified as specific mediator of ICAM-induced leukocyte diapedesis, as overexpression of a

tyrosine-phenylalanine point mutant blocked transendothelial migration (Allingham et al., 2007, Turowski et al., 2008).

Adherens junction phosphatases have been shown to enhance barrier characteristics and stabilize the junction complex. VE-PTP is an endothelial-specific phosphatase that associates directly with the EC domains of VE-Cadherin. Treatment with VE-PTP following VEGF stimulation dephosphorylated VE-Cadherin leading to an increase in barrier function (Wallez and Huber, 2008). Similarly, it has been shown that docking of neutrophils to the apical surface of EC's triggered the dissociation of VE-PTP from VE-Cadherin, thus implicating its involvement in neutrophil transmigration (Vestweber, 2008). Other phosphatases such as DEP-1 (Grazia Lampugnani et al., 2003), PTPμ (Sui et al., 2005) and SH2 - containing phosphotyrosine phosphatase (SHP2) (Ukropec et al., 2000) may interact with and dephosphorylate VE-Cadherin and thus enhance barrier properties.

Finally, VE-Cadherin itself is highly susceptible to enzymatic lysis, thus adding further explanation as to possible causes for heightened vascular permeability or leukocyte diapedesis. Exposure to various metalloproteases, elastase, cathepsin, or trypsin cleaves VE-Cadherin EC domains in cultured cells (Dejana et al., 2008).Thus both intracellular signalling processes and VE-Cadherin itself regulate the interaction/assembly of the cadherin-catenin junctional complex, uncovering a reciprocal signalling relationship. This has functional consequences for the membrane trafficking, internalization, degradation and post-translational modifications of VE-Cadherin with inevitable implications for barrier integrity. A more in-depth analysis, particularly from the in vivo situation will potentially shed more light on specific regulatory targets.

1.5.4 VE-Cadherin-catenin clinical implications

Due to the diverse range of endothelial functions regulated by the cadherin-catenin complex, it is not surprising that pathological conditioning of the endothelium with resulting increases in vascular permeability may precipitate via perturbations in the

homeostatic regulation of the adherens junction complex. Most severely, VE-Cadherin knockout mice are embryonic lethal, exhibiting a severely altered vascular phenotype compared to claudin-5 knockout mice which develop normally but die shortly after birth due to defective BBB functioning. With respect to specific diseases, alterations in the cell surface expression of VE-Cadherin is adversely regulated under conditions of inflammation (Alexander et al., 2000), diabetes (Navaratna et al., 2007) and viral infection (Dewi et al., 2008), with the latter two studies showing concomitant increases in vascular permeability. Anti-permeability factors which enhance VE-Cadherin membrane stabilization include angiopoietin-1, cAMP-elevating GPCR agonists, sphingosine 1 phosphate (S1P) and fibroblast growth factor, and therefore have direct implications as therapeutics targeting aberrant vascular leakiness (Gavard, 2009). Endothelial cell-cell adhesion is also compromised in tumor endothelium as large intercellular gaps are often present suggesting that VE-Cadherin function is altered, which is consistent with observations in epithelial-derived tumors (Hashizume et al., 2000, Berx and Van Roy, 2001). Interestingly and somewhat paradoxically though, VE-Cadherin was found to be expressed by highly aggressive melanoma tumor cells which were capable of inducing 'vasculogenic mimicry' (VM), i.e. the ability of tumor cells to form tubular-like structures (blood vessels) independent of angiogenesis (Hendrix et al., 2001). Based on its cell-cell adhesion functions, it is postulated that VE-Cadherin facilitates the connection of the VM channel to the host's blood vessel, thus acquiring essential growth factors for tumor survival, growth and metastasis. This phenotype has also been observed in several other malignant tumor types such as breast cancer, liver cancer, glioma and prostate cancer (Zhang et al., 2007). Therapeutic strategies targeting VE-Cadherin in this manner have been exploited through the use of antibodies against various epitopes of VE-Cadherin. Of particular significance was the mAb E4G10, which selectively blocked tumor growth in mice but did not affect normal blood vessels (Liao et al., 2002). Thus, exploiting knowledge on the functional regulation of VE-Cadherin and the catenin complex has real therapeutic value in a wide variety of clinical settings.

1.6 Intracellular signalling mechanisms

Amongst a plethora of intracellular mediators facilitating the transmission of circulatory conditions (both humoral and mechanical) with consequences for endothelial cell function is the Ras superfamily of small guanosine tripohosphatases (GTPases). The Ras superfamily comprises 5 family members, namely, the Ras, Rho, Ran, Rab and Arf GTPases, classified as such on the basis of structure and function. A total of 150 superfamily members have been identified in humans. They exist as monomeric G-proteins with molecular masses ranging between 20-30 kDa. The Ras sarcoma (Ras) genes were first identified as oncogenes of sarcoma viruses and are the earliest discovered members of the Ras family of GTPases, which control gene expression and regulate cell proliferation, differentiation and survival. The Ras like proteins in brain (Rab) family of GTPases and ADP-ribosylation factor (Arf) GTPases are involved in intracellular vesicular transport and trafficking of proteins between different organelles. The Ras like nuclear (Ran) protein is the most abundant GTPase in the cell which regulates nucleocytoplasmic transport of RNA and protein during cell cycle (G1-S-G2 phases) and microtubule organization during the metaphase (Matozaki et al., 2000, Wennerberg et al., 2005). The Ras like homologous (Rho) proteins are of particular interest to this thesis and are discussed in greater detail in section 1.6.1 below.

1.6.1 RhoGTPases

The RhoGTPases represents an intriguing family of signalling molecules, which are pivotal regulators of several signalling cascades activated by an array of receptor types, including mechanosensors (Tzima et al., 2001, Tzima et al., 2002). To date, 23 members of the Rho family of GTPases have been identified. They have being implicated in many signalling pathways in the vasculature regulating barrier function, inflammation, leukocyte extravasation and oxidative stress as well as smooth muscle cell contraction, migration, proliferation and differentiation. The relationship between RhoGTPases and endothelial function in physiology or pathology has been the subject of intensive investigation over the past decade and thus, their participation is discussed herein.

RhoGTPases, similar to other GTPase families function as molecular switches to initiate or terminate specific cell processes through their ability to bind to activate numerous downstream effectors leading to diverse signalling pathways. Each GTPase possesses a set of conserved G-box GTP/GDP binding motifs which exhibit a high binding affinity for GDP and GTP (see figure 1.13 below).

In response to upstream stimuli, the GTPase switches from an inactive (GDP-bound) to an active (GTP-bound) state, to induce conformational changes necessary to facilitate downstream effector binding within the core effector domain. Interestingly, the two nucleotide bound states have relatively similar conformations but contain pronounced differences at the switch I and II domains, allowing the effectors to 'sense' the nucleotide status of the small GTPase (Bishop and Hall, 2000). Another important structural feature of the majority of RhoGTPases is that they contain a C-terminal CAAX (Cysteine-Aliphatic-Aliphatic-X any amino acid) motif. This serves as a recognition sequence for farnesyltransferase and geranylgeranyltransferase I, which post-translationally modify the GTPase through the covalent attachment of an isoprenoid lipid, thus enhancing GTPase hydrophobicity and membrane insertion (Cox and Der, 2002). The principal regulatory processes that facilitate the switch between the active and inactive conformations are discussed in section 1.6.3.

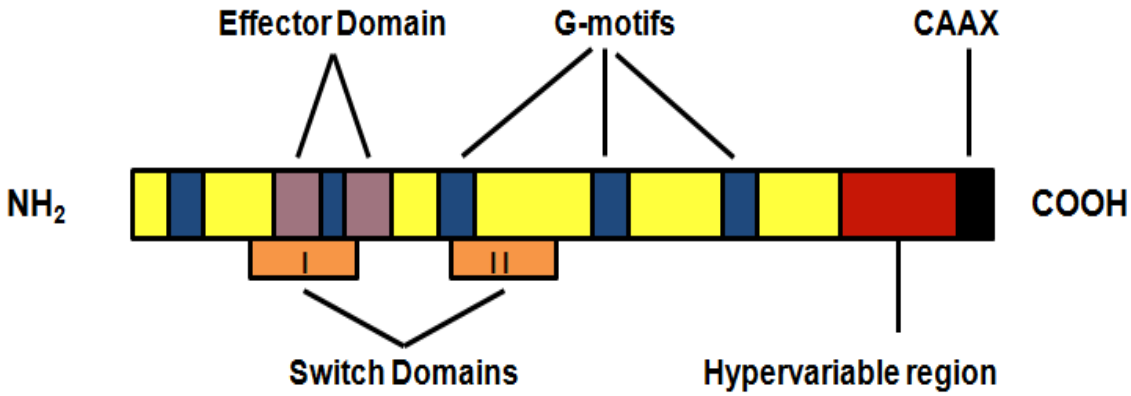

Fig. 1.13: Schematic of RhoGTPases. RhoGTPases contain a conserved structure and biochemistry with 5 G (GDP/GTP-binding) motifs, an effector domain for binding downstream targets controlled by conformational changes in switch domains (I and II). The hypervariable region differs between RhoGTPases and can contain a polybasic region and/or sites for palmitoylation. The CAAX box is important for membrane localization and is prenylated on the cysteine residue. Adapted from Ridley 2006.

1.6.2 RhoGTPase function

As mentioned earlier, RhoGTPases have been implicated in a range of endothelial functions. Of specific interest to this report however are their roles in regulating cell-cell adhesion and cytoskeletal dynamics. Detriments in adherens and tight junction assembly, and alterations in actin cytoskeleton-mediated associations with these intercellular junctions pose a genuine threat to physiology of the paracellular pathway. Moreover, there is ample evidence suggesting that the actin cytoskeleton is simply more than a structural component of junctional complexes, but dynamic changes in its expression and localization in response to spatially regulated cues are critically modulators of tight junction integrity and BBB permeability (Mark and Davis, 2002, Gloor et al., 2001, Vorbrodt and Dobrogowska, 2003). Unraveling the participation of RhoGTPases as regulators of endothelial barrier function will help clarify the cell and molecular processes behind BBB pathologies exhibiting leaky barriers.

From an endothelial perspective, RhoA, Rac1 and Cdc42 represent the three most extensively studied family members of RhoGTPases, and thus will be the subject of this discussion. Early work on the functions of these RhoGTPases in fibroblasts noted

dramatic capabilities of these signalling molecules to influence actin cytoskeletal dynamics; findings that were subsequently confirmed in EC's (Wojciak-Stothard et al., 1998). RhoA was first shown to promote the formation of stress fibers, contractile actomyosin bundles and focal adhesions, whereas Rac1 and Cdc42 were shown to induce the formation of lamellipodia and filopodia, respectively (Nobes and Hall, 1995). Lamellipodia are sheet-like protrusions of branching actin filaments commonly found at the leading edge of migrating cells while filopodia describe spike-like membrane protrusions containing parallel bundles of actin filaments.

1.6.2.1 RhoA

RhoA mediates its biological effects through a number of effector proteins including citron kinase, rhotekin, diaphanous related formins 1-2, and the more extensively studied Rho-associated kinase (ROCK). RhoA has been generally documented to promote barrier instability through its influence over actin cytoskeletal properties. In response to barrier destabilizing compounds such as thrombin, endothelin-1 and lipopolysaccharide (LPS), RhoA-GTP binds to ROCK to phosphorylate myosin light chain (MLC) via myosin light chain kinase (MCLK). ROCK can also enhance this process by inactivating myosin light chain phosphatase, an enzyme that dephosphorylates MLC. These changes in MLC enhance stress fiber formation and allow the myosin molecule to change conformation and interact with actin to induce actin-myosin contractility (Wojciak-Stothard and Ridley, 2002). This force generation is proposed to dissemble the intercellular junction complexes by physically 'tugging' trans-homophilic junctional proteins apart and enhance paracellular permeability (Sun et al., 2006, Birukova et al., 2004, Wojciak-Stothard et al., 2001a). Consistent with these findings is that inhibition of ROCK reduced baseline permeability of both post-capillary venules *in-vivo* and using microvascular EC's *in-vitro* (Adamson et al., 2002, Baumer et al., 2008).

RhoA activity has also been shown to be downregulated as endothelial monolayers reach confluence and the paracellular gap is sealed. Critical to this process is the binding of p120 catenin to the newly established adherens junction complex, which activates

p190RhoGAP (a regulator of RhoA activity) and inactivates RhoA (Wildenberg et al., 2006). More specific to the BBB, RhoA-mediated signalling has been associated with HIV infected monocyte infiltration across the BBB and in tight junction disassembly. Pretreatment with a ROCK inhibitor (Y-27632) was able to abrogate the monocyte induced post-translational modifications of tight junction proteins occludin and claudin-5, and the concomitant reduction in TEER (Persidsky et al., 2006a). Further experiments by Yamamoto and colleagues showed that ROCK could directly associate with both occludin and claudin-5 in brain microvascular EC's at phosphospecific residues, which paralleled with BBB dysfunction (Yamamoto et al., 2008). It is possible that the tight junction-associated RhoA activator GEF-H1/Lfc induced such profound responses. Although the majority of the literature points to the deleterious effects of RhoA on endothelial permeability, it has an important functional role in paracellular-mediated leukocyte extravasation to subendothelial sites of acute inflammation, however it would serve to the detriment of the tissue under a chronically inflamed state.

1.6.2.2 Rac1 and Cdc42

By contrast, Rac1 and Cdc42 are more renowned to antagonize the effects of RhoA and promote barrier-enhancing/stabilizing effects. Through the use of the pharmacological inhibitor NSC23766 and lethal toxin (LT) (block Rac1 and Cdc42 activity, respectively), microvascular endothelial barrier function was severely weakened, findings which were consistent with a report using dominant negative Rac1 mutants in macrovascular endothelium (Wojciak-Stothard et al., 2005, Baumer et al., 2009, Baumer et al., 2008). Both Rac1 and Cdc42 can target similar and/or diverse downstream effectors which regulate actin bundles and are thought to be associated with adherens and tight junctions. This includes the actin-binding protein cortactin, which has been heavily implicated in cortical actin assembly and reorganization and serves to strengthen endothelial barrier properties by stabilizing junctional proteins. (Dudek et al., 2004, Jacobson et al., 2006). Cortactin can bind directly to ZO-1 and may guide the spatial organization of actin within the tight junction. Another mechanism for stabilizing cortical actin fibers involves Rac1- and Cdc42-induced activation of LIM kinase via downstream effectors p21-activated kinase (PAK) 1-3, which directly phosphorylates

the actin-severing and depolymerizing protein cofilin, thereby inactivating it and stabilizing the actin filament arrays at the cell peripheries. Rac1 and Cdc42 can also stimulate actin polymerization via the actin-binding Arp (actin-related protein) 2/3 complex, albeit through diverse pathways. Cdc42 binds directly to the Wiskott-Aldrich syndrome protein (WASP) target, which directly binds to and activates Arp2/3, whereas Rac1 indirectly binds to the multi protein WASP Verpolin homologous (WAVE) complex via its targets Sra1 or IRSp53 to induce Arp2/3-associated actin nucleation (Ridley, 2006). Interestingly WASP-mediated stimulation of actin polymerization has been shown to be regulated by protein-protein interactions via the SH3 domain of cortactin, thus offering another mechanism for the accumulation of cortical actin.

Besides cytoskeletal dynamics, both Rac1 and Cdc42 are activated where junctional complexes are formed. A possible explanation for the relevance of this suggests; following VE-cadherin engagement, p120 catenin binding activates Rac1 and Cdc42, which bind to IQGAP (IQ motif containing GTPase-activating protein 1), thus retaining the GTPases in their active state. This facilitates the release of β-catenin from IQGAP to associate with α-catenin, which cross links with the cortical actin cytoskeleton and stabilizes the adherens junction (Beckers et al., 2010). At the tight junction, levels of ZO-1 were reduced following overexpression of a dominant negative Rac1 mutant as the localization pattern to cell borders was more fragmented (Wojciak-Stothard et al., 2001b). Moreover, a recent report by Schlegel *et al.* showed that claudin-5 staining at cell borders was reduced by LPS exposure (*in-vivo* and *in-vitro)* and this effect was dependent on the inactivation of Rac1 as opposed to activation of RhoA (Schlegel et al., 2009). The precise mechanism(s) of how Rac1/Cdc42 exerts its barrier-stabilizing effects on the tight junction remain elusive. The more obvious route would suggest direct modulation of cortical actin dynamics. However it is tempting to speculate the presence of upstream regulators (similar to GEF-H1/Lfc for RhoA) and/or downstream effectors embedded within the core plaque of proteins at the tight junction. Data is currently lacking in EC's but one such mechanism has been proposed in tight junctions of epithelial cells, where the scaffold protein angiomotin binds RICH1 (a regulator of Cdc42) suppressing its GTPase activity, thus allowing Cdc42-mediated barrier protection (Wells et al., 2006).

The information presented above depicts the generally well-accepted viewpoint that Rac1/Cdc42 serves to strengthen the intercellular junction whereas RhoA opposes these activities and is detrimental to endothelial permeability (see figure 1.14 below) however some controversy remains as to the precise roles of RhoGTPases in endothelial permeability regulation. A recent report by Amerongen *et al.* demonstrated that basal activity of Rho kinase was required for barrier maintenance and was required to sustain a basal tension necessary to enhance the affinity between the intercellular junctions and the cortical actin cytoskeleton (van Nieuw Amerongen et al., 2007). Furthermore, overexpression of a constitutively active Rac1 enhances breakdown of intercellular junctions consistent with reports which demonstrated that Rac1 activation mediated VEGF-induced tyrosine phosphorylation of occludin and VE-Cadherin causing hyperpermeability (Peng et al., 2009, Monaghan-Benson and Burridge, 2009). Thus, a subtle context-dependent balance in the regulation and relative ratios of the RhoGTPases appears essential for junctional integrity as excessively high GTP levels of one RhoGTPase can affect the activity of the other, thus altering their relative ratios affecting cellular physiology and endothelial permeability. Moreover, the specificity of the upstream stimulus acting on a particular RhoGTPase appears crucial in determining the specificity of the downstream effector(s) and cellular response.

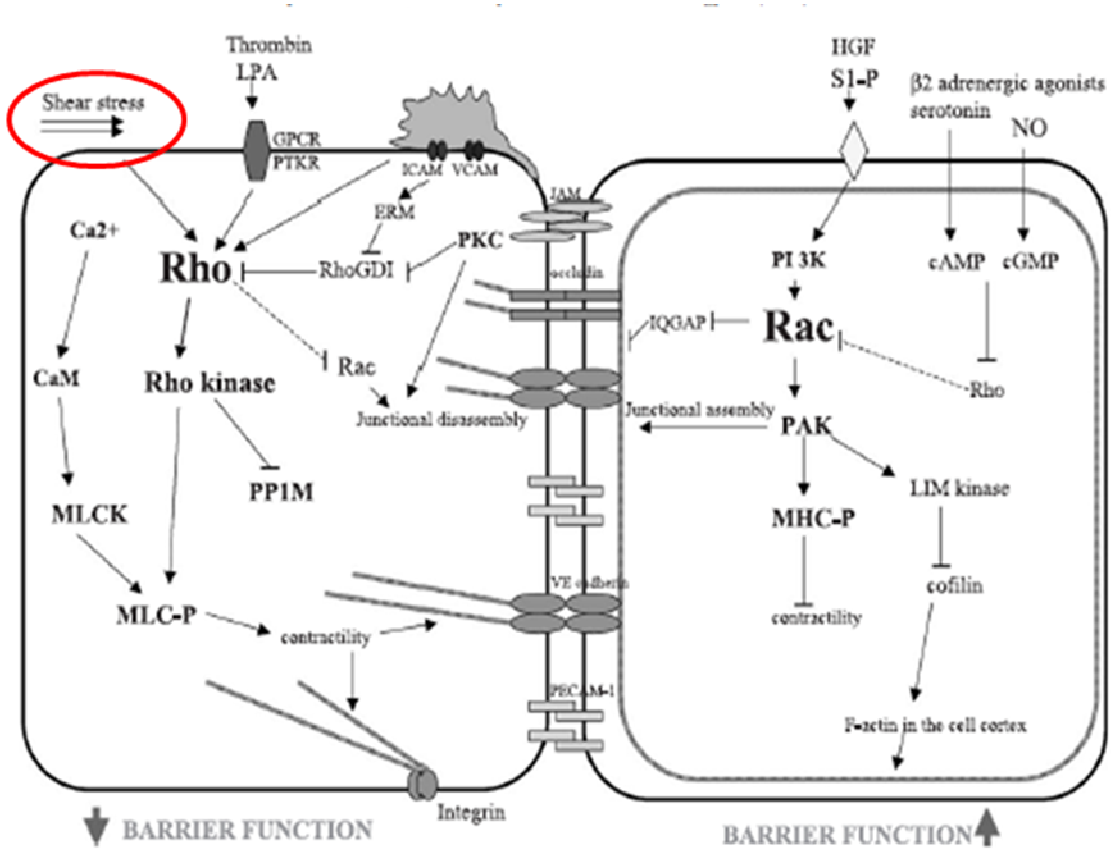

Fig. 1.14: Regulation of barrier function by Rho and Rac. This figure presents mechanisms of RhoGTPase (Rho/Rac) activation and alludes to the generally well accepted view that Rho activity is detrimental to barrier function and Rac enhances barrier integrity via alterations in intercellular junctions (Wojciak-Stothard and Ridley, 2002).

1.6.3 RhoGTPase regulation

To appreciate the role of the RhoGTPases in health and disease it will be essential to understand how they are regulated. The cycling of RhoGTPases between their active and inactive forms is finely tuned by three primary regulators, which are discussed below. It is however, important to note that a functional cross-talk between RhoGTPases exists, i.e. activation of one GTPase can have consequences for another, thus adding further complexity to RhoGTPase regulation. A hierarchical activation linking RhoA, Rac1 and Cdc42 was first demonstrated in Swiss 3T3 fibroblasts following agonist treatment, which activated Cdc42 inducing a rapid activation of Rac1 leading to RhoA

activation and subsequent actin stress fiber assembly (Kjoller and Hall, 1999). From an endothelial perspective, intensive effort has focused on the RhoA-Rac1 relationship where studies have shown that HGF-induced activation of Rac1 blocked the thrombin-induced activation of RhoA by interfering with p115RhoGEF (an activator of RhoA), while similarly cAMP-associated Rac1 activation also blocked thrombin-mediated RhoA activity (Birukova et al., 2007, Baumer et al., 2009). In view of this, EC's exposed to hypoxic conditions were shown to inactivate Rac1, which was followed by activation of RhoA; however the mechanism(s) underlying this sequential response needs to be clarified (Wojciak-Stothard et al., 2005). Furthermore, other small GTPases of different family members have been shown to influence the activity of RhoA, Rac1 and Cdc42, convoluting the regulation process even further (Matozaki et al., 2000). Understanding the coordinated regulation of these signalling molecules will constitute the next frontier in the study of RhoGTPases.

1.6.3.1 Rho guanine nucleotide exchange factors (RhoGEF's)

RhoGEF's are essential components driving RhoGTPase-mediated cellular behaviours in response to upstream stimuli. They catalyze the exchange of GDP for GTP in the switch region of the GTPase, which propagates specific downstream effector activation. RhoGEF's are generally large proteins (> 1000 amino acids) with multiple domains that facilitate protein-protein and protein-lipid interactions. This includes a Dbl homology (DH), SH2, SH3 and pleckstrin homology (PH) domains (Cerione and Zheng, 1996). The DH domain confers GEF specificity towards their GTPase substrate and catalyses the GDP-GTP exchange reaction. The PH domain interacts with phospholipids, facilitating RhoGEF interaction upon membrane association and subsequent GTPase activation to the membrane. Indeed, activation of Rac1 was induced by membrane localization of the cytosolic RhoGEF Tiam1 (Michiels et al., 1997). This particular interaction is of specific interest to this thesis and is depicted in figure 1.15 below. Certain RhoGEF's (p115RhoGEF, PDZ-RhoGEF) also contain a regulator of G-protein signalling (RGS) domain, which forms a molecular complex with the $G\alpha_{12/13}$ subunit of GPCR's enhancing the activation of RhoA (Hart et al., 1998, Siderovski and Willard, 2005). Furthermore, RhoGEF's can be regulated by phosphorylation via PKC isoforms

(Mehta and Malik, 2006), FAK (Chikumi et al., 2002) and RTK's via Src (Schiller, 2006). To date, 83 GEF's have been identified in the human genome, some of which are RhoGTPase specific while others activate multiple RhoGTPases. Given the fact that there are over 50 known effector targets for Rho, Rac and Cdc42 (Hall, 2005), the specificity of the upstream stimulus (i.e. RhoGEF) is essential for determining the specificity of the downstream effector target of the RhoGTPase.

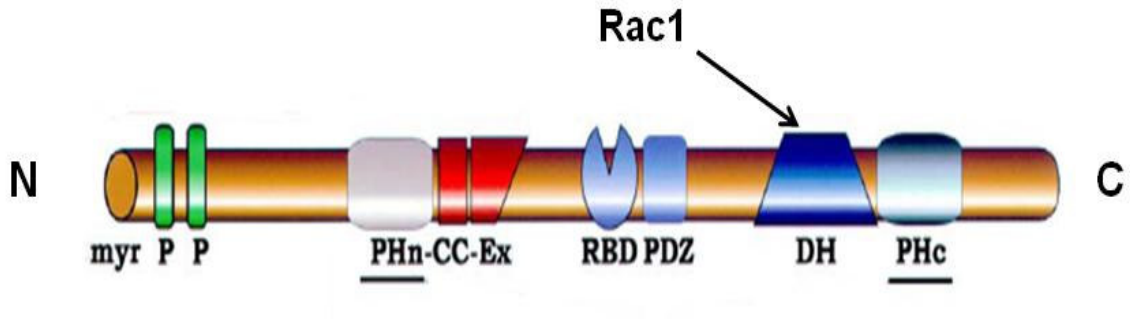

Fig. 1.15: Schematic structure of Tiam1. The specific domains indicated herein are from the N-terminus onwards: myr: myristoylation site; P: PEST sequence; PHn: N-terminal PH (pleckstrin homology) domain; CC: coiled coil region; Ex: extended structure; RBD: Ras binding domain; PDZ: PSD-95/DlgA/ZO-1 domain; DH: Dbl homology domain and PHc;C-terminal PH domain. Rac1 interacts with the DH domain of Tiam1 (Mertens et al., 2003).

1.6.3.2 RhoGTPase activating proteins (RhoGAP's)

Contrary to what their name implies, RhoGTPases have a relatively low intrinsic GTPase activity. RhoGAP's represent a family (70 known members in mammals) of regulatory proteins that bind to active GTPases and enhance the GTP hydrolysis, thereby inactivating the protein and terminating the signalling event. The expression of most RhoGAP's is ubiquitous; however one of them, p73RhoGAP has a preferential vascular expression which was crucial to angiogenesis (Hori et al., 2004). Similar to RhoGEF's, RhoGAP's can act on a single RhoGTPase, while others have preferential activity towards multiple proteins, thus explaining why RhoGTPase activities may simultaneously augment or diminish. Independent of their GAP activity, RhoGAP's molecular structure presents multiple functional domains to act as scaffold molecules mediating cross-talk between other GTPases and integrate signals from different pathways thereby specifying downstream signalling (Tcherkezian and Lamarche-Vane,

2007). RhoGAP activities appear to be regulated by different mechanisms including phosphorylation (Roof et al., 1998) and proteolytic degradation (Jenna et al., 2002).

1.6.3.3 Rho guanine dissociation inhibitors (RhoGDI's)

In a resting cell, the majority of RhoGTPases are cytosolic and complexed in their GDP-bound conformation despite the fact the GTP is more abundant in the cell. Sequestering of RhoGTPases in this conformation is finely regulated by RhoGDI's which have two structurally distinct regions. Their N-terminal flexible domain specifically interacts with the switch domains of the RhoGTPase to lock it in their inactive conformation while the C-terminal accommodates the isoprenyl moiety of the GTPase into its hydrophobic pocket, regulating cytosol/membrane partitioning (Dovas and Couchman, 2005). There are currently three RhoGDI's known; RhoGDI-1(α) which is ubiquitously expressed, RhoGDI-2(β) is expressed in hematopoietic cells and RhoGDI-3(γ) is preferentially expressed in organs (Beckers et al., 2010). *In-vivo* and *in-vitro* findings have shown that RhoGDI-1 binds to RhoA, Rac1 and Cdc42, although the mechanisms regulating the formation of stable, cytosolic RhoGDI complexes remain largely unknown. The dissociation of RhoGTPases from RhoGDI's however appears to be regulated by an array of factors including phosphorylation by PKCα (Mehta et al., 2001), PAK (DerMardirossian et al., 2004) and via protein-protein interaction with the ERM (Ezrin/Radixin/Moesin) family of proteins (Takahashi et al., 1997). Figure 1.16 below summarizes the mechanism of RhoGTPase regulation.

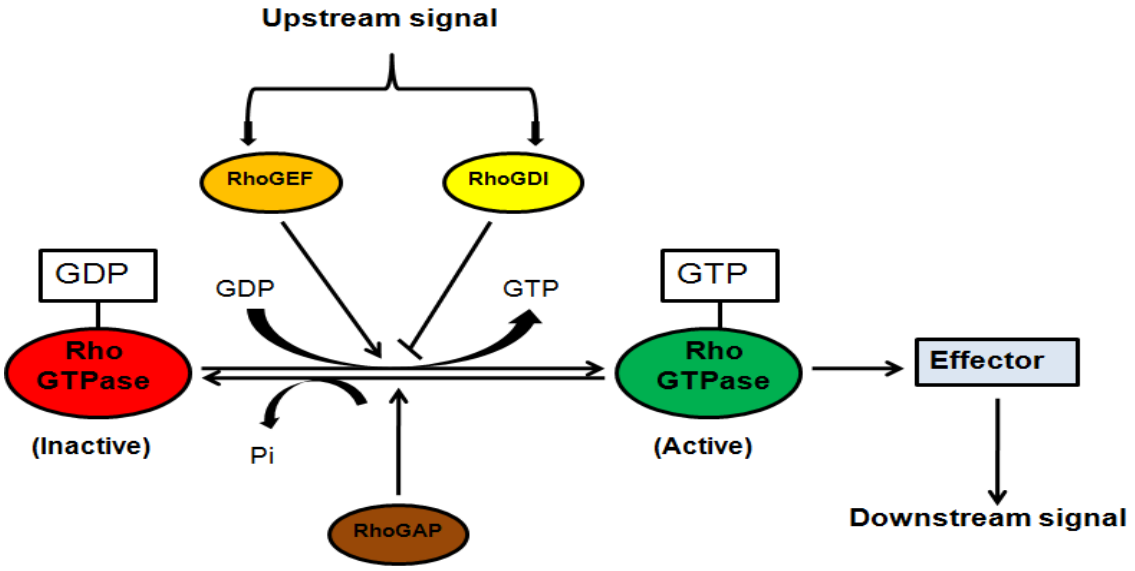

Fig. 1.16: RhoGTPase regulation by RhoGEF's, RhoGDI's and RhoGAP's. RhoGTPases are retained in their inactive GDP form by RhoGDI's. RhoGEF's facilitate the exchange of GDP for GTP following activation by upstream agonists, leading to downstream effector signalling. RhoGAP's accelerate the hydrolysis of GTP and accumulation of the inactive GDP-bound form.

1.6.3.4 Mechanoregulation of RhoGTPases

EC's exposed to laminar shear stress and cyclic stretch exhibit distinct patterns of cytoskeletal remodeling and changes in morphology. Amongst an array of possible intracellular signalling mechanisms mediating such effects, the RhoGTPases represent likely candidates based on their undoubted ability to influence cytoskeletal dynamics. Indeed, studies have shown that following flow onset, RhoA and Rac1 are both transiently activated in a sequential manner that appears to control the functional response, i.e. cellular/cytoskeletal realignment. RhoA is initially activated (peaks within 5 mins) leading to stress fiber formation and cell contraction. This facilitates cell depolarization allowing EC's to elongate more efficiently in the direction of the shear stress. The elongation process requires activation of Rac (within 15 mins) at the leading edge of the EC and subsequent deactivation of RhoA to allow optimal extension of membrane protrusions (Wojciak-Stothard and Ridley, 2003). Cdc42 is also activated in similar time pattern to Rac1 but there are conflicting reports as to whether or not its activation is essential to shear induced alignment (Li et al., 1999, Tzima, 2006).

Interestingly the expression of constitutively active (and dominant negative) mutants of Rho and Rac abolished the cytoskeletal reorientation of EC's in response to sustained shear stress. In the case of EC's expressing V12Rac1 (constitutively active Rac1), high levels of Rac1 activity were detected but lacked the spatial polarization towards the downstream edge of the cell following flow onset. Thus, although RhoA and Rac1 activation is a prerequisite for shear-induced morphological realignment, a precise temporal fine tuning of their relative GTP ratios and spatial organization will dictate the efficiency of their signal propagation and cellular responses. Moreover, these signalling mediators have been extensively linked to flow induced enhancements of endothelial permeability under physiological conditions, predominantly through their coordinated influences of the cortical actin cytoskeleton (Tzima et al., 2002, Birukova et al., 2008, Wojciak-Stothard and Ridley, 2002). Recent work by Miyazaki *et al.* demonstrated that disturbed flow conditions, which are associated with intercellular junction disassembly triggered an over-activation of RhoA (for 60mins) (Miyazaki et al., 2010). Although the authors didn't address Rac1 activity under similar conditions, it is possible that the aberrant RhoA signalling pattern ablated the characteristic Rac1 activation necessary to elicit a barrier-enhancing response. Furthermore, this is consistent with the notion that RhoA signalling is the common facilitator mediating permeability enhancement in response to upstream signalling.

The vast majority of these studies have however been performed in EC's of macrovascular origin where the magnitude of hemodynamic loading can vary drastically; therefore further studies will need to be performed in areas of the microvasculature such as the BBB to confirm to the roles of these signalling molecules. Although a role for integrins in force mediated changes in GTPase activity has been established (Tzima et al., 2002, Tzima et al., 2001), the contribution of intercellular junctions to force-dependent changes in these signalling molecules remains to be investigated. Understanding the mechanisms of mechanotransduction and involvement of RhoGTPases in the regulation of endothelial permeability will be essential to identifying key regulatory molecules or targets for drug therapies in diseases exhibiting vascular leakage. Future efforts must attempt to tie specific upstream signalling

mediators such as RhoGEF's/GDI's/GAP's to flow-mediated activation of RhoGTPases to further unravel the molecular mechanisms involved.

1.7 Summary and study rationale

The vascular endothelium represents a dynamic, heterogenic interface between blood constituents and the underlying interstitium, performing multifunctional roles in human health and disease. More specifically, the capillary endothelium of the cerebral microvasculature constitutes the BBB, a physical and metabolic barrier regulating blood-borne solute flux into the brain interstitial fluid (ISF). Disruption of this barrier is associated with multiple disease states; however the physiological characteristics of the BBB are the rate-limiting step in drug delivery. The burden of the physical barrier is borne primarily at the level of the tight junction; a series of transmembrane (occludin and claudin-5) and cytoplasmic (ZO-1) proteins that effectively seal the paracellular pathway. Acting in tandem with this complex is the adherens junction, comprising VE-Cadherin and catenins (α-, β-, p120-), which coordinate and regulate junctional assembly. Crucial to the regulation of these intercellular junctional complexes and thus, BBB permeability are the surrounding cells forming the NVU (astrocytes, pericytes, neurons and ECM components) and blood-borne hemodynamic forces, namely laminar shear stress. Indeed the latter component alone is of genuine physiological relevance considering the fact that EC's are continuously subjected to these forces *in-situ*. Moreover, altered shear stress is one of the contributing vascular causes of stroke and its microvascular consequences during cerebral ischemia.

The purpose of this study is to build on previous published findings from our laboratory assessing the effects of laminar shear stress on tight junction assembly and barrier function, and further examine the role of shear reduction (flow cessation) on these indices. It will primarily encompass elucidation of the signalling mechanism(s) pertaining to shear-dependent stabilization of barrier function within an *in-vitro,* monoculture model of the BBB. Clarification of how the BBB is regulated in physiology or pathology will further enhance our knowledge and thus serve as a platform to identify or develop novel therapeutic strategies targeting neurological diseases eliciting comprised barrier function.

1.8 Thesis Overview

The research data presented herein describes the physiological regulation of the tight junction complex in bovine brain microvascular endothelial cells (BBMvEC's) responding to laminar shear stress and various intracellular signalling intermediates. Tight junction assembly is assessed by the localization patterns of ZO-1 and claudin-5 and post-translational modifications of occludin in response to shear stress and various molecular/pharmacological knockout strategies. Permeability studies involving tracer fluorophores (FITC/APTS-dextran) were monitored in parallel to deduce if there is a direct association between shear induced tight junctional changes and endothelial barrier function, and furthermore to assess possible signalling intermediates pertaining to such effects. The findings are presented in the following manner.

Chapter 3: To monitor the effects of laminar shear stress and/or flow cessation on BBMvEC tight junction assembly and barrier function.

Chapter 4: To examine the contribution of RhoGTPases, Rac1 and RhoA, to shear-induced adaptation of BBMvEC tight junction assembly and barrier function.

Chapter 5: To assess the role of VE-Cadherin and Tiam1 in shear-induced upregulation of BBMvEC tight junction assembly and barrier function.

See figure 1.16 below for a schematic depiction of the experimental approached uses in this thesis.

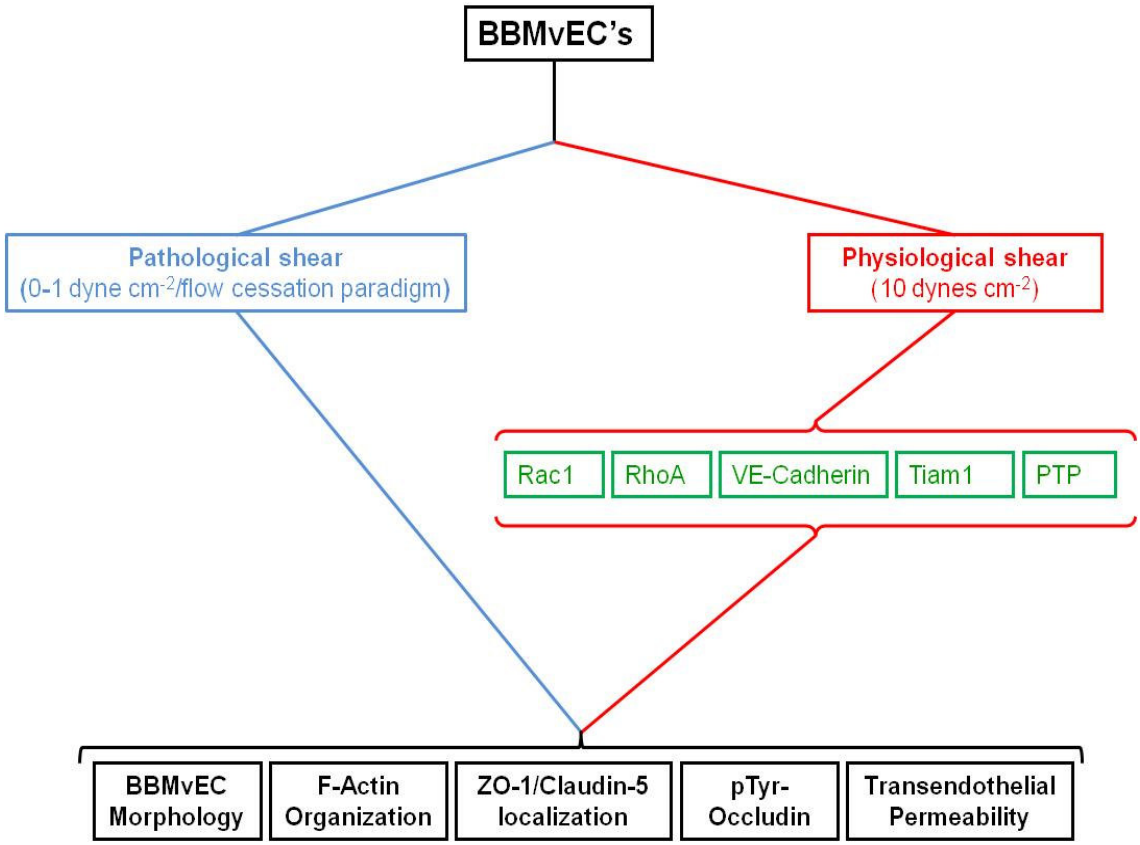

Fig. 1.17: Schematic depiction of experimental approach. Primary bovine brain microvascular endothelial cells (BBMvEC's) were subjected to different experimental paradigms; pathological shear conditions (blue) and physiological shear (red), and monitored for structural changes in morphology, functional alterations in permeability and biochemical changes in tight junction proteins. Various molecular and pharmacological inhibition strategies (green) were incorporated to assess potential involvement under physiological conditions.

Chapter 2:

Materials and Methods

2.1 Materials:

Acros Organics (NJ, USA)

Formaldehyde (37%).

Aktiengeselischaft and Company (Numbrecht, Germany)

1.5 mL micro tube with safety cap, 10, 200 and 1000 µL pipette tips, 15 and 50 mL falcon tubes, 2, 5, 10 and 25 mL serological pipettes, 6 and 24-well tissue culture plates, T-25 tissue culture flasks, T-75 tissue culture flasks, cell scrapers, 58 cm^2 tissue culture dishes.

Amaxa (Köln Germany)

Basic endothelial nucleofector kit.

Barloworld-Scientific (London, UK)

White flat-bottomed 96-well plates.

Becton Dickinson (NJ, USA)

FACS sheath fluid, FACS rinse, FACS clean, FACS tubes.

Bio-Rad, Hercules (CA, USA)

Thick mini trans-blot filter paper, Precision plus protein marker.

Calbiochem (San Diego, CA)

Dephostatin: Tyrosine phosphatase inhibitor, NSC23766: Rac-1 inhibitor, Y-27632:Rho-kinase inhibitor.

Cell Applications (San Francisco, USA)

Bovine brain microvascular endothelial cells (BBMvECs).

Cell Systems Inc (Kirkland, WA, USA)

Primary human brain microvascular endothelial cells (HBMvECs), CSC complete growth media, CSC attachment factor.

Cell Signalling Technology Inc (MA, USA)

HRP-conjugated anti-Rabbit IgG 2° antibody.

Cytoskeleton Inc (CO, USA)

Rac1 and RhoA G-LISA® activation assay kit, Mouse anti-Rac1 monoclonal antibody.

DAKO (CA, USA)

Rabbit anti-Von Willebrand Factor polyclonal antibody, Fluorescent mounting media.

Eppendorf (Cambridge, UK)

UVette: UV-disposable cuvettes.

GE-Healthcare (Buckinghamshire, UK)

HRP-conjugated anti-mouse IgG 2° antibody, ECL Hyperfilm, Protein-G Sepharose Beads.

Gibco (Scotland, UK)

Fetal calf serum.

Invitrogen (CA, USA)

Alexa Fluor® 488 F(ab')$_2$ fragment of goat anti-mouse IgG (H+L), Alexa Fluor® 488 F(ab')$_2$ fragment of goat anti-rabbit IgG (H+L), Alexa Fluor® 546 rhodamine phalloidin, *DH5α E-coli* competent cells, SyberSafe®.

Millipore (MA, USA)

bFGF – Recombinant human basic fibroblast growth factor, Millicell hanging cell

culture transwell inserts (6 well format, 0.4 μm pore size, 24 mm filter diameter).

Nalgene Nunc (NY, USA)

Cryogenic vials, Cryo freezing container

Pall Life Science (NY, USA)

Acrodisc 32 mm syringe filter with 0.2 μm super membrane, Nitrocellulose transfer membrane

Pierce Biotechnology (IL, USA)

BCA protein assay kit, Supersignal West Pico chemiluminescent substrate

Qiagen (West Sussex, UK)

HiSpeed Midi-prep kit.

Roche Diagnostics (Basal, Switzerland)

Protease and phosphatase inhibitor cocktail.

Santa Cruz Biotechnology (CA, USA)

Rabbit anti-GAPDH polyclonal antibody, Rabbit anti-Tiam1 polyclonal antibody.

Sigma Chemical Company (Dorset, UK)

2-mercaptoethanol, Acetic acid, Acetone, Ammonium Persulfate, ATPS (8-Aminopyrene-1,3,6-trisulfonic acid trisodium salt), Ampicillin (disodium salt), Agarose, Bovine serum albumin, Bromophenol blue, Citric acid, DAPI, Dextran, DMEM – High glucose D5796, EDTA, EGTA, FITC-dextran (40kDa), Forskolin, Glycerol, Glycine, Heparin, HEPES, Hydrochloric acid, Isopropanol, Kanamycin sulphate, LB agar, LB broth, Lauryl sulfate, PBS tablets, Penicillin-Streptomycin (100X), Ponceau S solution, Potassium chloride, Potassium phosphate, Potassium hydroxide, Sodium chloride, Sodium cyanborohydride, Sodium deoxycholate, Sodium orthovanadate, Sodium

phosphate-dibasic anhydrous, Sodium phosphate-monobasic anhydrous, TEMED, Thrombin, Triton® X-100, Trizma Base, Trypsin-EDTA (10X), Tween® 20.

Thermo Fisher Scientific (Leicestershire, UK)

Buffer solution pH 4 (phthalate), Buffer solution pH 7 (phosphate), Buffer solution pH 10 (borate).

VWR international Ltd (West Sussex, UK)

Methanol.

Zymed Laboratories (CA, USA)

Mouse anti-Occludin monoclonal antibody, Mouse anti-ZO-1 monoclonal antibody, Mouse anti-phosphotyrosine monoclonal PY-Plus™ antibody, Mouse anti-Claudin-5 monoclonal antibody.

2.2 Cell culture methods

All cell culture procedures were undertaken in a clean and sterile environment using a Bio Air 2000 MAC laminar flow cabinet. Cells were monitored daily for growth and morphology characteristics using an Olympus CK30 and/or Nikon Eclipse TS100 phase-contrast microscope.

2.2.1 Culture of bovine brain microvascular endothelial cells (BBMvEC's)

BBMvEC's are an adherent cell line that forms a contact-inhibited monolayer upon confluency with distinct *cobblestone* morphology. Cryopreserved passage two BBMvEC's were acquired from Cell Applications Inc., (Cat No. B840-05) California, USA. The cell line was tested free from bacteria, mycoplasma or fungal contaminants prior to shipping. Cells were characterized as endothelial by positive Dil-Ac-LDL uptake. BBMvEC's were routinely grown in high glucose DMEM supplemented with 10% foetal bovine serum (FBS), 3 μg/ml heparin, 3 ng/ml human recombinant basic fibroblast growth factor (bFGF), 100 U/ml penicillin and 100 μg/ml streptomycin. BBMvEC's were cultured in T25, T75 and 58 cm^2 culture flasks/dishes along with 6 and 24-well plates. Cells between passages 5-12 were used for experimental purposes, and were maintained in a humidified atmosphere of 5% CO2/95% air at 37°C.

2.2.2 Trypsinisation of BBMvEC's

As BBMvEC's are an adherent cell line, trypsinisation was necessary for sub-culturing. BBMvEC's were passaged at approximately 70-90% confluency. The trypsinisation process involved pre-equilibrating sterile phosphate buffered saline (PBS), trypsin/ethylenediamene tetracetic acid (5% v/v Trp/EDTA in PBS) and growth medium to 37°C. Using a sterile pipette, growth medium was aspirated from the culture flask and cells were washed with 4-6 mls of PBS for 30 sec to remove α-macroglobulin and other trypsin inhibitors present in the culture medium. Following removal, an appropriate volume of trypsin-EDTA was added to the cells and incubated for 2-3 mins at 37°C until

the cells were rounded but not detached. At this point the dish was gently tapped on the side to facilitate cellular detachment from the growth surface and subsequently an equal volume of culture media was added to prevent further trypsinisation. Cells were then removed from suspension by centrifugation at 700 rpm for 5 min at room temperature. The trypsin/growth medium was removed with the resulting cell pellet resuspended in growth or freeze media, and either counted for experimental procedures, split at a 1:4 ratio or cryopreserved.

2.2.3 Cryogenic preservation and recovery of BBMvEC's

For long term storage, BBMvEC's were preserved in a liquid nitrogen cryo-freezer unit (Taylor-Wharton, Al, USA). Following trypsinisation, cells were centrifuged at 700 rpm for 5 min at room temperature and the supernatant was removed. The resulting pellet was resuspended in an appropriate volume of freeze media; high glucose DMEM supplemented with 20% v/v FBS, 10% Dimethyl sulfoxide (DMSO), 3 μg/mL Heparin and 3 ng/mL bFGF, 100 U/ml Penicillin, 100 ug/ml Streptomycin and transferred in 1 mL aliquots to Nalgene cryovials and frozen in a -80^0C freezer at a rate of -1^0C/min using a Mr. Freeze® cryo-freezing container. Following this procedure, cryovials were transferred to the liquid nitrogen cyro-freezer unit until required.

For recovery of cells, cryovials were heated rapidly in a 37^0C water bath and added to a culture flask containing an appropriate volume of culture media pre-equilibrated at 37°C to dilute the DMSO. After 24 h, the media was removed, the cells were washed with sterile PBS and fresh culture media was added.

2.2.4 Cell counting

For efficient cell growth, BBMvEC's were seeded at precise numbers and densities to ensure consistency between experimental procedures. To achieve this, cell counts were performed using a Neubauer chamber haemocytometer and cell viability was assessed using trypan blue staining. This was incorporated for all experimental procedures with

the exception of seeding for transendothelial permeability assays, which utilized the Advanced Detection and Accurate Measurement (ADAM) counter.

2.2.4.1 Haemocytometer

For this procedure, the center chamber of the haemocytometer was mounted with a square coverslip until the Newton rings were visible. Approximately 20 µl of trypan blue was added to 100 µl of cell suspension and the haemocytometer chamber was filled by capillary action. Cells were visualized and counted in the four grids (G1-4) using a 4x objective under a phase-contrast microscope where viable cells excluded the trypan blue whilst non-viable (dead) cells stained blue. Viable cells touching the right and top corner were counted while those touching the left and bottom corner were excluded (Figure 2.1). The total number of cells in the all grids (G1-4) was divided by four to give the average count per 1 mm^2. The number of viable cells was calculated according to the equation:

Avg. cell no. x 1.2 (dilution factor) x 1x10^4 (conversion factor) = Viable cells/mL

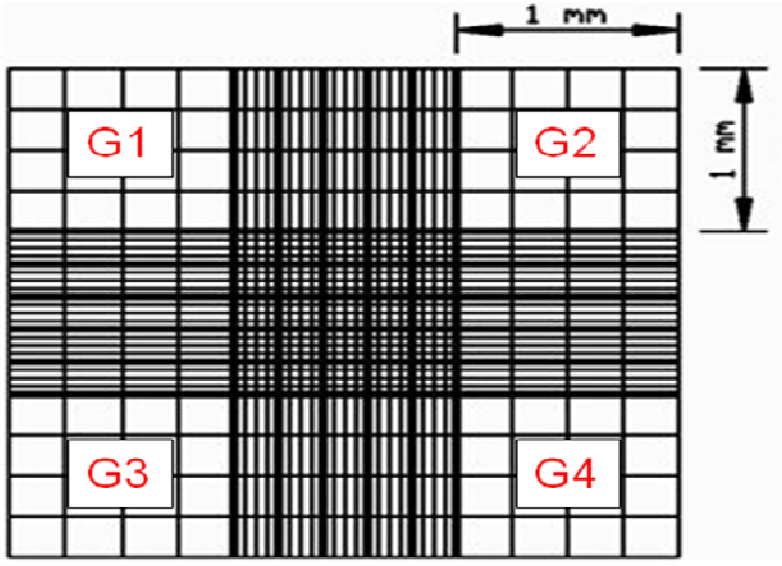

Fig. 2.1: The Haemocytometer

2.2.4.2 ADAM Counter

The ADAM Counter (Digital Bio, Korea) utilizes laser excitation and sensitive fluorescent optics connected to a charge coupled device (CCD) detection system to accurately measure viable cell suspension densities based on propidium iodide (PI) staining. Approximately 20 µl of cell suspension is mixed with 20 µl of solution T (containing PI and lysis buffer) and transferred (~30 µl) by capillary action into the 'T' channel of a microfluidic chip, giving a total cell count. Similarly 20 µl of cell suspension is mixed with 20 µl of solution N (containing PI, no lysis buffer), transferred to the 'N' channel giving a total non-viable cell count. The microfluidic chip is transferred to the ADAM counter and the results are calculated. Each N/T channel contains 22 grids, which are automatically counted, averaged and the resulting cell density of 'N' is subtracted from 'T' giving a viable cell count/ml of cell suspension (Figure 2.2).

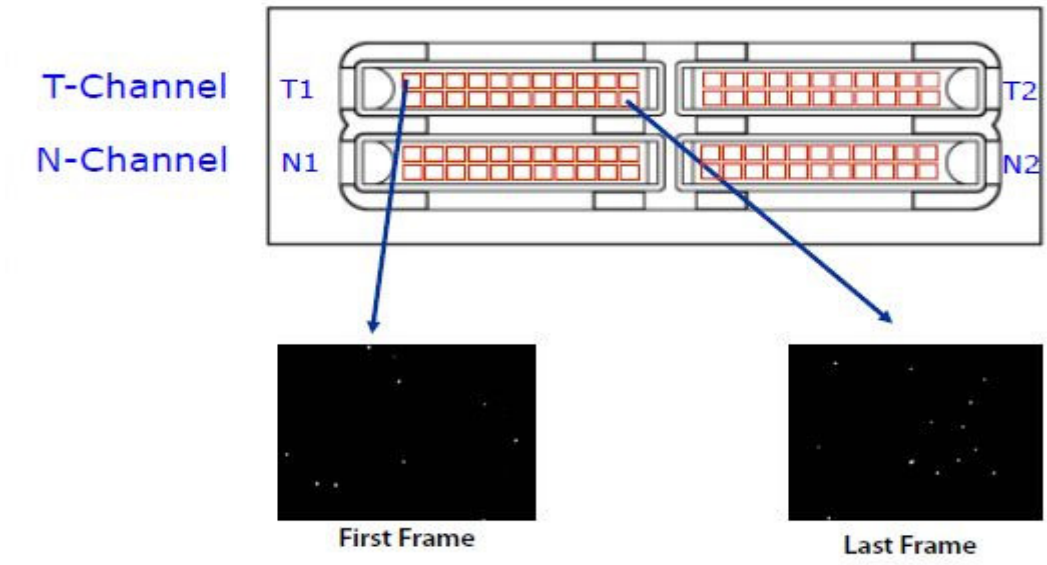

Fig. 2.2: ADAM counter microfluidic chip for viable cell counting.

2.2.5 Laminar shear stress studies

2.2.5.1 Laminar shear stress by orbital rotation

BBMVEC's were seeded at $1x10^5$ cells/well of a 6-well plate and grown to confluency (typically 4-5 days). Culture medium was then removed, replenished with 4 ml of fresh medium and cells were exposed to laminar shear stress (0 -10 dynes/cm^2, 0-24 h) using an orbital rotator (Stuart Scientific Mini Orbital Shaker) set to 150 rpm as determined by the following equation (Hendrickson et al., 1999). See figure 2.3 for schematic depiction of method.

$$ShearStress = \alpha\sqrt{\rho n(2\pi f)^3}$$

Where: α = radius of rotation (cm)

ρ = density of liquid (g/L)

$n = 7.5 \times 10^{-3}$ (dynes/cm^2 at 37^0C)

f = rotation per second

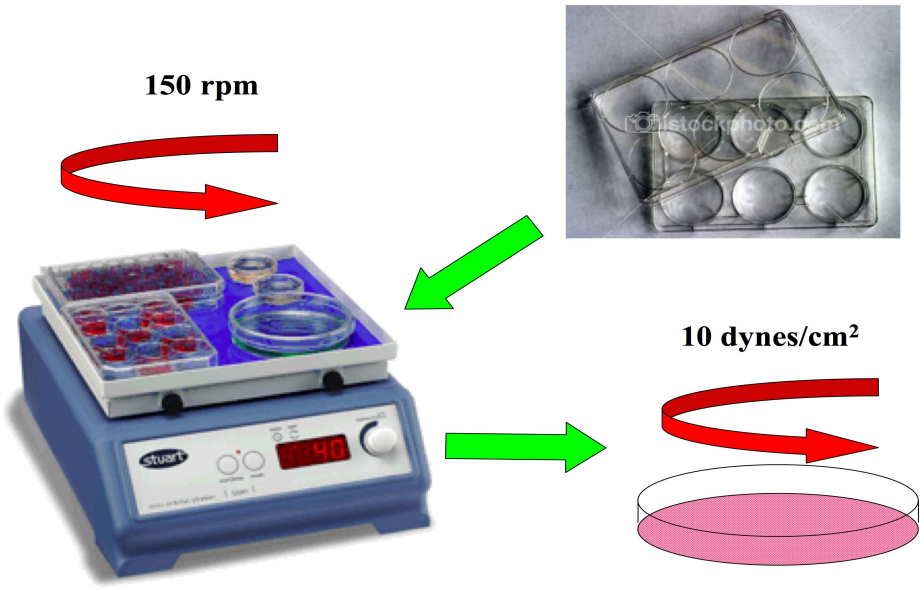

Fig. 2.3: Orbital Rotation model used in laminar shear stress studies.

2.2.5.2 Laminar shear stress by IBIDI® (Integrated BioDiagnostics) flow system

The IBIDI® pump system is a novel and recently acquired perfused flow system for exposing EC's to shear stress on IBIDI® μ-slides (Figure 2.4). Prior to seeding, slides and media were equilibrated overnight at 37°C in a tissue culture incubator. The following day, EC's were plated at a density of $1x10^5$ cells/slide and allowed to adhere. After allowing cells to adhere to the flow channel (1 h), 100μl of medium was added to each slide reservoir. EC's were allowed to grow to confluency at which point the μ-slides were connected to the pump system via its leur connectors in accordance with the manufacturer's instructions. The cells were then exposed to shear stress for the required time. This method was used for imaging purposes only and the immunocytochemistry (IC) protocol was carried out as described in section 2.5.2

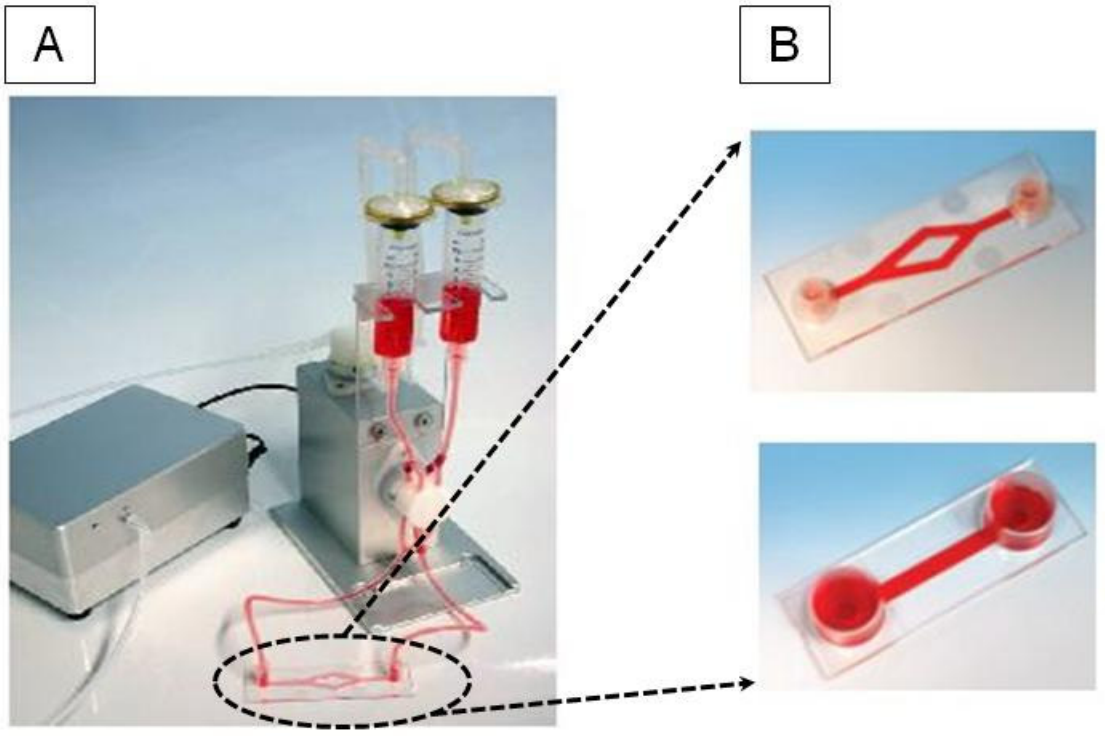

Fig. 2.4: IBIDI® flow system for laminar shear studies. (A): depicts the IBIDI® pressure pump connected to a fluidic unit containing two media reservoirs, with adjoining leur connectors which supply (B): EC's adhered to IBIDI® μ-slides with culture media at a specific shear rate.

2.2.6 Transendothelial permeability assay

Two different dextran substrates were employed to monitor BBMvEC transendothelial permeability. There preparations are outlined below.

2.2.6.1 Fluorescein isothiocyanate (FITC) – labelled dextran

For analysis of permeability, BBMvEC's following treatment were trypsinised and replated at high density ($1x10^6$ cells/well) into Millicell hanging cell culture inserts (6-well format, 0.4 µm pore size, 24 mm filter diameter). When cells had reached confluency (overnight) transendothelial permeability was monitored as previously described (Collins et al., 2006). In brief, fresh culture media was added to the upper (abluminal) and lower (sub-luminal) chambers of the Millicell insert within the 6-well dish (2 ml: upper, 4 ml: lower). At time (t)=0, FITC-labelled dextran (40 kDa) was added to the abluminal chamber (giving a final concentration of 250 µg/ml) and transwell diffusion allowed to proceed (Figure 2.5). Media samples (28 µl) were collected every 30 min from the sub-luminal compartment (for up to 3 h), diluted to a final volume of 400 µl with DMEM complete media, and monitored for FITC-dextran fluorescence (as 4x100 µl replicates in a 96-well fluorescence microplate). Using a TECAN Safire 2 fluorospectrometer (Tecan Group, Switzerland), excitation and emission wavelengths of 490 and 520 nm, respectively, were selected. % Trans Endothelial Exchange (%TEE) of FITC-dextran 40 kDa is expressed as the total subluminal fluorescence at a given time point (from 0-180 min) expressed as a percentage of total abluminal fluorescence at t=0 min.

2.2.6.2 8-Aminopyrene-1,3,6-trisulfonic acid trisodium salt (APTS) – labelled dextran

BBMvEC's were prepared as described in section 2.2.6.1. At t=0, the APTS dextran label, a fluorescent substrate specific to the paracellular space was incorporated in lieu of FITC dextran using the labeling reaction method of Neuhaus *et al.* (Neuhaus et al.,

2006). Briefly, a mixture consisting of 10 µl of 1 M ATPS, 15 µl of 1 M sodium cyanborohydride and 40 µl of dextran (6000 g/mol) was incubated at 85°C for 3.5 h. The resulting fluorescently-conjugated dextran was diluted 1:100 with complete culture media and added (2 ml) to the abluminal chamber. All remaining aspects of the transendothelial permeability assay for performed as described above in section 2.2.6.1.

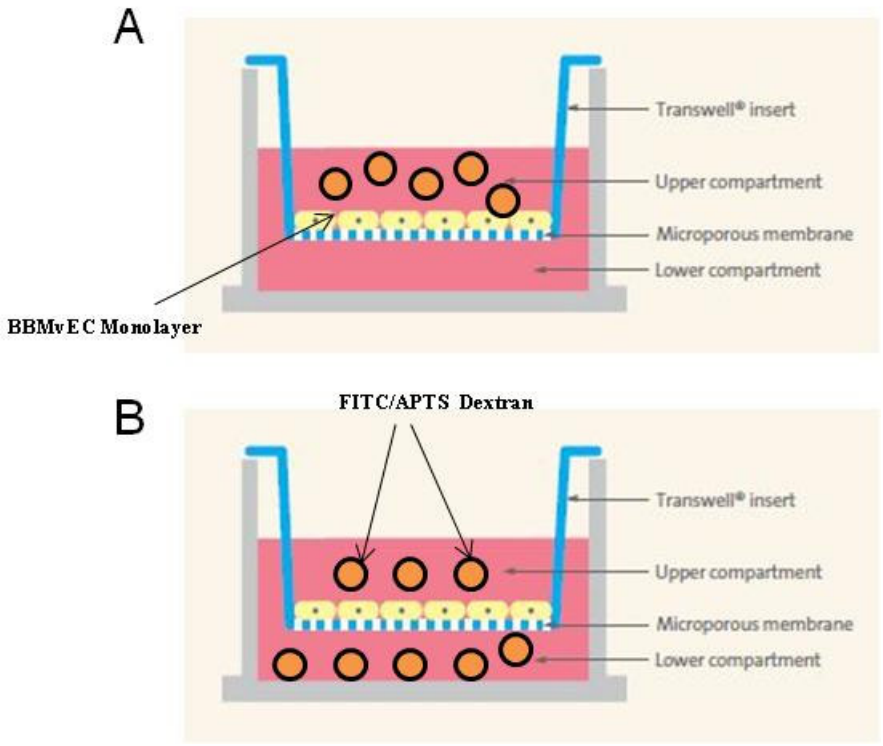

Fig. 2.5: Transendothelial permeability assay. A depicts the presence of FITC/APTS-labelled dextran into the upper compartment (abluminal chamber) at t=0, which diffuses through the BBMvEC monolayer and semi-permeable membrane, into the lower compartment (sub-luminal chamber) (B), from which samples (28 µl) are collected every 30 min.

2.2.7 Treatment with pharmacological inhibitors

For these experiments, BBMvEC's on 6-well plates were grown to confluency, after which the culture media was removed and cells were washed twice with sterile PBS. Inhibitors were diluted in culture media. For DMSO-soluble compounds, a suitable

stock concentration was prepared so that the final concentration of DMSO in working solutions was less than 0.5%.

For pharmacological inhibition studies, cells were incubated in culture media with 50 μM NSC23766 which inhibits Rac1, 10 μM Y-27632 which inhibits Rho-associated kinase (ROCK), and 20 μM Dephostatin, a tyrosine phosphatase inhibitor. These compounds were added approximately 1 h prior to the initiation of laminar shear stress. For Rac1/RhoA GLISA® activation assays, endogenous controls were incorporated to activate cellular pools of Rac1 and RhoA. For this procedure, BBMvEC's were incubated in complete media with 5 μM forskolin and 1 U/ml thrombin for 10 min to serve as positive controls for Rac1 and RhoA activation respectively (Waschke et al., 2004, Wojciak-Stothard et al., 2001).

Concentrations used in experiments were taken from recent literature and based on manufactures recommendations.

2.2.8 FACS analysis

Following transfection of BBMvEC's with a GFP-encoding plasmid construct, cells were monitored by fluorescent activating cell sorting (FACS) to detect GFP and assess the transfection efficiency. Approximately 24 h after GFP transfection, BBMvEC monolayers were washed twice with sterile PBS and harvested by trypsinisation. The cells were pelleted by centrifugation at 700 rpm for 5 min at room temperature and the resulting supernatant was removed. Cell pellets were then washed with 1 ml of ice-cold PBS supplemented with 0.1% w/v bovine serum albumin (BSA) and centrifuged once again. Following removal of the supernatant, the cell pellets were resuspended with 1 ml of ice-cold PBS (0.1% w/v BSA) and placed on ice. Samples were analysed by flow cytometry using a Becton Dickinson FACSCAN flow cytometer (NJ, USA).

2.3 Molecular biology techniques

2.3.1 Plasmid DNA reconstitution

Plasmid DNA constructs were received as small amounts of DNA (approximately 0.5 μg) spotted on air dried filter paper, which was stored at 4°C until use. To reconstitute the DNA, the small area (~1 cm^2) of the filter paper containing the appropriate plasmid was cut out using flame sterilized scissors and forceps, and added to a sterile 1.5 ml micro-centrifuge tube. Approximately 100 μl of sterile, endotoxin free, TE buffer (10 mM Tris base, 1 mM EDTA, pH 8.0) was added to the micro-centrifuge tube. This mixture was vortexed gently for 5-10 sec, incubated at room temperature for 5min and subsequently vortexed again. The tube was then centrifuged for 15 sec at 1000rpm. Approximately 1-10 μl of the supernatant was used for subsequent bacterial transformations.

2.3.2 Transformation of competent cells

Chemically modified DH5α *Escherichia-Coli* bacterial cells were transformed with the appropriate plasmid to facilitate rapid replication and subsequent purification of high quantities of plasmid DNA to be used for experimental procedures. The transformation protocol was as follows:

Approximately 1-10 μl of reconstituted plasmid DNA (10-50 ng) was gently added to 25-50 μl of competent bacterial cells as supplied in a micro-centrifuge tube. This bacterial-plasmid mixture was incubated on ice for 30 min. Following this, the competent cells were 'heat-shocked' at 42°C for 30 sec and subsequently returned to ice for 2 min. At this point, 500 μl of room temperature SOC media (2% w/v Tryptone, 0.5% w/v Yeast Extract, 10 mM NaCL, 2.5 mM KCl, 10 mM $MgCl_2$, 10 mM $MgSO_4$ and 20 mM Glucose) was added to the mixture and the cells were incubated for a further 30 min at 37°C on a bacterial culture shaker at 150 rpm. The resulting transformed bacterial cells were spread on two Luria-Burtani (L.B) agar plates containing the

appropriate selective antibiotics (Table 2.1) in volumes of 50 µl and 500 µl. Approximately 5 µl of competent cells (without plasmid DNA) were spread on selective agar plates to serve as negative controls for bacterial growth. The spread plates were inverted and incubated at 37°C overnight to facilitate optimal bacterial growth. Transformed colonies were isolated the following day.

Antibiotic	Solvent	Final Concentration (µg/ml)
Ampicillin	dH_2O	50 ug/ml
Chloramphenicol	EtOH	35 µg/ml
Kanamycin	dH_2O	50 µg/ml

Table 2.1: Antibiotic concentrations. Antibiotics dissolved in dH_2O were sterile filtered using a 0.25 µm filter.

2.3.3 Purification of plasmid DNA

Following bacterial transformation, successfully transformed colonies were isolated from the selective agar plates using a flame sterilized inoculating loop. The transformed colony was then grown overnight (approximately 16 h) in sterilized baffled flasks containing 150 ml of L.B broth (1% w/v Tryptone, 0.5% w/v Yeast Extract and 171 mM NaCL) supplemented with the appropriate antibiotics at 37°C with 150 rpm orbital shaking. Purification of plasmid DNA was carried out using a Qiagen plasmid midi-prep kit as per manufacturer's instructions.

In brief bacterial cells were pelted by centrifugation at 4000rpm for 15 min at 4°C and the resulting supernatant was decanted by tube inversion. The bacterial pellet was dissolved by vortexing in 6 ml of chilled P1 buffer. The bacterial suspension was subsequently lysed through the addition of 6 ml of P2 buffer and vigorous shaking for 30 sec followed by an incubation period of 5min at room temperature. The lysis activity

of P2 was neutralized by addition of 6 ml of chilled P3 buffer and was thoroughly mixed. The resulting cell lysate was poured into the barrel of a Qia midi-cartridge, inverted and incubated at room temperature for 10 min allowing cell debris to settle. Using a Qia midi-filter, the cell lysate was then filtered into a previously equilibrated hi-speed midi-prep tip containing a resin column where plasmid DNA binds. The column was then washed with 20 ml of QC buffer to flush out any bacterial cell proteins. Elution of DNA into a sterile 15 ml tube proceeded through the addition of 5 mls of QF buffer to the resin column, which was then followed by a 5 min precipitation period involving the addition of 3.5 mls of room temperature isopropanol. This isopropanol mixture was then filtered through a Qia-precipitator and the bound plasmid DNA was subsequently washed with 2 ml of 70% v/v ethanol. The precipitator was then air dried by flushing air through and the bound plasmid DNA eluted into a sterile 1.5 ml micro-centrifuge tube by the addition of 700 µl of sterile TE-buffer. The eluted DNA was flushed through the precipitator once again to remove any unbound DNA and was quantified by spectrophotometric analysis.

2.3.4 Spectrophotometric analysis of plasmid DNA

The concentration and purity of plasmid DNA from the bacterial culture was assessed by one of two methods, involving an automated NanoDrop 1000 spectrophotometer technique (Thermo Scientific, MA, USA) or measuring the absorbance (A) at 260 nm using an Eppendorf BioPhotometer (Eppendorf, Germany. It is assumed that 1 absorbance unit was equivalent to 50 µg/ml double-stranded DNA. This method involved a 1:100 dilution of purified plasmid DNA with TE-buffer in a plastic UVette. Plasmid concentration was calculated as follows;

$$Abs_{@260nm} \times 50 \times dilution\ factor = Concentration\ of\ DNA\ (\mu g/mL)$$

Plasmid purity was assessed by reading the absorbance at 260 nm and at 280 nm and then determining the ratio between the two (A_{260}/A_{280}). Pure DNA that has no bound protein impurities should have an A_{260}/A_{280} ratio of 1.8-1.9.

2.3.5 Agarose gel electrophoresis

Agarose gel electrophoresis was employed as a quality control to visualize and assess the quality of the purified plasmid. A 1% w/v agarose gel was prepared by adding 1 g of ultra pure agarose to a conical flask. This was brought to a volume of 100 ml by adding 1X Tris Borate EDTA (TBE) (90 mM Tris base, 90 mM Boric Acid, and 4 mM EDTA). The solution was boiled to dissolve the agarose until it became clear and transparent. Once cooled but still in liquid form, 10 µl (1X) Syber Safe® was added to the solution for visualization purposes. The mixture was then poured into a casting plate that had already been sealed with masking tape to prevent leakage of the gel. Immediately following this, a gel comb was inserted into the agarose gel, and allowed to solidify for approximately 20 min. The masking tape was then removed and the solid agarose gel was placed in the chamber within a horizontal gel rig and then filled with 1X TBE until the buffer overlaid the gel. For plasmid visualization, approximately 1 µg (4-5 µl) of plasmid DNA was mixed with 5 µl of 2X loading dye and loaded into the appropriate wells generated by comb. Approximately 5 µl of a 10 kilobase (kb) DNA ladder (New England BioLabs) was loaded in parallel for relative band size comparison. The gel was electrophoresised for 80 min at 40 mA or until the loading buffer appeared to have run three quarters of the way down the gel. DNA was visualized using a G-Box fluorescence gel documentation and analysis system (Syngene, UK)

2.4 Transfections - electroporation

Electroporation is a technique that enhances the electrical conductivity and permeability of the cell plasma membrane, thus serving as a pivotal tool in molecular biology in the delivery of a foreign substance (DNA/RNA) into a cell. Two different commercial means of electroporation were assessed for their ability to successfully deliver plasmid DNA into BBMvEC's without compromising overall cell viability (Figure 2.6 and 2.7).

2.4.1 Plasmid DNA nucleofection

Nucleofection is a novel technology that allows transfected DNA to directly enter the nucleus. It is a non-viral method that utilizes a unique combination of pre-designed electrical parameters and cell-type specific solutions. For BBMvEC's nucleofector transfections, the basic endothelial nucleofector cell kit was used in accordance with manufacturer's instructions. In brief, BBMvEC's were cultured to 70-80% confluency. On the day of transfection, approximately 2.5 ml of culture media without antibiotics was added to wells of a 6-well plate and equilibrated to 37°C in a cell culture incubator. BBMvEC's were trypsinised, counted and pelleted as described in section 2.2.2 and 2.2.4. Residual culture media was removed and the cell pellet was washed once with sterile PBS. BBMvEC's were then centrifuged at 700 rpm for 5 min, residual PBS removed by aspiration and cells were resuspended at a final concentration of $5x10^5$cells/100 µl, in nucleofector solution. Care was taken at this point not to store the cell suspension in the nucleofector solution for longer than 15 min as this would reduce cell viability and DNA transfer efficiency. For each sample, approximately 1.5 µg of DNA was mixed with the 100 µl cell suspension ($5x10^5$cells) and carefully transferred to a nucleofector cuvette. The cuvette was then checked to be free of air bubbles and sealed with a cap. The most appropriate programme to nucleofect BBMvEC's was U-11. Following nucleofection, 500 ul of pre-warmed culture media without antibiotics was added to the cuvette containing the sample, which was subsequently transferred to the pre-incubated well of the 6-well plate. Nucleofected samples were incubated overnight at 37°C and the culture media was replaced the next day.

Fig. 2.6: Amaxa nucleofection system. (A) The nucleofector apparatus for conducting the electroporation protocol and (B) nucleofector cuvette through which cell suspensions are contained during nucleofection (http://www.amaxa.com)

2.4.2 Microporation

Microporation is another novel method of electroporation but differs from the nucleofector as it utilizes a gold-plated tip as an electroporation space. This allows a more uniform electric field to be generated with minimal heat generation, metal ion dissolution, pH variation and oxide formation that are common problems experienced during the electroporation process. Microporation was carried out using a microporation kit in accordance with the manufacturer's instructions. The cell culture steps for microporation were performed as described in section 2.4.1 up until the cell counting procedure. At this point, BBMvEC's were pelleted by centrifugation at 700 rpm for 5 min, from which the supernatant was aspirated off and the cells were washed in sterile PBS. This cell suspension was centrifuged at 700 rpm for 5 min and residual PBS aspirated, from which the resulting cell pellet was resuspended to give a final concentration of $1.1x10^6$ cells/104 µl of transfection buffer-R solution. This cell-buffer R suspension was transferred to a sterile 1.5 ml micro-centrifuge tube and was mixed with 3.3 µg of plasmid DNA. Also at this point, 3 ml of E-buffer was added to a microporation tube and placed into the pipette docking station to form the microporation

unit (Figure 2.7). The cell-buffer R-DNA mixture was then pipetted into a 100 µl gold tip using the Microporator pipette before been inserted into the microporation docking unit. For BBMvEC's, the desired microporation conditions were set; 1000 pulse voltage, 30 pulse width (ms) and 2 pulse number. After microporation, the 100 µl sample was split between 2 wells of a 6-well plate containing pre-warmed culture media without antibiotics, giving approximately $5x10^5$ cells per well. BBMvEC's were allowed to recover overnight and the culture media was changed the following day.

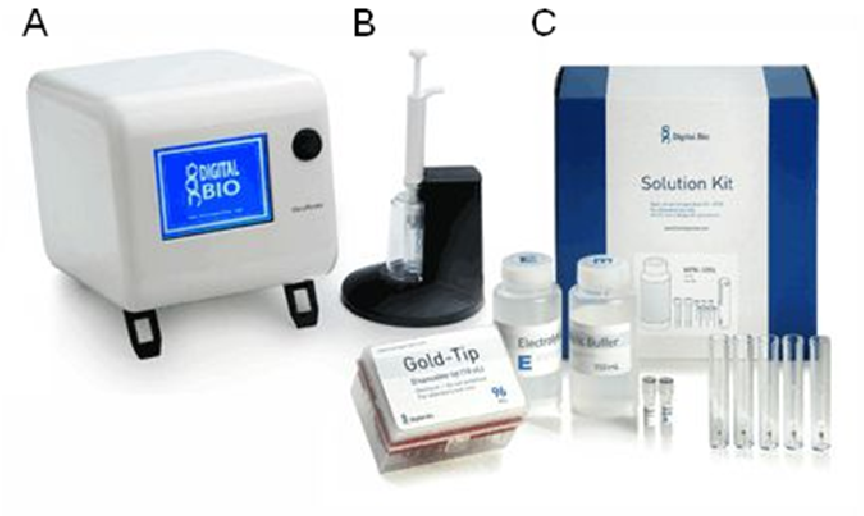

Fig. 2.7: Microporation System. (A) Microporation unit that generates the electrical parameters necessary for electroporation connected to (B) Microporation pipette docking unit consisting of microporation tubes containing electroporation buffer and the microporation pipette used to deliver electroporation to the cells through a gold plated pipette tip (C) Microporation kit with all the necessary solutions. (http://www.microporator.com)

2.5 Immunodetection techniques

2.5.1 Western blotting

2.5.1.1 Preparation of whole cell lysate

Post-treatment, confluent BBMvEC's were harvested for analysis by western blot or immunoprecipitation in the following manner. Either on ice or at 4°C, culture media was

removed by aspiration and cells were washed three times in chilled PBS. Following complete aspiration of PBS, cells were harvested using a cell scraper in radioimmunoprecipitation assay (RIPA) lysis buffer (64 mM HEPES pH 7.5, 192 mM NaCL, 1.28% w/v Triton X-100, 0.64% w/v sodium deoxycholate, 0.128% w/v sodium dodecyl sulfate SDS, supplemented with 0.5 M sodium fluoride, 0.5 M EDTA pH 8.0, 0.1 M sodium phosphate, 10 mM sodium orthovanadate, and 1X protease and phosphatase inhibitor cocktail) and transferred into a pre-chilled micro-centrifuge tube. Continuous lysate rotation persisted for 1 h at 4°C, prior to lysate clarification by centrifugation at 10000 rpm for 20 min at 4°C to sediment any triton-insoluble material. Subsequently clarified lysates were aliquoted into fresh tubes and were either stored at -80°C for future analysis or immediately subjected to a BCA assay and used for western blot/immunoprecipitation purposes.

2.5.1.2 Bicinchoninic acid (B.C.A) assay

The BCA assay is a biochemical assay used to quantify the amount of protein in solution. This assay is based on the principal that the protein under alkaline conditions will reduce copper (Cu^{2+}) ions to Cu^{1+} and secondly, the bicinchoninic acid (green) will chelate to each Cu^{1+} ion to form a complex (purple) than strongly absorbs at 562 nm. Two separate reagents were supplied in this commercially available assay kit (Pierce Chemicals), A; an alkaline bicarbonate solution and B; a copper sulphate solution, which were mixed at a ratio of 1 part (B) to 49 parts (A). Approximately 200 µL of this mixture was added to 10 µL of protein lysate or BSA standards (standard curve in the range 0-2 mg/mL) and monitored in triplicate form on a 96-well plate. The plate was incubated for 30 min at 37°C and the absorbance read at 562 nm using a EL*x*800 microplate reader (BioTek, VT, USA).

2.5.1.3 Immunoprecipitation (IP)

IP is technique that facilitates the precipitation of a specific protein out of solution by forming a stable antigen-antibody complex bound to a resin. This allows investigators to

concentrate levels of a target protein, monitor possible binding partners in multimember protein complexes and assess post-translational modifications of proteins. For our studies, this procedure was performed in conjunction with western blotting to isolate occludin protein from a sample of whole cell lysate and monitor changes in occludin tyrosine phosphorylation in response to biomechanical stimuli and molecular inhibition strategies.

Following preparation of whole cell lysate as described in section 2.5.1.1, lysates were monitored by IP analysis according to the method of Ferguson *et al.* with some minor modifications (Ferguson et al., 2000). In brief, lysate containing 200 µg of protein was pre-cleared with 20 µl of Protein G Sepharose beads for 1 h to minimize non specific binding. Beads were subsequently pelleted at 10000 rpm for 30 sec at 4°C. Pre-cleared lysate was transferred to a fresh tube and incubated with 2.5 µg of mouse anti-occludin monoclonal IgG, 10 µl of 10% w/v BSA, and 20 µl of fresh Protein G Sepharose beads, to give a final reaction volume of 500 µl. Incubation proceeded overnight with continuous eppendorf rotation at 4°C. Beads were then pelleted at 10000rpm for 30 sec at 4°C and washed extensively; twice in lysis buffer + 1% Triton X and twice in lysis buffer alone and resuspended in 2X sample solubilization buffer (2X SSB) (250 mM Tris-HCL pH 6.8, 8% SDS w/v, 40% glycerol v/v, 4% β-Mercaptoethanol v/v and 0.008% Bromophenol blue w/v) and heated for 5 mins at 95°C. Beads were pelleted by centrifugation at 10000 rpm for 30 sec at 4°C and supernatant (containing solubilized proteins) was transferred to a fresh eppendorf for western blot analysis.

2.5.1.4 Protein precipitation

Protein precipitation was performed using the organic solvent acetone to concentrate protein samples and ensure they could fit into the wells of an SDS-PAGE gel for Western blot analysis. In brief, 5 volumes of ice cold acetone were added to 1 volume of a known concentration of protein sample. This acetone-sample mixture was gently vortexed and centrifuged at 1000 rpm for 15 sec at 4°C. Samples were then incubated at

-20°C for 1 h with regular inversion every 10 min to prevent samples from freezing. Samples were then centrifuged at 10000 rpm for 5 min at 4°C and acetone-based supernatant was discarded. Subsequent protein pellets were allowed to air dry for 15 min and once all the acetone was removed, samples were resuspended in 30 µl 1X SSB and either stored at -20°C or used for subsequent western blot analysis.

2.5.1.5 Polyacrylamide gel electrophoresis (SDS-PAGE)

Sample separation by electrophoresis was carried out according to the method of Laemmli *et al. (Laemmli, 1970).* All components of the Mini-PROTEAN Tetra Cell® system (BioRad, CA, USA) were assembled according to the manufacturer's instructions. In brief, 10 x 100 mm glass plates (one short and one long with a 1.0 mm spacer; BioRad) were swabbed with 70% v/v ethanol and dried completely. The two plates were assembled accordingly and slotted into a casting frame, with the base space between the plates sealed by a gasket on a mounting stand. Resolving gels of 7.5% (Tiam1), 10% (Rac1, GADPH) and 12% (Occludin) polyacrylamide were prepared as described in Table 2.2 below. The TEMED was added last and approximately 5-6 mls of the resolving mixture was poured between the two plates. A small layer of 70% v/v ethanol was poured on top of the resolving gel to remove any surface air bubbles. The gel was then allowed to set for 30 min.

	7.5%	**10%**	**12%**
Distilled Water	4.85 ml	4.00 ml	4.35 ml
1.5M Tris HCL pH (8.8)	2.50 ml	2.50 ml	2.50 ml
Acrylamide/Bis-acrylamide	2.50 ml	3.33 ml	4.00 ml
10% SDS	100 µl	100 µl	100 µl
10% Ammonium persulfate	50 µl	50 µl	50 µl
TEMED	5 µl	5 µl	5 µl
Total Volume	**10 ml**	**10 ml**	**10 ml**

Table 2.2: SDS-PAGE resolving gel composition. The individual components and corresponding volumes of different percentage acrylamide resolving gels are presented.

A 4% v/v stacking gel was prepared for all SDS-PAGE experiments and the components were compiled in the order documented in Table 2.3 below.

	4%
Distilled Water	6.10 ml
1.5M Tris HCL pH (6.8)	2.50 ml
Acrylamide/Bis-acrylamide	1.30 ml
10% SDS	100 µl
10% Ammonium persulfate	100 µl
TEMED	10 µl
Total Volume	**10sml**

Table 2.3 SDS-Page stacking gel components. The individual components and corresponding volumes of a 4% acrylamide stacking gel is presented.

When the resolving gel had set, the 70% ethanol at the gel surface was poured off and the space in between dried with filter paper. TEMED was then added to the stacking gel mixture and poured (approximately 1-2 mls) on top of the polymerized resolving gel. Any residing bubbles were removed following which the comb was gently inserted, and the stacking gel was allowed to polymerise for 30 min. Upon polymerization, the gels were submerged in an electrophoresis tank with approximately 700 mls of running buffer (25 mM Tris, 192 mM Glycine, 0.1% SDS) and the combs were then removed. The wells in the stacking gel were then flushed using a micro-pipette to remove any unpolymerised acrylamide.

Table 2.4 below outlines the appropriate quantity of protein mixed with SSB and lysis buffer to give to a total loading volume of 30 µl. Once the samples were prepped, they were incubated for 5 min at 95°C on a heating block, before been cooled on ice and centrifuged briefly for 20 sec at 1000 rpm to collect any condensation on the lid of the

tube. Samples were loaded into the appropriate lanes along with 3 µl of Precision Plus® protein molecular weight marker (BioRad). Both samples and protein markers were electrophoretically separated for 90-120 min at 100 V.

Protein Name	Protein loaded per lane (µg)
Occludin	See section 2.5.1.3
Rac1	15**
Tiam1	50*
GAPDH	15**

Table 2.4: Protein concentrations loaded. The different proteins and their corresponding, optimised loading concentrations for Western blot procedures are presented. Asterisk (*) denotes the SSB concentration used, where * = 1XSSB and ** = 4XSSB.

2.5.1.6 Electrotransfer to nitrocellulose membrane

The wet or tank transfer method of Towbin *et al.* was utilized for electrotransfer of proteins to a gel in all circumstances (Towbin et al., 1979). This was accomplished using a Mini PROTEAN® Trans Blot Module (BioRad) according to the manufacturer's instructions. Following SDS-PAGE electrophoresis, gels were removed from glass plates and the stacking gel was discarded. The resolved gel was then soaked for 10 min in transfer buffer (25 mM Tris, 192 mM Glycine, 20% methanol) to remove any SDS complexes bound to the gel that could affect successful protein transfer. At this time, the transfer cassette was assembled and nitrocellulose membrane (Pall Biotrace) was cut to the exact dimensions of the resolving gel and allowed to soak in transfer buffer for 5-10 min. Following this the gel was assembled in the transfer cassette as described in Figure 2.8 below.

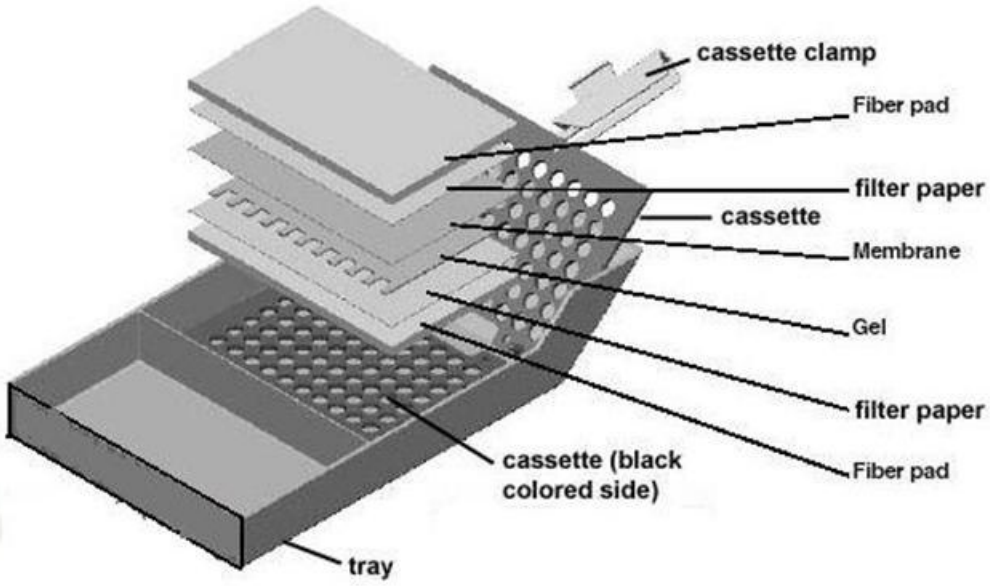

Fig. 2.8: Wet transfer cassette assembly. Figure describes the layout of the transfer cassette used to transfer electrophoresed proteins from an SDS-PAGE gel to nitrocellulose membrane. The black colored side is assembled face down, overlaid with a fiber pad, filter paper, resolved gel, nitrocellulose membrane, filter paper, and fiber pad and sealed on the non-colored side.

Once assembled, the cassette was checked to be free of air bubbles by rolling a 15 ml tube over the cassette while submerged in transfer buffer to remove any residual bubbles. The cassette was then placed in the Trans Blot Module with the correct orientation and subjected to 100 V for 2 h or 40 V overnight at 4°C. Following transfer completion, membranes were soaked in Ponceau S solution for 3 min to ensure even protein loading. The stain was subsequently removed by gentle washing in 1X PBS, 0.05% Tween-20® (PBS-Tween).

2.5.1.7 Immunoblotting and chemiluminescence band detection

Following removal of the Ponceau stain, membranes were blocked for 90 min in tris-buffered saline/Tween® (TBST: 25 mM Tris-HCL pH7.4, 150 mM NaCL and 0.05% Tween) containing 5% w/v BSA. Once membranes were blocked, they were briefly rinsed in TBS buffer to remove any excess blocking solution. Subsequently membranes were incubated with the appropriate primary antibody (see Table 2.5 below) in TBST

(5% BSA w/v) solution overnight at 4°C, with gentle agitation on a rocker (Stuart Scientific).

Following completion of primary incubations, membranes were washed 6 times for 5 min (30 min in total) in wash buffer (0.5% TBST for Rac1, GAPDH and Tiam1 or 1% TBST for Occludin or Phosphotyrosine blots). Membranes were subsequently incubated with the appropriate secondary antibody in TBST (5% BSA w/v) for 90 min with gentle agitation at room temperature. Membranes were then washed again using the same conditions described above.

Primary Antibody	Primary Dilution	Secondary Antibody	Secondary Dilution
Occludin (Zymed)	0.5 µg/ml	Mouse (GE-Healthcare)	1:3000
Phosphotyrosine (Zymed)	1 µg/ml	Mouse	1:3000
Rac1 (Cytoskeleton)	1 µg/ml	Mouse	1:3000
GAPDH (Santa Cruz)	0.4 µg/ml	Rabbit (Cell Signalling)	1:3000
Tiam1 (Santa Cruz)	0.4 µg/ml	Rabbit	1:2000

Table 2.5: Primary and secondary antibody dilutions. This table displays the optimised primary and secondary antibody dilutions for proteins monitored by Western blot, and the commercial sources of antibodies.

Supersignal® West Pico (Pierce) was the chemiluminescent substrate of choice for detection of HRP-conjugated secondary antibodies. This was prepared according to the manufacturer's instructions and incubated with the membranes for 5 min, following which excess substrate was removed and the chemiluminescent signal was detected in a dark room by autoradiography (GE-Healthcare). Resulting immunoblots were scanned and densitometric analysis was performed using NIH Image v1.61 software to obtain relative comparisons between bands.

2.5.2 Immunocytochemistry

In order to monitor the expression and/or subcellular localization of proteins, BBMvECs were prepared for immunocytochemical (IC) analysis according to the method of Groarke *et al.* with minor modifications (Groarke et al., 2001). Briefly, cells were washed twice in PBS and fixed with 3% formaldehyde for 15 mins. Cells were then washed, permeabilised with 0.2% Triton X-100 for 15 mins, and blocked in 5% w/v BSA for 30 mins. Cells were then incubated at room temperature with the appropriate primary antibody or stain as displayed in Table 2.6. Samples were then washed twice in PBS and incubated for 1 h in the dark with an Alexa Fluor 488-conjugated goat anti-mouse IgG (1:400 for Z0-1, 1:400 for claudin-5) (Molecular Probes, OR, USA) and Alexa Fluor 488-conjugated goat-anti rabbit IgG (1:400 for FLAG®, Tiam1 and vWF) (Molecular Probes). Nuclear DAPI staining was routinely performed by incubating cells with 0.5 x 10^{-6} µg/mL DAPI for 3 min. Following two washes with PBS, BBMvEC's were sealed with DAKO mounting media (DAKO, UK) and coverslips for visualisation by fluorescent microscopy (Olympus BX50, Germany). Appropriate controls (such as primary antibody omission) were routinely incorporated into all immunocytochemical experiments.

1° Antibody/Stain	1° Antibody/Stain Dilution
ZO-1 (Zymed)	0.5 µg/ml (2 h)
Claudin-5 (Zymed)	1 µg/ml (3 h)
Tiam1 (Santa Cruz)	2 µg/ml (2 h)
FLAG® (DYKDDDDK) (Cell Signalling)	0.4 µg/ml (3 h)
von Willebrand Factor (DAKO)	1:1000 (2 h)
Rhodamine-Conjugated Phalloidin (Molecular Probes)	1:80 (40 min)

Table 2.6: Immunocytochemistry primary antibody dilutions. Table 2.6 displays the optimised incubations for all primary antibody and stain dilutions of proteins monitored by immunocytochemistry.

2.6 RhoGTPase G-LISA® activation assays

2.6.1 Lysate reparation

Following shear experiments, BBMvEC's were harvested for analysis of active (GTP) levels of Rac1 and RhoA using the Rac1 and/or RhoA G-LISA™ activation assay kits (Cytoskeleton Inc., CO, USA). This assay utilizes the p21-binding domain (PDB) of p21-activated kinase 1 (Pak1) for Rac1 and Rho binding domain (RBD) of rhotekin for RhoA, coupled to GST as bait to selectively isolate active "GTP-bound" Rac1 and or RhoA (Stofega et al., 2006). All aspects of the assay protocol were performed as per the manufacturer specifications

In brief, BMvECs were grown to 80% confluence, serum-starved overnight (0.2% FBS) and replenished with full-serum culture media immediately prior to the initiation of shear stress. Following shear cessation, cells were maintained on ice and rapidly processed to reduce GTP hydrolysis. BBMvEC's were washed twice in ice-cold PBS and harvested with a cell scraper in the supplied lysis buffer, and transferred to a pre-chilled micro-centrifuge tube. Lysate clarification proceeded at 14000 rpm for 2 min at 4°C, following which the sample protein concentration was assayed within 1 min using the supplied Precision Red™ protein assay reagent as per manufacturer's instructions. Sample concentrations were then equalized by diluting the most concentrated sample(s) with lysis buffer, aliquoted in 100 µl volumes and 'flash frozen' in liquid nitrogen and stored at -80°C for subsequent analysis. Typical protein concentrations were in the range of 0.7-1 mg/ml.

2.6.2 G-LISA® procedure and immunodetection

Again all aspects were prepared in accordance with the manufacturer's instructions. In brief samples were rapidly thawed in a room temperature water bath and 60 µl of sample was diluted with 60 µl of ice-cold binding buffer. Samples were transferred (in duplicate, 50 µl per well) to appropriate wells on a 'RhoGTPase affinity plate', pre-

coated with the respective binding domains for active Rac1 and RhoA. Positive and negative controls were routinely incorporated and added to the affinity plate under the following conditions; 60 µl of lysis buffer was added to 60 µl of binding buffer (negative control) and 12 µl of the supplied Rac1/RhoA control protein added with 108 µl of binding buffer (positive control). The pulldown of active GTP levels proceeded by placing the affinity plate on an orbital shaker at 300 rpm for 30 min at 4°C.

Following this, the solution was removed from the wells and washed twice in the supplied wash buffer. Solution removal consisted of a vigorous flick of the plate and 6-7 hard pats onto paper towels. Then 200 µl of antigen presenting buffer was added to each well for 2 min, following which the wells were washed three times with wash buffer. Primary antibody incubation proceeded at 300 rpm for 45 min at room temperature in antibody dilution buffer (1:250 dilutions for Rac1 and RhoA). Wells were subsequently washed three times with wash buffer and incubated at 300 rpm for 45 min at room temperature in antibody dilution buffer containing secondary antibodies (1:200 for Rac1 and 1:62.5 for RhoA). Wells were then washed 3 times with wash buffer, with complete solution removal after the final wash before the appropriate substrate was added to the samples. Quantification of Rac1 was by luminescence using a Synergy HT Multi-Mode Microplate Reader (BioTek) and RhoA was monitored using a TECAN Safire 2 fluorospectrometer. Figure 2.9 below depicts the principle of the GLISA® assay.

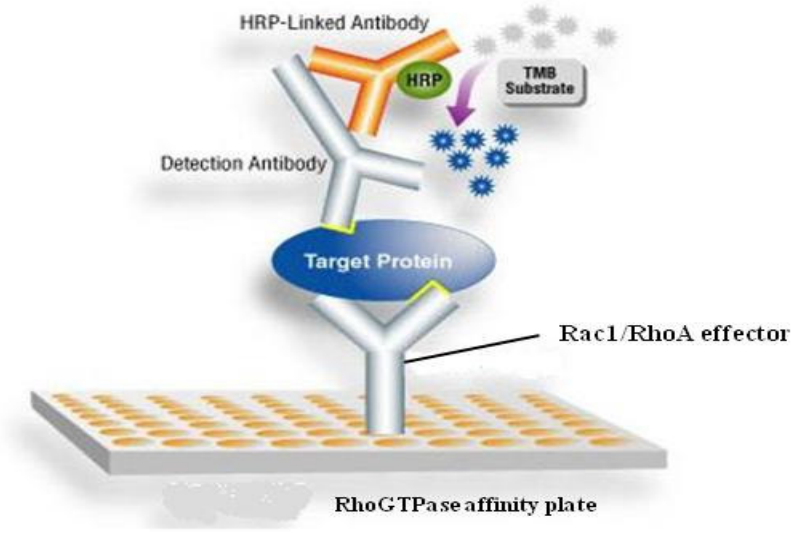

Fig. 2.9: G-LISA principle. A 96-well plate is pre-coated with an effector domain for particular RhoGTPases forming an affinity plate to selectively isolate active RhoGTPases. The assay proceeds with sample addition and a standard primary and secondary based immunodetection protocol with subsequent quantification via substrate association with the HRP-secondary antibody conjugate.

2.7 Statistical analysis

Results are expressed as mean±sem. Experimental points were performed in triplicate with a minimum of three independent experiments (n=3). Statistical comparisons between controls versus treated groups were made by Student's unpaired *t*-test and Wilcoxon Signed-Rank test (for non-parametric comparisons). A value of *P≤0.05 (or ϕP≤0.05) was considered significant.

Chapter 3:

The effects of laminar shear stress and/or flow cessation on BBMvEC tight junction assembly and barrier function.

3.1 Introduction

Vascular endothelial cells of the cerebral vascular network constitute a highly restrictive barrier phenotype forming the blood brain barrier. They establish a dynamic interface between cerebral blood flow and the central nervous system, a mechanism essential to controlling blood borne fluid and solute flux into the brain microenvironment (Persidsky et al., 2006). Surveillance of these BBB specific processes is tightly controlled and requires coordinated regulation via specific transcellular and paracellular pathway machinery. Indeed, the latter component involves a coordinated interaction of intercellular adherens and tight junction protein complexes, which mutually cooperate to stabilize barrier properties of the paracellular pathway. An abundance of clinical and experimental evidence exists, which implicate perturbations of intercellular junction complexes in various CNS disorders such as stroke, meningitis, multiple sclerosis, Alzheimer's disease and epilepsy (Hawkins and Davis, 2005, Persidsky et al., 2006, Weiss et al., 2008).

Both *in-vivo* and *in-vitro,* the functional BBB phenotype is highly sensitive to physiological and pathological variables encompassing both humoral (cytokines, immune cells, growth factors and infectious agents) and hemodynamic (shear stress) variables. The lateral component, blood flow-associated shear is of crucial importance, which through complex mechanosensing mechanisms regulates intracellular signaling, cytoskeletal dynamics and differential gene expression with profound consequences for vessel integrity and remodeling (del Zoppo, 2008, Schwartz, 2009). Moreover, shear stress promotes cerebral homeostasis and is postulated to exert protective effects against the pathophysiology of several neurological disorders (Krizanac-Bengez et al., 2004). However, a detailed understanding of the cellular mechanisms of shear-induced up-regulation of BBB function is somewhat lacking. With this in mind, we re-visit the previous BBMvEC model of Colgan *et al.* to further clarify the shear-induced upregulation of BBB permeability, with specific relevance to tight junction assembly (Colgan et al., 2007).

In this chapter we examine the effect of physiological laminar shear stress on BBMvEC morphological characteristics, tight junction assembly and barrier function. Particular emphasis is also placed on claudin-5 and ZO-1 subcellular localization and occludin phosphotyrosine levels. Moreover, the effects of flow cessation following shear pre-conditioning of BBMvEC's are examined with respect to the aforementioned barrier indices.

3.2 Results

3.2.1: Morphology and positive characterization of BBMvEC's by von Willebrand Factor and claudin-5 staining

BBMvEC's were grown to confluency and monitored by phase-contrast microscopy for characteristic growth patterns (doubling time of approximately 24 h) and typical 'cobblestone' shaped morphology (Fig. 3.1 A). BBMvEC's cultured under similar conditions were fixed in situ and monitored by fluorescent microscopy following immunocytochemical (IC) staining protocol for expression of two endothelial specific markers. BBMvEC's stained positively for von Willebrand Factor (Fig. 3.1 B i) and claudin-5 (Fig. 3.2.1 B iii). Negative controls (Fig. 3.1 B ii, iv) showed no detectable, non-specific secondary antibody issues.

3.2.2: Exposure of BBMvEC's to laminar shear stress-induced cellular and filamentous (F)-actin realignment in the direction of the flow vector

Confluent BBMvEC's were subjected to laminar shear stress (10 dynes cm^{-2}, 24 h) and monitored for cellular realignment by phase-contrast microscopy (Fig. 3.2 i-ii) and fluorescent microscopy following IC protocol for F-actin (Fig. 3.2 iii-iv). Under sheared conditions, BBMvEC's and F-actin filaments realigned in the direction of the flow (Fig. 3.2 ii, iv). Under static (unsheared, 0 dynes cm^{-2}) conditions, BBMvEC's were randomly organised, with high expression levels of F-actin stress fibers exhibiting a random pattern of distribution (Fig. 3.2 i, iii).

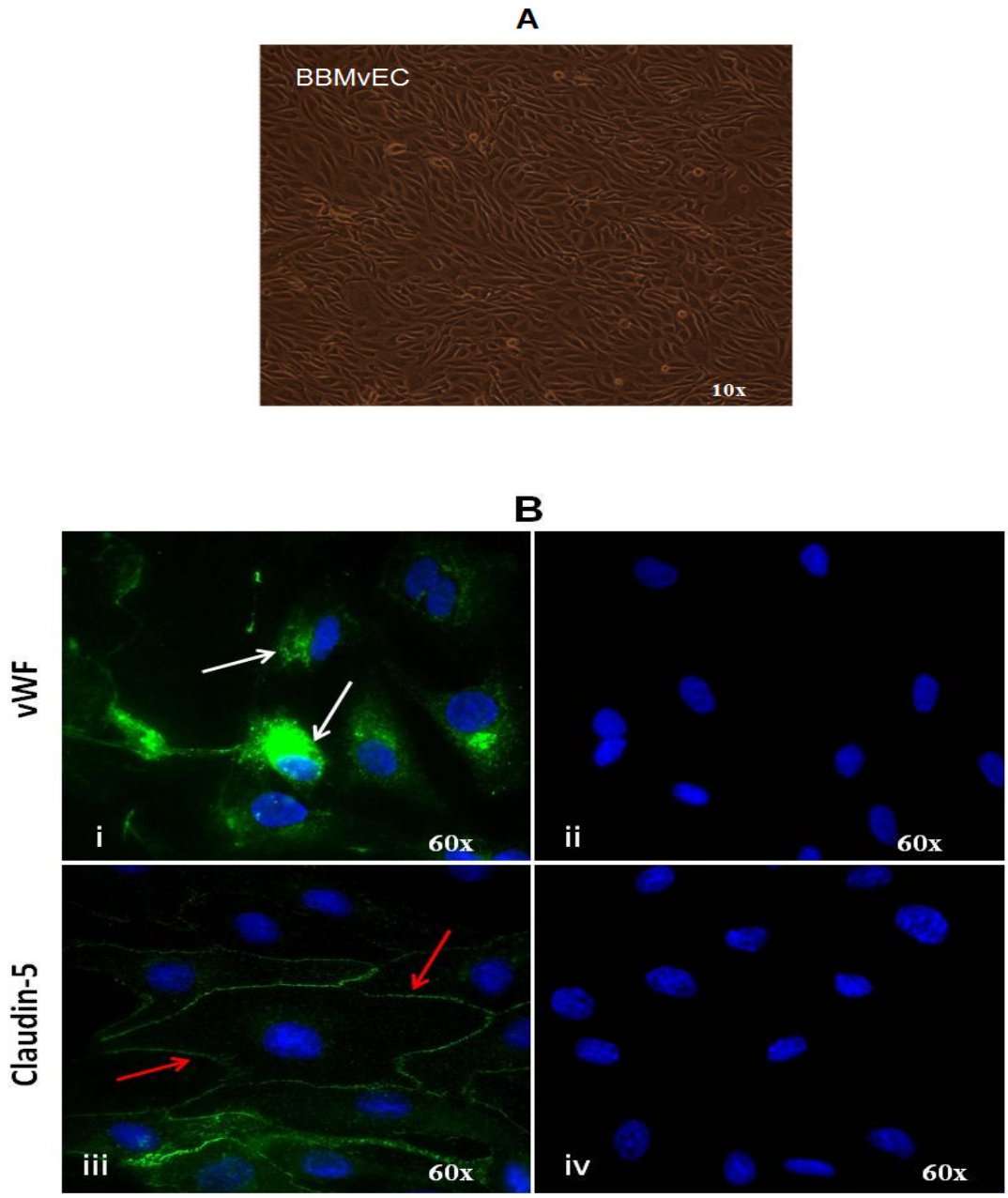

Fig. 3.1: Characterization of BBMvEC's. (A) Endothelial "cobblestone" morphology: (B) BBMvEC's were grown to confluency and monitored by fluorescent microscopy for: (i) Von Willebrand Factor (vWF) expression (green) as indicated by white arrows; (ii) vWF negative control – primary antibody exclusion with DAPI stained nuclei; (iii) Claudin-5 expression (green) and cell-cell border localization in BBMvEC as indicated by red arrows; (iv) Claudin-5 negative control – no primary antibody with DAPI stained nuclei. Images are representative.

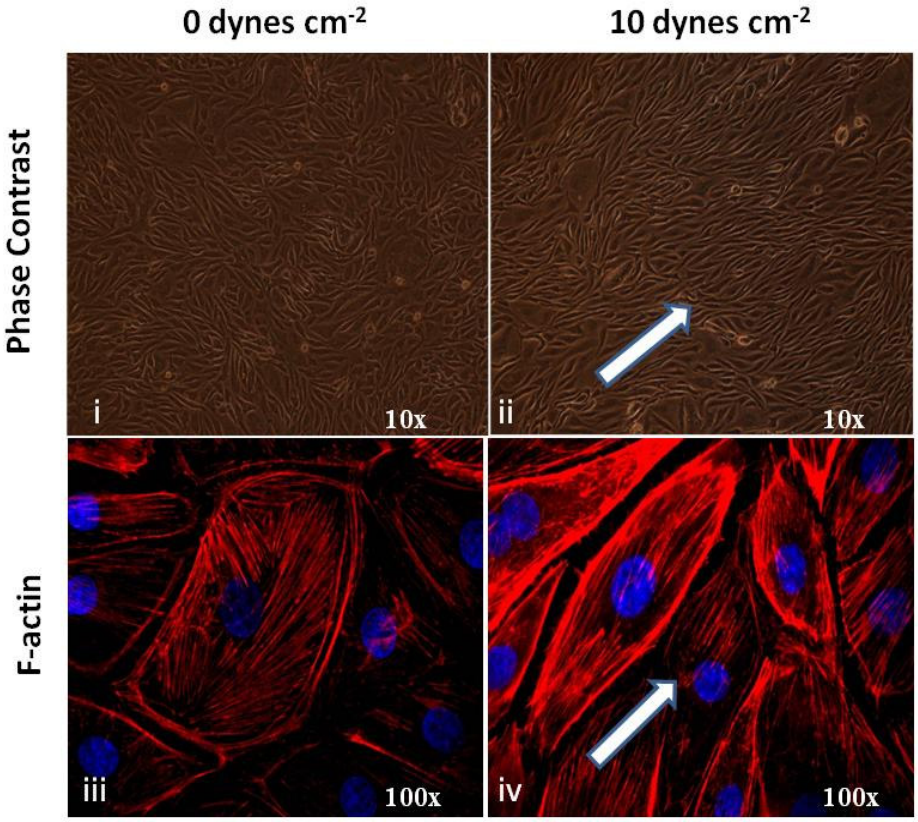

Fig. 3.2: Effect of laminar shear stress on BBMvEC and F-actin re-alignment. Confluent BBMvEC's were exposed to laminar shear stress (10 dynes cm^{-2}, 24 h) and monitored for morphological realignment by phase-contrast microscopy (i-ii) and fluorescent microscopy (rhodamine phalloidin stain for F-actin) (iii-iv). White arrows indicate the direction of the flow vector. DAPI stained nuclei (iii-iv) are clearly visible. Images are representative.

3.2.3: The impact of laminar shear stress on BBMvEC morphology and barrier function is magnitude-dependent

BBMvEC's at confluency were investigated for the effect of static (0 dyne cm^{-2}), low (1 dyne cm^{-2}) and high (10 dyne cm^{-2}) shear (24 h) on BBMvEC morphology and permeability as monitored by phase-contrast microscopy (Fig. 3.3 A) and transendothelial permeability assay (Fig. 3.3 B, C). Low levels of shear (Fig. 3.3 A ii) induced a random pattern of cellular organization as observed in static cultures (Fig. 3.3 A i) and did not resemble the characteristic BBMvEC realignment as observed following high shear exposure (Fig. 3.3 A iii). The trend for permeability, i.e. transendothelial exchange (TEE) of FITC-dextran 40 kDa (FD40) between different shear rates is depicted by Fig. 3.3 B. Taking the data for a specific time point (e.g. 120 min), a significant reduction in permeability (i.e. indicative of enhanced barrier function) was observed following high shear but not low shear (Fig. 3.3 C). No significant difference in permeability between static and low shear conditions were detected. All subseqent transendothelial permeability assays presented within this thesis will be depicted by a histogram using data from the 120 min time point.

3.2.4: Laminar shear-induced upregulation of BBMvEC barrier function and cellular realignment requires prolonged shear exposure

BBMvEC's were exposed to varying durations of laminar shear stress (10 dynes cm^{-2} 0-24 h) and monitored by phase-contrast microscopy for changes in cellular realignment (Fig. 3.4 A) and barrier function (Fig. 3.4 B). BBMvEC realignment in the direction of the flow only became evident 12 h post shear initiation with full realignment observed by 24 h of shear stress (Fig. 3.4 A). The changes in permeability (%TEE of FD40) versus shear exposure time is presented in Fig. 3.4 B. Significant reductions in transendothelial permeability became evident 6 h post shear initiation, with the most significant fold reductions observed at 12 and 24 h respectively.

Fig. 3.3

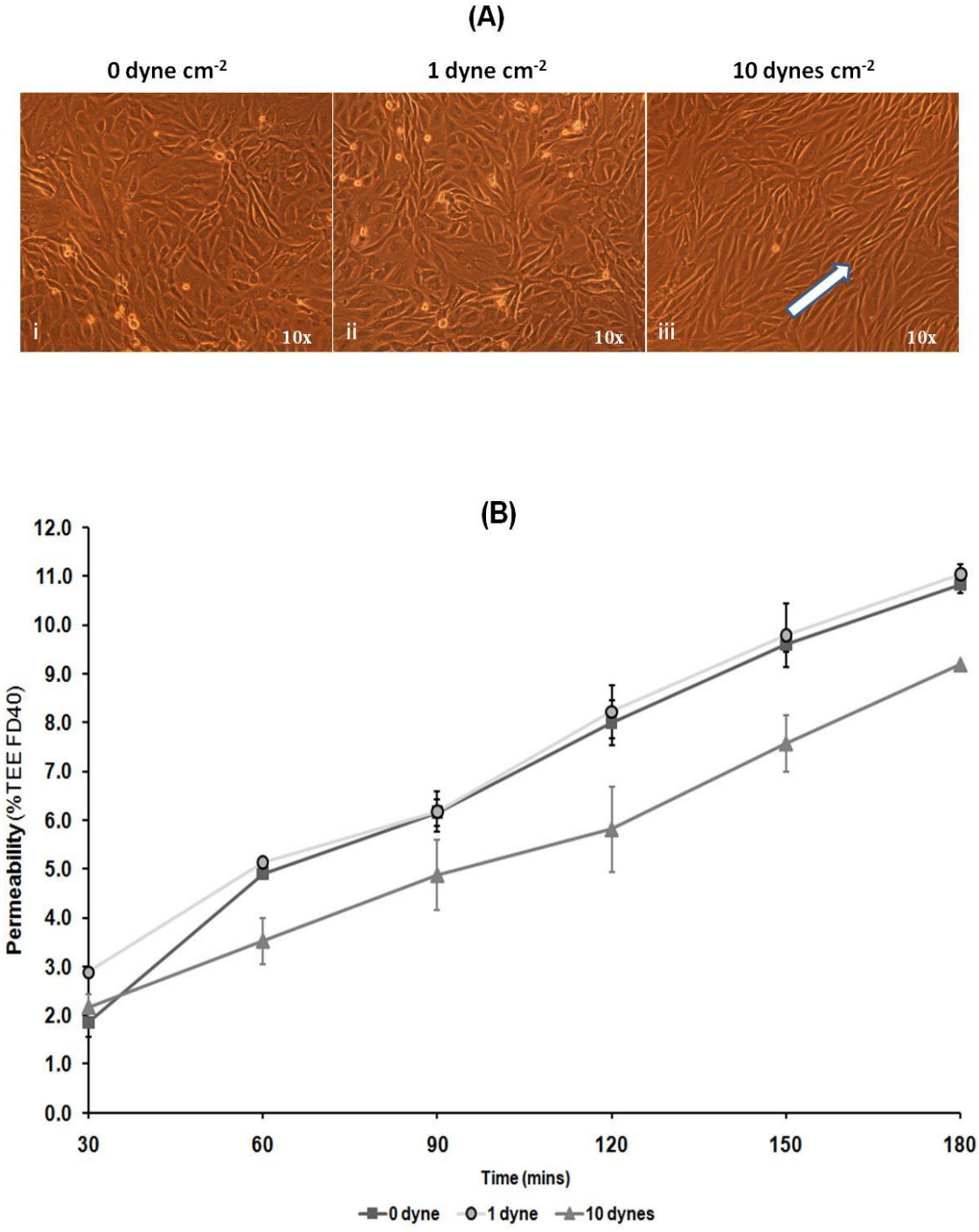
(A)
0 dyne cm-2
1 dyne cm-2
10 dynes cm-2
i
10x
ii
10x
iii
10x
(B)
Permeability (%TEE FD40)
12.0
11.0
10.0
9.0
8.0
7.0
6.0
5.0
4.0
3.0
2.0
1.0
0.0
30
60
90
120
150
180
Time (mins)
0 dyne
1 dyne
10 dynes

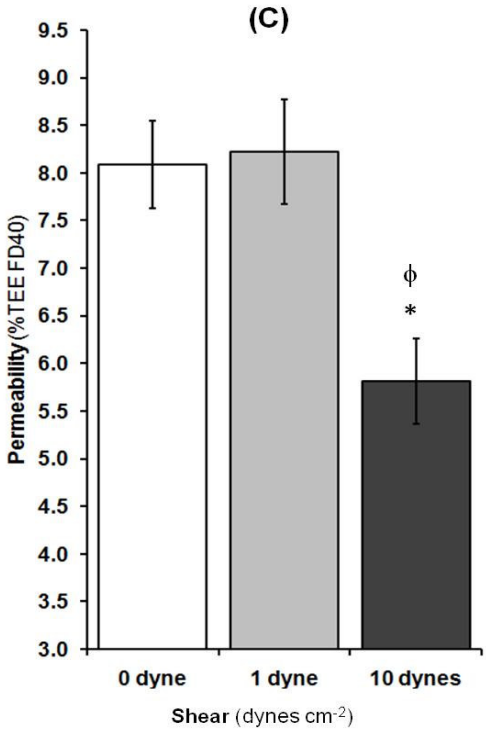

Fig. 3.3: Magnitude-dependent effects of shear stress on BBMvEC permeability and morphological realignment. Confluent BBMvEC's were subjected to non-physiological (1 dyne cm^{-2}) and physiological (10 dynes cm^{-2}) levels of laminar shear stress and monitored by: (A) Phase-contrast microscopy: (B, C) Transendothelial permeability. White arrow indicates direction of the flow vector (A iii). Line graph and histogram data points show change in permeability (% TEE FD40) at a given time point(s) (0-180 min, B), (time (t) =120 min, C). Results are averaged from three independent experiments ±SEM; $*P \leq 0.05$ vs static, $\phi P \leq 0.05$ vs 1 dyne cm^{-2}. Images are representative.

Fig. 3.4

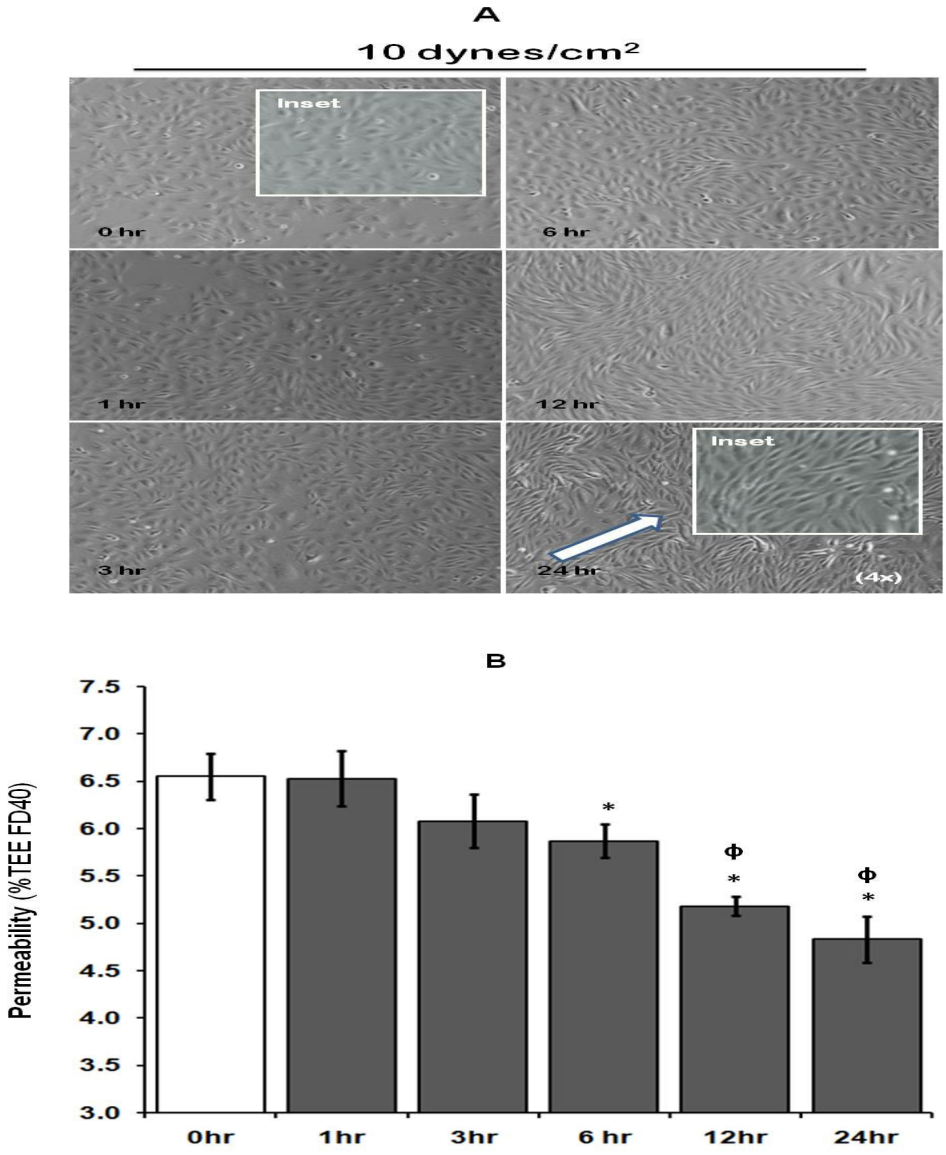

Fig. 3.4: Time dependent effects of shear stress on BBMvEC permeability and morphological realignment. Following laminar shear stress (10 dynes cm^{-2}, 0-24 h), BBMvEC's were monitored for morphological realignment by: (A) phase-contrast microscopy: (B) barrier function by transendothelial permeability assay. White arrow indicates the direction of the flow vector (A 24 h). (B) Histogram data points show change in permeability (% TEE FD40 at t=120 min) Results are averaged from three independent experiments ±SEM; *$P \leq 0.05$ vs static (0 h) ϕ$P \leq 0.05$ vs 6h. Images are representative.

3.2.5: Exposure of BBMvEC's to laminar shear stress enhances the cell-cell border localization of tight junction proteins, ZO-1 and claudin-5

Confluent BBMvEC's were exposed to laminar shear stress (10 dynes cm^{-2}, 24 h) and fixed in situ to be assessed by fluorescent microcopy following IC protocol for the subcellular localization of two pivotal tight junction proteins; ZO-1 and claudin-5 (Fig. 3.5). For unsheared samples (Fig. 3.5 i, iii), the staining pattern for ZO-1 and claudin-5 was quite jagged and discontinuous at the cell-cell border. This is in stark contrast to the enhanced immunoreactivity and continuous localization pattern of both ZO-1 (Fig. 3.5 ii) and claudin-5 (Fig. 3.5 iv) at cell-cell borders following shear stress.

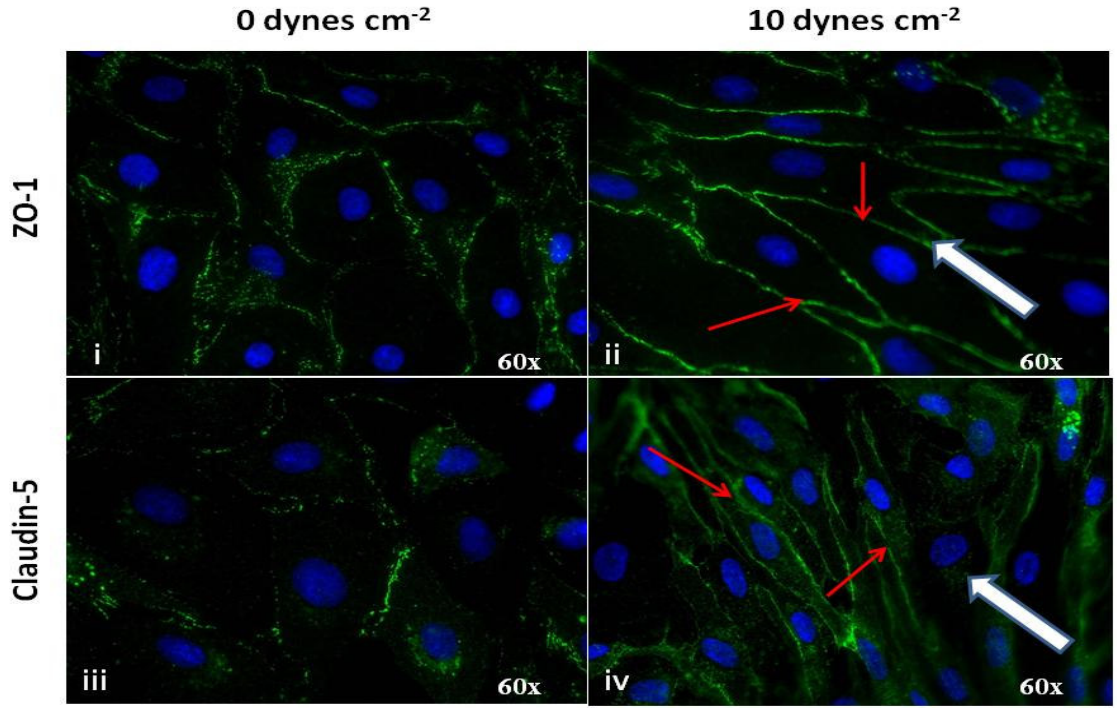

Fig. 3.5: Effect of laminar shear stress on ZO-1 and Claudin-5 localization. Confluent BBMvEC's were exposed to laminar shear stress (10 dynes cm^{-2}, 24 h) and monitored for staining patterns of the tight junction proteins ZO-1 (i-ii) and claudin-5 (iii-iv) by fluorescent microscopy. Red arrows (ii, iv) indicate sharp localization of tight junction proteins to cell-cell borders. White arrows (ii, iv) denote the direction of the flow vector. DAPI stained nuclei (i-iv) are clearly visible. Images are representative

3.2.6: Prolonged exposure of BBMvEC's to shear stress reduces occludin phosphotyrosine levels

Following exposure to laminar shear stress (10 dynes cm^{-2}, 0-24 h), BBMvEC's were subjected to immunoprecipitation (IP) and immunoblot (IB) analysis for phosphotyrosine (pTyr)-occludin levels. PTyr-occludin levels were substantially elevated following acute shear exposure to 1.76 fold±0.09 at 30 min shear and 1.39 fold ±0.10 following 60 min exposure. These values are in stark contrast to the pTyr-occludin levels observed following chronic shear (24 h), which were significantly below static baseline levels (0.38 fold±0.03) (Fig. 3.6 A, B).

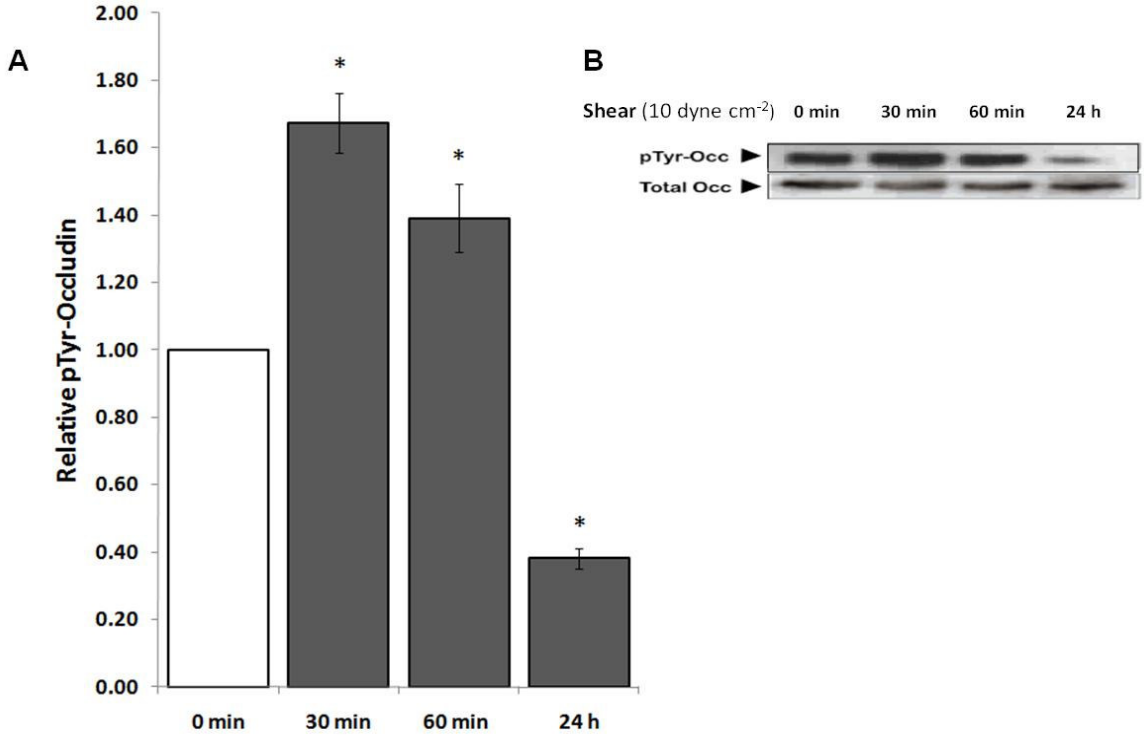

Fig. 3.6: Effect of laminar shear stress on occludin tyrosine phosphorylation. BBMvEC's were grown to confluence and subjected to laminar shear stress (10 dynes cm^{-2}) following which they were harvested at varying time points (0, 30, 60 min and 24 h) and monitored by IP/IB analysis for pTyr-occludin and total occludin levels. Histogram (A) represents relative pTyr-occludin (i.e. pTyr-occludin/total occludin derived by scanning densitometry from blots in B). Results are averaged from three independent experiments ±SEM; **P* ≤0.05 vs 0min. Scanned blots in (B) are representative.

3.2.7: Laminar shear-induced enhancement of BBMvEC barrier integrity involves tyrosine phosphatase activity

BBMvEC's at confluency were exposed to laminar shear stress (10 dynes cm^{-2}, 24 h) in the absence or presence dephostatin and monitored for changes in barrier function via transendothelial permeability assay. Shear significantly reduced permeability (%TEE of FD40) by 3.61% compared to the static control. However this shear-induced reduction in permeability was attenuated by 57.9% when dephostatin was present (following correction for the baseline increase with dephostatin under static conditions) (Fig. 3.7).

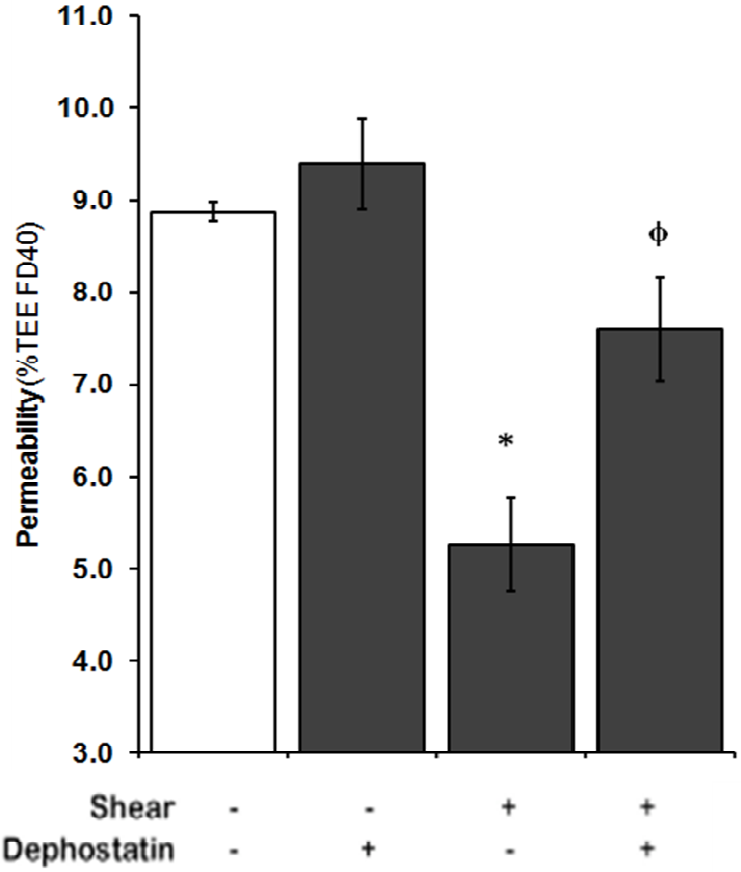

Fig. 3.7: Effect of dephostatin on laminar shear-induced BBMvEC barrier enhancement. Confluent BBMvEC cultures were either maintained under static conditions or exposed to laminar shear stress (10 dynes cm^{-2}, 24 h) in the absence and presence of the protein tyrosine phosphatase inhibitor, dephostatin and monitored for transendothelial permeability. Histogram data points show change in permeability (% TEE FD40 at t=120 min). Histogram is averaged from three independent experiments ±SEM; *$P \leq 0.05$ vs unhibited static, ϕ$P \leq 0.05$ vs unhibited shear.

3.2.8: Flow reduction following shear pre-conditioning of BBMvEC's leads to a reversal of shear-induced barrier stabilization, ZO-1 localization and increase in pTyr-occludin level

BBMvEC's were pre-sheared at 10 dyne cm^{-2} for 24 h after which, cells were split into two groups – those allowed to continue shearing at a sustained rate for 24 h and those allowed to continue shearing at a reduced rate of 1 dyne cm^{-2}, in both instances for a further 24 h (histogram inset in Fig. 3.8 A). Using an identical shearing protocol, BBMvEC's were monitored for cellular realignment by phase-contrast microscopy (Fig. 3.8 B i-iii) and fluorescent microscopy following IC protocol for ZO-1 (Fig. 3.8 B iv-vi). Following flow reduction, BBMvEC morphology reverted from the characteristic 'flow-aligned' phenotype (Fig. 3.8 B ii) to a more cobblestone pattern of cellular organization (Fig. 3.8 B iii) similar to observations in static cultures (Fig. 3.8 B i). Furthermore, ZO-1 localization at cell-cell borders was abrogated under flow reversal conditions (Fig. 3.8 B vi) compared to the characteristic cell-cell border localization of ZO-1 observed under sustained shearing conditions at 10 dyne cm^{-2} (Fig. 3.8 B v). BBMvEC's were then monitored for barrier as assessed by transendothelial permeability assay. A significant increase in permeability (%TEE FD40) was observed as pre-sheared BBMvEC's were reduced to 1 dyne cm^{-2} (Fig. 3.8 C). Finally this shear regime was employed to monitor pTyr-occludin levels. The characteristic decrease in pTyr-occludin levels (0.20 fold±0.04) in response to sustained shear at 10 dynes cm^{-2} relative to static control was substantially reversed (to 0.71 fold±0.054) by flow reduction to 1 dyne cm^{-2} (Fig. 3.8 D i-ii).

Fig. 3.8

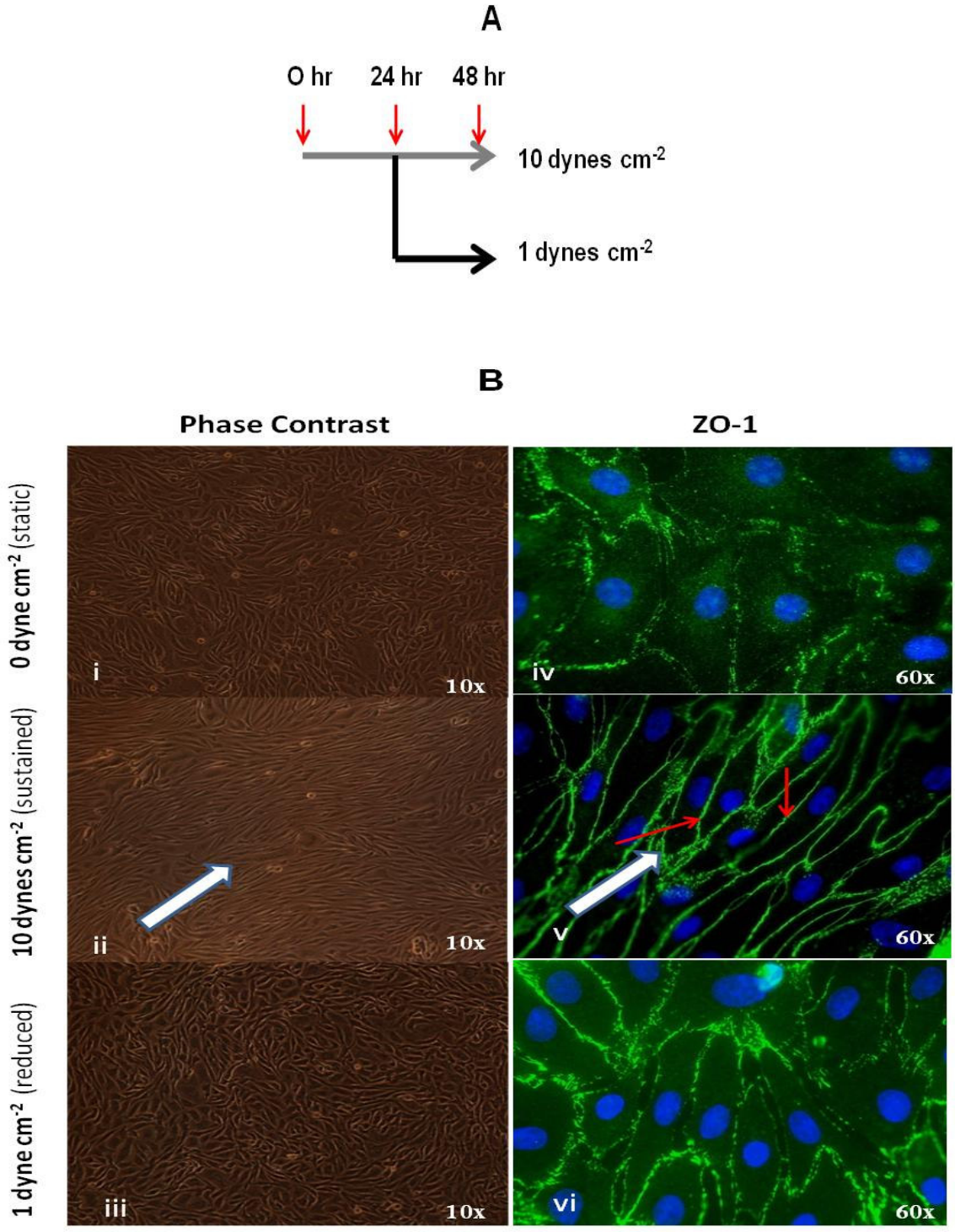
A
0 hr
24 hr
48 hr
10 dynes cm-2
1 dynes cm-2
B
Phase Contrast
ZO-1
0 dyne cm-2 (static)
10 dynes cm-2 (sustained)
1 dyne cm-2 (reduced)
i
10x
ii
10x
iii
10x
iv
60x
v
60x
vi
60x

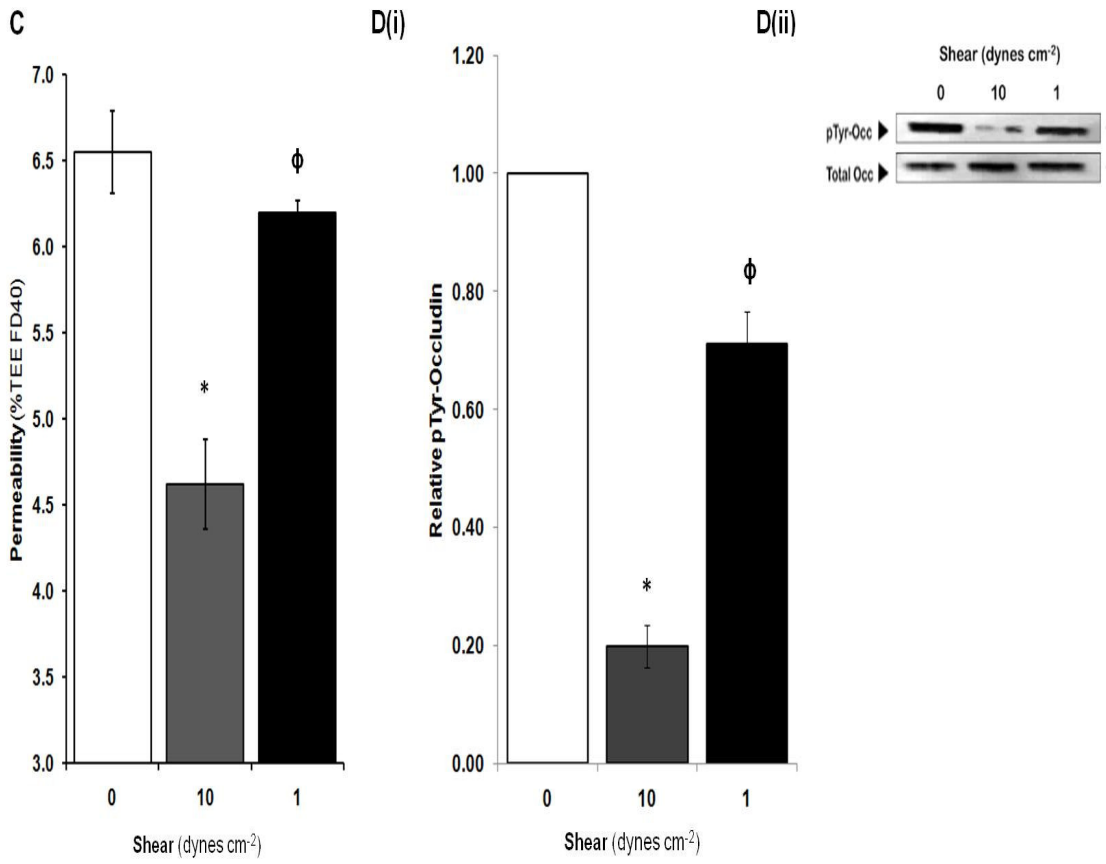

Fig. 3.8: Effect of flow reduction on the barrier properties of shear-preconditioned BBMvEC's. (A) In confluent cultures of laminar shear-preconditioned BBMvEC's (10 dynes cm^{-2}, 24 h), flow was either sustained at 10 dynes cm^{-2} for a further 24 h or reduced to 1 dyne cm^{-2} (24 h) as shown by schematic inset. (B): Following flow reduction protocol, BBMvEC's were monitored for morphological realignment by phase- contrast microscopy (i-iii) and ZO-1 staining by fluorescent microscopy (iv-vi). Red arrows (v) indicate localization of ZO-1 to cell-cell borders. White arrows (ii and v) denote direction of the flow vector. DAPI stained nuclei (iv-vi) are clearly visible. Images are representative. (C): BBMvEC's were then monitored for barrier function by transendothelial permeability assay. Histogram data points show change in permeability (% TEE FD40 at t=120 min). Histogram is averaged from three independent experiments ±SEM; *$P \leq 0.05$ vs 0 dynes cm^{-2} (static) ϕ$P \leq 0.05$ vs 10 dynes cm^{-2} (sustained). (D): Illustrates the effect of shear pre-conditioning (10 dynes cm^{-2}, 24 h) followed by sustained flow (10 dynes cm^{-2}, 24 h) or flow reduction (1 dyne cm^{-2}, 24 h) on pTyr-occludin and total occludin levels. Histogram represents relative pTyr-occludin (i.e. pTyr-occludin/total occludin as derived by scanning densitometry from blots in D ii). Results are averaged from three independent experiments ±SEM; *$P \leq 0.05$ vs static, ϕ$P \leq 0.05$ vs shear 10 dynes cm^{-2}. Blots are representative (D ii).

3.2.9: Shear-dependent enhancement of BBMvEC barrier function occurs via paracellular mechanisms

A control study was conducted in which BBMvEC's at confluency were exposed to laminar shear stress (10 dynes cm^{-2} 24 h) and monitored for changes in paracellular permeability using APTS-dextran. This molecule has been previously validated to be a paracellular specific marker (Neuhaus et al., 2006). Using ATPS-dextran, shear reduced permeability (%TEE FD40) from 23.1% to 18.35%, (i.e. 0.21±0.03 fold reduction), which is very similar to the fold reduction in permeability observed with FITC-dextran (Fig. 3.9).

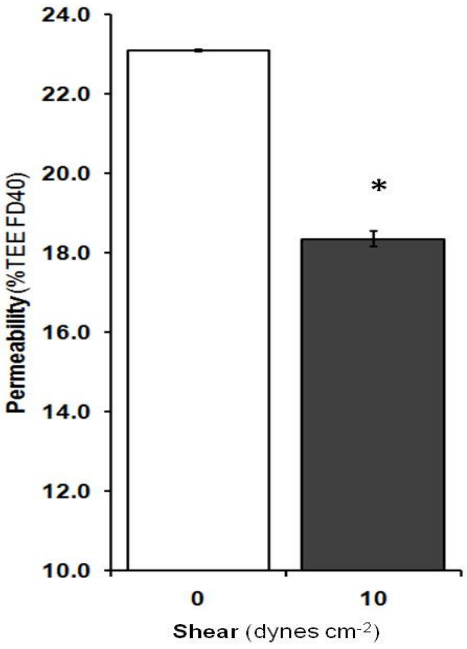

Fig. 3.9: Effect of shear stress on BBMvEC permeability using the "paracellular" marker, APTS-dextran. Confluent BBMvEC were exposed to laminar shear stress (10 dynes cm^{-2}, 24 h), and monitored for transendothelial permeability using the paracellular-specific label APTS-dextran. Histogram data points show change in permeability (% TEE FD40 at t=120 min). Histogram is averaged from three independent experiments ±SEM; *$P \leq 0.05$ vs 0 dynes cm^{-2}.

3.3 Discussion.

EC's of the BBB *in-vivo* are physiologically regulated by a multitude of signaling mediators that encompass both humoral and hemodynamic stimuli. A further dimension to BBB regulation involves local, chemical input from the surrounding neurovascular unit. Together these contribute to a functional BBB phenotype that protects the CNS from fluctuations in changes in concentrations of ions, neurotransmitters, blood-borne factors and various toxins/pathogens that could affect neuronal and/or glial function. Traditionally, the majority of experimental evidence from *in-vitro* studies has utilized various co-culture or tri-culture model systems consisting of brain EC's, astrocytes and/or pericytes to recapture the in situ 'conditioning' of brain EC's (for comprehensive review see Deli *et al.* 2005). These models have proved to be invaluable tools in expanding our understanding in the induction of BBB specific properties, such as high TEER, expression of BBB-specific transporters and ion channels and thus serve as more viable methods to study BBB function. However, the major disadvantage of some of these models is that they lack the input of flow-associated shear stress.

Efforts in more recent years have sought to overcome this, with the establishment of the DIV-BBB (dynamic *in-vitro*) model, which allows real time monitoring of barrier function (Cucullo et al., 2002). Notwithstanding this there is still a genuine lack of knowledge regarding the cellular signaling processes involved in the flow-induced regulation of BBB function. Previous work conducted in this laboratory by Colgan *et al.* investigated the regulation of brain microvascular endothelial tight junction assembly and barrier function by laminar shear stress using a mono-culture BBMvEC model (Colgan et al., 2007). With this particular chapter, we sought to expand on these basic findings and further develop our insight into the cellular phenomenology regarding shear-dependent enhancement of BBB function.

Throughout the course of this project, BBMvEC's were routinely monitored for endothelial specific markers vWF and claudin-5, to ensure they retained their properties *in-vitro*. Furthermore we observed the characteristic shear-induced realignment of EC's in the direction of the flow following laminar shear stress (10 dynes cm^{-2}, 24 h) relative

to static (unsheared) controls, findings consistent with the parallel organization of F-actin stress fibers in the direction of flow. This cellular adaptation to blood flow is an essential process EC's undergo to reduce mechanical loading and subsequent injury. Moreover, based on the immunocytochemical staining pattern of F-actin, there was enhanced cortical actin localization at the cell-cell borders suggesting increased association with intercellular junction components, i.e. adherens and tight junctions. This morphological feature of EC's is frequently associated with vessel homeostasis and indicative of an upregulated barrier phenotype (Lai et al., 2005, Jacobson et al., 2006, Spindler et al., 2010).

Although the preliminary BBMvEC experimental work discussed above was performed using the static (unsheared/0 dyne cm^{-2}) condition as control, we also sought to investigate the effect of a more physiologically relevant control within the context of vascular flow patterns to assess any possible discrepancies in using static cultures. To this end, we used low shear stress (1 dyne cm^{-2}), which falls within a non-physiological paradigm and is prevalent in atherosclerotic-prone and flow compromised regions of the vasculature (Krizanac-Bengez et al., 2004, Davies, 2009). There was however no detectable difference in BBMvEC permeability between static and low shear protocols. Furthermore, BBMvEC's under low shear were unable to realign with the flow, clearly exhibiting a morphological resemblance to static BBMvEC cultures. In view of this, subsequent experiments routinely employed the static condition as control.

As a control to ensure our permeability assay with FITC-dextran was indeed measuring paracellular (not transcellular) flux, we prepared a fluorescent ATPS-dextran conjugated label from first principles. This molecule is extremely hydrophilic with 3 negatively charged sulfonic acid groups and its structural characteristics hamper its binding to transcellular active transport systems, thus making it a paracellular specific marker (Neuhaus et al., 2006). Our experiments demonstrated that the shear-induced fold decrease in permeability was very similar with either APTS-dextran (paracellular only) or FITC-dextran, suggesting that the latter marker is principally recording paracellular transport.

Studies have previously shown that prolonged (> 24 h) exposure of physiological levels of shear stress enhances the barrier properties of brain endothelial monolayers (Colgan et al., 2007, Siddharthan et al., 2007). We sought to expand on this knowledge and temporally monitor shear-induced enhancement of BBMvEC barrier integrity. In this regard, significant decreases in permeability became evident 6 h post shear initiation, however the most noticeable responses observed following chronic shear exposure at 12 and 24 h. In a subsequent control experiment, no detectable difference in permeability between 24 and 48 h was detected (data not shown). Furthermore, the pattern of cellular realignment under shear stress appeared to mimic these functional responses as the most noticeable changes in BBMvEC realignment with flow were observed at the 12 and 24 h points. Interestingly, shear initiation (1 h) did not significantly alter BBMvEC barrier function. This period of flow onset is associated with dramatic cytoskeletal remodeling and pro-inflammatory conditions, which would imply that the endothelial barrier would be compromised and permeability increased (Hahn and Schwartz, 2009). Perhaps a more sensitive model which allows for real-time monitoring of barrier integrity by transendothelial electrical resistance would refine such a possible discrepancy.

Having established a reliable model of shear-induced (10 dynes cm^{-2}, 24 h) regulation of BBMvEC barrier function, our focus shifted to the tight junction components likely mediating these effects. Apically located tight junctions represent the primary form of maintenance to paracellular permeability, and alterations in their regulation contribute to permeability changes in a variety of disease states (Harhaj and Antonetti, 2004, Lee et al., 2004, Liu et al., 2008). Consistent with our findings of enhanced barrier function following shear (10 dynes cm^{-2}, 24 h), we observed enhanced immunoreactivity of claudin-5 and ZO-1 at intercellular junctions. ZO-1 presents a structural anchor for the insertion of other tight junction proteins such as claudin-5 and occludin, which provide the physical barrier to solute flux via homo/heterophilic interaction with partners from adjacent EC's. Unsheared BBMvEC's exhibited a substantially decreased immunoreactivity of both ZO-1 and claudin-5 at cell borders with a discontinuous, broken staining pattern.

We further extended our understanding of the mechano-regulation of BBB function by assessing post-translational modifications of the tight junction component occludin, on tyrosine residues. The significance of phosphotyrosine (pTyr) occludin levels to barrier integrity has been frequently cited in the literature. Following shear onset (0-60 min), we observed a significant increase in pTyr-occludin above static levels, a finding consistent with previous work using a similar shear regimen in bovine aortic endothelial cells (DeMaio et al., 2001). However, this acute increase is in complete contrast to the profound reduction in pTyr-occludin observed following chronic shear exposure (24 h) suggesting pTyr-occludin is essential for BBB adaptation to, and function under flow. This somewhat paradoxical shift in pTyr-occludin levels could be explained by the profound remodeling processes that EC's undergo during the acute phase of shear initiation (Hahn and Schwartz, 2009). Furthermore, tyrosine phosphorylation of occludin is known to lead to reduced association with ZO-1, which likely explains the scattered ZO-1 localization observed in static BBMvEC's (Kale et al., 2003). In addition, the two extracellular loops of occludin are rich in tyrosine residues and their phosphorylation status could possibly dictate the strength of the homophilic binding between opposing occludin strands, or its interlocking with ZO-1, either of which would have a significant impact on paracellular permeability. In a further development of this finding, we assessed the effect of protein tyrosine phosphatase (PTP) inhibition on shear-induced regulation of barrier function using dephostatin (Imoto et al., 1993). Molecular inhibition of PTP significantly attenuated the shear-induced increase in barrier integrity by 57.9% suggesting a putative role for PTP's in maintaining barrier function.

Cerebral ischemia is an irreversible neurodegenerative disorder of which decreased shear stress is believed to be one of three major initiating components of 'Virchow's Triad' (along with thrombosis and loss of microvascular barrier function) (Krizanac-Bengez et al., 2006b, Krizanac-Bengez et al., 2006a, del Zoppo, 2008). We therefore sought to investigate the effect of decreased flow on BBMvEC barrier function. Our findings demonstrate that when flow is reduced (1 dyne cm^{-2}, 24 h) following preconditioning at 10 dyne cm^{-2} (24 h), both BBMvEC permeability and

phosphotyrosine occludin levels return to pre-shear levels, in parallel with a complete loss of shear-induced cellular realignment. Moreover, ZO-1 cell border immunoreactivity was abrogated as inter-endothelial gaps between cells became apparent. Molecular alterations of tight junction proteins during ischemic stroke progression have previously been reported in the literature. Kago and colleagues showed a reduced expression of occludin and ZO-1, in addition to increased pTyr-occludin levels following cerebral ischemia, whilst more recent experiments by Takenaga *et al.* implicating the protein tyrosine kinase (PTK) Src as a putative mediator of this post-translational phosphorylation state of occludin (Kago et al., 2006, Takenaga et al., 2009). Interestingly, recent work by Salle and Burrdige implicated a specific role for the tyrosine phosphatase DEP-1 (density enhanced phosphatase-1) in dephosphorylating occludin and ZO-1, consistent with increased barrier function, albeit in epithelial cells (Sallee and Burridge, 2009). It seems apparent that a coordinated activation/de-activation of PTK's and PTP's is crucial to tight junction assembly, and thus barrier function, including BBB function in response to flow. As a complete attenuation of shear-induced barrier regulation with PTP was not achieved within our model using dephostatin, it is plausible that PTK's are also involved in regulating pTyr-occludin levels. Future work could address this issue and also attempt to identify the specific phosphatase(s) and kinase(s) involved.

Chapter 4:

The contribution of RhoGTPases, Rac1 and RhoA, to shear-induced adaptation of BBMvEC tight junction assembly and barrier function.

4.1 Introduction

Maintenance of a dynamic yet stable BBB is a prerequisite for CNS homeostasis. In this regard, physiological levels of blood flow-associated laminar shear stress are of crucial importance, and have been extensively documented to control the structural integrity of the endothelial monolayer (Stanness et al., 1999, Krizanac-Bengez et al., 2004, Colgan et al., 2007, Siddharthan et al., 2007). Vascular EC's responding to such physiological conditions undergo dramatic actin-cytoskeletal remodeling, which induces an elongated cellular phenotype aligned in the direction of the flow, aswell as enhanced cortical actin accumulation at the cell periphery. Most notably, tight and adherens junction complexes are associated with the cortical actin cytoskeleton through associations with adaptor molecules ZO-1 and catenin (α-, β-, p120-) family members respectively. It is widely accepted that these associations enhance the 'stiffness' of the cell periphery, thus stabilizing the endothelial barrier (Jacobson et al., 2006, Waschke et al., 2006). Conversely, breakdown of endothelial integrity is believed to be a consequence of increased centripetal tension created by actomyosin contractility, thus destabilizing intercellular adhesion (Wojciak-Stothard and Ridley, 2002).

The RhoGTPases, and in particular its family members RhoA, Rac1 and Cdc42 have been extensively documented for their ability to profoundly influence cytoskeletal dynamics. There is a wealth of evidence from *in-vivo* and *in-vitro* studies incorporating EC's predominantly of macrovascular origin, culminating in a generally well-accepted view that RhoA disrupts the endothelial barrier, whereas Rac1 serves to strengthen/stabilize cell-cell junctions (Spindler et al., 2010, Beckers et al., 2010). Studies on Cdc42 have shown that its activation is essential to barrier restoration subsequent to injury (Kouklis et al., 2004, Waschke et al., 2006). Moreover, these GTPases have been shown to be hemodynamically sensitive. However, coupled to the fact that there is genuine lack of knowledge regarding laminar shear-induced upregulation of tight junction assembly at the BBB, there is little or no evidence of studies that have assessed signaling mechanisms pertaining to such effects in the cerebral microvasculature.

In this chapter we examine the potential role of the RhoGTPases, Rac1 and RhoA in the shear-dependent regulation of BBMvEC tight junction assembly and barrier function.

4.2 Results

4.2.1: Post-transfection efficiency/viability: Microporation versus Amaxa Nucleofection.

BBMvEC's were monitored by two different electroporation mechanisms (Amaxa nucleofection and microporation) to determine the most appropriate method of plasmid DNA delivery for genetic manipulation studies. Initial optimization of each system required fine tuning of electrical parameters, plasmid DNA concentration and cell number. Once this was achieved, the two systems were compared for cell viability and transfection efficiency. BBMvEC's monitored by phase-contrast microscopy 24 h post transfection revealed noticeably better cell viability (and morphology) with microporation compared to nucleofection (Fig. 4.1 A i-ii). Analysis of enhanced Green Fluorescent Protein (eGFP) expression by fluorescent microscopy revealed a negligible difference in eGFP uptake between the two methods (Fig. 4.1 A iii-iv), although quantitative evaluation of eGFP by FACS analysis revealed a transfection efficiency of 52.92% compared to 35.05% in favour of microporation (Fig. 4.1 B). As a result, all subsequent transfections were performed using microporation.

4.2.2: Laminar shear stress regulates BBMvEC Rac1-GTP activity.

BBMvEC's subjected to laminar shear stress (10 dynes cm^{-2}, 0-24 h), were monitored for acute (0-60 min) and chronic (24 h) effects on Rac1 total protein and Rac1-GTP levels. Acute and chronic shear exposure did not alter Rac1 protein levels (Fig. 4.2 A i). Interestingly, shear onset (within 1 min) triggered a small decrease (to 0.74±0.09 fold) in Rac1-GTP followed by a 1.54±0.06 fold increase of Rac1-GTP above static levels at 60 min shear. Levels of Rac1-GTP following chronic exposure of shear stress were 1.75±0.08 fold above static values. Forskolin and NSC23766 exerted their respective positive (1.31±0.01 fold) and negative (0.72±0.07 fold) control effects on Rac1-GTP levels (Fig. 4.2 A ii).

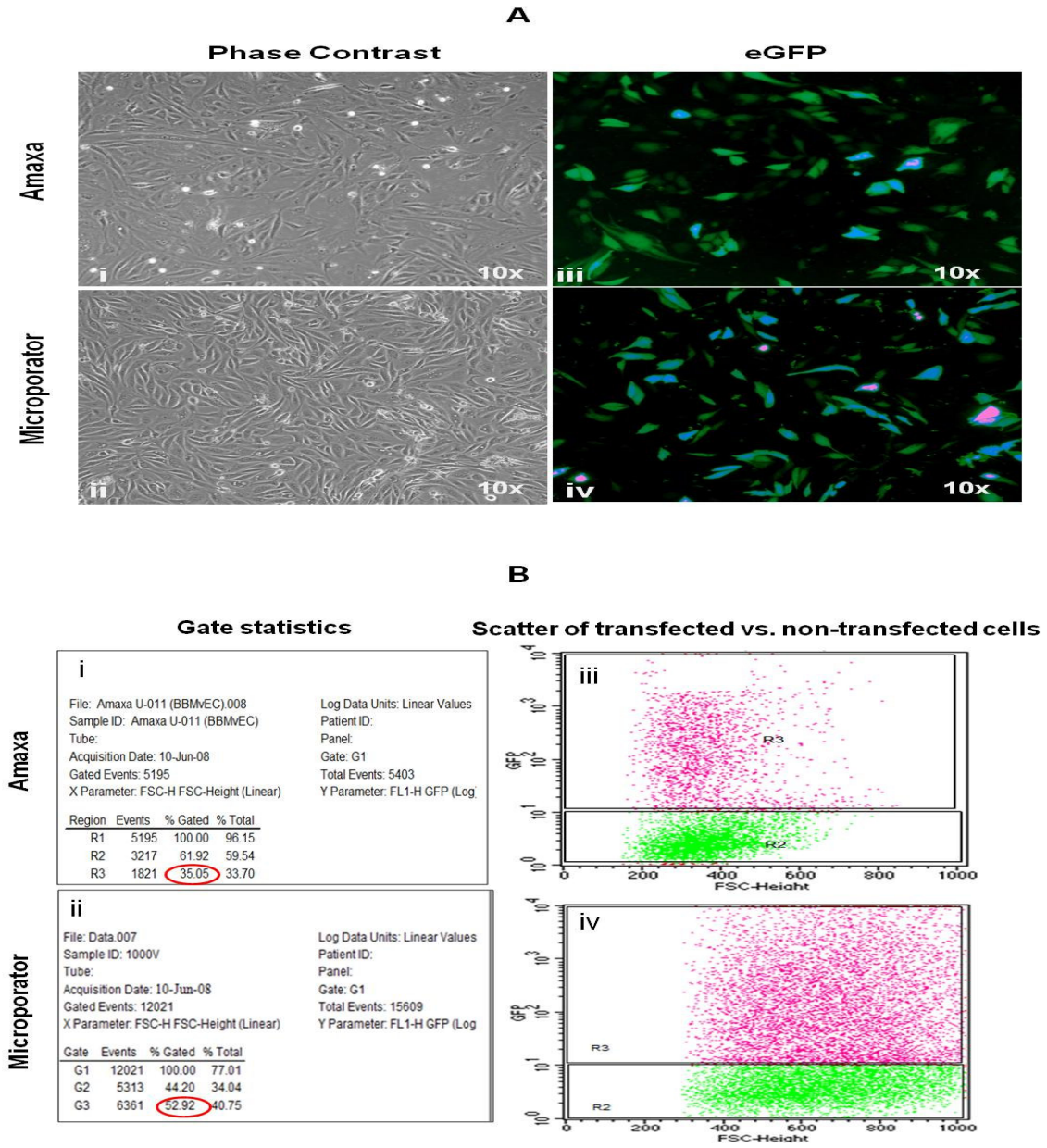

Fig. 4.1: Assessment of plasmid DNA transfection viability and efficiency via Amaxa nucleofection and microporation. BBMvEC's were grown to 70-80% confluency and subjected to electroporation protocols described in sections 2.4.1 and 2.4.2. The following day, BBMvEC's were monitored for cell viability by: (A i-ii) phase-contrast microscopy, and eGFP transfection efficiency via: (A iii-iv) fluorescent microscopy and: (B) FACS analysis. Scatter plots in (B iii-iv) show the regions of non-transfected cells (R2) vs. the region of transfected cells (R3), which represent the gate statistics generated (B i-ii) and the overall transfection efficiency encircled in red. Images shown are representative.

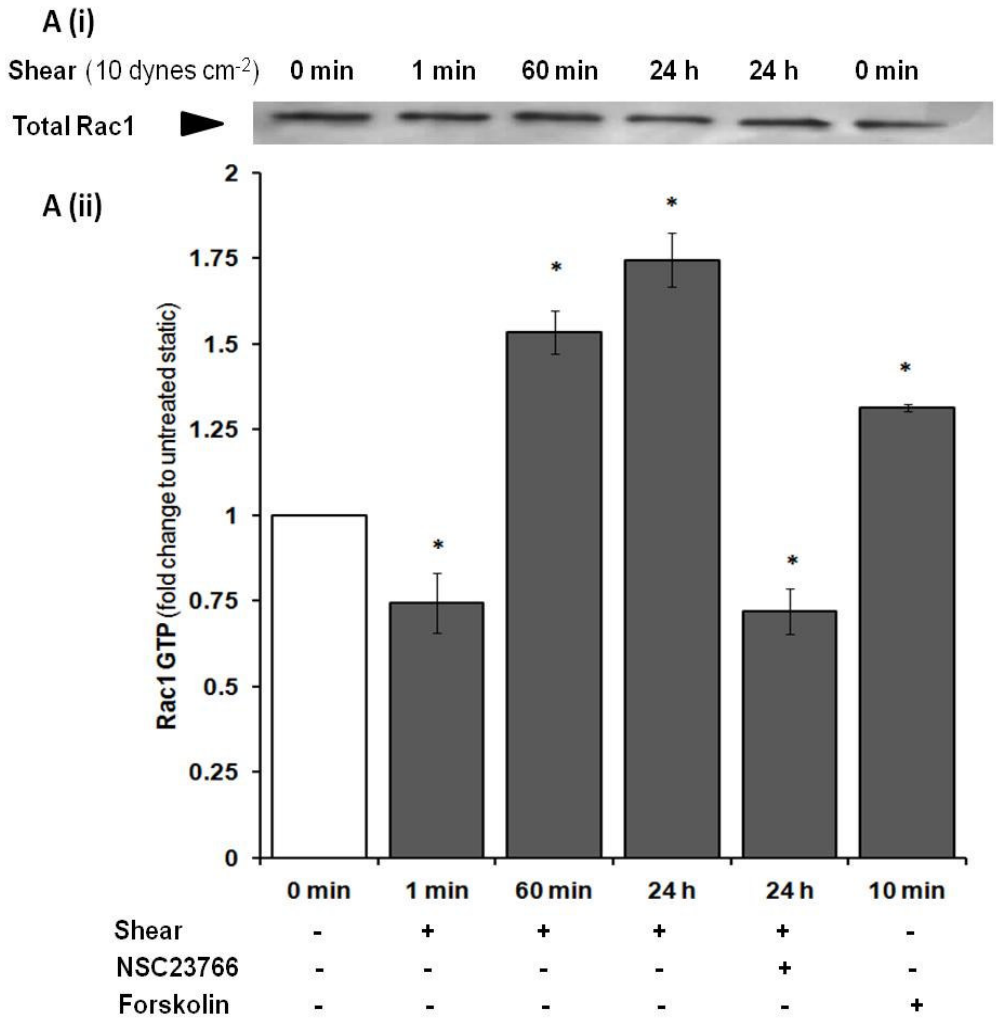

Fig. 4.2: Effect of laminar shear stress on Rac1 activation. BBMvEC's were cultured as described in section 2.6.1 and exposed to laminar shear stress (10 dynes cm^2), following which they were harvested at varying time points (0-60 min and 24 h) and monitored by: (A i) IB analysis for total Rac1 levels and (A ii) Rac1-GLISA® activation assay for Rac1 GTP levels. Forskolin (5 μM, 10 min treatment) and NSC23766 (50 μM, 24 h treatment) were included as positive and negative controls, respectively, for Rac1 activation. Results are averaged from three independent experiments ±SEM; *P≤0.05 vs. 0 min. Blots are representative.

4.2.3: Laminar shear stress-induced BBMvEC morphological/cytoskeletal realignment is Rac1-dependent.

As observed in section 3.2.2, the common characteristic response of EC's to prolonged laminar shear stress (10 dynes cm^{-2}, 24 h) is their morphological and F-actin realignment in the direction of the flow vector in tandem with cortical actin accumulation at the cell periphery. These responses were found to be Rac1-dependent as blockade of Rac1 activation via NSC23766 strongly attenuated shear-induced BBMvEC morphological (Fig. 4.3 A iv) and F-actin (Fig. 4.3 B iv) realignment, and diminished cortical actin assembly. Treatment with NSC23766 had no observable impact on static BBMvEC morphology as observed by phase-contrast microscopy (Fig. 4.3 A ii).

4.2.4: Laminar shear stress-induced upregulation of BBMvEC barrier function is Rac1 dependent.

As observed in section 3.2.4, laminar shear stress (10 dynes cm^{-2}, 24 h) reduces BBMvEC permeability (i.e. upregulates barrier function). We therefore employed two methods of Rac1 inhibition using NSC23766 and T17N (dominant negative mutant) to assess the potential role of Rac1 in the shear-dependent enhancement of BBMvEC barrier function. At t =120 min, shear significantly reduced permeability (%TEE of FD40), however the shear-induced reduction in permeability was attenuated by 88.7% and 76.6% with NSC23766 and T17N respectively (following correction for the baseline increase with NSC23766/T17N under static conditions) (Fig. 4.4 A/B i). Overexpression of T17N was confirmed by IB analysis for total Rac1 levels (Fig. 4.4 B ii).

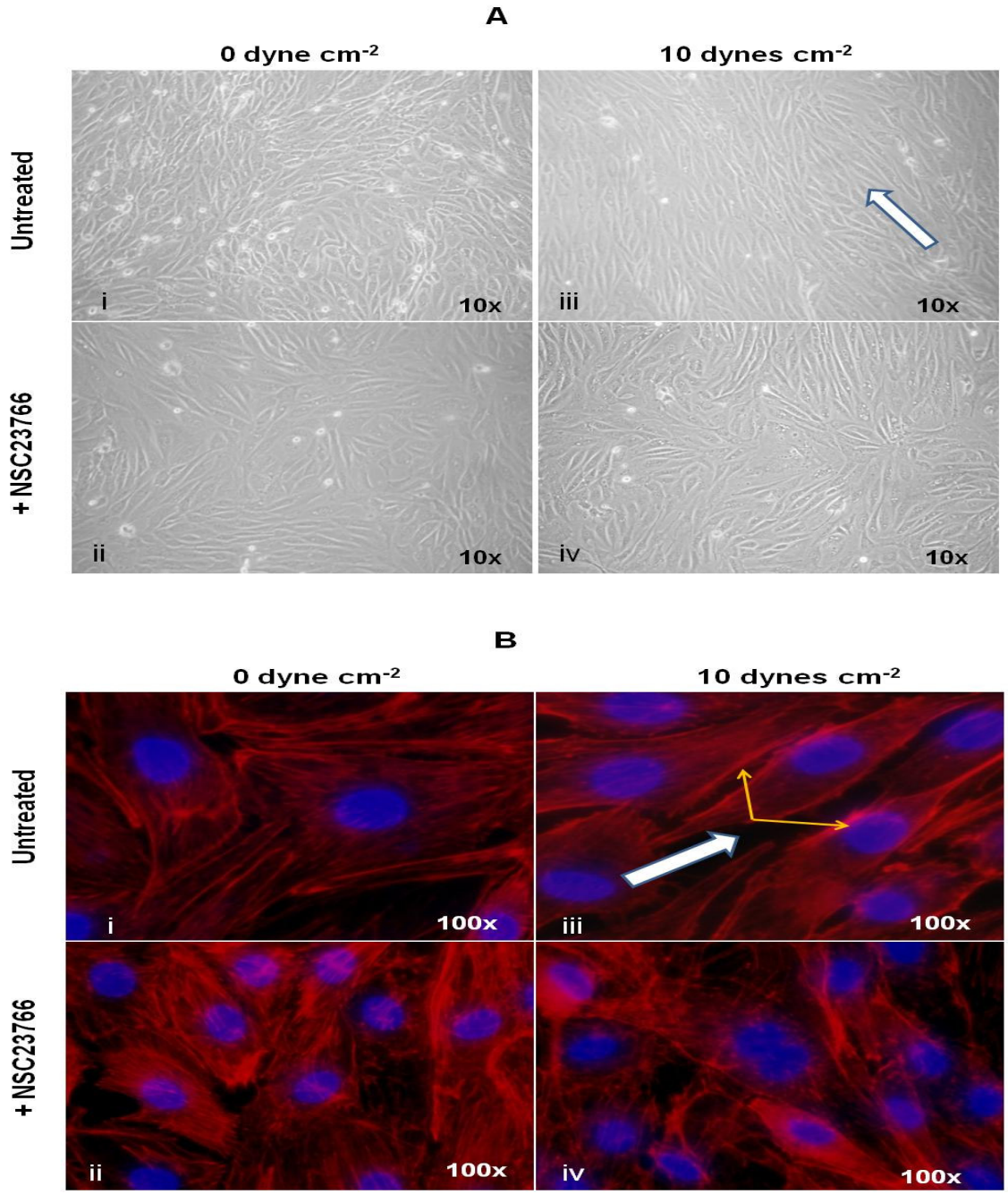

Fig. 4.3: Effect of Rac1 inhibition on laminar shear-induced BBMvEC morphological and F-actin realignment. Following exposure to laminar shear (10 dynes cm^{-2} 24 h) in the absence and presence of 50 μM NSC23766, BBMvEC realignment was monitored by: (A) phase-contrast microscopy and (B) fluorescent microscopy (rhodamine-phalloidin stain for F-actin). White arrows indicate direction of the flow vector (A/B iii). Yellow arrows indicate cortical actin (B iii). DAPI stained nuclei (blue) are clearly visible (Bi-iv). Images are representative.

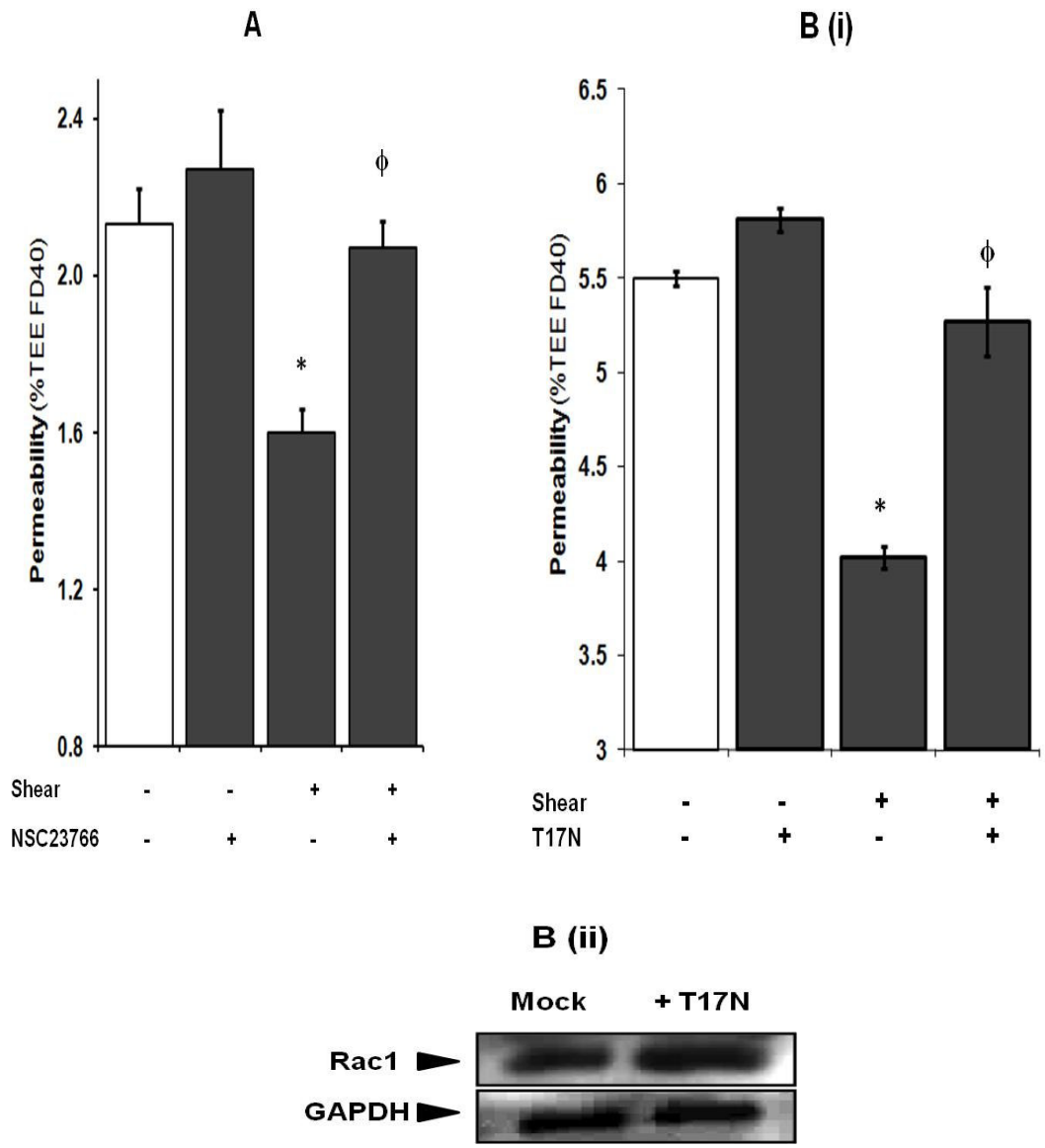

Fig. 4.4: Effect of Rac1 blockade on laminar shear-induced regulation of BBMvEC permeability. Confluent BBMvEC cultures were either maintained under static conditions or exposed to laminar shear stress (10 dynes cm^{-2}, 24 h) in the absence and presence of NSC23766 and T17N monitored for transendothelial permeability. Histogram data points show change in permeability (% TEE FD40 at t=120 min) (A/B i). Histogram is averaged from three independent experiments ±SEM; **P*≤0.05 vs uninhibited static, ϕ*P*≤0.05 vs uninhibited shear. Overexpression of Rac1 in tandem with GAPDH (as loading control) was assessed by IB (B ii). Blots are representative.

4.2.5: Laminar shear stress-induced localization of ZO-1 requires Rac1 activation.

Consistent with an intact endothelial barrier, ZO-1 immunoreactivity in response to laminar shear stress (10 dynes cm^{-2}, 24 h) displays a continuous, well-defined localization pattern along cell-cell borders (section 3.2.5). Two methods of Rac1 inhibition (NSC23766 and T17N) were incorporated to assess their potential involvement in this shear-dependent process. Both molecular and pharmacological inhibition strategies abrogated shear-induced ZO-1 alignment at cell-cell junctions (Fig. 4.5 i-vi). Baseline effects of both NSC23766 and T17N (i.e. relative to untreated static BBMvEC's) were not apparent.

4.2.6: Laminar shear stress-induced tyrosine dephosphorylation of occludin is Rac1 dependent.

Having already established that prolonged shear exposure (10 dynes cm^{-2}, 24 h) induces a significant reduction in occludin phosphotyrosine (pTyr-occludin) levels (section 3.2.6), we next investigated the potential involvement of Rac1 in this process. In this regard, laminar shear induced a substantial reduction in pTyr-occludin levels, which could be substantially attenuated (65.1%) by pretreatment of BBMvEC's with NSC23766 (following correction for the baseline decrease with NSC23766 under static conditions) (Fig. 4.6 A i-ii).

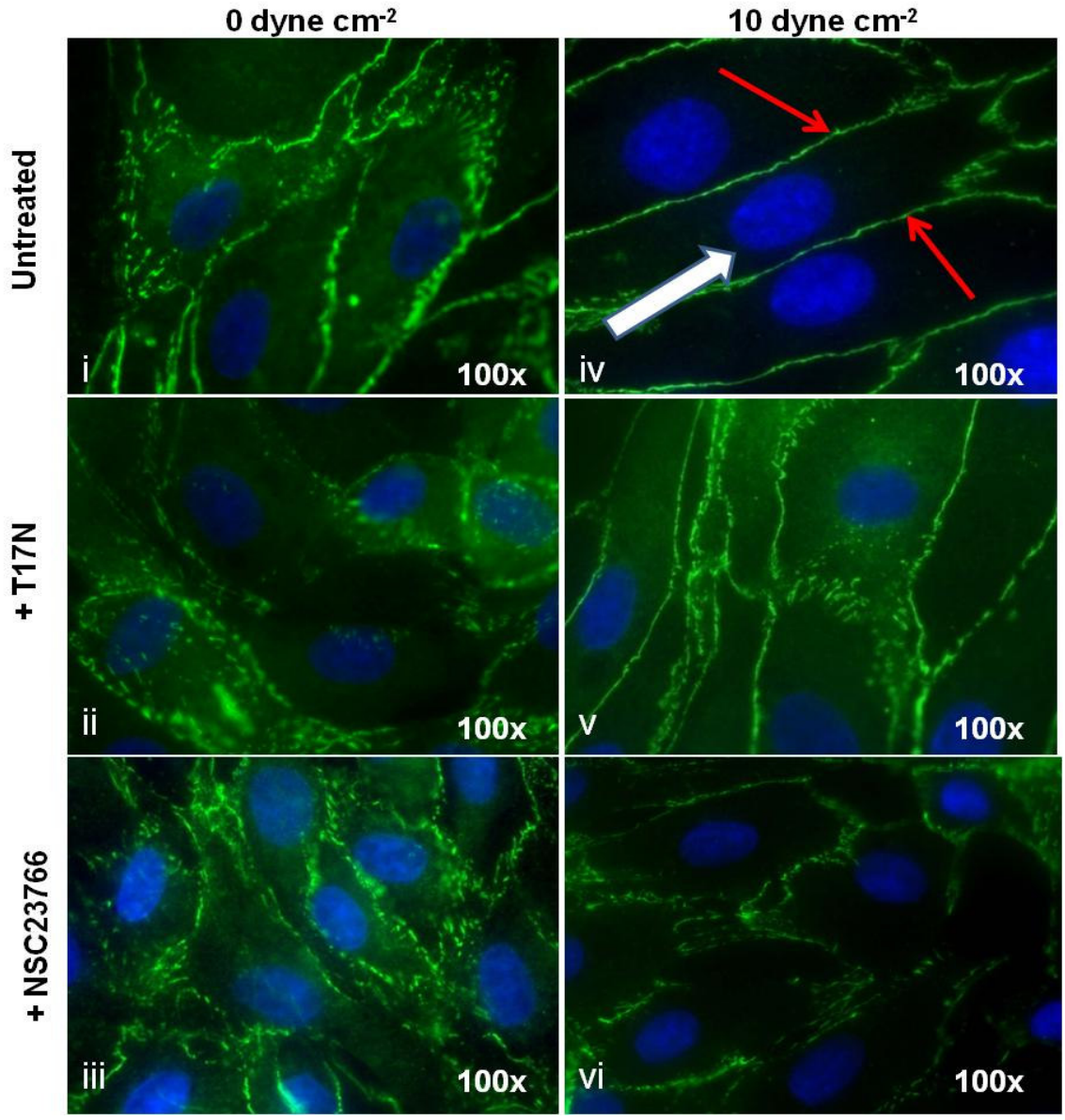

Fig. 4.5: Effect of Rac1 blockade on laminar shear-induced localization of ZO-1. Following transfection with (or without) T17N or pre-treatment with (or without) NSC23766, BBMvEC's at confluency were either maintained under static conditions or exposed to laminar shear stress (10 dyne cm^{-2}, 24 h) and monitored for ZO-1 localization by fluorescent microscopy. Red arrows denote sharp, continuous localization of ZO-1 to cell-cell borders (iv). White arrow indicates direction of the flow vector (iv). DAPI stained nuclei (blue) are clearly visible (i-vi). Images are representative.

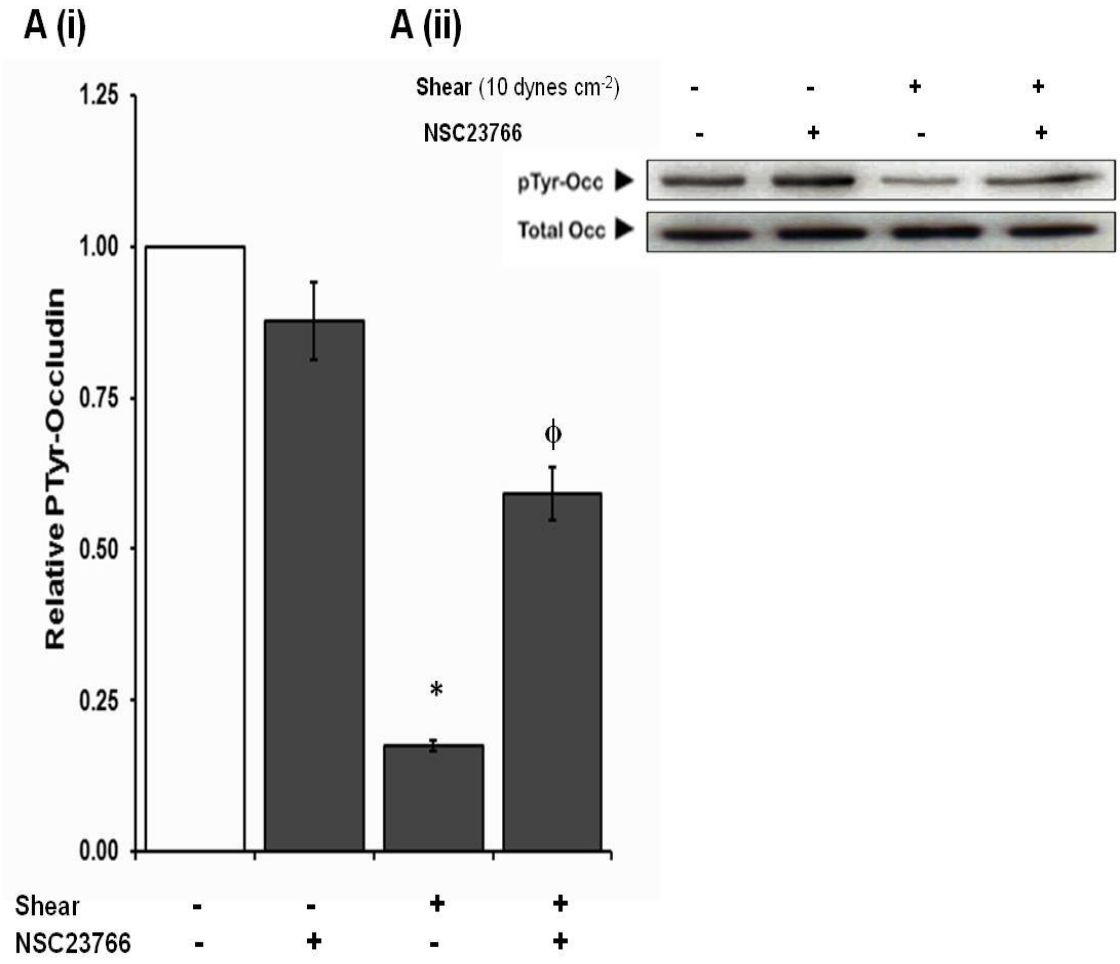

Fig. 4.6: Effect of Rac1 inhibition on laminar shear stress-induced occludin tyrosine dephosphorylation. Confluent BBMvEC cultures were either maintained under static conditions or exposed to laminar shear stress (10 dyne cm^{-2}, 24 h) in the absence and presence of NSC23766 and monitored for pTyr-occludin and total occludin levels. Histogram (A i) represents relative pTyr-occludin (i.e. pTyr-occludin/total occludin derived by scanning densitometry from blots in A ii). Results are averaged from three independent experiments ±SEM; **P* ≤0.05 vs unihibited static. ϕP≤0.05 vs. uninhibited shear. Blots are representative.

4.2.7: Laminar shear stress regulates BBMvEC RhoA-GTP activity.

BBMvEC's were subjected to laminar shear stress (10 dyne cm^{-2}) and monitored for acute (0-60 min) and chronic (24 h) effects on RhoA-GTP levels. Shear onset (within 1 min), triggered a 1.32±0.02 fold increase in RhoA-GTP followed by a return to baseline (static) levels at 60 min shear. Levels of RhoA-GTP following chronic shear were significantly reduced to 0.57±0.05 fold below baseline values. Thrombin was included as a positive control on RhoA activation (Fig. 4.7).

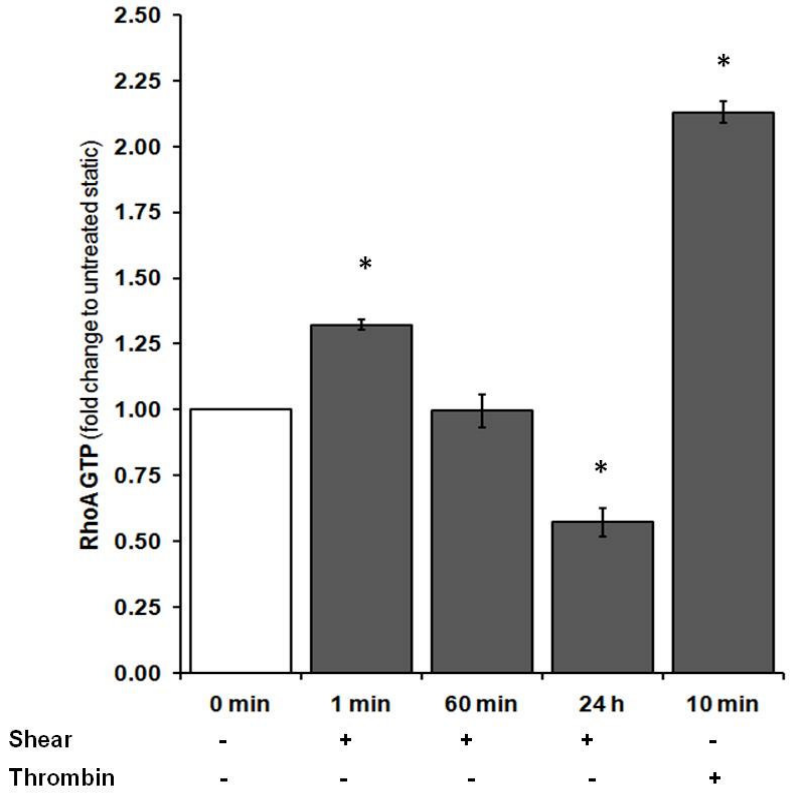

Fig. 4.7: Effect of laminar shear stress on RhoA activation. BBMvEC's were cultured as described in section 2.6.1 and exposed to laminar shear stress (10 dynes cm^2) following which they were harvested at varying time points (0-60 min and 24 h) and monitored by RhoA-GLISA®. Thrombin (1 U/ml, 10 min treatment) was included as a positive control for RhoA activation. Results are averaged from two independent experiments ±SEM; *P≤0.05 vs. 0 min.

4.2.8: Rho-associated kinase (ROCK) inhibition attenuates shear-induced BBMvEC morphological realignment and diminishes actin stress fiber formation.

The effect of ROCK inhibition (downstream effector of RhoA) on the shear-induced realignment of BBMvEC's was investigated. Pretreatment with Y-27632 (pharmacological inhibitor of ROCK) abolished the characteristic realignment of BBMvEC's to laminar flow with no noticeable baseline effects on static cells (Fig. 4.8 A i-iv). ROCK inhibition severely diminished cytoskeletal F-actin stress fiber formation, but retained cortical actin at cell peripheries in both static and sheared BBMvEC's (Fig. 4.8 B i-iv).

4.2.9: Laminar shear-induced upregulation of BBMvEC permeability involves ROCK activity.

BBMvEC's were monitored for transendothelial permeability to assess the potential involvement of ROCK in the shear-dependent (10 dynes cm^{-2}, 24 h) enhancement of barrier function. At t =120 min, static BBMvEC's treated with Y-27632 had significantly reduced permeability (%TEE FD40) compared to untreated static BBMvEC's. The shear-induced reduction in permeability yielded similar findings in BBMvEC's sheared in the presence of Y-27632, however restoration of the baseline effect of Y-27632 in static BBMvEC's reveals that the shear-induced reduction in permeability is attenuated by 74.1% in the presence of Y-27632 (Fig. 4.9).

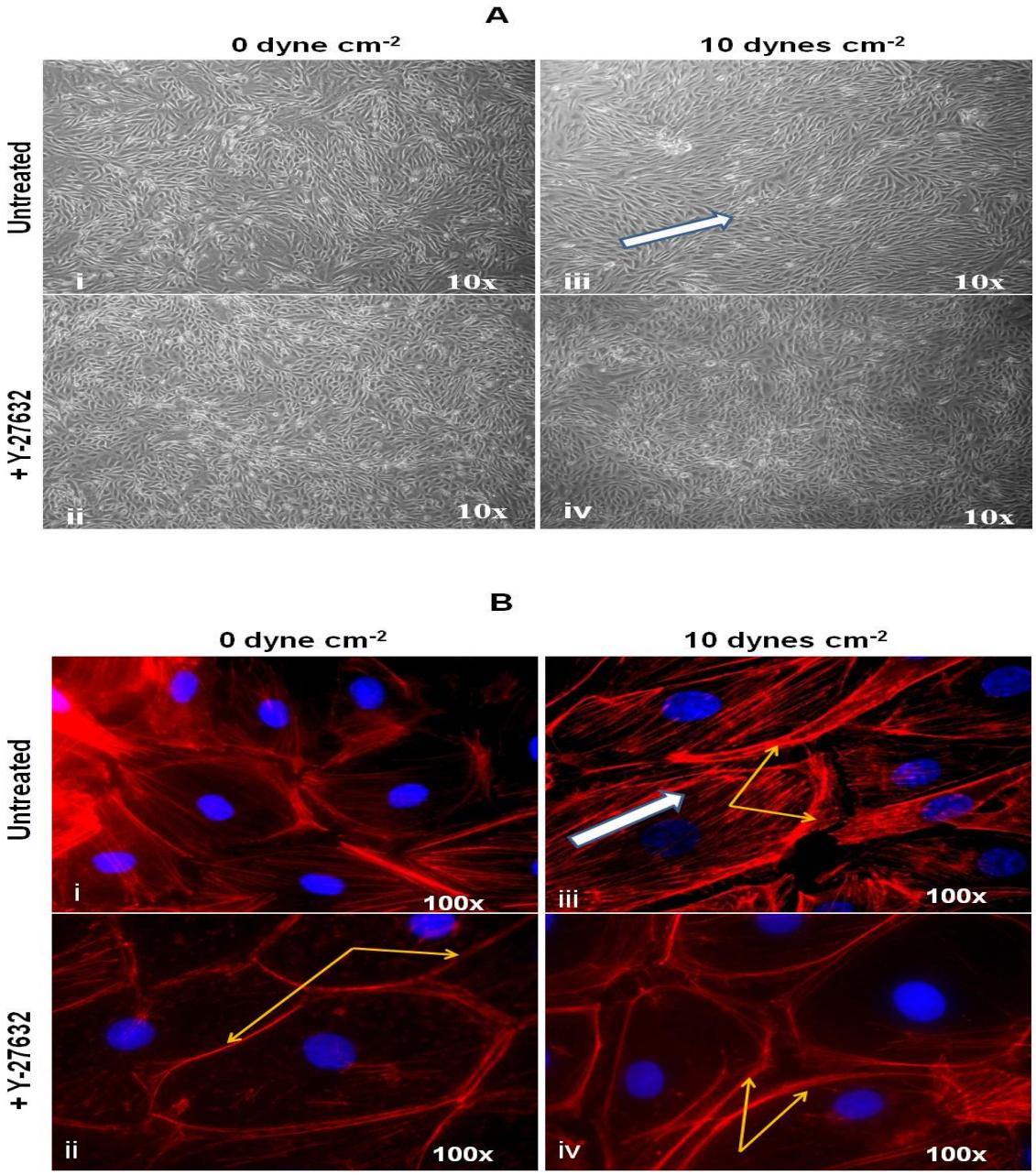

Fig. 4.8: Effect ROCK inhibition on shear-induced BBMvEC morphological and F-actin realignment. Following exposure to laminar shear (10 dynes cm^{-2}, 24 h) in the absence and presence of 10 μM Y-27632 (ROCK inhibitor), BBMvEC realignment was monitored by: (A) phase-contrast microscopy and (B) fluorescent microscopy (rhodamine-phalloidin stain for F-actin). White arrows indicate direction of the flow vector (A/B iii). Yellow arrows indicate cortical actin (B ii-iv). DAPI stained nuclei (blue) are clearly visible (B i-iv). Images are representative.

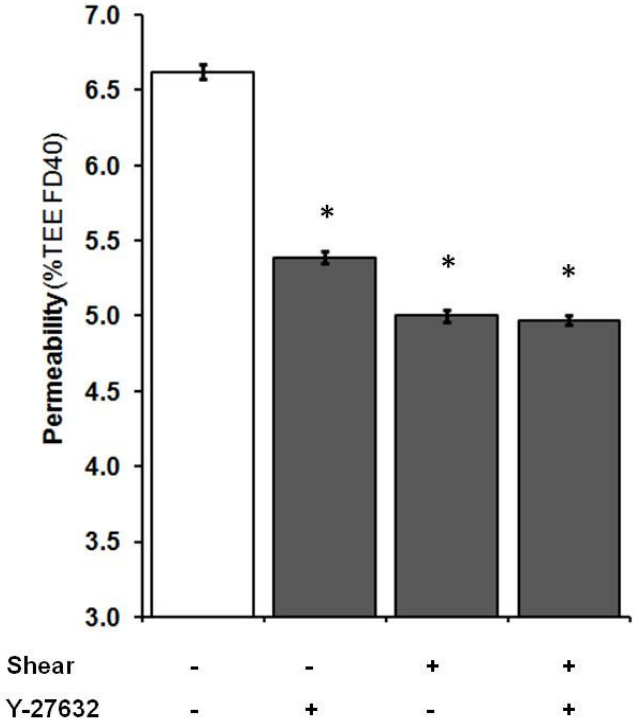

Fig. 4.9: Effect of ROCK inhibition on shear-induced regulation of BBMvEC permeability. Confluent BBMvEC cultures were either maintained under static conditions or exposed to laminar shear stress (10 dyne cm^{-2}, 24 h) in the absence and presence of 10 μM Y-27632 and monitored for transendothelial permeability. Histogram data points show change in permeability (% TEE FD40 at t=120 min). Histogram is averaged from three independent experiments ±SEM; *$P \leq 0.05$ vs uninhibited static.

4.2.10: Shear-induced localization of ZO-1 does not involve ROCK activity.

Following BBMvEC exposure to laminar shear stress (10 dynes cm^{-2}, 24 h) in the absence and presence of Y-27632, subcellular localization of ZO-1 was monitored. Findings show that static BBMvEC's cultured in the presence of Y-27632 (ii) displayed enhanced ZO-1 immunoreactivity at the cell-cell border compared to untreated static controls (i). Shear-induced cell-cell localization of ZO-1 (iii) did not appear to be affected by pre-treatment with Y-27632 (iv) (Fig. 4.10 i-iv).

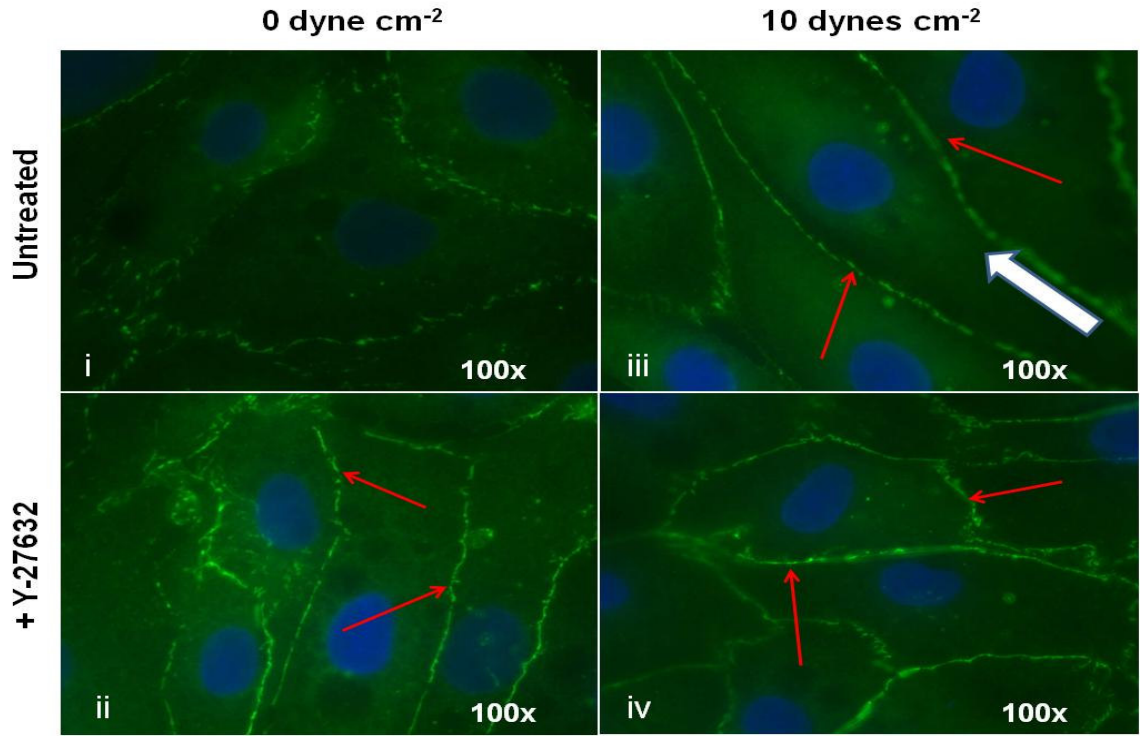

Fig 4.10: Effect of ROCK inhibition on shear-induced regulation of ZO-1 localization. Confluent BBMvEC cultures were either maintained under static conditions or exposed to laminar shear stress (10 dynes cm^{-2}, 24 h) in the absence and presence of 10 μM Y-27632 and monitored for ZO-1 localization by fluorescent microscopy. Red arrows denote sharp, continuous localization of ZO-1 to cell-cell borders (ii-iv). White arrow indicates direction of the flow vector (iii). DAPI stained nuclei (blue) are clearly visible (i-iv). Images are representative.

4.3 Discussion

Transport across the BBB occurs via two distinct pathways; directly through the cell (transcellular) or between adjacent cells linked by intercellular junction complexes (paracellular). The latter mechanism is of specific interest to this report. It is commonly accepted that paracellular permeability is regulated by a finely tuned balance between pro-adhesive forces generated by intercellular junction complexes on the one hand, and pro-contractile forces generated by the actin cytoskeleton on the other. Moreover, shear stress is well known to alter both the organization of the actin cytoskeleton and intercellular junctions (Birukov et al., 2002, Mehta and Malik, 2006). Given the fact that a wealth of knowledge implicates the RhoGTPases RhoA and Rac1 in actin-cytoskeletal dynamics, we sought to investigate their potential role in the shear-dependent regulation of tight junction assembly and barrier function within the BBB context.

Our first objective was to monitor the shear-induced activation of RhoGTPases in BBMvEC's following acute and chronic shear exposure. Previous authors have addressed the acute effects of shear on RhoGTPase activity in EC's of macrovascular origin, however data from the microvasculature is scarce (Tzima, 2006). Our results show that shear onset triggers a rapid (1 min) activation of RhoA, concomitant with a significant reduction of Rac1 activation below basal levels. By 60 mins however, an inverse shift in this trend indicated significantly elevated Rac1 activity while RhoA activation returned to baseline levels. This reciprocating trend in RhoGTPase activation suggests that the initial activation of RhoA following shear onset triggers a transient phase of cell contraction followed by Rac-1 mediated lamellipodia formation and extension in the direction of the flow. This two-stage mechanism has previously been suggested to be important for cellular reorientation in response to flow onset (Wojciak-Stothard and Ridley, 2003).

Most work to-date on shear-induced RhoGTPase activity has monitored acute responses (< 2 h shear), during which Rac1 activity returns to basal levels (Tzima et al., 2002, Wojciak-Stothard and Ridley, 2003). However, a recent report by Liu *et al.* showed that pulmonary artery EC's exposed to more prolonged hemodynamic stimuli (6 h cyclic

strain) retained significantly elevated levels of Rac1-GTP relative to static cells (Liu et al., 2007). Consistent with this, we observed Rac1GTP levels were significantly elevated 24 h post-shear, while RhoA-GTP was significantly below basal levels after similar shear duration. In the case of Rac1-GTP, it would be reasonable to speculate that shear-dependent regulation of Rac1 activation undergoes a biphasic response, whereby Rac1-GTP peaks and returns to baseline during the acute shear phase, followed by a later increase in Rac1-GTP during the chronic shear phase. This would be consistent with the notion of RhoGTPases functioning as molecular switches capable of sensing and activating in response to cell shape and morphology (Takai et al., 2001, Etienne-Manneville and Hall, 2002). Furthermore, as described in section 3.2.3, full BBMvEC realignment was only observed between 12 and 24 h, implying that dynamic cellular remodeling events are still evident in the chronic phase. The observation that RhoA-GTP levels were substantially below basal levels at 24 h (in conjunction with elevated Rac1) emphasizes the decreased state of cell contractility at this point that would favour intercellular junctional assembly, and thus stabilize barrier integrity (Wojciak-Stothard and Ridley, 2002).

In order to dissect the putative role of RhoGTPase signaling in our BBB model, selective RhoGTPase inhibition strategies were employed in shearing experiments following which cells were monitored for various indices of barrier integrity. Pharmacological inhibitors NSC23766 and Y-27632 have been extensively cited throughout the scientific literature for their respective blockade capabilities of the Rac1 and RhoA-ROCK signaling pathways (Gao et al., 2004, Sun et al., 2006, Yamamoto et al., 2008). Moreover, we achieved very good transfection efficiency (>50%) with T17N, a Rac1 dominant negative mutant (Jou et al., 1998).

Using these inhibitory approaches, we sought to investigate the involvement of RhoGTPases in the shear-dependent barrier improvements observed. In this regard, Rac1 has been previously implicated in shear-mediated cytoskeletal realignment (Tzima et al., 2002, Tzima et al., 2001). Consistent with this, pre-treatment of BBMvEC's with NSC23766 prevented the shear-induced cellular morphology realignment. The

corresponding shear-induced realignment of F-actin stress fibers was also disorientated with Rac1 inhibition, concurrent with a complete loss of cortical actin accumulation at cell-cell borders. The enhancement of cortical accumulation has been frequently associated with improvements in barrier function (Waschke et al., 2006, Dudek et al., 2004, Jacobson et al., 2006) We extended these inhibition strategies to our model of transendothelial permeability, to determine functional consequences of Rac1 inhibition on shear-dependent enhancement of barrier function. Initial experiments with NSC23766 revealed a significant attenuation of the shear-induced reduction in permeability. To undoubtedly confirm Rac1 participation in this effect, we repeated these experiments using a Rac1 T17N dominant negative mutant, which yielded a relatively similar inhibitory effect. This mutant contains a threonine (T) to asparagine (N) substitution at amino acid 17 within the Rac core effector domain, which cannot bind downstream effectors and also competes with endogenous Rac1 for guanine exchange factor (GEF) binding (Feig, 1999).

We extended our investigations with Rac1 to assess potential involvement in the shear-induced regulation of tight junction assembly. Previous reports have shown that constitutively active or dominant negative mutants of both Rac1 and RhoA can adversely affect junctional localization of occludin and ZO-1(Wojciak-Stothard et al., 2001). By blocking shear-dependent Rac1 activation with NSC23766 and T17N, we observed a reduced ZO-1 immunoreactivity at cell-cell borders, thus adding further weight to a role for Rac1 in shear-induced enhancement of barrier function.

We next revisited our earlier finding that prolonged shear exposure reduces pTyr-occludin levels and we found that pre-treatment with NSC23766 significantly attenuated this shear-dependent response. Recent work by Peng *et al.* showed VEGF-induced hyperpermeability in glomerular EC's was acting through a Rac1-pTyr-occludin mechanism (Peng et al., 2009), while Benson and Burridge using a similar mechanism of VEGF stimulation in pulmonary EC's uncovered a Rac1-ROS (reactive oxygen species)-pTyr-VE-Cadherin-dependent pathway of barrier disruption (Monaghan-Benson and Burridge, 2009). Consistent with our results was the observation that

elevated pTyr-occludin correlates with weaker endothelial barrier, however Peng *et al.* showed that Rac1 elevates pTyr-occludin, whereas shear-induced activation of Rac1 in our model reduces pTyr-occludin. These somewhat contradictory findings are most likely attributable to the specificity of the upstream stimulus, i.e. ligand-dependent activation of VEGFR2 via VEGF has been shown to induce a divergent intracellular signaling cascade compared to shear-induced (ligand-independent) activation of VEGFR2 (Shay-Salit et al., 2002). This effect could determine Rho guanine nucleotide exchange factor (RhoGEF) recruitment and also the specificity of the downstream effectors of Rac1. Collectively, these findings implicate Rac1 activation in the shear-dependent upregulation of BBMvEC barrier function and tight junction assembly at multiple levels.

It is a well-accepted notion that RhoA and Rac1 have antagonizing effects with respect to barrier function, where Rac1 promotes barrier stabilization and RhoA destabilizes barrier integrity (Wojciak-Stothard and Ridley, 2002, Wojciak-Stothard et al., 2001, Jacobson et al., 2006). Having clarified a definitive shear-dependent role for Rac1, we sought to investigate a potential reciprocal role for RhoA in our BBMvEC model. Under *static* conditions, pretreatment with Y-27632 had no observable effect on BBMvEC morphology, however it significantly diminished actin stress fiber formation, with BBMvEC's retaining a dense band of cortical actin at cell-cell junctions. In a further series of experiments, ROCK inhibition significantly reduced permeability under basal conditions, and displayed an enhanced junctional immunoreactivity of ZO-1 to cell-cell border. Under *shearing* conditions, pretreatment with Y-27632 prevented shear-induced cellular morphology realignment, which is consistent with previous findings using a dominant negative mutant of RhoA (Tzima et al., 2001). Moreover, the data implicates that ROCK inhibition attenuates the shear-induced regulation of BBMvEC permeability, following correction of the baseline effect with Y-27632 under static conditions. BBMvEC's sheared in the presence of Y-27632 also displayed decreased stress fiber formation, but retained a band of cortical actin and ZO-1 immunolocalization at the cell-cell junction similar to static conditions,

We can interpret these results on a number of levels. Firstly, our initial finding that ROCK inhibition blocked the shear-induced morphology realignment led us to hypothesize that the initial increase of Rho-GTP in the acute shear-onset phase is a significant factor necessary for BBMvEC morphological realignment in the chronic shear phase. It would appear that this initial phase of cell contraction 'primes' the EC for a cascade of signaling events associated with morphology realignment under sustained shear conditions (Wojciak-Stothard and Ridley, 2003). The finding that Y-27632 severely diminished actin stress fiber assembly under both static and shearing conditions supports the concept of weakening cell contraction. Moreover, the observation of enhanced cortical actin accumulation under these conditions would provide a favourable environment for stabilizing intercellular adhesion (Sun et al., 2006). Interestingly, previous reports have shown that ROCK inhibition can stimulate Rac1 activation, which could potentially explain the observed enhancement of cortical actin under such conditions (Desai et al., 2004, Tsuji et al., 2002, Wang and Dudek, 2009).

Our observation that Y-27632 treatment reduces BBMvEC permeability under static conditions, yet attenuates the shear-induced reduction in permeability may initially seem ambiguous. It would appear that under static conditions, basal levels of RhoA-GTP are sufficient to contribute to barrier disassembly, such that inhibition of RhoA signaling with Y-27632 disrupts this mechanism, possibly via enhanced cortical actin accumulation. A large amount of experimental evidence exists to show that Y-27632 exerts barrier-stabilizing effects when EC's are challenged with hyperpermeability mediators that initiate their effects through modulation of RhoA-ROCK activity (Birukova et al., 2004, Sun et al., 2006, Miyazaki et al., 2010). With prolonged shear exposure we observed a significant drop in RhoA activity below basal values (concomitant with elevated Rac1 activity). We hypothesize that shearing in the presence of Y-27632 blocks the early contraction phase necessary for barrier establishment; hence the reversal of shear induced permeability but would also further reduce/completely diminish RhoA-ROCK signaling to non-physiological levels. Moreover, this effect could potentially elevate Rac1-GTP above physiological levels normally observed following prolonged shear. When interpreting findings on

RhoGTPase activity, it is important to recognize that these molecules are spatially and temporally regulated (as under shearing conditions), thus any inappropriate induction/changes of their GTPase activities would alter the homeostatic balance and thus compromise the functional response, i.e. barrier stability (Tzima, 2006, Connolly et al., 2002).

Following pretreatment with Y-27632 we observed enhanced junctional localization of ZO-1 under static conditions, thus offering further explanation for the reduction in BBMvEC permeability under such conditions. Interestingly, ROCK inhibition did not disrupt the shear-induced junctional localization of ZO-1, a result seemingly at odds with the effect of Y-27632 on permeability under shear conditions. However, our observation that BBMvEC's sheared in the presence of Y-27632 retained a dense band of cortical actin would suggest that this likely facilitated the retention of ZO-1 localization to the cell periphery (Fanning et al., 2002, Van Itallie et al., 2009). Thus, Y-27632 likely blocks shear-dependent permeability reduction in BBMvEC's by a *ZO-1 independent mechanism*. In this regard, recent findings by *van Nieuw et al.* showed that basal levels of ROCK activity were essential for barrier maintenance by regulating expression levels of VE-Cadherin, thus offering a possible alternative mechanism for barrier disassembly (van Nieuw Amerongen et al., 2007).

To summarize, blockade of RhoA signaling via ROCK inhibition enhances junctional stability in BBMvEC's under static conditions. However, from a shear context, RhoA activity appears crucial to the upregulation of BBMvEC barrier function during the early shear-onset phase/adaptation. An inverse shift in RhoGTPase activity towards Rac1 predominates during the chronic shear phase, after necessary Rho-dependent cellular morphological adaptations have occurred. This response is more closely associated with the *in-vivo* condition of EC's in undisturbed, laminar regions of the vasculature, thus placing a greater emphasis on Rac1 in shear-dependent maintenance of barrier function (Noria et al., 2004, Hahn and Schwartz, 2009).

The signaling mechanisms connecting RhoGTPase activation to post-translational modification of junctional proteins is poorly understood. Given the fact that post-

translational modifications of tight and adherens junction proteins (elevated tyrosine phosphorylation in particular) can have such a profound effect on endothelial permeability, it would be logical to imply a role for protein tyrosine phosphatases (PTP's) and protein tyrosine kinases (PTK's) as downstream effectors of RhoGTPase activity. Furthermore, our initial studies showing that shear-induced activation of Rac1 regulates both ZO-1 localization and pTyr-occludin comply with a notion that Rac1 is targeting the tight junction, albeit through unknown mechanisms. Evidence from the literature on upstream regulators and/or downstream effectors (e.g. PTP's) of Rac1 within endothelium is currently lacking, however recent findings from epithelial cells suggest that the tight junction imbedded protein paracingulin (homologous to cingulin) can associate with and regulate RhoA and Rac1 GEF's, GEF-H1 and Tiam1 respectively (Guillemot et al., 2008). The RhoA effector ROCK has already been implicated in direct association and modulation of tight junction components (Yamamoto et al., 2008). Thus, identification of targets modulating tight function assembly could not only be of genuine therapeutic benefit to pathologies exhibiting vascular leakiness, but also in the delivery of therapeutic compounds to the underlying interstitium via temporal manipulation of the tight junction 'seal' to facilitate paracellular delivery of the compound.

Chapter 5:

The role of VE-Cadherin and Tiam1 in shear-induced upregulation of BBMvEC tight junction assembly and barrier function.

5.1 Introduction

Understanding the mechanosensory and intracellular signaling mechanism mediating the physiological/pathological consequences of hemodynamic force stimulation of the endothelium has been the subject of intense investigation over recent decades, with the intention of identifying key molecular targets in health and disease. Adding to the complexity of this matter are findings demonstrating that a host of apical, lateral and basolaterally situated EC mechanosensors in tandem with the actin cytoskeleton can all instigate profound shear-induced consequences on EC functions (Chen et al., 1999, Deli et al., 2005, Hahn and Schwartz, 2009). This would imply that no single mechanosensing mechanism exits, but possibly requires a synchronous activation of several mechanosensory systems, as evidenced by the signaling triad involving PECAM-1, VE-Cadherin and VEGFR2 (Tzima et al., 2005).

Within our model of shear-induced enhancement of BBMvEC barrier function, our attention turned to VE-Cadherin as a possible mechanosensory adaptor protein participating in the shear-dependent induction of these events. The contribution of VE-Cadherin in the adaptation of EC's to flow is well established in compliance with its multifaceted role in other EC functions, including barrier maintenance and RhoGTPase regulation. Moreover, recent evidence has demonstrated that VE-Cadherin can regulate claudin-5 expression, by preventing nuclear accumulation of Fox01 and β-Catenin (repressors of claudin-5 expression), thereby alluding to a functional cross-talk mechanism between endothelial adherens and tight junction structures (Taddei et al., 2008). Furthermore, VE-Cadherin is also known to regulate membrane association of the guanine nucleotide exchange factor (GEF) Tiam1, a known activator of Rac1 (Lampugnani et al., 2002). Increasing evidence has suggested a putative role for Tiam1-mediated activation of Rac1 in models of barrier enhancement (Birukova et al., 2007a, Birukova et al., 2008). However, to the best of our knowledge no group has examined the contribution of intercellular junctions (VE-Cadherin) to shear-mediated changes in RhoGTPase activity, particularly at the BBB.

In this chapter we examine the contribution of VE-Cadherin and Tiam1 to laminar shear-induced changes in Rac1 activity, with downstream consequences for tight junction assembly and barrier function. For these studies we used VE-Cad ΔEXD (extracellular domain deletion mutant) and Tiam1 C580 (mutant lacking PHn and DHR domains) plasmid constructs to inhibit VE-Cadherin and Tiam1 function.

5.2 Results

5.2.1: Illustration of VE-Cadherin WT and ΔEXD mutant and confirmation of ΔEXD expression in BBMvEC's.

Fig. 5.1 A depicts the core domains of wild type (WT) VE-Cadherin compared to VE-Cad ΔEXD lacking the extracellular cadherin repeats (1-5), which are essential for homophilic cell-cell adhesion. This 'non-junctional' mutant form of VE-Cadherin has the external repeats replaced by a FLAG® (octapeptide) tag. Following transfection of BBMvEC's with and without (mock) VE-Cad ΔEXD, mutant over-expression was confirmed by immunocytochemistry (IC) using an anti-FLAG® antibody (Fig. 5.1 B ii).

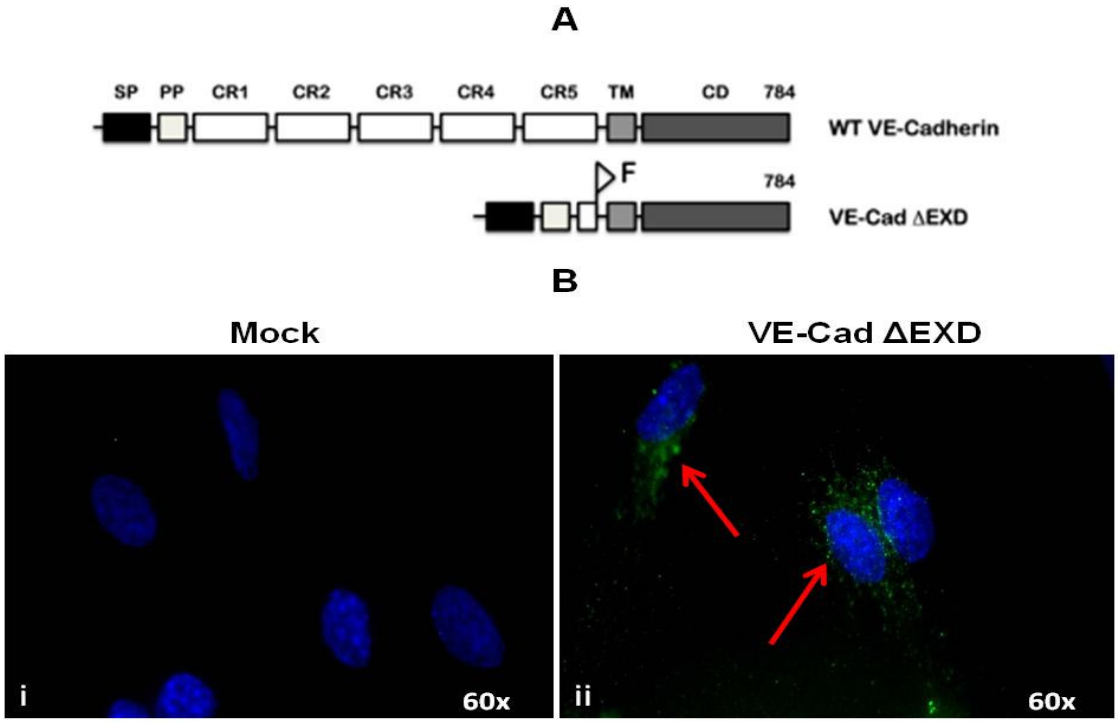

Fig. 5.1: Illustration and overexpression of VE-Cad ΔEXD in BBMvEC's. (A): Illustration of VE-Cadherin wild type and ΔEXD mutant. SP, signal peptide; PP, pre-peptide; CR, cadherin repeat; TM, transmembrane domain; CD, cytoplasmic domain; F, FLAG® epitope. (B): Following transfection of BBMvEC's, VE-Cad ΔEXD expression was monitored by IC. Arrows in red indicate FLAG® epitope staining (ii). DAPI stained nuclei (blue) are clearly visible (i-ii). Images are representative.

5.2.2: Laminar shear stress-induced activation of Rac1 is VE-Cadherin-dependent.

In section 4.2.2 we observed that acute exposure of laminar shear stress (10 dynes cm^{-2}, 60 min) induced a significant increase in Rac1-GTP. We therefore monitored the effects of VE-Cadherin inhibition on shear-dependent Rac1 activation following 60 min shear exposure. No detectable changes in Rac1 protein levels were observed following treatment (Fig 5.2 A i). However, sheared BBMvEC's caused a 1.89±0.08 fold increase in Rac1-GTP, a response that was significantly attenuated by 73.03% in the presence of VE-Cad ΔEXD (following correction for the baseline increase with VE-Cad ΔEXD under static conditions) (Fig. 5.2 A ii).

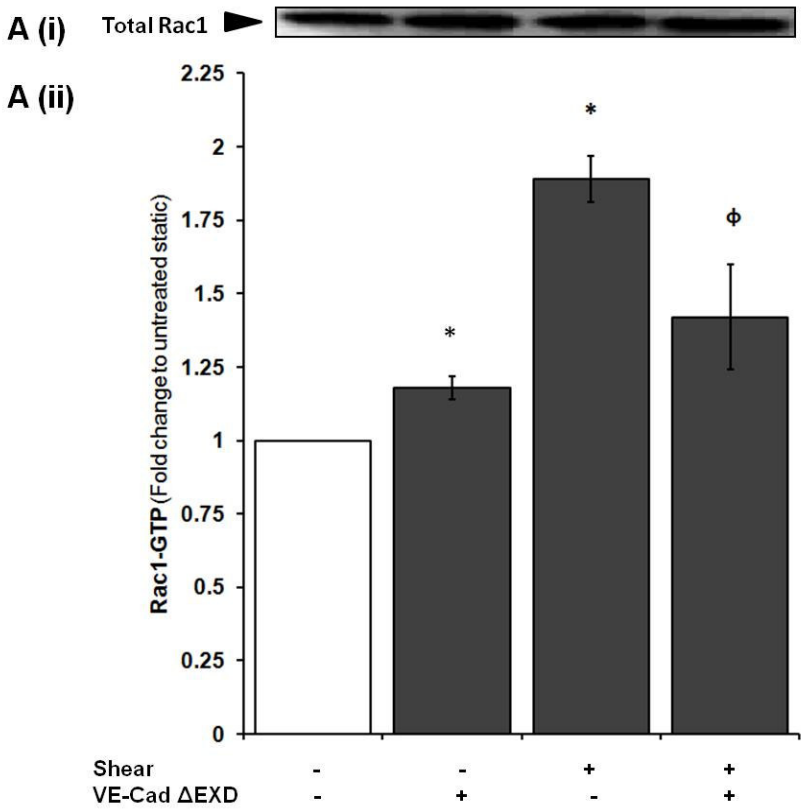

Fig. 5.2: Effect of VE-Cadherin inhibition on laminar shear induced-Rac1 activation. Cultures of BBMvEC's were either maintained under static conditions or exposed to laminar shear stress (10 dynes cm^{-2}, 60 min) in the absence and presence of VE-Cad ΔEXD, following which they were harvested and monitored by: (A i) IB analysis for total Rac1 levels and (A ii) Rac1-GLISA® for Rac1-GTP. Results are averaged from three independent experiments ±SEM; *P≤0.05 vs. uninhibited static, ϕP≤0.05 vs. uninhibited shear. Blots are representative.

5.2.3: Laminar shear stress-induced upregulation of BBMvEC barrier function is VE-Cadherin-dependent.

BBMvEC's transfected in the absence (mock) or presence of VE-Cad ΔEXD were monitored for their effects on shear-dependent enhancement of barrier function. As expected, shear significantly reduced permeability (%TEE of FD40) compared to the static control. However, this shear-induced reduction in permeability was attenuated by 79.8% in the presence of VE-Cad ΔEXD (following correction for the baseline increase with VE-Cad ΔEXD under static conditions) (Fig. 5.3).

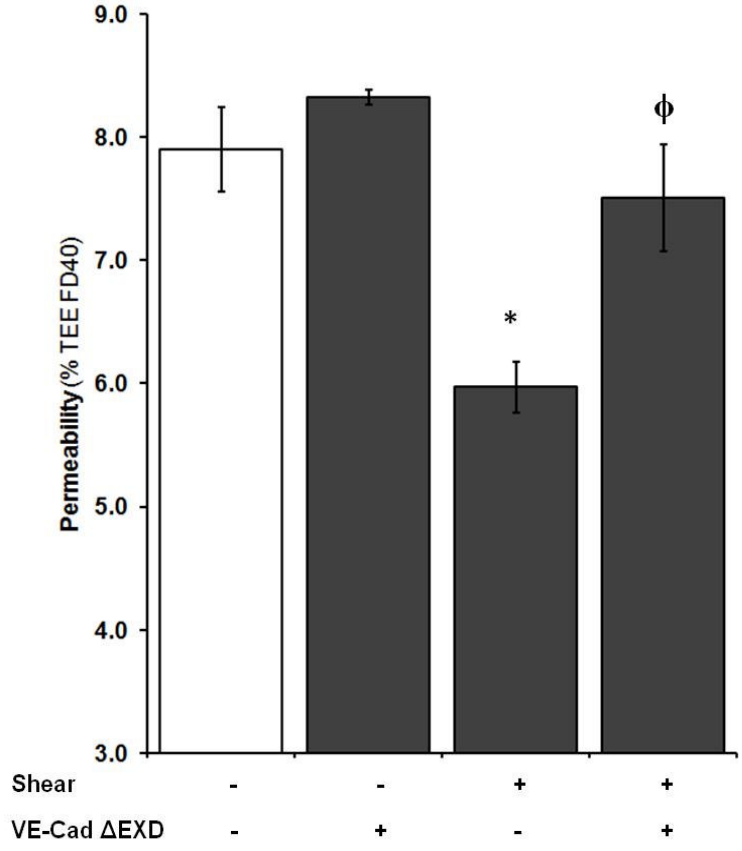

Fig. 5.3: Effect of VE-Cadherin inhibition on laminar shear-induced regulation of BBMvEC permeability. Confluent BBMvEC's transfected with or without (mock) VE-Cad ΔEXD were either maintained under static conditions or exposed to laminar shear stress (10 dynes cm^{-2}, 24 h) and monitored for transendothelial permeability. Histogram data points show change in permeability (%TEE FD40 at t=120 min). Histogram is averaged from three independent experiments ±SEM; *$P \leq 0.05$ vs uninhibited static, ϕ$P \leq 0.05$ vs uninhibited shear.

5.2.4: Laminar shear-induced localization of ZO-1 is VE-Cadherin dependent.

Following BBMvEC exposure to laminar shear stress (10 dynes cm^{-2}, 24 h) in the absence (mock) or presence of VE-Cad ΔEXD, subcellular localization of ZO-1 was monitored. Results indicate that the typical shear-induced re-localization of ZO-1 immunoreactivity to the cell-cell borders was completely abrogated following transfection with VE-Cad ΔEXD, leaving a broken, discontinuous pattern of ZO-1 staining at cell peripheries (Fig. 5.4 i-iv).

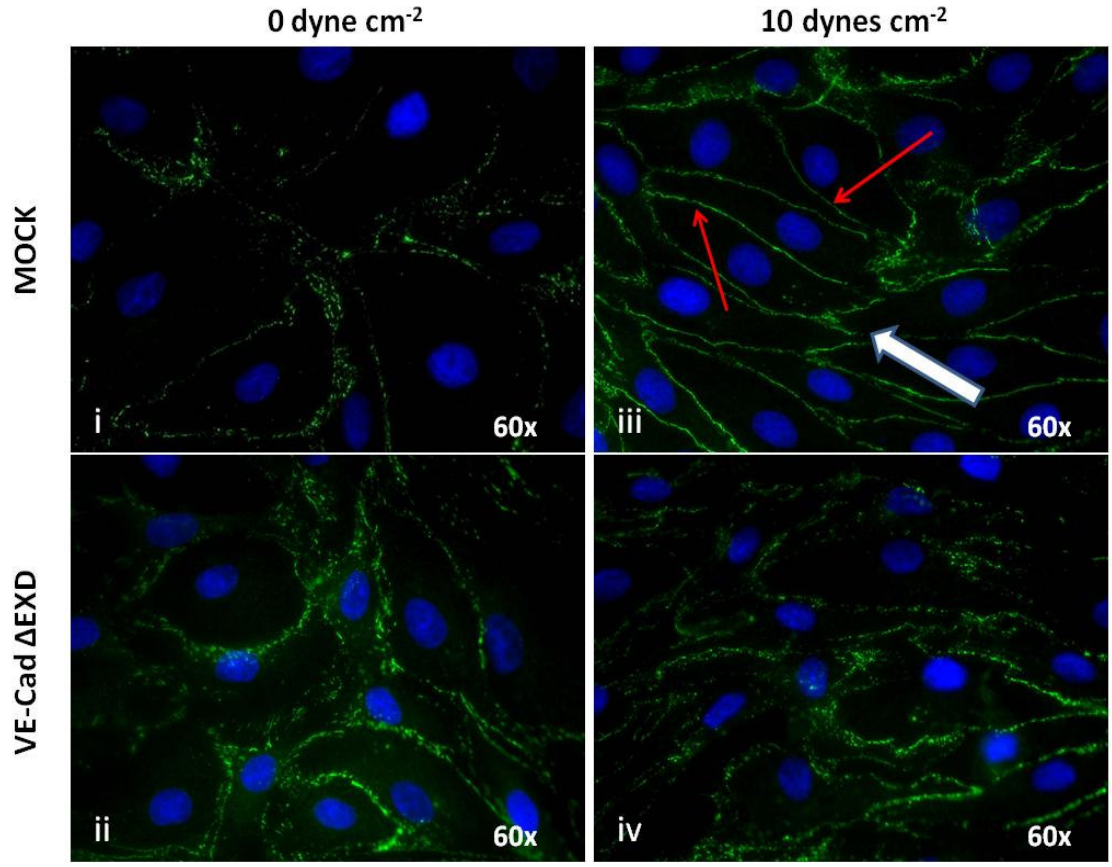

Fig. 5.4: Effect of VE-Cadherin inhibition on laminar shear-induced ZO-1 localization. Transfected BBMvEC's with or without (mock) VE-Cad ΔEXD were grown to confluency and either maintained under static conditions or exposed to laminar shear stress (10 dyne cm^{-2}, 24 h) and monitored for ZO-1 localization by fluorescent microscopy. Red arrows denote sharp, continuous localization of ZO-1 to cell-cell borders (iii). White arrow indicates direction of the flow vector (iii). DAPI stained nuclei (blue) are clearly visible (i-iv). Images are representative.

5.2.5: Laminar shear-induced localization of claudin-5 is VE-Cadherin dependent.

Following BBMvEC exposure to laminar shear stress (10 dynes cm^{-2}, 24 h) in the absence (mock) or presence of VE-Cad ΔEXD, subcellular localization of claudin-5 was monitored. Results indicate that the continuous and well-defined organization of claudin-5 immunoreactivity initially observed along the plasma membrane in response to laminar shear stress was completely ablated by treatment with VE-Cad ΔEXD, reverting to a jagged and somewhat diminished pattern of claudin-5 along the cell-cell border (Fig. 5.5 i-iv).

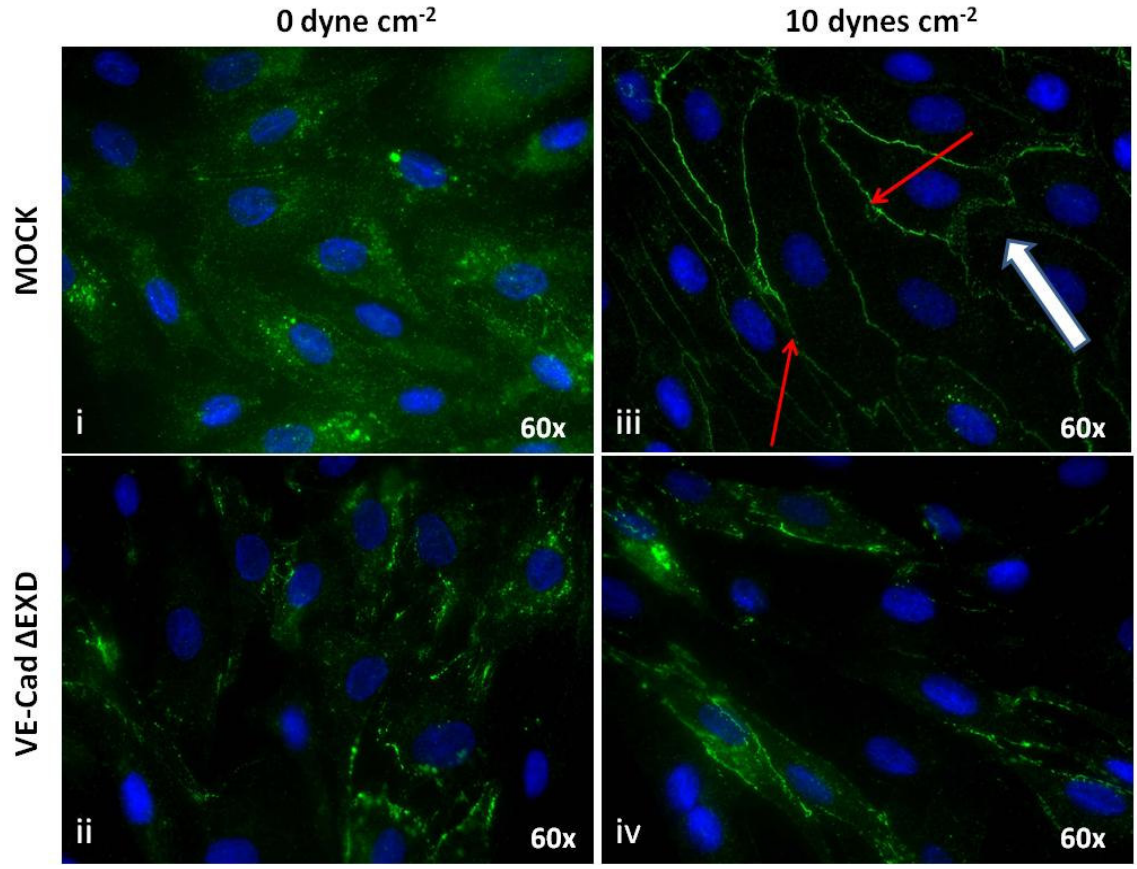

Fig. 5.5: Effect of VE-Cadherin inhibition on laminar shear-induced claudin-5 localization. Transfected BBMvEC's with or without (mock) VE-Cad ΔEXD were grown to confluency and either maintained under static conditions or exposed to laminar shear stress (10 dyne cm^{-2}, 24 h) and monitored for claudin-5 localization by fluorescent microscopy. Red arrows denote sharp, continuous localization of claudin-5 to cell-cell borders (iii). White arrow indicates direction of the flow vector (iii). DAPI stained nuclei (blue) are clearly visible (i-iv). Images are representative.

5.2.6: Laminar shear-induced tyrosine dephosphorylation of occludin is VE-Cadherin-dependent.

We extended our investigations of the shear-induced (10 dynes cm^{-2}, 24 h) reduction in phosphotyrosine (pTyr)-occludin levels to assess potential involvement of VE-Cadherin. Following transfection in the absence and presence (mock) of VE-Cad ΔEXD, BBMvEC's were harvested and monitored for changes in pTyr-occludin level by IP and IB. The shear-induced reduction in pTyr-occludin (to 0.08±0.01 fold of control) was attenuated by 89.13% in the presence of VE-Cad ΔEXD (following correction for the baseline decrease with VE-Cad ΔEXD under static conditions) (Fig. 5.6).

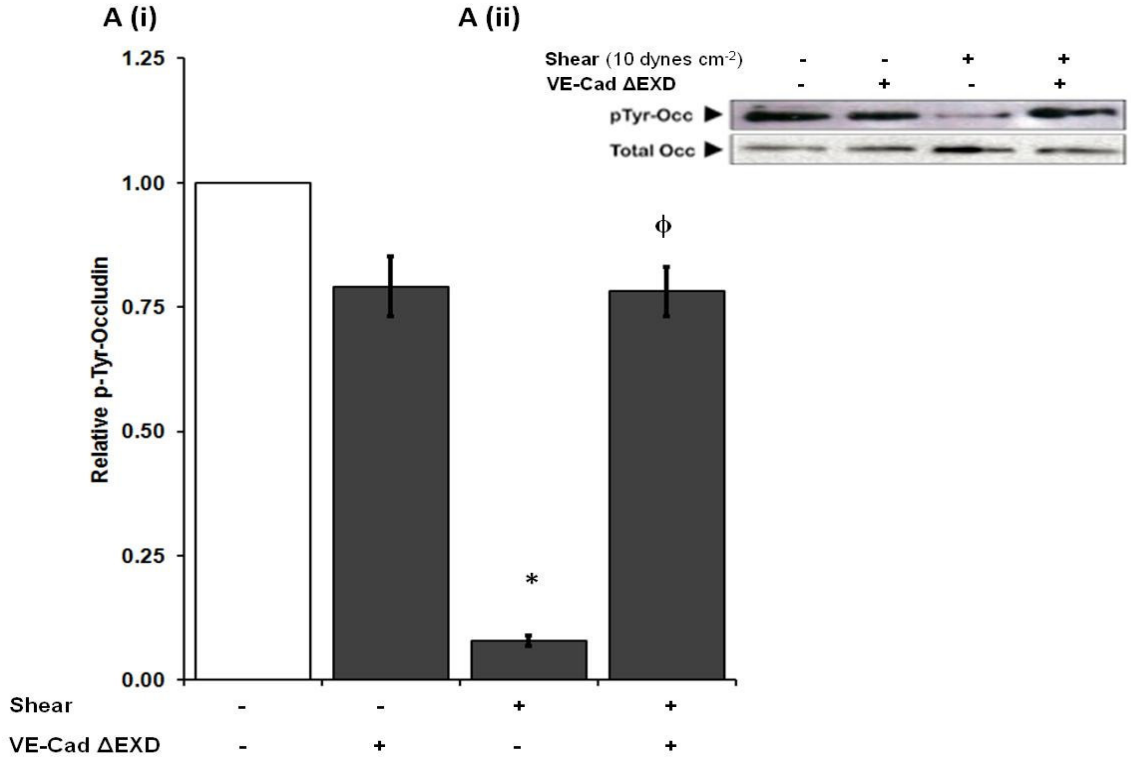

Fig. 5.6: Effect of VE-Cadherin inhibition on laminar shear-induced occludin tyrosine dephosphorylation. Transfected BBMvEC's with or without (mock) VE-Cad ΔEXD were grown to confluency and either maintained under static conditions or exposed to laminar shear stress (10 dyne cm^{-2}, 24 h) and monitored for pTyr-occludin and total occludin levels. Histogram (A i) represents relative pTyr-occludin (i.e. pTyr-occludin/total occludin derived by scanning densitometry from blots in A ii). Results are averaged from three independent experiments ±SEM; $*P \leq 0.05$ vs uninhibited static, $\phi P \leq 0.05$ vs. uninhibited shear. Blots are representative.

5.2.7: Illustration of Tima1 WT and C580 mutant and confirmation of C580 expression in BBMvEC's.

Fig. 5.7 A depicts the core domains of the guanine nucleotide exchange factor Tiam1 WT compared to Tiam1 C580 (lacking the PHn and DHR domains, which are responsible for membrane trafficking of Tiam1). Following transfection of BBMvEC's with and without (mock) Tiam1 C580, overexpression of Tiam1 was confirmed by IC using an anti-Tiam1 C16 antibody specific to an epitope on the C-terminus of Tiam1 (Fig. 5.7 B ii).

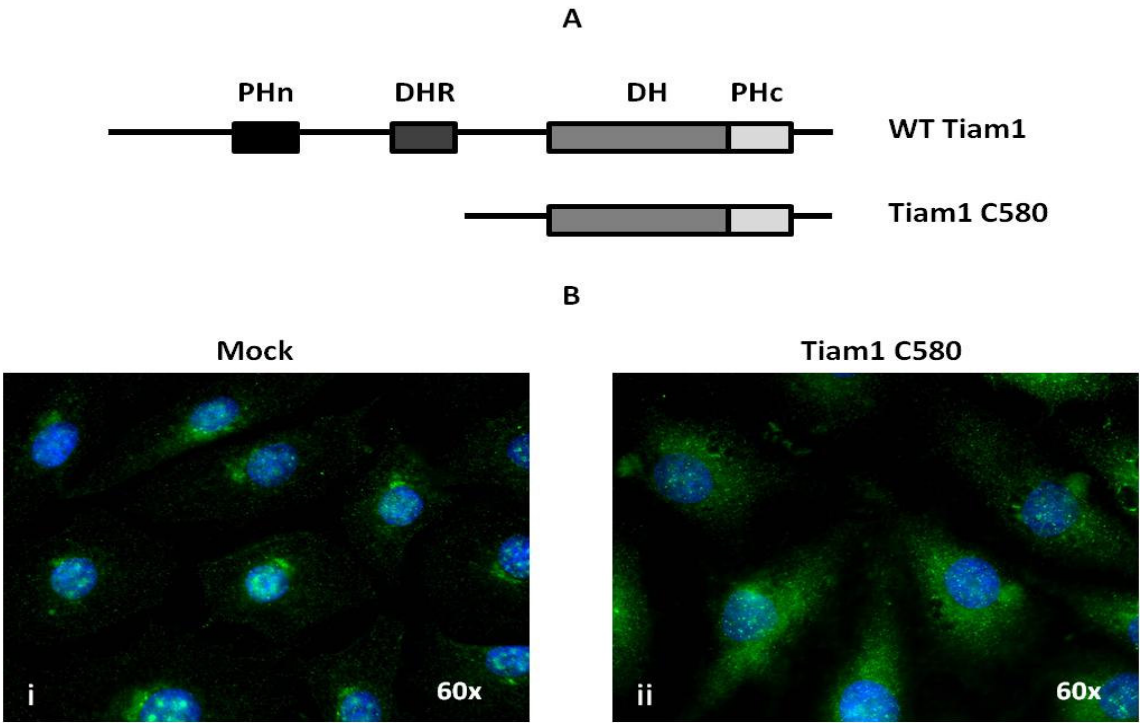

Fig. 5.7: Illustration and overexpression of Tiam1 C580 in BBMvEC's. (A) Illustration of Tiam1 WT and C580 mutant. PHn, N-terminal pleckstrin homology domain; DHR, disc homology region; DH, Dbl-homology domain; PHc, C-terminal pleckstrin homology domain. (B) Following transfection of BBMvEC's with and without (mock) Tiam1 C580, Tiam1 expression (green) was monitored by IC. DAPI stained nuclei (blue) are clearly visible (i-ii). Images are representative.

5.2.8: Laminar shear stress-induced activation of Rac1 is Tiam1-dependent

We assessed the potential upstream signaling role of Tiam1 using Tiam1 C580. Initially, the effects of Tiam1 inhibition on shear-dependent Rac1 activation following 60 min shear was monitored. No detectable changes in Rac1 protein levels were observed following treatment (Fig 5.8 A i). However sheared BBMvEC's caused a 1.69±0.11 fold increase in Rac1-GTP, a response that was significantly attenuated by 60.87% in the presence of Tiam1 C580 (following correction for the baseline decrease with Tiam1 C580 under static conditions) (Fig. 5.8 A ii).

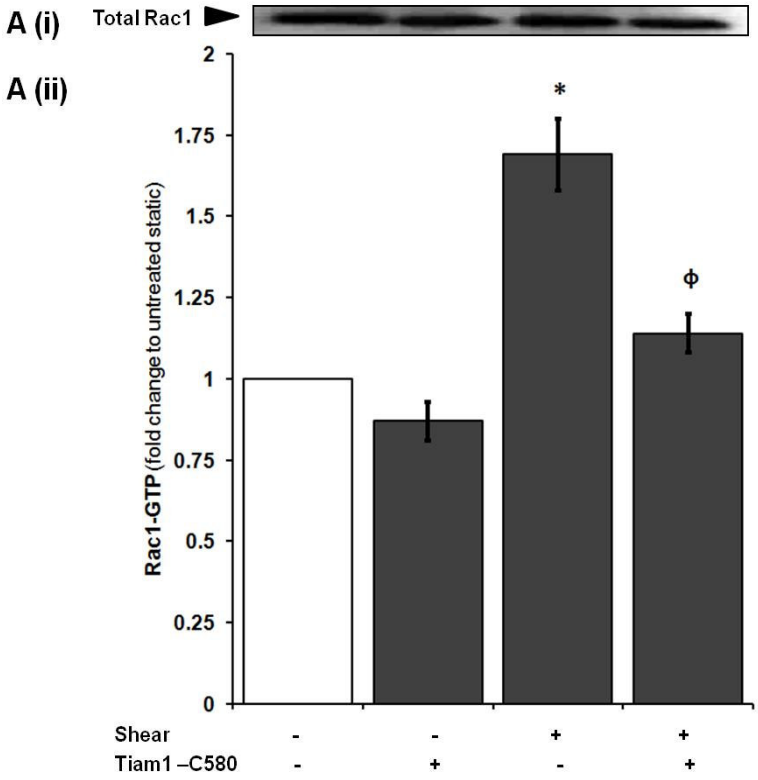

Fig. 5.8: Effect of Tiam1 inhibition on laminar shear-induced Rac1 activation. Cultures of BBMvEC's were either maintained under static conditions or exposed to laminar shear stress in the absence and presence of Tiam1 C580, following which they were harvested and monitored by: (A i) IB analysis for total Rac1 levels and (A ii) Rac1-GLISA® for Rac1-GTP. Results are averaged from three independent experiments ±SEM; *P≤0.05 vs. uninhibited static, ϕP≤0.05 vs. uninhibited shear. Blots are representative.

5.2.9: Laminar shear stress-induced BBMvEC cellular realignment is Tiam1-dependent.

Following transfection in the absence (mock) or presence of Tiam1 C580, BBMvEC's were left static or exposed to laminar shear stress (10 dynes cm^{-2}, 24 h) and monitored for cellular realignment by phase-contrast microscopy. Inhibition of Tiam1 signaling severely abrogated the typical shear-induced realignment of BBMvEC's (Fig. 5.9 i-iv).

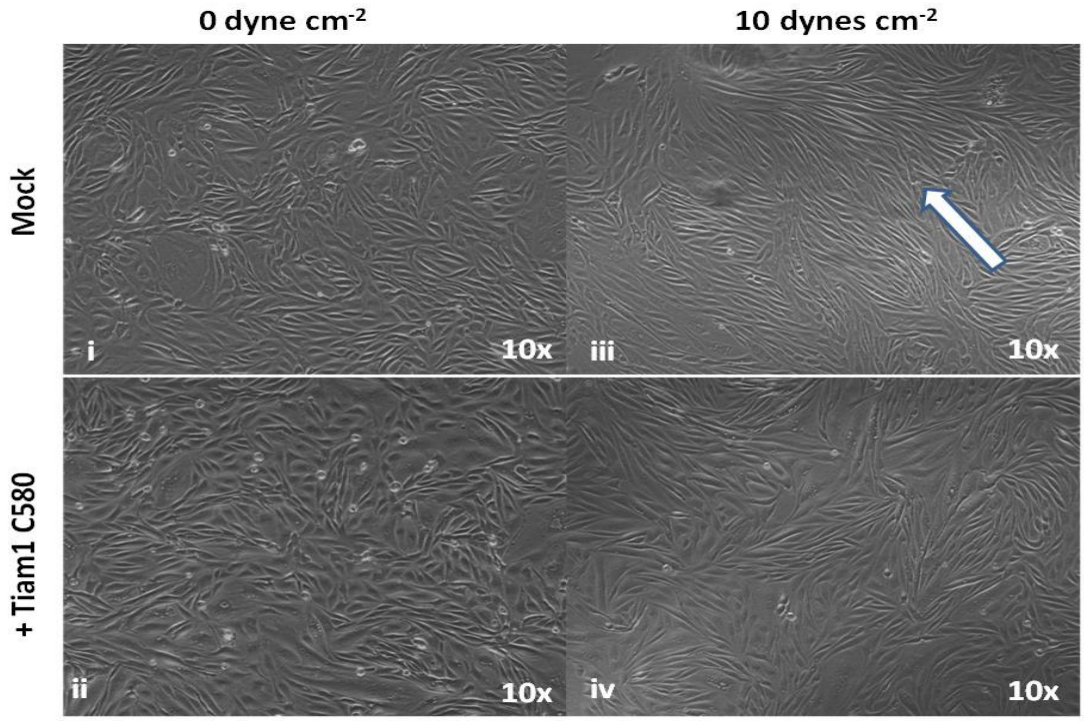

Fig. 5.9: Effect of Tiam1 inhibition on laminar shear-induced cellular realignment. BBMvEC's transfected with or without (mock) Tiam1 C580 were either maintained under static conditions or exposed to laminar shear stress (10 dynes cm^{-2}, 24 h) and monitored for cellular realignment by phase-contrast microscopy. White arrow indicates the direction of the flow vector (iii). Images are representative.

5.2.10: Laminar shear stress-induced upregulation of BBMvEC barrier function is Tiam1-dependent.

BBMvEC's transfected in the absence (mock) and presence of Tiam1 C580 were monitored for their effects on shear-dependent enhancement of barrier function. As expected, shear significantly reduced permeability (%TEE of FD40) compared to the static control. However, this shear-induced reduction in permeability was attenuated by 76.4% in the presence of Tiam1 C580 (following correction for the baseline decrease with Tiam1 C580 under static conditions) (Fig. 5.10).

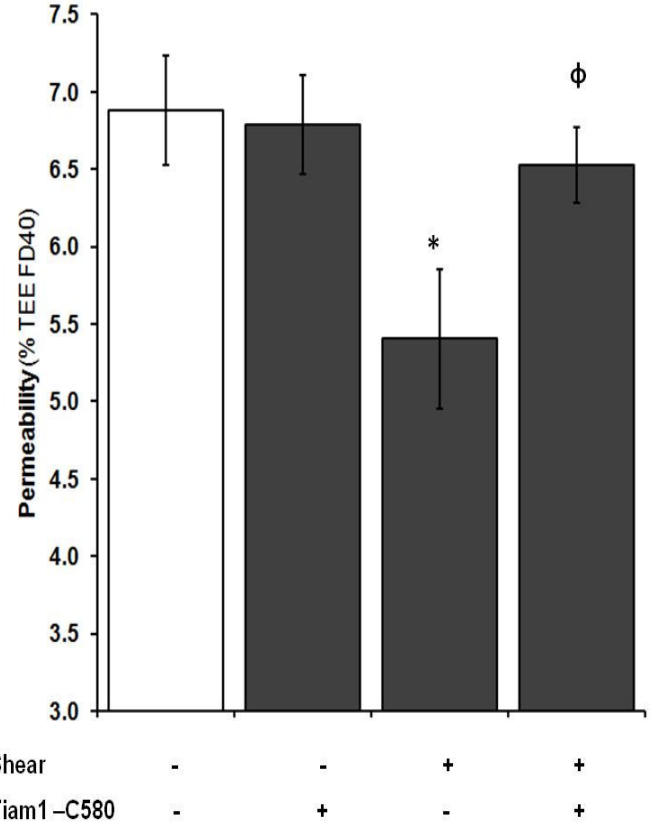

Fig. 5.10: Effect of Tiam1 inhibition on laminar shear-induced regulation of BBMvEC permeability. Transfected BBMvEC's with or without (mock) Tiam1 C580 were either maintained under static conditions or exposed to laminar shear stress (10 dynes cm^{-2}, 24 h) and monitored for transendothelial permeability. Histogram data points show change in permeability (%TEE FD40 at t=120 min). Histogram is averaged from three independent experiments ±SEM; *$P \leq 0.05$ vs uninhibited static, ϕ$P \leq 0.05$ vs uninhibited shear.

5.2.11: Laminar shear-induced localization of ZO-1 is Tiam1 dependent.

Following BBMvEC exposure to laminar shear stress (10 dynes cm^{-2}, 24 h) in the absence (mock) or presence of Tiam1 C580, subcellular localization of ZO-1 was monitored. As previously described, undisturbed laminar flow induced a profound immunoreactivity of ZO-1 along the plasma membrane, which was completely disrupted with Tiam1 C580 treatment, exhibiting a more discontinuous, broken pattern of ZO-1 at cell-cell borders (Fig. 5.11 i-iv).

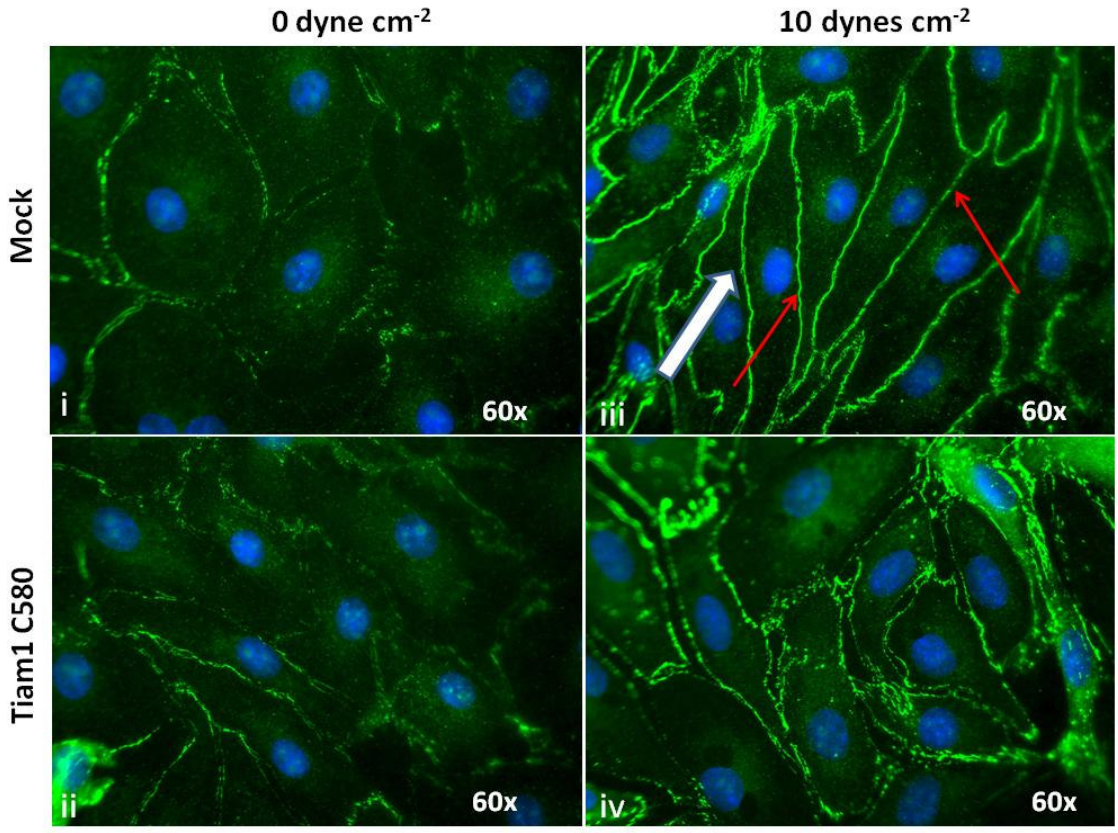

Fig. 5.11: Effect of Tiam1 inhibition on laminar shear-induced ZO-1 localization. Transfected BBMvEC's with or without (mock) Tiam1 C580 were grown to confluency and either maintained under static conditions or exposed to laminar shear stress (10 dyne cm^{-2}, 24 h) to be monitored for ZO-1 localization by fluorescent microscopy. Red arrows denote sharp, continuous localization of ZO-1 to cell-cell borders (iii). White arrow indicates direction of the flow vector (iii). DAPI stained nuclei (blue) are clearly visible (i-iv). Images are representative.

5.2.12: Laminar shear-induced tyrosine dephosphorylation of occludin is Tiam1-dependent.

Following transfection in the absence (mock) or presence of Tiam1 C580, BBMvEC's were harvested and monitored for changes in pTyr-occludin level by IP and IB. The shear-induced reduction in pTyr-occludin (to 0.09±0.06 fold of control) was significantly attenuated by 37.36% in the presence of Tiam1 C580 (following correction for the baseline increase with Tiam1 C580 under static conditions) (Fig. 5.12 A i-ii).

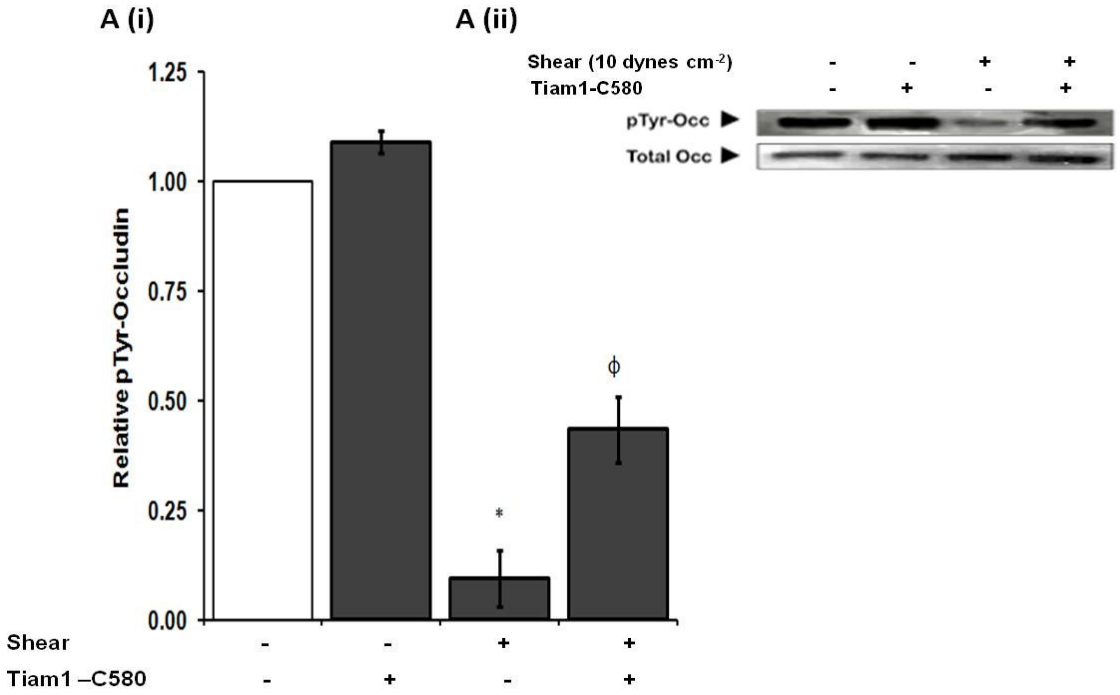

Fig. 5.12: Effect of Tiam1 C580 inhibition on laminar shear-induced occludin tyrosine dephosphorylation. Transfected BBMvEC's with or without (mock) Tiam1 C580 were grown to confluency and either maintained under static conditions or exposed to laminar shear stress (10 dyne cm^{-2}, 24 h) and monitored for pTyr-occludin and total occludin levels. Histogram (A i) represents relative pTyr-occludin (i.e. pTyr-occludin/total occludin derived by scanning densitometry from blots in A ii). Results are averaged from three independent experiments ±SEM; *$P \leq 0.05$ vs uninhibited static, ϕP≤0.05 vs. uninhibited shear. Blots are representative.

5.3 Discussion

In-vitro models of blood flow have yielded a comprehensive insight into potential *in-vivo* mechanostransduction processes that might mediate responses to flow-associated shear stress and uncover mechanisms that contribute to disease progression. Chapters 3 and 4 clearly demonstrate the role of laminar shear stress in the assembly of tight junction proteins, consistent with an enhancement of BBMvEC barrier function. Furthermore, putative intracellular signaling roles for the GTPase Rac1 (and to an extent, RhoA) in the shear-induced regulation of BBMvEC barrier function was clarified. We now extend these findings to examine potential upstream regulators of shear-induced Rac1 activity and BBMvEC barrier function, specifically monitoring the mechanosensory adaptor protein, VE-Cadherin and the Rho GEF, Tiam1.

In order to block VE-Cadherin function, BBMvEC's were transfected with a VE-Cad ΔEXD plasmid construct (mutant form of VE-Cadherin lacking extracellular cadherin repeat domains 1-5). Thus, whilst VE-Cad ΔEXD can localize to adherens junctions and associate as normal with cytoplasmic binding partners, homotypic intercellular adhesion with wild type VE-Cadherin is completely disrupted (Kouklis et al., 2003, Orrington-Myers et al., 2006). Furthermore it has been shown that over-expressing VE-Cadherin cytoplasmic domains (lacking EC repeat domains) titrates β-Catenin from its downstream effectors and suppresses the endogenous expression of VE-Cadherin (Venkiteswaran et al., 2002). Following transfection of BBMvEC's with VE-Cad ΔEXD, the shear-induced activation of Rac1 following 60 min shear exposure was significantly attenuated suggesting a plausible role for VE-Cadherin mechano-signaling in our model. Consistent with our findings, a recent report by Liu *et al.* showed that VE-Cadherin engagement (i.e. homotypic binding of adjacent EC domains) was necessary for cyclic strain-induced activation of Rac1, by using blocking antibodies specific to EC domains of VE-Cadherin. The authors proposed a model whereby a primary junctional structure (PECAM-1?) transduces the hemodynamic stimuli, which alters the engagement of cadherins and in turn leads to Rac1 signaling, i.e. outside-in signaling (Liu et al., 2007). Also, as discussed in section 1.5.1, VE-Cadherin is organised through

cis dimerization/trimerization of EC domains, a mechanism that would potentially be disrupted through VE-Cad ΔEXD expression.

Downstream of VE-Cadherin mechano-signaling, we sought to investigate the potential role of Tiam1 in shear-induced activation of Rac1 in BBMvEC's. It has been previously demonstrated that VE-cadherin engagement can activate Rac1 via recruitment of Tiam1 (Lampugnani et al., 2002). In order to block Tiam1 function, BBMvEC's were transfected with a Tiam1 C580 plasmid construct (mutant form lacking PHn; pleckstrin homology N-terminus domain and DHR; discs-large homology region). Although endogenous Tiam1 contains two PH domains (PHn and PHc), the PHn domain has been specifically shown to be critical for the membrane localization of Tiam1 and downstream signaling through Rac1 (Hordijk et al., 1997). In our model, shear-induced Rac1 activation was significantly attenuated following Tiam1 C580 expression suggesting a definitive role for Tiam1 in this process. Furthermore, Tiam1 inhibition disrupted the shear-induced realignment of BBMvEC's, consistent with findings observed with the Rac1 inhibitor NSC23766 in section 4.2.3, confirming Tiam1 as a critical GEF regulating shear-mediated activation of Rac1. The molecular linkage of VE-Cadherin to Tiam1 activation is unknown, however an attractive linkage is proposed herein. Shear-induced activation of the 'PECAM-1/VE-Cadherin/VEGFR2' mechanosensory complex is known to regulate PI3K activity, which can lead to the production of the membrane-associated lipid product, phosphatidylinositol 3,4,5-triphosphate (PIP_3). PIP_3 has been shown to bind to at least 3 GEFs (Tiam1, Vav and Sos) through associations with their PH domains, which would relieve their inhibitory effect and elicit the conformational changes necessary to activate the GEF, thus signaling to their respective GTPases (Kjoller and Hall, 1999, Tzima et al., 2005). This mechanism would however appear somewhat controversial as it 'bypasses' integrin-mediated mechanosensing processes, which have also been implicated in shear-induced activation of Rac1 (discussed further in chapter 6) (Tzima et al., 2002).

The specificity of the upstream signal activating a particular RhoGTPase is essential for specific downstream effector activation and functional response. Thus, having

confirmed that both VE-Cadherin and Tiam1 were acting upstream of shear-induced Rac1 signaling, we employed similar inhibition strategies to monitor for potential effects on downstream indices of barrier function. Both VE-Cadherin and Tiam1 inhibition significantly attenuated the shear-induced enhancement of barrier function (79.8% and 76.4% respectively) as measured by transendothelial permeability assay, alluding to a coupled signaling relationship between the two molecules. Previous *in-vitro* and *in-vitro* findings have shown that VE-Cad ΔEXD expression induces junctional disassembly (Orrington-Myers et al., 2006, Broman et al., 2006). Interestingly though, expression of VE-Cad ΔEXD in BBMvEC's didn't provoke a statistically significant increase in permeability relative to static, mock-transfected BBMvEC's, but was pivotal to shear-induced responses. One possible explanation is that under static conditions tight junctions are able to compensate for the reduction in VE-Cadherin homotypic adhesion experienced with VE-Cad ΔEXD. Furthermore, the observed modifications (localization, phosphorylation) in tight junction proteins following prolonged, physiological levels of shear appear to explain the concomitant reduction in permeability, thus placing tight junctions at the hub of paracellular permeability regulation at the BBB. This is consistent with the well-accepted view that tight junction proteins at the BBB are of the highest complexity and best equipped to limit paracellular flux compared to endothelial tight junctions of non-BBB origin (Kniesel and Wolburg, 2000, Wolburg and Lippoldt, 2002).

To this end, we extended our inhibition studies with VE-Cad ΔEXD and Tiam1 C580 to examine biochemical changes in tight junction proteins with respect to ZO-1 and/or claudin-5 localization. Both inhibition strategies clearly abrogated the shear-induced immunoreactivity of ZO-1 at cell-cell borders. ZO-1 is an essential adaptor protein that facilitates correct spatial organization of tight junction proteins and associations with cortical actin, and is thus crucial to stability of the endothelial barrier (Umeda et al., 2006, Fanning and Anderson, 2009). The loss of shear-induced ZO-1 localization at the cell membrane would offer in part, an explanation for the observed increase in BBMvEC permeability under conditions of VE-Cadherin and Tiam1 inhibition. The specific finding that VE-Cadherin could influence shear-induced ZO-1 organization

adds further weight to the recently established concept of a functional "cross-talk" mechanism between adherens and tight junction complexes. Taddei *et al.* identified this concept by showing that VE-Cadherin inhibition represses claudin-5 expression, which paralleled with increases in permeability, thereby offering a novel mechanism of barrier disruption via VE-Cadherin ablation (Taddei et al., 2008). With this in mind, we examined the effect of shear-induced claudin-5 subcellular localization following VE-Cad ΔEXD expression. Similar to ZO-1, the shear-mediated cell-cell border immunoreactivity of claudin-5 was completely disrupted with VE-Cad ΔEXD, thus confirming that shear stress promotes a junctional cross-talk within BBMvEC's. Although quantification of claudin-5 expression was not assessed with VE-Cad ΔEXD treatment, the immunocytochemical staining pattern appeared to reveal a diminished expression of claudin-5, in tandem with a discontinuity along the plasma membrane.

Finally, we observed that both VE-Cadherin and Tiam1 inhibition significantly attenuated the shear-induced reduction in pTyr-occludin by 89.13% and 37.36% respectively. This finding with VE-Cad ΔEXD on pTyr-occludin confirmed that shear-induced regulation of VE-Cadherin was able to target all three tight junction components (occludin, claudin-5 and ZO-1), placing the mechanosensory adaptor molecule as a core mediator of shear-induced regulation of BBMvEC barrier function, possibly through a Tiam1-Rac1 signaling axis. Interestingly, the shear-induced attenuation of pTyr-occludin with Tiam1 inhibition only represented 57.38% of the shear-induced attenuation of pTyr-occludin observed with NSC23766 (Rac1 inhibition). Consistent with this was the finding that Tiam1 inhibition attenuated the shear-induced activation of Rac1 by 60.87%. Not owing to possible discrepancies in transfection efficiency, this observation could suggest the involvement of integrins or even the possibility of other GEF'(s) in shear-mediated Rac1 activation and barrier function. In this regard, the RhoGEF Vav2 has been shown to promote Rac1 activity consistent with an enhancement of barrier integrity (Birukova et al., 2007b, Birukova et al., 2008). Future work using a molecular knockout of Vav2 would help clarify this issue.

In concluding, our findings build substantially on the earlier work of Colgan *et al.* and establish a series of shear-induced changes in tight junction proteins that are consistent with an upregulated BBMvEC barrier phenotype (Colgan et al., 2007). This includes shear-induced enhancement of occludin and ZO-1 expression levels (mRNA and protein); enhanced localization of occludin, ZO-1 and claudin-5 to the cell-cell border; reduction in pTyr-occludin and increased occludin-ZO-1 association. Our recent findings have shed some light on possible mechanosensing (VE-Cadherin) and intracellular signaling mechanisms (Tiam1, Rac1) putatively mediating these effects. Future work will attempt to expand on the molecular link between VE-Cadherin and GEF and/or integrin-mediated activation of Rac1. Furthermore, the events downstream of Rac1-mediated regulation of tight junction proteins will need to be assessed, with a specific emphasis on the tyrosine kinase and phosphatase mechanisms involved in tight junction protein modification.

Chapter 6:

Final Summary

6.1 Final Summary

Physiological maintenance of cerebral homeostasis and thus neuronal/glial function is governed by the blood brain barrier (BBB). This highly stringent barrier is formed by cerebral microvascular endothelial cells (EC's), which shield the brain from blood-borne toxins, supplies the brain with essential nutrients and filters harmful compounds from the brain back into the bloodstream. Crucial to regulation of these processes are the transcellular and paracellular pathways. The former contains multiple transport systems and enzymatic barriers to control molecular traffic through the cell. The latter describes a continuum of intercellular tight and adherens junction complexes between adjacent cerebral microvascular endothelial cells (EC's), generating a relatively impermeable barrier to the flow of ions, proteins, hydrophilic molecules and hormones between EC's, thereby protecting the brain from harmful fluctuations in these molecules. Together, both pathways establish a highly restrictive barrier phenotype, and as a consequence make the BBB the rate limiting step in the delivery of therapeutic agents to the CNS (Pardridge, 2007). Conversely, BBB disruption has been associated with the pathophysiology of various neurological disorders, including HIV-encephalitis, ischemia, tumors, Parkinson's disease, multiple sclerosis and Alzheimer's disease (Persidsky et al., 2006).

Of particular interest to the present thesis is the paracellular pathway. It is a well-accepted concept that tight junctions are the primary structures responsible for the paracellular barrier properties present at the BBB (Wolburg and Lippoldt, 2002, Vorbrodt and Dobrogowska, 2003, Engelhardt, 2003). Much effort in recent decades has been made to indentify the molecular composition of the tight junction complex, the interaction with adaptor/peripheral proteins and their regulation by adhesion molecules, extracellular matrix components and signal transduction pathways. Understanding the mechanisms by which intercellular junction complexes (tight junctions) are regulated in physiology and/or pathology will be essential to the development of pharmacotherapeutic strategies modulating BBB function. Unfortunately, most of the findings to date have been gathered in epithelial cells or endothelial cells of non-

neuronal origin thus making accurate inferences about tight junction permeability regulation at the BBB more difficult. The probable reasons for this are direct investigation of BBB *in-vivo* is hindered because of anatomical and topographic obstacles, and furthermore it is challenging for *in-vitro* models to encompass all essential surrounding influences such as astrocytes, pericytes, neurons, extracellular matrix and flow-associated shear-stress. Indeed, the latter component, laminar shear stress is widely considered to be a principal differentiative stimulus influencing endothelial phenotype at multiple levels, with profound consequences for blood vessel integrity and remodeling (Krizanac-Bengez et al., 2004, del Zoppo, 2008, Hahn and Schwartz, 2009).

With this in mind, the aim of this study was to examine the effects of shear stress (acute vs. chronic) on endothelial tight junction assembly at both the molecular and functional level in an *in-vitro* BBMvEC model. We hypothesised that physiological shear stress would induce BBMvEC barrier phenotypes as assessed by various responses, including changes in BBMvEC cellular and F-actin morphology, biochemical changes in tight junction proteins (occludin, ZO-1 and claudin-5) and functional changes in permeability. Furthermore, we investigated the effects of flow reduction following an initial pre-conditioning phase of high shear and monitored for changes in BBMvEC barrier phenotype.

In an effort to delineate the signaling pathways mediating shear-dependent changes in BBMvEC barrier function, we employed a series of pharmacological and molecular inhibition strategies specifically targeting the RhoGTPases, RhoA and Rac1, the guanine nucleotide exchange factor (GEF) Tiam1, and the mechanosensory adaptor protein VE-Cadherin. It was anticipated that the latter studies elucidating signal transduction pathways would identify potential molecular targets involved in tight junction regulation at the BBB, which would be invaluable in CNS disorders exhibiting a dysfunctional barrier. Figure 6.1 below schematically depicts the experimental approach used in this body of research.

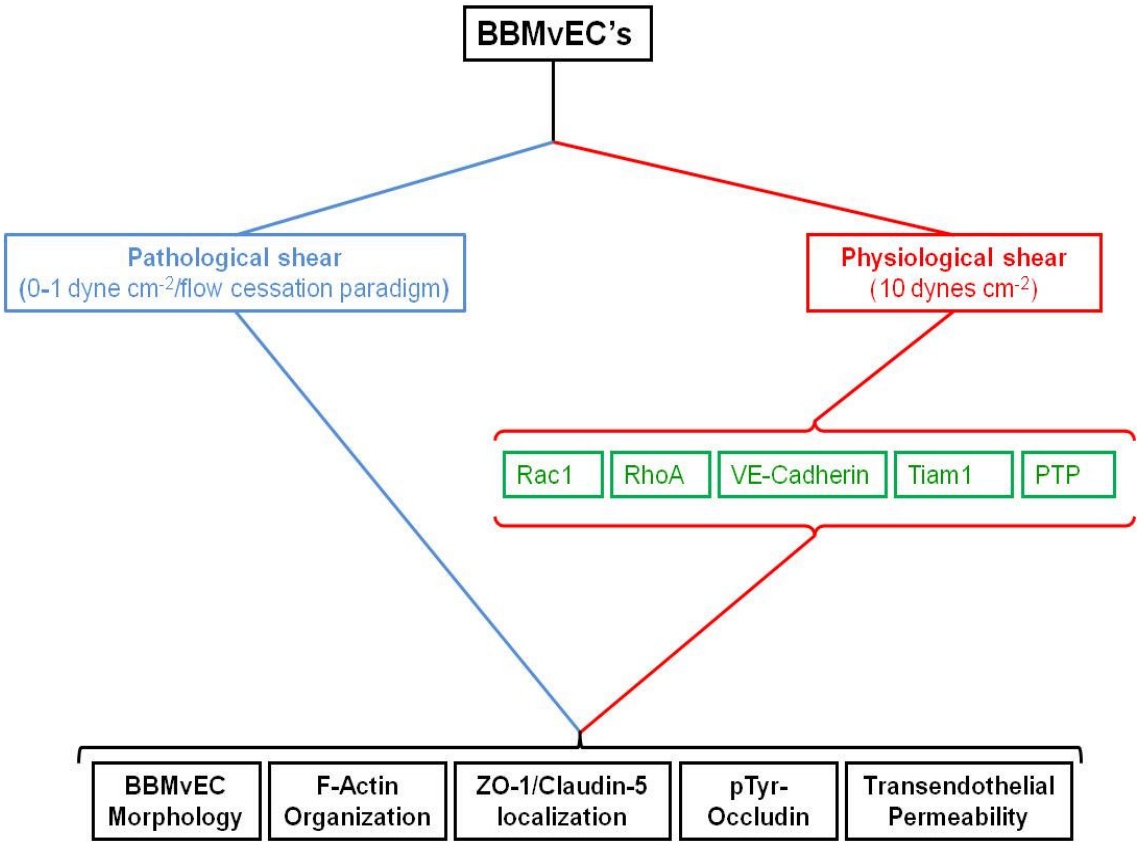

Fig. 6.1: Schematic depiction of experimental approach. Bovine brain microvascular endothelial cells (BBMvEC's) were subjected to different experimental paradigms; pathological shear conditions (blue) and physiological shear (red), and monitored for structural changes in morphology, functional alterations in permeability and biochemical changes in tight junction proteins. Various molecular and pharmacological inhibition strategies (green) were incorporated to assess potential involvement under physiological conditions.

Hemodynamic forces are a functionally relevant stimulus, which have previously been described as critical regulators of BBB induction and regulation (Stanness et al., 1997, Siddharthan et al., 2007, Cucullo et al., 2008). Furthermore, recent findings from our laboratory have implicated hemodynamic forces as a putative stimulus regulating endothelial tight junction assembly and barrier function (Collins et al., 2006, Colgan et al., 2007). With this in mind, we sought to re-visit and expand on the basic findings of Colgan *et al.* using physiological and non-physiological paradigms of blood flow-associated shear stress and examine the cellular signaling mechanism regulating BBMvEC function under shear. Our initial experiments revealed that non-physiological

levels of laminar shear stress (1 dyne cm^{-2} 24 h) correlated with findings from unsheared BBMvEC's with respect to cellular morphology and transendothelial permeability, thus strengthening the applicability of the static condition as a suitable control when comparing to physiological levels of shear (10 dynes cm^{-2}). In a parallel series of experiments we temporally monitored shear-enhanced barrier function at 10 dynes/cm^{-2} over a 24 h period. The most significant shear-induced reductions in permeability only became evident in the latter chronic stages (12-24 h), which paralleled with the pattern of cellular realignment in the direction of the flow. EC realignment to flow involves a complex process of actin-cytoskeletal remodeling that spans a rapid (within mins) to prolonged (up to 24 h) time course of events (Rizzo, 2007, Noria et al., 2004). Thus, although shear-onset initiates a rapid phase of cytoskeletal adaptations, it appears that the cellular elongation and realignment processes that accompany extended shear exposure necessitate/facilitate appropriate assembly of intercellular junction components that stabilize barrier integrity.

To further extend our physiological flow paradigm, we monitored the effects of chronic shear on biochemical alterations in tight junction proteins. The tight junction-associated adaptor molecule ZO-1 plays a multifunctional role at the intercellular junction by facilitating protein-protein interactions, membrane trafficking of other tight junction proteins and bridging associations with the cortical based actin-cytoskeleton (Fanning and Anderson, 2009). The tight junction protein claudin-5 plays a more physical role in barrier maintenance through the 'sealing' properties of its extracellular domains within the intercellular cleft (Krause et al., 2008). We therefore hypothesized that membrane localization of ZO-1 and claudin-5 would be crucial to the structural assembly and/or associations of the tight junction complex. Within our BBMvEC model, we observed that chronic shear exposure induced significant enhancements of both ZO-1 and claudin-5 immunoreactivity at cell-cell borders, which is consistent with the observed decrease in permeability at similar time points. Moreover, loss of these junctional structures has been frequently associated with various pathological conditions at the BBB, thereby strengthening the functional relevance of these molecules at the tight junction following shear exposure (Dallasta et al., 1999, Andras et al., 2003, Liu et al., 2008a, Chen et al.,

2009). Furthermore, these events coincided with the shear-induced re-arrangement of the actin cytoskeleton, as F-actin staining revealed an enhanced assembly of cortical actin. This forms an important structural association with ZO-1 and thus, indirect association with other tight junction components and has been frequently associated with enhanced barrier integrity (Birukova et al., 2007a). Consistent with this was the observation by Colgan *et al.* that shear exposure enhanced the co-association of ZO-1 with occludin in BBMvEC's (Colgan et al., 2007). Thus, it appears that prolonged shear enhances the structural assembly and integrity of tight complexes, but the mechanistic link mediating these shear-induced structural alterations in tight junction components needs to be deciphered.

Recent findings from our laboratory indicated that inhibition of *de-novo* protein synthesis (by cycloheximide) could only partially attenuate the shear-induced increase in ZO-1-occludin co-association, thereby suggesting that post-translation modifications of the tight junction pool were essential for enhanced tight junction co-association, in tandem with increased protein expression (Collins et al., 2006, Colgan et al., 2007). We found that shear exposure in BBMvEC's triggers a shift in pTyr-occludin levels, from being initially elevated in the acute shear phase (1 h) to being significantly attenuated well below basal levels in the chronic shear phase (24 h). Indeed, the latter finding on pTyr-occludin status (i.e. tyrosine dephosphorylated) is consistent with previous reports showing that pTyr-occludin levels are essential for barrier maintenance (Kago et al., 2006, Peng et al., 2009). To further confirm the hypothesis that this post-translational state was imperative to tight junction assembly and barrier function, we observed that protein tyrosine phosphatase (PTP) inhibition with dephostatin significantly attenuated the shear-induced reduction with permeability. Recent work by Elias *et al.* identified specific pTyr-residues on occludin that were essential for its interaction with ZO-1 (at the C-terminus), a process which was regulated by the tyrosine kinase c-Src (Elias et al., 2009). Based on all these findings it would imply that possibly other PTP's (not inhibited by dephostatin) and protein tyrosine kinases (PTK's) are mechano-regulated to target the tight junction, albeit through unknown mechanisms. Importantly though, these findings are consistent with previous reports by Lohmann *et al.* and Wachtel *et al.* who

showed that pharmacological blockade of tyrosine phosphatases alters barrier function at the BBB and peripheral vasculature respectively (Lohmann et al., 2004, Wachtel et al., 1999). Identifying the molecular link(s) and specific PTP's and PTK's regulating these functions would be of genuine therapeutic relevance.

Having established a series of structural and biochemical responses in BBMvEC's to physiological shear, our attention turned towards potential signaling molecules mediating such effects. The RhoGTPases RhoA and Rac1 have been implicated as definitive regulators of cytoskeletal dynamics and vascular permeability, and as such we hypothesized that these molecules would participate in shear-dependent barrier regulation within BBMvEC's (Hall, 1998, Spindler et al., 2010). GTPases function like molecular switches in response to upstream stimuli (i.e. shear stress) that propagate downstream signaling pathways through appropriate effector binding. In this regard, RhoA has been extensively linked with barrier dysfunction through its effector Rho-associated kinase (ROCK) which drives actin-mediated cell contractility and intercellular junction disassembly (Birukova et al., 2004, Sun et al., 2006). By contrast, Rac1 has been well documented for its barrier-stabilizing effects by promoting cortical actin accumulation and intercellular junction assembly (Jacobson et al., 2006, Baumer et al., 2009).

Both GTPases were shown to be mechanosensitive in BBMvEC's, albeit with significant temporal disparity between their activation states. RhoA was rapidly activated following shear-onset (while Rac1-GTP was decreased), and we hypothesize that this initial, acute shear-phase response is essential to the cellular morphological adaptations and barrier enhancement observed following prolonged shear exposure (Wojciak-Stothard and Ridley, 2003). However, as the time course of shear exposure advances, a reciprocating trend towards Rac1 activity became more prominent, particularly in the chronic shear phase (24 h) as levels of Rac1-GTP at this stage were significantly elevated above basal levels whereas RhoA activity was significantly below baseline levels. This suggests a more central role for Rac1 in the maintenance of barrier

integrity under continued shear exposure, and as result, we decided to look more closely at the Rac1 participation in our shear-dependent model.

To test this hypothesis further, we used two different strategies of Rac1 inhibition (NSC23766 and T17N), and we confirmed that Rac1 activity is essential to shear-induced BBMvEC morphological realignment, enhancement of barrier function, cell-cell border localization of ZO-1 and reduction in pTyr-occludin levels following prolonged shear exposure. Significantly though, these findings show that within BBMvEC's, RhoGTPases can target the tight junction, which is consistent with previous findings (Wojciak-Stothard et al., 2001, Yamamoto et al., 2008). Thus, from this point on our primary focus was to expand on the signaling events linking shear-induced activation of Rac1 to changes in tight junction assembly and barrier function.

Moving upstream of shear-mediated Rac1 activity, our focus shifted toward the mechanosensory adaptor protein VE-Cadherin which has been previously implicated in endothelial mechanotransduction processes (Shay-Salit et al., 2002, Tzima et al., 2005). Inhibition of VE-Cadherin by over-expressing VE-CadΔEXD significantly abrogated the shear-induced activation of Rac1. VE-Cadherin has been previously shown to regulate RhoGTPase activity, to our knowledge however, no group has investigated the contribution of intercellular junctions to shear-dependent changes in Rac1 activity (Liu et al., 2007, Wallez and Huber, 2008). Moreover, we extended this inhibition strategy with VE-Cad ΔEXD to indices of BBMvEC barrier function and observed that shear-induced membrane localization of ZO-1 and claudin-5, reduction in pTyr-occludin and enhancement of barrier function was significantly disrupted following VE-Cadherin inhibition. Thus, we confirm that under shear conditions, VE-Cadherin is targeting the tight junction, possibly via Rac1. This conforms to recent findings by Taddei *et al.* who identified a functional crosstalk mechanism between adherens and tight junctions, whereby VE-Cadherin was able to regulate claudin-5 expression (Taddei et al., 2008). Previous work by Orrington Myers *et al.* confirmed that VE-Cad ΔEXD disrupts lung endothelial barrier function *in-vivo* (Orrington-Myers et al., 2006). We anticipate that by restoring VE-Cadherin adhesion and function may not only alleviate vascular leakage,

but could rescue BBB function in associated pathologies by providing positive feedback on tight junction proteins. Thus, future work should focus on further clarification of the molecular mechanisms by which shear-induced regulation of VE-Cadherin regulates tight junction assembly.

In an effort to further delineate this shear-induced signaling network, we assessed the participation of the Rho guanine nucleotide exchange factor (GEF) Tiam1 in our model. Tiam1 is Rac1-specific RhoGEF that is regulated by diverse signaling pathways including PI3K-dependent, protein-kinase A-dependent, tyrosine-kinase dependent and Epac-Rap1-dependent pathways (Arthur et al., 2004, O'Connor and Mercurio, 2001, Servitja et al., 2003, Welch et al., 2003). Furthermore, VE-Cadherin mediated cell-cell adhesion has been shown to activate Tiam1, thus forming our hypothesis that shear-mediated activation of Rac1 via VE-Cadherin requires Tiam1 (Lampugnani et al., 2002). Indeed, shear-induced activation of Rac1 in BBMvEC's was significantly attenuated by Tiam1 C580. When this inhibition strategy was incorporated into indices of barrier function, we noticed that the shear-mediated immunoreactivity of ZO-1 at cell-cell borders, reduction in pTyr-occludin and enhancement of barrier function was significantly disrupted following Tiam1 inhibition. We conclude that Tiam1 is essential to shear-mediated responses in our BBMvEC model, however as complete attenuation of shear-induced activation of Rac1 was not achieved with Tiam1 inhibition, we suspect that other GEF's may be involved. Given the fact that Rac1 can regulate such diverse cellular processes, identification of these specific upstream mediators of shear-induced Rac1 activity will help identify appropriate molecular targets (Bosco et al., 2009).

Based on our observations in BBMvEC's and accepted findings throughout the literature, we now propose a signaling model by which shear stress upregulates barrier function and tight junction assembly (Figure 6.2). In brief, shear stress activates the mechanosensory complex (PECAM-1-VE-Cadherin-VEGFR2), which induces Tiam1 and/or integrin-mediated Rac1 activation via PI3K (Tzima et al., 2005). Downstream effector(s) activation by Rac1 promotes the assembly of cortical actin, and the regulation of PTK's and PTP's, which together control pTyr-occludin levels and cell-

cell border localization of ZO-1 and claudin-5 thus promoting tight junction assembly and barrier stability.

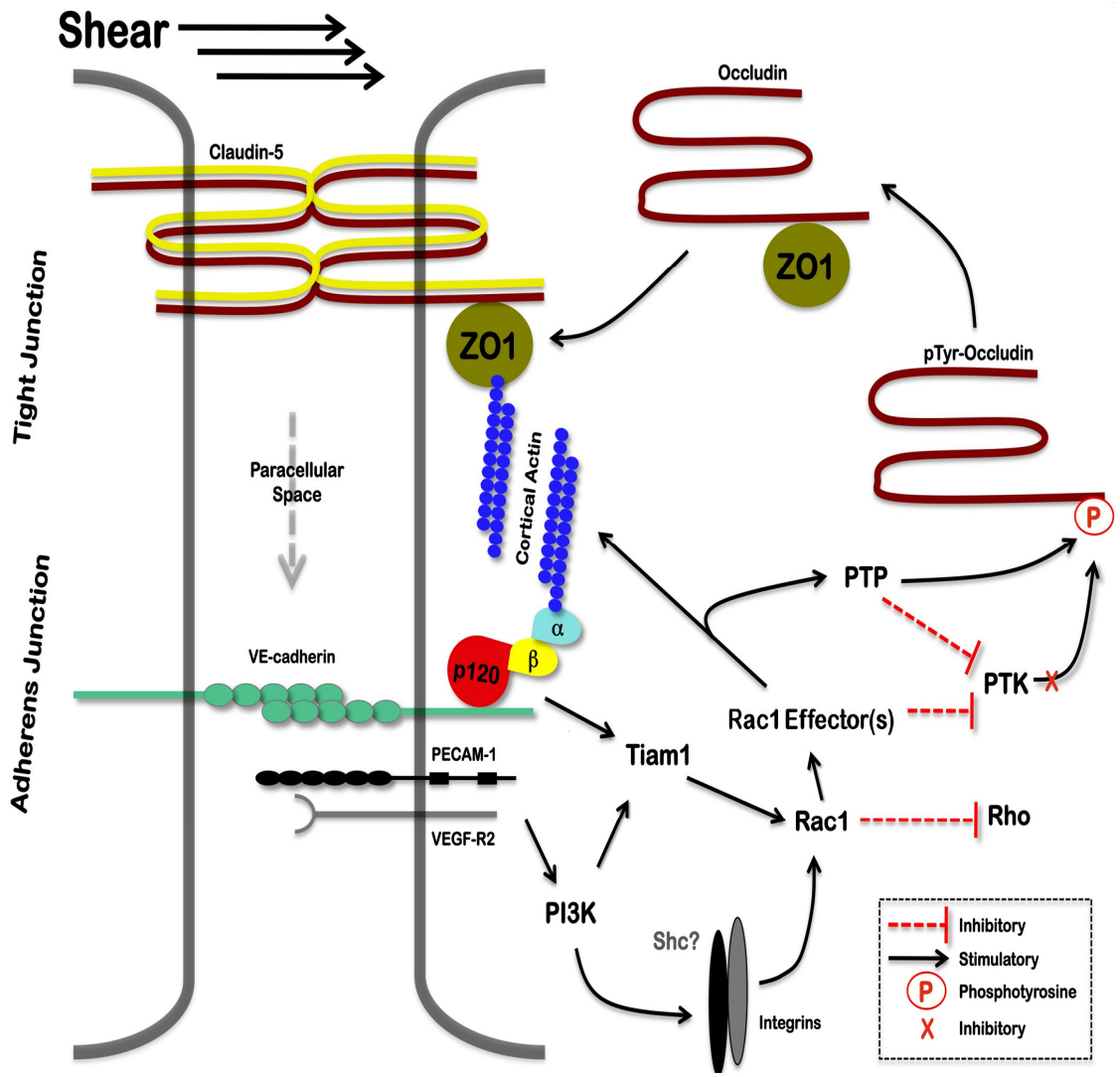

Fig. 6.2: Signaling mechanisms mediating the barrier-stabilizing influence of shear stress in BBMvEC's. PECAM-1, platelet endothelial cell adhesion molecule 1; VEGFR2, vascular endothelial growth factor receptor 2; p120/α/β-catenins; PI3K, phosphoinisotide 3-OH-kinsae; Shc, Src-homology SH2 domain adaptor protein; PTP, protein tyrosine phosphatase; PTK, protein tyrosine kinase; ZO-1, zonula occludens 1.

Although not examined in this body of research, we acknowledge the possible contribution of integrins to the barrier stabilizing influence of shear in BBMvEC's. Integrins comprise a family of transmembrane receptors that facilitate cell-matrix adhesion but have been implicated in flow-mediated responses. In this regard, shear-dependent activation of the mechanosensory complex has been shown to activate PI3K, consequently leading to integrin (αvβ3) activation, which imply a degree of cross talk of mechanosensing mechanisms originating from cell-cell and cell-matrix contacts (Tzima et al., 2005). Furthermore, Rac1 activation has been shown to occur downstream of shear-induced integrin activation (Tzima et al., 2002). Crucial to the integration of both signaling mechanisms is Shc, an SH2 adaptor protein which orchestrates signals from both cell-cell and cell-matrix adhesions to elicit flow-induced signaling (Liu et al., 2008b, Sweet and Tzima, 2009). Future work should therefore clarify the contribution of integrins (and Shc), in conjunction with VE-Cadherin, to the shear signaling cascade during BBB stabilization.

In an attempt to mimic the evolution of cerebrovascular injury experienced during cerebral ischemia, we investigated the effect of flow reduction on BBMvEC barrier function (Krizanac-Bengez et al., 2004, del Zoppo, 2008). This experimental paradigm involved a "pre-conditioning" phase under physiological conditions (10 dynes cm^{-2}, 24 h) followed by a sustained (10 dynes cm^{-2}, for a further 24 h) or reduced (1 dyne cm^{-2}, 24 h) flow phase. Significantly, flow reduction attenuated the shear-induced BBMvEC morphological realignment, enhancement of barrier function, ZO-1 cell-cell border localization and reduction in pTyr-occludin. Indeed, the latter finding is consistent with recent findings from *in-vivo* BBB models showing that cerebral ischemia enhances pTyr-occludin levels, therefore supporting the applicability of our model (Kago et al., 2006, Takenaga et al., 2009). Therefore, future work should explore the signaling mechanisms pertaining to these effects. In this regard, we hypothesize that decreased shear would alter cytoskeletal machinery leading to barrier disassembly, possibly via RhoA. Moreover, this pathological state is associated with increased levels of reactive oxygen species (ROS) which have been previously shown to disrupt barrier integrity,

and their participation within this context should also be addressed (Lee et al., 2004, Monaghan-Benson and Burridge, 2009).

Although our shearing model of orbital rotation has been previously validated and was suitable for generating substantive quantities of sheared cells for IB, IP and IC analyses, BBMvEC permeability via transendothelial permeability assay could be not monitored in real time (Pearce et al., 1996, Fitzpatrick et al., 2009, Colgan et al., 2007, Hendrickson et al., 1999). Shearing of BBMvEC's in transwell inserts was not feasible as cells would be exposed to basolateral turbulence, and thus would not reflect the *in-situ* condition of apical shear exposure. As a consequence, BBMvEC's following shearing protocols had to be replated and left to adhere overnight on transwell inserts before permeability could be monitored. In this regard, EC's have previously demonstrated 'mechanical memory' capabilities under a similar protocol following prolonged exposure of cyclic strain in bovine aortic endothelial cells (Collins et al., 2006). The dynamic *in-vitro* (DIV)-BBB model would be a suitable alternative as it allows for real-time monitoring of BBB function under flow conditions by direct quantification of transendothelial electrical resistance (TEER) (Flocel Inc., Cleveland, Ohio). DIV-BBB is a novel, tri-dimensional, perfused trans-capillary apparatus consisting of an enclosed bundle of 19 semi-permeable (0.2μm) Pronectin®-coated capillaries within a DIV-BBB cartridge, through which medium from a reservoir is pumped at a chosen flow rate. (Figure 6.3). Each cartridge contains built in electrodes which connect to a computer controlled device for monitoring TEER. Moreover, the DIV-BBB allows for co-culturing of cell-types within spatially distinct compartments i.e. intralumenial space (EC's) and extralumenial space (astrocytes) whilst facilitating solute diffusion via 0.2μm trans-capillary pores, giving a closer representation of the *in-vivo* brain micro-environment and an accurate *in-vitro* model to study BBB function (Krizanac-Bengez et al., 2006, Santaguida et al., 2006). Thus, acquiring such a multi-dimensional model would be invaluable for future cell modeling work assessing molecular/pharmacological based inhibition strategies targeting BBB permeability.

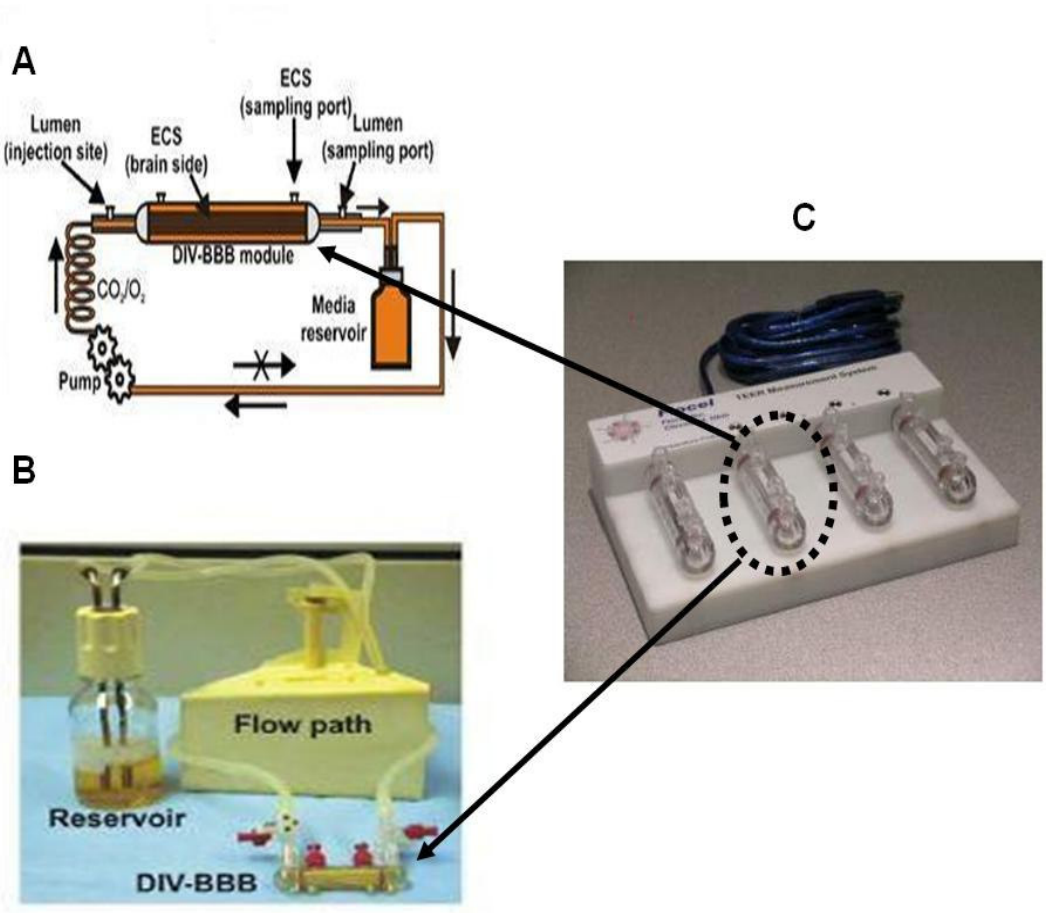

Fig. 6.3: Representation of DIV-BBB model and computer controlled TEER monitoring device. (A): Schematic representation of the DIV-BBB module cartridge and model set-up, (B): actual set-up of DIV-BBB with flow path and medium reservoir, (C): DIV-BBB cartridges contain electrodes in the lower half of the module and are connected to the TEER measurement system (Flocel Inc.) allowing for computer controlled monitoring of BBB function in real time.

Finally, although bovine models are a suitable surrogate system for biological research, proof-of-concept experiments on BBB function should be replicated in human primary cells. In this regard, we recently acquired primary, human brain microvascular endothelial cells (HBMvEC's), from which we hypothesize that future experiments on BBB function will yield similar findings to those observed within our BBMvEC model. Indeed, initial findings with HBMvEC's demonstrating shear-induced (10 dyne cm^{-2}, 24 h) morphological realignment and enhanced ZO-1 immunoreactivity at cell-cell borders

are consistent with our observations from the BBMvEC model (Figure 6.4). Future work should expand on these basic findings and monitor the role of various signaling mediators, i.e. Rac1, integrins, RhoGEF's in shear-dependent regulation. Moreover, the RasGTPase 'Rap1' has received much recent attention for its role in regulating cell-cell adhesion and as an upstream mediator of Rac1-induced barrier stability, however its participation in shear-mediated processes remains to investigated (Adamson et al., 2008, Birukova et al., 2007b, Birukova et al., 2008, Spindler et al., 2010).

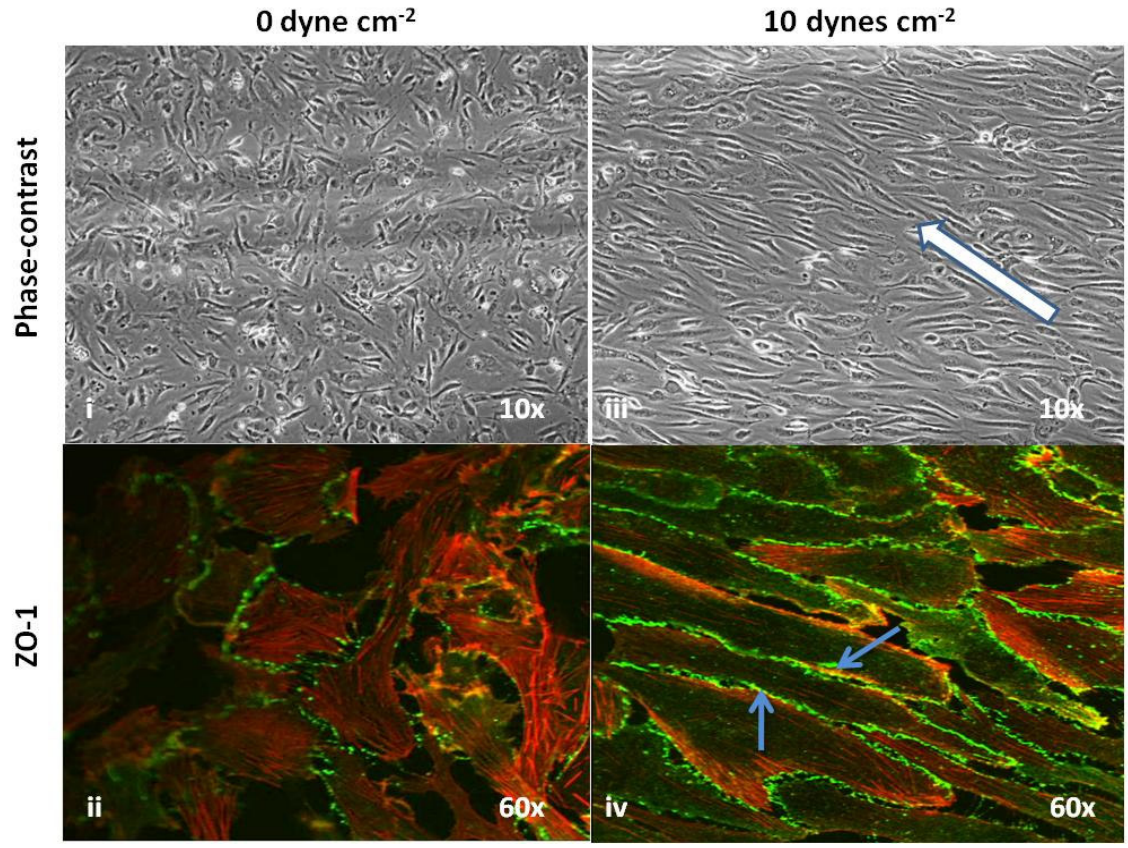

Fig. 6.4: Effect of laminar shear stress on HBMvEC re-alignment, F-actin organization and ZO-1 localization. Confluent HBMvEC's were exposed to laminar shear stress (10 dynes cm^{-2}, 24 h) using a novel IBIDI® perfusion flow system and monitored for morphological realignment by phase-contrast microscopy (i-ii) and fluorescent microscopy (Olympus, FV10i confocal microscope) using a double-stain procedure for F-actin (red) and ZO-1 (green) (iii-iv). White arrow indicates direction of the flow (iii). Blue arrow indicates ZO-1 cell-cell border localization (iv). Images are representative.

In conclusion, it was demonstrated that laminar shear stress is a dynamic regulator of tight junction assembly and barrier function within BBMvEC's. Our findings implicate a putative link between shear-induced regulation of tight junction proteins (ZO-1, occludin, claudin-5) and endothelial permeability. Furthermore, we partially elucidated the signaling mechanism mediating the shear-dependent induction of tight junction assembly, which involved a *VE-Cadherin-Tiam1-Rac1* signaling axis. Multiple signaling pathways (including RhoGTPases) have been previously implicated in tight junction regulation, including heterotrimeric G-proteins, serine-, threonine-, and tyrosine kinases, intracellular calcium levels, cytokines and extracellular matrix proteins (Wolburg et al., 1994, Schulze et al., 1997, Lu et al., 2000, Wolburg and Lippoldt, 2002). However it is our belief that we are the first group to specifically investigate the signaling mechanism(s) mediating shear-induced regulation of tight junctions specifically within the BBB, thus establishing molecular targets of genuine relevance to neurological diseases manifesting through manipulations of BBB tight junctions. It is anticipated that these findings may also transfer to other areas of the vasculature, and thus impact on non-neurological diseases associated with endothelial barrier dysfunction in peripheral vasculature, e.g. atherosclerosis in coronary arteries leading to myocardial infarction.

Bibliography

ABBOTT, N. J. (2004) Evidence for bulk flow of brain interstitial fluid: significance for physiology and pathology. *Neurochem Int,* 45**,** 545-52.

ABBOTT, N. J. (2005) Dynamics of CNS barriers: evolution, differentiation, and modulation. *Cell Mol Neurobiol,* 25**,** 5-23.

ABBOTT, N. J., RONNBACK, L. & HANSSON, E. (2006) Astrocyte-endothelial interactions at the blood-brain barrier. *Nat Rev Neurosci,* 7**,** 41-53.

ADAMSON, P., ETIENNE, S., COURAUD, P. O., CALDER, V. & GREENWOOD, J. (1999) Lymphocyte migration through brain endothelial cell monolayers involves signaling through endothelial ICAM-1 via a rho-dependent pathway. *J Immunol,* 162**,** 2964-73.

ADAMSON, R. H., CURRY, F. E., ADAMSON, G., LIU, B., JIANG, Y., AKTORIES, K., BARTH, H., DAIGELER, A., GOLENHOFEN, N., NESS, W. & DRENCKHAHN, D. (2002) Rho and rho kinase modulation of barrier properties: cultured endothelial cells and intact microvessels of rats and mice. *J Physiol,* 539**,** 295-308.

ADAMSON, R. H., LY, J. C., SARAI, R. K., LENZ, J. F., ALTANGEREL, A., DRENCKHAHN, D. & CURRY, F. E. (2008) Epac/Rap1 pathway regulates microvascular hyperpermeability induced by PAF in rat mesentery. *Am J Physiol Heart Circ Physiol,* 294**,** H1188-96.

AIRD, W. C. (2005) Spatial and temporal dynamics of the endothelium. *J Thromb Haemost,* 3**,** 1392-406.

AIRD, W. C. (2007) Phenotypic heterogeneity of the endothelium: I. Structure, function, and mechanisms. *Circ Res,* 100**,** 158-73.

AKIMOTO, S., MITSUMATA, M., SASAGURI, T. & YOSHIDA, Y. (2000) Laminar shear stress inhibits vascular endothelial cell proliferation by inducing cyclin-dependent kinase inhibitor p21(Sdi1/Cip1/Waf1). *Circ Res,* 86**,** 185-90.

ALEXANDER, J. S., ALEXANDER, B. C., EPPIHIMER, L. A., GOODYEAR, N., HAQUE, R., DAVIS, C. P., KALOGERIS, T. J., CARDEN, D. L., ZHU, Y. N. & KEVIL, C. G. (2000) Inflammatory mediators induce sequestration of VE-cadherin in cultured human endothelial cells. *Inflammation,* 24**,** 99-113.

ALLINGHAM, M. J., VAN BUUL, J. D. & BURRIDGE, K. (2007) ICAM-1-mediated, Src- and Pyk2-dependent vascular endothelial cadherin tyrosine phosphorylation is required for leukocyte transendothelial migration. *J Immunol,* 179**,** 4053-64.

ANDO, J. & YAMAMOTO, K. (2009) Vascular mechanobiology: endothelial cell responses to fluid shear stress. *Circ J,* 73**,** 1983-92.

ANDO, J., KOMATSUDA, T. & KAMIYA, A. (1988) Cytoplasmic calcium response to fluid shear stress in cultured vascular endothelial cells. *In Vitro Cell Dev Biol,* 24**,** 871-7.

ANDO-AKATSUKA, Y., SAITOU, M., HIRASE, T., KISHI, M., SAKAKIBARA, A., ITOH, M., YONEMURA, S., FURUSE, M. & TSUKITA, S. (1996) Interspecies diversity of the occludin sequence: cDNA cloning of human, mouse, dog, and rat-kangaroo homologues. *J Cell Biol,* 133**,** 43-7.

ANDRAS, I. E., PU, H., DELI, M. A., NATH, A., HENNIG, B. & TOBOREK, M. (2003) HIV-1 Tat protein alters tight junction protein expression and distribution in cultured brain endothelial cells. *J Neurosci Res,* 74**,** 255-65.

ANDRIOPOULOU, P., NAVARRO, P., ZANETTI, A., LAMPUGNANI, M. G. & DEJANA, E. (1999) Histamine induces tyrosine phosphorylation of endothelial cell-to-cell adherens junctions. *Arterioscler Thromb Vasc Biol,* 19**,** 2286-97.

ANGELINI, D. J., HYUN, S. W., GRIGORYEV, D. N., GARG, P., GONG, P., SINGH, I. S., PASSANITI, A., HASDAY, J. D. & GOLDBLUM, S. E. (2006) TNF-alpha increases tyrosine phosphorylation of vascular endothelial cadherin and opens the paracellular pathway through fyn activation in human lung endothelia. *Am J Physiol Lung Cell Mol Physiol,* 291**,** L1232-45.

ANTONETTI, D. A., BARBER, A. J., HOLLINGER, L. A., WOLPERT, E. B. & GARDNER, T. W. (1999) Vascular endothelial growth factor induces rapid phosphorylation of tight junction proteins occludin and zonula occluden 1. A potential mechanism for vascular permeability in diabetic retinopathy and tumors. *J Biol Chem,* 274**,** 23463-7.

ARTHUR, W. T., QUILLIAM, L. A. & COOPER, J. A. (2004) Rap1 promotes cell spreading by localizing Rac guanine nucleotide exchange factors. *J Cell Biol,* 167**,** 111-22.

BALDA, M. S., GONZALEZ-MARISCAL, L., MATTER, K., CEREIJIDO, M. & ANDERSON, J. M. (1993) Assembly of the tight junction: the role of diacylglycerol. *J Cell Biol,* 123**,** 293-302.

BALDA, M. S., WHITNEY, J. A., FLORES, C., GONZALEZ, S., CEREIJIDO, M. & MATTER, K. (1996) Functional dissociation of paracellular permeability and transepithelial electrical resistance and disruption of the apical-basolateral intramembrane diffusion barrier by expression of a mutant tight junction membrane protein. *J Cell Biol,* 134**,** 1031-49.

BALDA, M. S. & MATTER, K. (2000) The tight junction protein ZO-1 and an interacting transcription factor regulate ErbB-2 expression. *EMBO J,* 19**,** 2024-33.

BALLABH, P., BRAUN, A. & NEDERGAARD, M. (2004) The blood-brain barrier: an overview: structure, regulation, and clinical implications. *Neurobiol Dis,* 16**,** 1-13.

BAMFORTH, S. D., KNIESEL, U., WOLBURG, H., ENGELHARDT, B. & RISAU, W. (1999) A dominant mutant of occludin disrupts tight junction structure and function. *J Cell Sci,* 112 (Pt 12)**,** 1879-88.

BAUMER, Y., BURGER, S., CURRY, F. E., GOLENHOFEN, N., DRENCKHAHN, D. & WASCHKE, J. (2008) Differential role of Rho GTPases in endothelial barrier regulation dependent on endothelial cell origin. *Histochem Cell Biol,* 129**,** 179-91.

BAUMER, Y., SPINDLER, V., WERTHMANN, R. C., BUNEMANN, M. & WASCHKE, J. (2009) Role of Rac 1 and cAMP in endothelial barrier stabilization and thrombin-induced barrier breakdown. *J Cell Physiol,* 220**,** 716-26.

BECKERS, C. M., VAN HINSBERGH, V. W. & VAN NIEUW AMERONGEN, G. P. (2010) Driving Rho GTPase activity in endothelial cells regulates barrier integrity. *Thromb Haemost,* 103**,** 40-55.

BEN-MENACHEM, E., JOHANSSON, B. B. & SVENSSON, T. H. (1982) Increased vulnerability of the blood-brain barrier to acute hypertension following depletion of brain noradrenaline. *J Neural Transm,* 53**,** 159-67.

BERGAYA, S., MENETON, P., BLOCH-FAURE, M., MATHIEU, E., ALHENC-GELAS, F., LEVY, B. I. & BOULANGER, C. M. (2001) Decreased flow-dependent dilation in carotid arteries of tissue kallikrein-knockout mice. *Circ Res,* 88**,** 593-9.

BERK, B. C., ABE, J. I., MIN, W., SURAPISITCHAT, J. & YAN, C. (2001) Endothelial atheroprotective and anti-inflammatory mechanisms. *Ann N Y Acad Sci,* 947**,** 93-109; discussion 109-11.

BERX, G. & VAN ROY, F. (2001) The E-cadherin/catenin complex: an important gatekeeper in breast cancer tumorigenesis and malignant progression. *Breast Cancer Res,* 3**,** 289-93.

BHULLAR, I. S., LI, Y. S., MIAO, H., ZANDI, E., KIM, M., SHYY, J. Y. & CHIEN, S. (1998) Fluid shear stress activation of IkappaB kinase is integrin-dependent. *J Biol Chem,* 273**,** 30544-9.

BIRUKOVA, A. A., SMUROVA, K., BIRUKOV, K. G., KAIBUCHI, K., GARCIA, J. G. & VERIN, A. D. (2004) Role of Rho GTPases in thrombin-induced lung vascular endothelial cells barrier dysfunction. *Microvasc Res,* 67**,** 64-77.

BIRUKOVA A. A., ALEKSEEVA E., MIKAELYAN A. and BIRUKOV K. G. (2007a) HGF attenuates thrombin-induced endothelial permeability by Tiam1-mediated

activation of the Rac pathway and by Tiam1/Rac-dependent inhibition of the Rho pathway. *FASEB J* **21,** 2776-2786.

BIRUKOVA A. A., ZAGRANICHNAYA T., ALEKSEEVA E., CHEN W., JACOBSON J. R. and BIRUKOV K. G. (2007b) Prostaglandins PGE(2) and PGI(2) promote endothelial barrier enhancement via PKA- and Epac1/Rap1-dependent Rac activation. *Exp Cell Res* **313,** 2504-2520.

BIRUKOVA A. A., ZAGRANICHNAYA T., ALEKSEEVA E., BOKOCK G. M. and BIRUKOV K. G. (2008) Epac/Rap and PKA are novel mechanisms of ANP-induced Rac-mediated pulmonary endothelial barrier protection. *J Cell Physiol* **215,** 715-724.

BIRUKOVA, A. A., MOLDOBAEVA, N., XING, J. & BIRUKOV, K. G. (2008) Magnitude-dependent effects of cyclic stretch on HGF- and VEGF-induced pulmonary endothelial remodeling and barrier regulation. *Am J Physiol Lung Cell Mol Physiol,* 295**,** L612-23.

BISHOP, A. L. & HALL, A. (2000) Rho GTPases and their effector proteins. *Biochem J,* 348 Pt 2**,** 241-55.

BOSCO, E. E., MULLOY, J. C. & ZHENG, Y. (2009) Rac1 GTPase: a "Rac" of all trades. *Cell Mol Life Sci,* 66**,** 370-4.

BOUIS, D., HOSPERS, G. A., MEIJER, C., MOLEMA, G. & MULDER, N. H. (2001) Endothelium in vitro: a review of human vascular endothelial cell lines for blood vessel-related research. *Angiogenesis,* 4**,** 91-102.

BREVIARIO, F., CAVEDA, L., CORADA, M., MARTIN-PADURA, I., NAVARRO, P., GOLAY, J., INTRONA, M., GULINO, D., LAMPUGNANI, M. G. & DEJANA, E. (1995) Functional properties of human vascular endothelial cadherin (7B4/cadherin-5), an endothelium-specific cadherin. *Arterioscler Thromb Vasc Biol,* 15**,** 1229-39.

BRIGHTMAN, M. W. & REESE, T. S. (1969) Junctions between intimately apposed cell membranes in the vertebrate brain. *J Cell Biol,* 40**,** 648-77.

BRIGHTMAN, M. W. (1977) Morphology of blood-brain interfaces. *Exp Eye Res,* 25 Suppl**,** 1-25.

BROMAN M. T., KOUKLIS P., GAO X., RAMCHANDRAN R., NEAMU R. F., MINSHALL R. D. and MALIK A. B. (2006) Cdc42 regulates adherens junction stability and endothelial permeability by inducing alpha-catenin interaction with the vascular endothelial cadherin complex. *Circ Res,* 98**,** 73-80.

BURGEL, N., BOJARSKI, C., MANKERTZ, J., ZEITZ, M., FROMM, M. & SCHULZKE, J. D. (2002) Mechanisms of diarrhea in collagenous colitis. *Gastroenterology,* 123**,** 433-43.

BUSCH, C., HANSSEN, T. A., WAGENER, C. & B, O. B. (2002) Down-regulation of CEACAM1 in human prostate cancer: correlation with loss of cell polarity, increased proliferation rate, and Gleason grade 3 to 4 transition. *Hum Pathol,* 33**,** 290-8.

BUSSE, R. & FLEMING, I. (2003) Regulation of endothelium-derived vasoactive autacoid production by hemodynamic forces. *Trends Pharmacol Sci,* 24**,** 24-9.

CARMELIET, P., LAMPUGNANI, M. G., MOONS, L., BREVIARIO, F., COMPERNOLLE, V., BONO, F., BALCONI, G., SPAGNUOLO, R., OOSTHUYSE, B., DEWERCHIN, M., ZANETTI, A., ANGELLILO, A., MATTOT, V., NUYENS, D., LUTGENS, E., CLOTMAN, F., DE RUITER, M. C., GITTENBERGER-DE GROOT, A., POELMANN, R., LUPU, F., HERBERT, J. M., COLLEN, D. & DEJANA, E. (1999) Targeted deficiency or cytosolic truncation of the VE-cadherin gene in mice impairs VEGF-mediated endothelial survival and angiogenesis. *Cell,* 98**,** 147-57.

CAVEDA, L., MARTIN-PADURA, I., NAVARRO, P., BREVIARIO, F., CORADA, M., GULINO, D., LAMPUGNANI, M. G. & DEJANA, E. (1996) Inhibition of cultured cell growth by vascular endothelial cadherin (cadherin-5/VE-cadherin). *J Clin Invest,* 98**,** 886-93.

CERIONE, R. A. & ZHENG, Y. (1996) The Dbl family of oncogenes. *Curr Opin Cell Biol,* 8**,** 216-22.

CHAPPELL, D. C., VARNER, S. E., NEREM, R. M., MEDFORD, R. M. & ALEXANDER, R. W. (1998) Oscillatory shear stress stimulates adhesion molecule expression in cultured human endothelium. *Circ Res,* 82**,** 532-9.

CHATZIZISIS, Y. S., JONAS, M., COSKUN, A. U., BEIGEL, R., STONE, B. V., MAYNARD, C., GERRITY, R. G., DALEY, W., ROGERS, C., EDELMAN, E. R., FELDMAN, C. L. & STONE, P. H. (2008) Prediction of the localization of high-risk coronary atherosclerotic plaques on the basis of low endothelial shear stress: an intravascular ultrasound and histopathology natural history study. *Circulation,* 117**,** 993-1002.

CHEN K. D., LI Y. S., KIM M., LI S., YUAN S., CHIEN S. and SHYY J. Y. (1999) Mechanotransduction in response to shear stress. Roles of receptor tyrosine kinases, integrins, and Shc. *J Biol Chem* **274,** 18393-18400.

CHEN, F., OHASHI, N., LI, W., ECKMAN, C. & NGUYEN, J. H. (2009) Disruptions of occludin and claudin-5 in brain endothelial cells in vitro and in brains of mice with acute liver failure. *Hepatology,* 50**,** 1914-23.

CHEN, Y., MCCARRON, R. M., AZZAM, N., BEMBRY, J., REUTZLER, C., LENZ, F. A. & SPATZ, M. (2000) Endothelin-1 and nitric oxide affect human cerebromicrovascular endothelial responses and signal transduction. *Acta Neurochir Suppl,* 76**,** 131-5.

CHIKUMI, H., FUKUHARA, S. & GUTKIND, J. S. (2002) Regulation of G protein-linked guanine nucleotide exchange factors for Rho, PDZ-RhoGEF, and LARG by tyrosine phosphorylation: evidence of a role for focal adhesion kinase. *J Biol Chem,* 277**,** 12463-73.

CHOBANIAN, A. V. & ALEXANDER, R. W. (1996) Exacerbation of atherosclerosis by hypertension. Potential mechanisms and clinical implications. *Arch Intern Med,* 156**,** 1952-6.

CLARKE, H., SOLER, A. P. & MULLIN, J. M. (2000) Protein kinase C activation leads to dephosphorylation of occludin and tight junction permeability increase in LLC-PK1 epithelial cell sheets. *J Cell Sci,* 113 (Pt 18)**,** 3187-96.

COLGAN, O. C., COLLINS, N. T., FERGUSON, G., MURPHY, R. P., BIRNEY, Y. A., CAHILL, P. A. & CUMMINS, P. M. (2007) Regulation of Bovine Brain Microvascular Endothelial Tight Junction Assembly and Barrier Function by Laminar Shear Stress. *Am J Physiol Heart Circ Physiol*, 292, H3190-7.

COLGAN, O. C., COLLINS, N. T., FERGUSON, G., MURPHY, R. P., BIRNEY, Y. A., CAHILL, P. A. & CUMMINS, P. M. (2008) Influence of basolateral condition on the regulation of brain microvascular endothelial tight junction properties and barrier function. *Brain Res,* 1193**,** 84-92.

COLLINS, N. T., CUMMINS, P. M., COLGAN, O. C., FERGUSON, G., BIRNEY, Y. A., MURPHY, R. P., MEADE, G. & CAHILL, P. A. (2006) Cyclic strain-mediated regulation of vascular endothelial occludin and ZO-1: influence on intercellular tight junction assembly and function. *Arterioscler Thromb Vasc Biol,* 26**,** 62-8.

CONKLIN, B. S., ZHONG, D. S., ZHAO, W., LIN, P. H. & CHEN, C. (2002) Shear stress regulates occludin and VEGF expression in porcine arterial endothelial cells. *J Surg Res,* 102**,** 13-21.

CONNOLLY, J. O., SIMPSON, N., HEWLETT, L. & HALL, A. (2002) Rac regulates endothelial morphogenesis and capillary assembly. *Mol Biol Cell,* 13**,** 2474-85.

CORDENONSI, M., D'ATRI, F., HAMMAR, E., PARRY, D. A., KENDRICK-JONES, J., SHORE, D. & CITI, S. (1999) Cingulin contains globular and coiled-coil domains and interacts with ZO-1, ZO-2, ZO-3, and myosin. *J Cell Biol,* 147**,** 1569-82.

COULTAS, L., CHAWENGSAKSOPHAK, K. & ROSSANT, J. (2005) Endothelial cells and VEGF in vascular development. *Nature,* 438**,** 937-45.

COX, A. D. & DER, C. J. (2002) Ras family signaling: therapeutic targeting. *Cancer Biol Ther,* 1**,** 599-606.

CUCULLO, L., COURAUD, P. O., WEKSLER, B., ROMERO, I. A., HOSSAIN, M., RAPP, E. & JANIGRO, D. (2008) Immortalized human brain endothelial cells and flow-based vascular modeling: a marriage of convenience for rational neurovascular studies. *J Cereb Blood Flow Metab,* 28**,** 312-28.

CUCULLO, L., MCALLISTER, M. S., KIGHT, K., KRIZANAC-BENGEZ, L., MARRONI, M., MAYBERG, M. R., STANNESS, K. A. & JANIGRO, D. (2002) A new dynamic in vitro model for the multidimensional study of astrocyte-endothelial cell interactions at the blood-brain barrier. *Brain Res,* 951**,** 243-54.

CUNNINGHAM, K. S. & GOTLIEB, A. I. (2005) The role of shear stress in the pathogenesis of atherosclerosis. *Lab Invest,* 85**,** 9-23.

DALLASTA, L. M., PISAROV, L. A., ESPLEN, J. E., WERLEY, J. V., MOSES, A. V., NELSON, J. A. & ACHIM, C. L. (1999) Blood-brain barrier tight junction disruption in human immunodeficiency virus-1 encephalitis. *Am J Pathol,* 155**,** 1915-27.

DAVIES, D. C. (2002) Blood-brain barrier breakdown in septic encephalopathy and brain tumours. *J Anat,* 200**,** 639-46.

DAVIES, P. F. (2009) Hemodynamic shear stress and the endothelium in cardiovascular pathophysiology. *Nat Clin Pract Cardiovasc Med,* 6**,** 16-26.

DE KEULENAER, G. W., CHAPPELL, D. C., ISHIZAKA, N., NEREM, R. M., ALEXANDER, R. W. & GRIENDLING, K. K. (1998) Oscillatory and steady laminar shear stress differentially affect human endothelial redox state: role of a superoxide-producing NADH oxidase. *Circ Res,* 82**,** 1094-101.

DEJANA, E. (2004) Endothelial cell-cell junctions: happy together. *Nat Rev Mol Cell Biol,* 5**,** 261-70.

DEJANA, E., ORSENIGO, F. & LAMPUGNANI, M. G. (2008) The role of adherens junctions and VE-cadherin in the control of vascular permeability. *J Cell Sci,* 121**,** 2115-22.

DEL ZOPPO, G. J., MILNER, R., MABUCHI, T., HUNG, S., WANG, X. & KOZIOL, J. A. (2006) Vascular matrix adhesion and the blood-brain barrier. *Biochem Soc Trans,* 34**,** 1261-6.

DEL ZOPPO, G. J. (2008) Virchow's triad: the vascular basis of cerebral injury. *Rev Neurol Dis,* 5 Suppl 1**,** S12-21.

DELI, M. A., ABRAHAM, C. S., KATAOKA, Y. & NIWA, M. (2005) Permeability studies on in vitro blood-brain barrier models: physiology, pathology, and pharmacology. *Cell Mol Neurobiol,* 25**,** 59-127.

DEMAIO, L., CHANG, Y. S., GARDNER, T. W., TARBELL, J. M. & ANTONETTI, D. A. (2001) Shear stress regulates occludin content and phosphorylation. *Am J Physiol Heart Circ Physiol,* 281**,** H105-13.

DERMARDIROSSIAN, C., SCHNELZER, A. & BOKOCH, G. M. (2004) Phosphorylation of RhoGDI by Pak1 mediates dissociation of Rac GTPase. *Mol Cell,* 15**,** 117-27.

DESAI, L. P., ARYAL, A. M., CEACAREANU, B., HASSID, A. & WATERS, C. M. (2004) RhoA and Rac1 are both required for efficient wound closure of airway epithelial cells. *Am J Physiol Lung Cell Mol Physiol,* 287**,** L1134-44.

DESAI, S. Y., MARRONI, M., CUCULLO, L., KRIZANAC-BENGEZ, L., MAYBERG, M. R., HOSSAIN, M. T., GRANT, G. G. & JANIGRO, D. (2002) Mechanisms of endothelial survival under shear stress. *Endothelium,* 9**,** 89-102.

DEWEY, C. F., JR., BUSSOLARI, S. R., GIMBRONE, M. A., JR. & DAVIES, P. F. (1981) The dynamic response of vascular endothelial cells to fluid shear stress. *J Biomech Eng,* 103**,** 177-85.

DEWI, B. E., TAKASAKI, T. & KURANE, I. (2008) Peripheral blood mononuclear cells increase the permeability of dengue virus-infected endothelial cells in association with downregulation of vascular endothelial cadherin. *J Gen Virol,* 89**,** 642-52.

DIMMELER, S., HAENDELER, J., NEHLS, M. & ZEIHER, A. M. (1997) Suppression of apoptosis by nitric oxide via inhibition of interleukin-1beta-converting enzyme (ICE)-like and cysteine protease protein (CPP)-32-like proteases. *J Exp Med,* 185**,** 601-7.

DOVAS, A. & COUCHMAN, J. R. (2005) RhoGDI: multiple functions in the regulation of Rho family GTPase activities. *Biochem J,* 390**,** 1-9.

D'SOUZA, T., AGARWAL, R. & MORIN, P. J. (2005) Phosphorylation of claudin-3 at threonine 192 by cAMP-dependent protein kinase regulates tight junction barrier function in ovarian cancer cells. *J Biol Chem,* 280**,** 26233-40.

DUDEK, S. M., JACOBSON, J. R., CHIANG, E. T., BIRUKOV, K. G., WANG, P., ZHAN, X. & GARCIA, J. G. (2004) Pulmonary endothelial cell barrier enhancement by sphingosine 1-phosphate: roles for cortactin and myosin light chain kinase. *J Biol Chem,* 279**,** 24692-700.

EHRLICH (1904) U¨ ber die Beziehung chemischer Constitution, Verteilung, und pharmakologischer Wirkung. Gesammelte Arbeiten zur Immunitatsforschung.

EL-BACHA, R. S. & MINN, A. (1999) Drug metabolizing enzymes in cerebrovascular endothelial cells afford a metabolic protection to the brain. *Cell Mol Biol (Noisy-le-grand),* 45**,** 15-23.

ELIAS, B. C., SUZUKI, T., SETH, A., GIORGIANNI, F., KALE, G., SHEN, L., TURNER, J. R., NAREN, A., DESIDERIO, D. M. & RAO, R. (2009) Phosphorylation of Tyr-398 and Tyr-402 in occludin prevents its interaction with ZO-1 and destabilizes its assembly at the tight junctions. *J Biol Chem,* 284**,** 1559-69.

ENGELHARDT, B. (2003) Development of the blood-brain barrier. *Cell Tissue Res,* 314**,** 119-29.

ERIN, N., WANG, N., XIN, P., BUI, V., WEISZ, J., BARKAN, G. A., ZHAO, W., SHEARER, D. & CLAWSON, G. A. (2009) Altered gene expression in breast cancer liver metastases. *Int J Cancer,* 124**,** 1503-16.

ESPER R. J., NORDABY R. A., VILARINO J. O., PARAGANO A., CACHARRON J. L. and MACHADO R. A. (2006) Endothelial dysfunction: a comprehensive appraisal. *Cardiovasc Diabetol* **5,** 4.

ESSER, S., LAMPUGNANI, M. G., CORADA, M., DEJANA, E. & RISAU, W. (1998) Vascular endothelial growth factor induces VE-cadherin tyrosine phosphorylation in endothelial cells. *J Cell Sci,* 111 (Pt 13)**,** 1853-65.

ETIENNE-MANNEVILLE, S. & HALL, A. (2002) Rho GTPases in cell biology. *Nature,* 420**,** 629-35.

FANG, Y., SCHRAM, G., ROMANENKO, V. G., SHI, C., CONTI, L., VANDENBERG, C. A., DAVIES, P. F., NATTEL, S. & LEVITAN, I. (2005) Functional expression of Kir2.x in human aortic endothelial cells: the dominant role of Kir2.2. *Am J Physiol Cell Physiol,* 289**,** C1134-44.

FANNING, A. S., MA, T. Y. & ANDERSON, J. M. (2002) Isolation and functional characterization of the actin binding region in the tight junction protein ZO-1. *FASEB J,* 16**,** 1835-7.

FANNING, A. S., JAMESON, B. J., JESAITIS, L. A. & ANDERSON, J. M. (1998) The tight junction protein ZO-1 establishes a link between the transmembrane protein occludin and the actin cytoskeleton. *J Biol Chem,* 273**,** 29745-53.

FANNING, A. S., LITTLE, B. P., RAHNER, C., UTEPBERGENOV, D., WALTHER, Z. & ANDERSON, J. M. (2007) The unique-5 and -6 motifs of ZO-1 regulate tight junction strand localization and scaffolding properties. *Mol Biol Cell,* 18**,** 721-31.

FANNING A. S. and ANDERSON J. M. (2009) Zonula occludens-1 and -2 are cytosolic scaffolds that regulate the assembly of cellular junctions. *Ann N Y Acad Sci* **1165,** 113-120.

FARRELL, C. R., STEWART, P. A., FARRELL, C. L. & DEL MAESTRO, R. F. (1987) Pericytes in human cerebral microvasculature. *Anat Rec,* 218**,** 466-9.

FEDWICK, J. P., LAPOINTE, T. K., MEDDINGS, J. B., SHERMAN, P. M. & BURET, A. G. (2005) Helicobacter pylori activates myosin light-chain kinase to disrupt claudin-4 and claudin-5 and increase epithelial permeability. *Infect Immun,* 73**,** 7844-52.

FEIG, L. A. (1999) Tools of the trade: use of dominant-inhibitory mutants of Ras-family GTPases. *Nat Cell Biol,* 1**,** E25-7.

FELDMAN, G. J., MULLIN, J. M. & RYAN, M. P. (2005) Occludin: structure, function and regulation. *Adv Drug Deliv Rev,* 57**,** 883-917.

FERGUSON, G., WATTERSON, K. R. & PALMER, T. M. (2000) Subtype-specific kinetics of inhibitory adenosine receptor internalization are determined by sensitivity to phosphorylation by G protein-coupled receptor kinases. *Mol Pharmacol,* 57**,** 546-52.

FINDLEY, M. K. & KOVAL, M. (2009) Regulation and roles for claudin-family tight junction proteins. *IUBMB Life,* 61**,** 431-7.

FITZPATRICK, P. A., GUINAN, A. F., WALSH, T. G., MURPHY, R. P., KILLEEN, M. T., TOBIN, N. P., PIEROTTI, A. R. & CUMMINS, P. M. (2009) Down-regulation of neprilysin (EC3.4.24.11) expression in vascular endothelial cells by laminar shear stress involves NADPH oxidase-dependent ROS production. *Int J Biochem Cell Biol,* 41**,** 2287-94.

FLEMING, I. (2000) Cytochrome P450 2C is an EDHF synthase in coronary arteries. *Trends Cardiovasc Med,* 10**,** 166-70.

FLORIAN, J. A., KOSKY, J. R., AINSLIE, K., PANG, Z., DULL, R. O. & TARBELL, J. M. (2003) Heparan sulfate proteoglycan is a mechanosensor on endothelial cells. *Circ Res,* 93**,** e136-42.

FRANK, R. N., DUTTA, S. & MANCINI, M. A. (1987) Pericyte coverage is greater in the retinal than in the cerebral capillaries of the rat. *Invest Ophthalmol Vis Sci,* 28**,** 1086-91.

FUJIBE, M., CHIBA, H., KOJIMA, T., SOMA, T., WADA, T., YAMASHITA, T. & SAWADA, N. (2004) Thr203 of claudin-1, a putative phosphorylation site for MAP kinase, is required to promote the barrier function of tight junctions. *Exp Cell Res,* 295**,** 36-47.

FUJITA, K., KATAHIRA, J., HORIGUCHI, Y., SONODA, N., FURUSE, M. & TSUKITA, S. (2000) Clostridium perfringens enterotoxin binds to the second extracellular loop of claudin-3, a tight junction integral membrane protein. *FEBS Lett,* 476**,** 258-61.

FUJIWARA, K. (2006) Platelet endothelial cell adhesion molecule-1 and mechanotransduction in vascular endothelial cells. *J Intern Med,* 259**,** 373-80.

FUKUHARA, A., IRIE, K., NAKANISHI, H., TAKEKUNI, K., KAWAKATSU, T., IKEDA, W., YAMADA, A., KATATA, T., HONDA, T., SATO, T., SHIMIZU, K., OZAKI, H., HORIUCHI, H., KITA, T. & TAKAI, Y. (2002) Involvement of nectin in the localization of junctional adhesion molecule at tight junctions. *Oncogene,* 21**,** 7642-55.

FURCHGOTT, R. F. & ZAWADZKI, J. V. (1980) The obligatory role of endothelial cells in the relaxation of arterial smooth muscle by acetylcholine. *Nature,* 288**,** 373-6.

FURUSE, M., HIRASE, T., ITOH, M., NAGAFUCHI, A., YONEMURA, S., TSUKITA, S. & TSUKITA, S. (1993) Occludin: a novel integral membrane protein localizing at tight junctions. *J Cell Biol,* 123**,** 1777-88.

FURUSE, M., ITOH, M., HIRASE, T., NAGAFUCHI, A., YONEMURA, S., TSUKITA, S. & TSUKITA, S. (1994) Direct association of occludin with ZO-1 and its possible involvement in the localization of occludin at tight junctions. *J Cell Biol,* 127**,** 1617-26.

FURUSE, M., FUJITA, K., HIIRAGI, T., FUJIMOTO, K. & TSUKITA, S. (1998a) Claudin-1 and -2: novel integral membrane proteins localizing at tight junctions with no sequence similarity to occludin. *J Cell Biol,* 141**,** 1539-50.

FURUSE, M., SASAKI, H., FUJIMOTO, K. & TSUKITA, S. (1998b) A single gene product, claudin-1 or -2, reconstitutes tight junction strands and recruits occludin in fibroblasts. *J Cell Biol,* 143**,** 391-401.

FURUSE, M., FURUSE, K., SASAKI, H. & TSUKITA, S. (2001) Conversion of zonulae occludentes from tight to leaky strand type by introducing claudin-2 into Madin-Darby canine kidney I cells. *J Cell Biol,* 153**,** 263-72.

GALBRAITH, C. G., SKALAK, R. & CHIEN, S. (1998) Shear stress induces spatial reorganization of the endothelial cell cytoskeleton. *Cell Motil Cytoskeleton,* 40**,** 317-30.

GAO, Y., DICKERSON, J. B., GUO, F., ZHENG, J. & ZHENG, Y. (2004) Rational design and characterization of a Rac GTPase-specific small molecule inhibitor. *Proc Natl Acad Sci U S A,* 101**,** 7618-23.

GARCIA-CARDENA, G. & GIMBRONE, M. A., JR. (2006) Biomechanical modulation of endothelial phenotype: implications for health and disease. *Handb Exp Pharmacol***,** 79-95.

GAVARD, J. (2009) Breaking the VE-cadherin bonds. *FEBS Lett,* 583**,** 1-6.

GEE, J. R. & KELLER, J. N. (2005) Astrocytes: regulation of brain homeostasis via apolipoprotein E. *Int J Biochem Cell Biol,* 37**,** 1145-50.

GEORGES-LABOUESSE, E., MESSADDEQ, N., YEHIA, G., CADALBERT, L., DIERICH, A. & LE MEUR, M. (1996) Absence of integrin alpha 6 leads to epidermolysis bullosa and neonatal death in mice. *Nat Genet,* 13**,** 370-3.

GERRITSEN, M. E. (1987) Functional heterogeneity of vascular endothelial cells. *Biochem Pharmacol,* 36**,** 2701-11.

GIANNOTTI, G. & LANDMESSER, U. (2007) Endothelial dysfunction as an early sign of atherosclerosis. *Herz,* 32**,** 568-72.

GLOOR, S. M., WACHTEL, M., BOLLIGER, M. F., ISHIHARA, H., LANDMANN, R. & FREI, K. (2001) Molecular and cellular permeability control at the blood-brain barrier. *Brain Res Brain Res Rev,* 36**,** 258-64.

GOLDMANN (1913) Vitalfa¨rbung am Zentralnervensystem. Agh Preuss Akad Wissensch PhysMath. 1–60.

GONUL, E., DUZ, B., KAHRAMAN, S., KAYALI, H., KUBAR, A. & TIMURKAYNAK, E. (2002) Early pericyte response to brain hypoxia in cats: an ultrastructural study. *Microvasc Res,* 64**,** 116-9.

GONZALEZ-MARISCAL, L., BETANZOS, A. & AVILA-FLORES, A. (2000) MAGUK proteins: structure and role in the tight junction. *Semin Cell Dev Biol,* 11**,** 315-24.

GONZALEZ-MARISCAL, L., BETANZOS, A., NAVA, P. & JARAMILLO, B. E. (2003) Tight junction proteins. *Prog Biophys Mol Biol,* 81**,** 1-44.

GORY-FAURE, S., PRANDINI, M. H., POINTU, H., ROULLOT, V., PIGNOT-PAINTRAND, I., VERNET, M. & HUBER, P. (1999) Role of vascular endothelial-cadherin in vascular morphogenesis. *Development,* 126**,** 2093-102.

GOTSCH, U., BORGES, E., BOSSE, R., BOGGEMEYER, E., SIMON, M., MOSSMANN, H. & VESTWEBER, D. (1997) VE-cadherin antibody accelerates neutrophil recruitment in vivo. *J Cell Sci,* 110 (Pt 5)**,** 583-8.

GOTTARDI, C. J., ARPIN, M., FANNING, A. S. & LOUVARD, D. (1996) The junction-associated protein, zonula occludens-1, localizes to the nucleus before the maturation and during the remodeling of cell-cell contacts. *Proc Natl Acad Sci U S A,* 93**,** 10779-84.

GRANDERATH, S., STOLLEWERK, A., GREIG, S., GOODMAN, C. S., O'KANE, C. J. & KLAMBT, C. (1999) loco encodes an RGS protein required for Drosophila glial differentiation. *Development,* 126**,** 1781-91.

GRAZIA LAMPUGNANI, M., ZANETTI, A., CORADA, M., TAKAHASHI, T., BALCONI, G., BREVIARIO, F., ORSENIGO, F., CATTELINO, A., KEMLER, R., DANIEL, T. O. & DEJANA, E. (2003) Contact inhibition of VEGF-induced proliferation requires vascular endothelial cadherin, beta-catenin, and the phosphatase DEP-1/CD148. *J Cell Biol,* 161**,** 793-804.

GROARKE, D. A., DRMOTA, T., BAHIA, D. S., EVANS, N. A., WILSON, S. & MILLIGAN, G. (2001) Analysis of the C-terminal tail of the rat thyrotropin-releasing hormone receptor-1 in interactions and cointernalization with beta-arrestin 1-green fluorescent protein. *Mol Pharmacol,* 59**,** 375-85.

GUDI, S. R., CLARK, C. B. & FRANGOS, J. A. (1996) Fluid flow rapidly activates G proteins in human endothelial cells. Involvement of G proteins in mechanochemical signal transduction. *Circ Res,* 79**,** 834-9.

GUDI, S., HUVAR, I., WHITE, C. R., MCKNIGHT, N. L., DUSSERRE, N., BOSS, G. R. & FRANGOS, J. A. (2003) Rapid activation of Ras by fluid flow is mediated by Galpha(q) and Gbetagamma subunits of heterotrimeric G proteins in human endothelial cells. *Arterioscler Thromb Vasc Biol,* 23**,** 994-1000.

GUILLEMOT, L., PASCHOUD, S., JOND, L., FOGLIA, A. & CITI, S. (2008) Paracingulin regulates the activity of Rac1 and RhoA GTPases by recruiting Tiam1 and GEF-H1 to epithelial junctions. *Mol Biol Cell,* 19**,** 4442-53.

GUMBINER, B. & SIMONS, K. (1986) A functional assay for proteins involved in establishing an epithelial occluding barrier: identification of a uvomorulin-like polypeptide. *J Cell Biol,* 102**,** 457-68.

GUMBINER, B. M. (2005) Regulation of cadherin-mediated adhesion in morphogenesis. *Nat Rev Mol Cell Biol,* 6**,** 622-34.

HADDY, F. J., VANHOUTTE, P. M. & FELETOU, M. (2006) Role of potassium in regulating blood flow and blood pressure. *Am J Physiol Regul Integr Comp Physiol,* 290**,** R546-52.

HAGA, M., CHEN, A., GORTLER, D., DARDIK, A. & SUMPIO, B. E. (2003) Shear stress and cyclic strain may suppress apoptosis in endothelial cells by different pathways. *Endothelium,* 10**,** 149-57.

HAHN, C. & SCHWARTZ, M. A. (2009) Mechanotransduction in vascular physiology and atherogenesis. *Nat Rev Mol Cell Biol,* 10**,** 53-62.

HALBLEIB, J. M. & NELSON, W. J. (2006) Cadherins in development: cell adhesion, sorting, and tissue morphogenesis. *Genes Dev,* 20**,** 3199-214.

HALL, A. (1998) Rho GTPases and the actin cytoskeleton. *Science,* 279**,** 509-14.

HALL, A. (2005) Rho GTPases and the control of cell behaviour. *Biochem Soc Trans,* 33**,** 891-5.

HARHAJ, N. S. & ANTONETTI, D. A. (2004) Regulation of tight junctions and loss of barrier function in pathophysiology. *Int J Biochem Cell Biol,* 36**,** 1206-37.

HARHAJ, N. S., FELINSKI, E. A., WOLPERT, E. B., SUNDSTROM, J. M., GARDNER, T. W. & ANTONETTI, D. A. (2006) VEGF activation of protein kinase C stimulates occludin phosphorylation and contributes to endothelial permeability. *Invest Ophthalmol Vis Sci,* 47**,** 5106-15.

HARRISON, D. G., WIDDER, J., GRUMBACH, I., CHEN, W., WEBER, M. & SEARLES, C. (2006) Endothelial mechanotransduction, nitric oxide and vascular inflammation. *J Intern Med,* 259**,** 351-63.

HART, M. J., JIANG, X., KOZASA, T., ROSCOE, W., SINGER, W. D., GILMAN, A. G., STERNWEIS, P. C. & BOLLAG, G. (1998) Direct stimulation of the guanine nucleotide exchange activity of p115 RhoGEF by Galpha13. *Science,* 280**,** 2112-4.

HARTSOCK, A. & NELSON, W. J. (2008) Adherens and tight junctions: structure, function and connections to the actin cytoskeleton. *Biochim Biophys Acta,* 1778**,** 660-9.

HASELOFF, R. F., BLASIG, I. E., BAUER, H. C. & BAUER, H. (2005) In search of the astrocytic factor(s) modulating blood-brain barrier functions in brain capillary endothelial cells in vitro. *Cell Mol Neurobiol,* 25**,** 25-39.

HASHIZUME, H., BALUK, P., MORIKAWA, S., MCLEAN, J. W., THURSTON, G., ROBERGE, S., JAIN, R. K. & MCDONALD, D. M. (2000) Openings between defective endothelial cells explain tumor vessel leakiness. *Am J Pathol,* 156**,** 1363-80.

HASKINS, J., GU, L., WITTCHEN, E. S., HIBBARD, J. & STEVENSON, B. R. (1998) ZO-3, a novel member of the MAGUK protein family found at the tight junction, interacts with ZO-1 and occludin. *J Cell Biol,* 141**,** 199-208.

HAWKINS, B. T. & DAVIS, T. P. (2005) The blood-brain barrier/neurovascular unit in health and disease. *Pharmacol Rev,* 57**,** 173-85.

HEIMARK, R. L., DEGNER, M. & SCHWARTZ, S. M. (1990) Identification of a Ca2(+)-dependent cell-cell adhesion molecule in endothelial cells. *J Cell Biol,* 110**,** 1745-56.

HELMKE, B. P. & DAVIES, P. F. (2002) The cytoskeleton under external fluid mechanical forces: hemodynamic forces acting on the endothelium. *Ann Biomed Eng,* 30**,** 284-96.

HELMKE, B. P., THAKKER, D. B., GOLDMAN, R. D. & DAVIES, P. F. (2001) Spatiotemporal analysis of flow-induced intermediate filament displacement in living endothelial cells. *Biophys J,* 80**,** 184-94.

HENDRICKSON, R. J., CAHILL, P. A., SITZMANN, J. V. & REDMOND, E. M. (1999) Ethanol enhances basal and flow-stimulated nitric oxide synthase activity in vitro by activating an inhibitory guanine nucleotide binding protein. *J Pharmacol Exp Ther,* 289**,** 1293-300.

HENDRIX, M. J., SEFTOR, E. A., MELTZER, P. S., GARDNER, L. M., HESS, A. R., KIRSCHMANN, D. A., SCHATTEMAN, G. C. & SEFTOR, R. E. (2001) Expression and functional significance of VE-cadherin in aggressive human melanoma cells: role in vasculogenic mimicry. *Proc Natl Acad Sci U S A,* 98**,** 8018-23.

HEWAT, E. A., DURMORT, C., JACQUAMET, L., CONCORD, E. & GULINO-DEBRAC, D. (2007) Architecture of the VE-cadherin hexamer. *J Mol Biol,* 365**,** 744-51.

HOPKINS, A. M., WALSH, S. V., VERKADE, P., BOQUET, P. & NUSRAT, A. (2003) Constitutive activation of Rho proteins by CNF-1 influences tight junction structure and epithelial barrier function. *J Cell Sci,* 116**,** 725-42.

HORDIJK P. L., TEN KLOOSTER J. P., VAN DER KAMMEN R. A., MICHIELS F., OOMEN L. C. and COLLARD J. G. (1997) Inhibition of invasion of epithelial cells by Tiam1-Rac signaling. *Science* **278,** 1464-1466.

HORI, S., OHTSUKI, S., HOSOYA, K., NAKASHIMA, E. & TERASAKI, T. (2004) A pericyte-derived angiopoietin-1 multimeric complex induces occludin gene expression in brain capillary endothelial cells through Tie-2 activation in vitro. *J Neurochem,* 89**,** 503-13.

HOU, J., PAUL, D. L. & GOODENOUGH, D. A. (2005) Paracellin-1 and the modulation of ion selectivity of tight junctions. *J Cell Sci,* 118**,** 5109-18.

HU, Y., BOCK, G., WICK, G. & XU, Q. (1998) Activation of PDGF receptor alpha in vascular smooth muscle cells by mechanical stress. *FASEB J,* 12**,** 1135-42.

HUBER, J. D., EGLETON, R. D. & DAVIS, T. P. (2001) Molecular physiology and pathophysiology of tight junctions in the blood-brain barrier. *Trends Neurosci,* 24**,** 719-25.

HUNT, B. J. (2002) *An introduction to vascular biology: from basic science to clinical practice*, Cambridge University Press, 186-216.

HUTCHESON, I. R. & GRIFFITH, T. M. (1996) Mechanotransduction through the endothelial cytoskeleton: mediation of flow- but not agonist-induced EDRF release. *Br J Pharmacol,* 118**,** 720-6.

IADECOLA, C. (2004) Neurovascular regulation in the normal brain and in Alzheimer's disease. *Nat Rev Neurosci,* 5**,** 347-60.

ILZECKA, J. (1996) The structure and function of blood-brain barrier in ischaemic brain stroke process. *Ann Univ Mariae Curie Sklodowska Med,* 51**,** 123-7.

IMBERTI, B., MORIGI, M., ZOJA, C., ANGIOLETTI, S., ABBATE, M., REMUZZI, A. & REMUZZI, G. (2000) Shear stress-induced cytoskeleton rearrangement mediates NF-kappaB-dependent endothelial expression of ICAM-1. *Microvasc Res,* 60**,** 182-8.

IMOTO, M., KAKEYA, H., SAWA, T., HAYASHI, C., HAMADA, M., TAKEUCHI, T. & UMEZAWA, K. (1993) Dephostatin, a novel protein tyrosine phosphatase inhibitor produced by Streptomyces. I. Taxonomy, isolation, and characterization. *J Antibiot (Tokyo),* 46**,** 1342-6.

INAI, T., KOBAYASHI, J. & SHIBATA, Y. (1999) Claudin-1 contributes to the epithelial barrier function in MDCK cells. *Eur J Cell Biol,* 78**,** 849-55.

ISHII, H., SALEM, H. H., BELL, C. E., LAPOSATA, E. A. & MAJERUS, P. W. (1986) Thrombomodulin, an endothelial anticoagulant protein, is absent from the human brain. *Blood,* 67**,** 362-5.

ISHIZAKI, T., CHIBA, H., KOJIMA, T., FUJIBE, M., SOMA, T., MIYAJIMA, H., NAGASAWA, K., WADA, I. & SAWADA, N. (2003) Cyclic AMP induces phosphorylation of claudin-5 immunoprecipitates and expression of claudin-5 gene in blood-brain-barrier endothelial cells via protein kinase A-dependent and -independent pathways. *Exp Cell Res,* 290**,** 275-88.

ITOH, M., NAGAFUCHI, A., YONEMURA, S., KITANI-YASUDA, T., TSUKITA, S. & TSUKITA, S. (1993) The 220-kD protein colocalizing with cadherins in non-epithelial cells is identical to ZO-1, a tight junction-associated protein in epithelial cells: cDNA cloning and immunoelectron microscopy. *J Cell Biol,* 121**,** 491-502.

JACOBSON, J. R., DUDEK, S. M., SINGLETON, P. A., KOLOSOVA, I. A., VERIN, A. D. & GARCIA, J. G. (2006) Endothelial cell barrier enhancement by ATP is mediated by the small GTPase Rac and cortactin. *Am J Physiol Lung Cell Mol Physiol,* 291**,** L289-95.

JENNA, S., HUSSAIN, N. K., DANEK, E. I., TRIKI, I., WASIAK, S., MCPHERSON, P. S. & LAMARCHE-VANE, N. (2002) The activity of the GTPase-activating protein CdGAP is regulated by the endocytic protein intersectin. *J Biol Chem,* 277**,** 6366-73.

JESAITIS, L. A. & GOODENOUGH, D. A. (1994) Molecular characterization and tissue distribution of ZO-2, a tight junction protein homologous to ZO-1 and the Drosophila discs-large tumor suppressor protein. *J Cell Biol,* 124**,** 949-61.

JIANG, W. G., MARTIN, T. A., MATSUMOTO, K., NAKAMURA, T. & MANSEL, R. E. (1999) Hepatocyte growth factor/scatter factor decreases the expression of occludin and transendothelial resistance (TER) and increases paracellular permeability in human vascular endothelial cells. *J Cell Physiol,* 181**,** 319-29.

JIN, Z. G., UEBA, H., TANIMOTO, T., LUNGU, A. O., FRAME, M. D. & BERK, B. C. (2003) Ligand-independent activation of vascular endothelial growth factor receptor 2 by fluid shear stress regulates activation of endothelial nitric oxide synthase. *Circ Res,* 93**,** 354-63.

JO, H., SIPOS, K., GO, Y. M., LAW, R., RONG, J. & MCDONALD, J. M. (1997) Differential effect of shear stress on extracellular signal-regulated kinase and N-terminal Jun kinase in endothelial cells. Gi2- and Gbeta/gamma-dependent signaling pathways. *J Biol Chem,* 272**,** 1395-401.

JOU, T. S., SCHNEEBERGER, E. E. & NELSON, W. J. (1998) Structural and functional regulation of tight junctions by RhoA and Rac1 small GTPases. *J Cell Biol,* 142**,** 101-15.

KAGO, T., TAKAGI, N., DATE, I., TAKENAGA, Y., TAKAGI, K. & TAKEO, S. (2006) Cerebral ischemia enhances tyrosine phosphorylation of occludin in brain capillaries. *Biochem Biophys Res Commun,* 339**,** 1197-203.

KALE, G., NAREN, A. P., SHETH, P. & RAO, R. K. (2003) Tyrosine phosphorylation of occludin attenuates its interactions with ZO-1, ZO-2, and ZO-3. *Biochem Biophys Res Commun,* 302**,** 324-9.

KATSUNO, T., UMEDA, K., MATSUI, T., HATA, M., TAMURA, A., ITOH, M., TAKEUCHI, K., FUJIMORI, T., NABESHIMA, Y., NODA, T., TSUKITA, S. & TSUKITA, S. (2008) Deficiency of zonula occludens-1 causes embryonic lethal phenotype associated with defected yolk sac angiogenesis and apoptosis of embryonic cells. *Mol Biol Cell,* 19**,** 2465-75.

KAUSALYA, P. J., PHUA, D. C. & HUNZIKER, W. (2004) Association of ARVCF with zonula occludens (ZO)-1 and ZO-2: binding to PDZ-domain proteins and cell-cell adhesion regulate plasma membrane and nuclear localization of ARVCF. *Mol Biol Cell,* 15**,** 5503-15.

KEVIL, C. G., OKAYAMA, N., TROCHA, S. D., KALOGERIS, T. J., COE, L. L., SPECIAN, R. D., DAVIS, C. P. & ALEXANDER, J. S. (1998) Expression of zonula occludens and adherens junctional proteins in human venous and arterial endothelial cells: role of occludin in endothelial solute barriers. *Microcirculation,* 5**,** 197-210.

KHACHIGIAN, L. M., RESNICK, N., GIMBRONE, M. A., JR. & COLLINS, T. (1995) Nuclear factor-kappa B interacts functionally with the platelet-derived growth factor B-chain shear-stress response element in vascular endothelial cells exposed to fluid shear stress. *J Clin Invest,* 96**,** 1169-75.

KJOLLER, L. & HALL, A. (1999) Signaling to Rho GTPases. *Exp Cell Res,* 253**,** 166-79.

KNIESEL U. and WOLBURG H. (2000) Tight junctions of the blood-brain barrier. *Cell Mol Neurobiol* **20,** 57-76.

KNIESEL, U., RISAU, W. & WOLBURG, H. (1996) Development of blood-brain barrier tight junctions in the rat cortex. *Brain Res Dev Brain Res,* 96**,** 229-40.

KOBAYASHI, J., INAI, T. & SHIBATA, Y. (2002) Formation of tight junction strands by expression of claudin-1 mutants in their ZO-1 binding site in MDCK cells. *Histochem Cell Biol,* 117**,** 29-39.

KONRAD, M., SCHALLER, A., SEELOW, D., PANDEY, A. V., WALDEGGER, S., LESSLAUER, A., VITZTHUM, H., SUZUKI, Y., LUK, J. M., BECKER, C., SCHLINGMANN, K. P., SCHMID, M., RODRIGUEZ-SORIANO, J., ARICETA, G., CANO, F., ENRIQUEZ, R., JUPPNER, H., BAKKALOGLU, S. A., HEDIGER, M. A., GALLATI, S., NEUHAUSS, S. C., NURNBERG, P. & WEBER, S. (2006) Mutations in the tight-junction gene claudin 19 (CLDN19) are associated with renal magnesium wasting, renal failure, and severe ocular involvement. *Am J Hum Genet,* 79**,** 949-57.

KOUKLIS P., KONSTANTOULAKI M. and MALIK A. B. (2003) VE-cadherin-induced Cdc42 signaling regulates formation of membrane protrusions in endothelial cells. *J Biol Chem* **278,** 16230-16236.

KOUKLIS, P., KONSTANTOULAKI, M., VOGEL, S., BROMAN, M. & MALIK, A. B. (2004) Cdc42 regulates the restoration of endothelial barrier function. *Circ Res,* 94**,** 159-66.

KRAUSE, G., WINKLER, L., MUELLER, S. L., HASELOFF, R. F., PIONTEK, J. & BLASIG, I. E. (2008) Structure and function of claudins. *Biochim Biophys Acta,* 1778**,** 631-45.

KRIZANAC-BENGEZ, L., MAYBERG, M. R. & JANIGRO, D. (2004) The cerebral vasculature as a therapeutic target for neurological disorders and the role of shear stress in vascular homeostatis and pathophysiology. *Neurol Res,* 26**,** 846-53.

KRIZANAC-BENGEZ, L., HOSSAIN, M., FAZIO, V., MAYBERG, M. & JANIGRO, D. (2006a) Loss of flow induces leukocyte-mediated MMP/TIMP imbalance in dynamic in vitro blood-brain barrier model: role of pro-inflammatory cytokines. *Am J Physiol Cell Physiol,* 291**,** C740-9.

KRIZANAC-BENGEZ, L., MAYBERG, M. R., CUNNINGHAM, E., HOSSAIN, M., PONNAMPALAM, S., PARKINSON, F. E. & JANIGRO, D. (2006b) Loss of shear stress induces leukocyte-mediated cytokine release and blood-brain barrier failure in dynamic in vitro blood-brain barrier model. *J Cell Physiol,* 206**,** 68-77.

KUCHARZIK, T., WALSH, S. V., CHEN, J., PARKOS, C. A. & NUSRAT, A. (2001) Neutrophil transmigration in inflammatory bowel disease is associated with differential expression of epithelial intercellular junction proteins. *Am J Pathol,* 159**,** 2001-9.

KUSTOVA, Y., GRINBERG, A. & BASILE, A. S. (1999) Increased blood-brain barrier permeability in LP-BM5 infected mice is mediated by neuroexcitatory mechanisms. *Brain Res,* 839**,** 153-63.

LAEMMLI, U. K. (1970) Cleavage of structural proteins during the assembly of the head of bacteriophage T4. *Nature,* 227**,** 680-5.

LAI, C. H. & KUO, K. H. (2005) The critical component to establish in vitro BBB model: Pericyte. *Brain Res Brain Res Rev,* 50**,** 258-65.

LAMPUGNANI, M. G., RESNATI, M., RAITERI, M., PIGOTT, R., PISACANE, A., HOUEN, G., RUCO, L. P. & DEJANA, E. (1992) A novel endothelial-specific membrane protein is a marker of cell-cell contacts. *J Cell Biol,* 118**,** 1511-22.

LAMPUGNANI, M. G., ZANETTI, A., BREVIARIO, F., BALCONI, G., ORSENIGO, F., CORADA, M., SPAGNUOLO, R., BETSON, M., BRAGA, V. & DEJANA, E. (2002) VE-cadherin regulates endothelial actin activating Rac and increasing membrane association of Tiam. *Mol Biol Cell,* 13**,** 1175-89.

LAPLACE, E. (1899) I. A New Forceps for Intestinal Anastomosis. *Ann Surg,* 29**,** 297-305.

LEE, E. J., HUNG, Y. C. & LEE, M. Y. (1999) Early alterations in cerebral hemodynamics, brain metabolism, and blood-brain barrier permeability in experimental intracerebral hemorrhage. *J Neurosurg,* 91**,** 1013-9.

LEE, H. S., NAMKOONG, K., KIM, D. H., KIM, K. J., CHEONG, Y. H., KIM, S. S., LEE, W. B. & KIM, K. Y. (2004) Hydrogen peroxide-induced alterations of tight junction proteins in bovine brain microvascular endothelial cells. *Microvasc Res,* 68**,** 231-8.

LEHOUX, S. & TEDGUI, A. (2003) Cellular mechanics and gene expression in blood vessels. *J Biomech,* 36**,** 631-43.

LEHOUX, S., CASTIER, Y. & TEDGUI, A. (2006) Molecular mechanisms of the vascular responses to haemodynamic forces. *J Intern Med,* 259**,** 381-92.

LI Y. S., HAGA J. H. and CHIEN S. (2005) Molecular basis of the effects of shear stress on vascular endothelial cells. *J Biomech* **38,** 1949-1971.

LI, S., CHEN, B. P., AZUMA, N., HU, Y. L., WU, S. Z., SUMPIO, B. E., SHYY, J. Y. & CHIEN, S. (1999) Distinct roles for the small GTPases Cdc42 and Rho in endothelial responses to shear stress. *J Clin Invest,* 103**,** 1141-50.

LIAO, F., DOODY, J. F., OVERHOLSER, J., FINNERTY, B., BASSI, R., WU, Y., DEJANA, E., KUSSIE, P., BOHLEN, P. & HICKLIN, D. J. (2002) Selective targeting of angiogenic tumor vasculature by vascular endothelial-cadherin antibody inhibits tumor growth without affecting vascular permeability. *Cancer Res,* 62**,** 2567-75.

LIU W. F., NELSON C. M., TAN J. L. and CHEN C. S. (2007) Cadherins, RhoA, and Rac1 are differentially required for stretch-mediated proliferation in endothelial versus smooth muscle cells. *Circ Res* **101,** e44-52.

LIU, L. B., XUE, Y. X., LIU, Y. H. & WANG, Y. B. (2008) Bradykinin increases blood-tumor barrier permeability by down-regulating the expression levels of ZO-1, occludin, and claudin-5 and rearranging actin cytoskeleton. *J Neurosci Res,* 86**,** 1153-68.

LIU, Y., SWEET, D. T., IRANI-TEHRANI, M., MAEDA, N. & TZIMA, E. (2008) Shc coordinates signals from intercellular junctions and integrins to regulate flow-induced inflammation. *J Cell Biol,* 182**,** 185-96.

LOHMANN, C., KRISCHKE, M., WEGENER, J. & GALLA, H. J. (2004) Tyrosine phosphatase inhibition induces loss of blood-brain barrier integrity by matrix metalloproteinase-dependent and -independent pathways. *Brain Res,* 995**,** 184-96.

LU, R., WANG, W., UZZAU, S., VIGORITO, R., ZIELKE, H. R. & FASANO, A. (2000) Affinity purification and partial characterization of the zonulin/zonula occludens toxin (Zot) receptor from human brain. *J Neurochem,* 74**,** 320-6.

MA, T. Y., IWAMOTO, G. K., HOA, N. T., AKOTIA, V., PEDRAM, A., BOIVIN, M. A. & SAID, H. M. (2004) TNF-alpha-induced increase in intestinal epithelial tight

junction permeability requires NF-kappa B activation. *Am J Physiol Gastrointest Liver Physiol,* 286**,** G367-76.

MAGISTRETTI, P. J., PELLERIN, L., ROTHMAN, D. L. & SHULMAN, R. G. (1999) Energy on demand. *Science,* 283**,** 496-7.

MALEK, A. M., ZHANG, J., JIANG, J., ALPER, S. L. & IZUMO, S. (1999) Endothelin-1 gene suppression by shear stress: pharmacological evaluation of the role of tyrosine kinase, intracellular calcium, cytoskeleton, and mechanosensitive channels. *J Mol Cell Cardiol,* 31**,** 387-99.

MANKERTZ, J., WALLER, J. S., HILLENBRAND, B., TAVALALI, S., FLORIAN, P., SCHONEBERG, T., FROMM, M. & SCHULZKE, J. D. (2002) Gene expression of the tight junction protein occludin includes differential splicing and alternative promoter usage. *Biochem Biophys Res Commun,* 298**,** 657-66.

MARK, K. S. & DAVIS, T. P. (2002) Cerebral microvascular changes in permeability and tight junctions induced by hypoxia-reoxygenation. *Am J Physiol Heart Circ Physiol,* 282**,** H1485-94.

MASUDA, M. & FUJIWARA, K. (1993) Morphological responses of single endothelial cells exposed to physiological levels of fluid shear stress. *Front Med Biol Eng,* 5**,** 79-87.

MATOZAKI, T., NAKANISHI, H. & TAKAI, Y. (2000) Small G-protein networks: their crosstalk and signal cascades. *Cell Signal,* 12**,** 515-24.

MCCARTHY, K. M., SKARE, I. B., STANKEWICH, M. C., FURUSE, M., TSUKITA, S., ROGERS, R. A., LYNCH, R. D. & SCHNEEBERGER, E. E. (1996) Occludin is a functional component of the tight junction. *J Cell Sci,* 109 (Pt 9)**,** 2287-98.

MCNALLY, J. S., DAVIS, M. E., GIDDENS, D. P., SAHA, A., HWANG, J., DIKALOV, S., JO, H. & HARRISON, D. G. (2003) Role of xanthine oxidoreductase and NAD(P)H oxidase in endothelial superoxide production in response to oscillatory shear stress. *Am J Physiol Heart Circ Physiol,* 285**,** H2290-7.

MEDINA, R., RAHNER, C., MITIC, L. L., ANDERSON, J. M. & VAN ITALLIE, C. M. (2000) Occludin localization at the tight junction requires the second extracellular loop. *J Membr Biol,* 178**,** 235-47.

MEHTA, D., RAHMAN, A. & MALIK, A. B. (2001) Protein kinase C-alpha signals rho-guanine nucleotide dissociation inhibitor phosphorylation and rho activation and regulates the endothelial cell barrier function. *J Biol Chem,* 276**,** 22614-20.

MEHTA, D. & MALIK, A. B. (2006) Signaling mechanisms regulating endothelial permeability. *Physiol Rev,* 86**,** 279-367.

MERTENS, A. E., ROOVERS, R. C. & COLLARD, J. G. (2003) Regulation of Tiam1-Rac signalling. *FEBS Lett,* 546**,** 11-6.

MICHIELS, F., STAM, J. C., HORDIJK, P. L., VAN DER KAMMEN, R. A., RUULS-VAN STALLE, L., FELTKAMP, C. A. & COLLARD, J. G. (1997) Regulated membrane localization of Tiam1, mediated by the NH2-terminal pleckstrin homology domain, is required for Rac-dependent membrane ruffling and C-Jun NH2-terminal kinase activation. *J Cell Biol,* 137**,** 387-98.

MINAGAR, A., OSTANIN, D., LONG, A. C., JENNINGS, M., KELLEY, R. E., SASAKI, M. & ALEXANDER, J. S. (2003) Serum from patients with multiple sclerosis downregulates occludin and VE-cadherin expression in cultured endothelial cells. *Mult Scler,* 9**,** 235-8.

MINAGAR, A. & ALEXANDER, J. S. (2003) Blood-brain barrier disruption in multiple sclerosis. *Mult Scler,* 9**,** 540-9.

MIYAZAKI, T., HONDA, K. & OHATA, H. (2010) m-Calpain antagonizes RhoA overactivation and endothelial barrier dysfunction under disturbed shear conditions. *Cardiovasc Res,* 85**,** 530-41.

MOCHIZUKI, N., YAMASHITA, S., KUROKAWA, K., OHBA, Y., NAGAI, T., MIYAWAKI, A. & MATSUDA, M. (2001) Spatio-temporal images of growth-factor-induced activation of Ras and Rap1. *Nature,* 411**,** 1065-8.

MONAGHAN-BENSON, E. & BURRIDGE, K. (2009) The regulation of vascular endothelial growth factor-induced microvascular permeability requires Rac and reactive oxygen species. *J Biol Chem,* 284**,** 25602-11.

MOORADIAN, A. D., HAAS, M. J. & CHEHADE, J. M. (2003) Age-related changes in rat cerebral occludin and zonula occludens-1 (ZO-1). *Mech Ageing Dev,* 124**,** 143-6.

MORGANTI-KOSSMANN, M. C., RANCAN, M., STAHEL, P. F. & KOSSMANN, T. (2002) Inflammatory response in acute traumatic brain injury: a double-edged sword. *Curr Opin Crit Care,* 8**,** 101-5.

MORITA, K., SASAKI, H., FURUSE, M. & TSUKITA, S. (1999) Endothelial claudin: claudin-5/TMVCF constitutes tight junction strands in endothelial cells. *J Cell Biol,* 147**,** 185-94.

MULLER, J. M., CHILIAN, W. M. & DAVIS, M. J. (1997) Integrin signaling transduces shear stress--dependent vasodilation of coronary arterioles. *Circ Res,* 80**,** 320-6.

NAG, S. (1995) Role of the endothelial cytoskeleton in blood-brain-barrier permeability to protein. *Acta Neuropathol,* 90**,** 454-60.

NAGY, Z., PETERS, H. & HUTTNER, I. (1984) Fracture faces of cell junctions in cerebral endothelium during normal and hyperosmotic conditions. *Lab Invest,* 50**,** 313-22.

NAKADA, M. T., AMIN, K., CHRISTOFIDOU-SOLOMIDOU, M., O'BRIEN, C. D., SUN, J., GURUBHAGAVATULA, I., HEAVNER, G. A., TAYLOR, A. H., PADDOCK, C., SUN, Q. H., ZEHNDER, J. L., NEWMAN, P. J., ALBELDA, S. M. & DELISSER, H. M. (2000) Antibodies against the first Ig-like domain of human platelet endothelial cell adhesion molecule-1 (PECAM-1) that inhibit PECAM-1-dependent homophilic adhesion block in vivo neutrophil recruitment. *J Immunol,* 164**,** 452-62.

NAKAGAWA, S., DELI, M. A., KAWAGUCHI, H., SHIMIZUDANI, T., SHIMONO, T., KITTEL, A., TANAKA, K. & NIWA, M. (2009) A new blood-brain barrier model using primary rat brain endothelial cells, pericytes and astrocytes. *Neurochem Int,* 54**,** 253-63.

NAVARATNA, D., MCGUIRE, P. G., MENICUCCI, G. & DAS, A. (2007) Proteolytic degradation of VE-cadherin alters the blood-retinal barrier in diabetes. *Diabetes,* 56**,** 2380-7.

NEUHAUS, W., BOGNER, E., WIRTH, M., TRZECIAK, J., LACHMANN, B., GABOR, F. & NOE, C. R. (2006) A novel tool to characterize paracellular transport: the APTS-dextran ladder. *Pharm Res,* 23**,** 1491-501.

NOBES, C. D. & HALL, A. (1995) Rho, rac, and cdc42 GTPases regulate the assembly of multimolecular focal complexes associated with actin stress fibers, lamellipodia, and filopodia. *Cell,* 81**,** 53-62.

NORIA, S., COWAN, D. B., GOTLIEB, A. I. & LANGILLE, B. L. (1999) Transient and steady-state effects of shear stress on endothelial cell adherens junctions. *Circ Res,* 85**,** 504-14.

NORIA, S., XU, F., MCCUE, S., JONES, M., GOTLIEB, A. I. & LANGILLE, B. L. (2004) Assembly and reorientation of stress fibers drives morphological changes to endothelial cells exposed to shear stress. *Am J Pathol,* 164**,** 1211-23.

NUNBHAKDI-CRAIG, V., MACHLEIDT, T., OGRIS, E., BELLOTTO, D., WHITE, C. L., 3RD & SONTAG, E. (2002) Protein phosphatase 2A associates with and regulates atypical PKC and the epithelial tight junction complex. *J Cell Biol,* 158**,** 967-78.

O'CONNOR, K. L. & MERCURIO, A. M. (2001) Protein kinase A regulates Rac and is required for the growth factor-stimulated migration of carcinoma cells. *J Biol Chem,* 276**,** 47895-900.

OHTANI, S., TERASHIMA, M., SATOH, J., SOETA, N., SAZE, Z., KASHIMURA, S., OHSUKA, F., HOSHINO, Y., KOGURE, M. & GOTOH, M. (2009) Expression of tight-junction-associated proteins in human gastric cancer: downregulation of claudin-4 correlates with tumor aggressiveness and survival. *Gastric Cancer,* 12**,** 43-51.

OLDENDORF, W. H. (1971) Brain uptake of radiolabeled amino acids, amines, and hexoses after arterial injection. *Am J Physiol,* 221**,** 1629-39.

ORR, A. W., SANDERS, J. M., BEVARD, M., COLEMAN, E., SAREMBOCK, I. J. & SCHWARTZ, M. A. (2005) The subendothelial extracellular matrix modulates NF-kappaB activation by flow: a potential role in atherosclerosis. *J Cell Biol,* 169**,** 191-202.

ORRINGTON-MYERS, J., GAO, X., KOUKLIS, P., BROMAN, M., RAHMAN, A., VOGEL, S. M. & MALIK, A. B. (2006) Regulation of lung neutrophil recruitment by VE-cadherin. *Am J Physiol Lung Cell Mol Physiol,* 291**,** L764-71.

OSAWA, M., MASUDA, M., KUSANO, K. & FUJIWARA, K. (2002) Evidence for a role of platelet endothelial cell adhesion molecule-1 in endothelial cell mechanosignal transduction: is it a mechanoresponsive molecule? *J Cell Biol,* 158**,** 773-85.

OSTERUD, B., BAJAJ, M. S. & BAJAJ, S. P. (1995) Sites of tissue factor pathway inhibitor (TFPI) and tissue factor expression under physiologic and pathologic conditions. On behalf of the Subcommittee on Tissue factor Pathway Inhibitor (TFPI) of the Scientific and Standardization Committee of the ISTH. *Thromb Haemost,* 73**,** 873-5.

PAEMELEIRE, K. (2002) The cellular basis of neurovascular metabolic coupling. *Acta Neurol Belg,* 102**,** 153-7.

PAPADOPOULOS, M. C., SAADOUN, S., WOODROW, C. J., DAVIES, D. C., COSTA-MARTINS, P., MOSS, R. F., KRISHNA, S. & BELL, B. A. (2001) Occludin expression in microvessels of neoplastic and non-neoplastic human brain. *Neuropathol Appl Neurobiol,* 27**,** 384-95.

PARDRIDGE, W. M. (2002) Drug and gene delivery to the brain: the vascular route. *Neuron,* 36**,** 555-8.

PARDRIDGE, W. M. (2007) Drug targeting to the brain. *Pharm Res,* 24**,** 1733-44.

PARMAR, K. M., LARMAN, H. B., DAI, G., ZHANG, Y., WANG, E. T., MOORTHY, S. N., KRATZ, J. R., LIN, Z., JAIN, M. K., GIMBRONE, M. A., JR. & GARCIA-CARDENA, G. (2006) Integration of flow-dependent endothelial phenotypes by Kruppel-like factor 2. *J Clin Invest,* 116**,** 49-58.

PAWSON, T. (1994) Tyrosine kinase signalling pathways. *Princess Takamatsu Symp,* 24**,** 303-22.

PEARCE, M. J., MCINTYRE, T. M., PRESCOTT, S. M., ZIMMERMAN, G. A. & WHATLEY, R. E. (1996) Shear stress activates cytosolic phospholipase A2 (cPLA2) and MAP kinase in human endothelial cells. *Biochem Biophys Res Commun,* 218**,** 500-4.

PENG, H., WANG, C., YE, Z. C., CHEN, Y. R., ZHANG, J., CHEN, Z. J., YU, X. Q. & LOU, T. Q. (2009) How increased VEGF induces glomerular hyperpermeability: a potential signaling pathway of Rac1 activation. *Acta Diabetol* [Epub ahead of print].

PERSIDSKY, Y., GHORPADE, A., RASMUSSEN, J., LIMOGES, J., LIU, X. J., STINS, M., FIALA, M., WAY, D., KIM, K. S., WITTE, M. H., WEINAND, M., CARHART, L. & GENDELMAN, H. E. (1999) Microglial and astrocyte chemokines regulate monocyte migration through the blood-brain barrier in human immunodeficiency virus-1 encephalitis. *Am J Pathol,* 155**,** 1599-611.

PERSIDSKY, Y., HEILMAN, D., HAORAH, J., ZELIVYANSKAYA, M., PERSIDSKY, R., WEBER, G. A., SHIMOKAWA, H., KAIBUCHI, K. & IKEZU, T. (2006a) Rho-mediated regulation of tight junctions during monocyte migration across the blood-brain barrier in HIV-1 encephalitis (HIVE). *Blood,* 107**,** 4770-80.

PERSIDSKY, Y., RAMIREZ, S. H., HAORAH, J. & KANMOGNE, G. D. (2006b) Blood-brain barrier: structural components and function under physiologic and pathologic conditions. *J Neuroimmune Pharmacol,* 1**,** 223-36.

PIERCE, M., WANG, C., STUMP, M. & KAMB, A. (2003) Overexpression of the beta-catenin binding domain of cadherin selectively kills colorectal cancer cells. *Int J Cancer,* 107**,** 229-37.

PIONTEK, J., WINKLER, L., WOLBURG, H., MULLER, S. L., ZULEGER, N., PIEHL, C., WIESNER, B., KRAUSE, G. & BLASIG, I. E. (2008) Formation of tight junction: determinants of homophilic interaction between classic claudins. *FASEB J,* 22**,** 146-58.

PRASAD, S., MINGRINO, R., KAUKINEN, K., HAYES, K. L., POWELL, R. M., MACDONALD, T. T. & COLLINS, J. E. (2005) Inflammatory processes have differential effects on claudins 2, 3 and 4 in colonic epithelial cells. *Lab Invest,* 85**,** 1139-62.

RAMSAUER, M., KRAUSE, D. & DERMIETZEL, R. (2002) Angiogenesis of the blood-brain barrier in vitro and the function of cerebral pericytes. *FASEB J,* 16**,** 1274-6.

RANSOM, C. B. & SONTHEIMER, H. (1995) Biophysical and pharmacological characterization of inwardly rectifying K+ currents in rat spinal cord astrocytes. *J Neurophysiol,* 73**,** 333-46.

RAO, R. K., BASUROY, S., RAO, V. U., KARNAKY JR, K. J. & GUPTA, A. (2002) Tyrosine phosphorylation and dissociation of occludin-ZO-1 and E-cadherin-beta-catenin complexes from the cytoskeleton by oxidative stress. *Biochem J,* 368**,** 471-81.

RASCHER, G., FISCHMANN, A., KROGER, S., DUFFNER, F., GROTE, E. H. & WOLBURG, H. (2002) Extracellular matrix and the blood-brain barrier in glioblastoma multiforme: spatial segregation of tenascin and agrin. *Acta Neuropathol,* 104**,** 85-91.

REESE, T. S. & KARNOVSKY, M. J. (1967) Fine structural localization of a blood-brain barrier to exogenous peroxidase. *J Cell Biol,* 34**,** 207-17.

RESNICK, N., COLLINS, T., ATKINSON, W., BONTHRON, D. T., DEWEY, C. F., JR. & GIMBRONE, M. A., JR. (1993) Platelet-derived growth factor B chain promoter contains a cis-acting fluid shear-stress-responsive element. *Proc Natl Acad Sci U S A,* 90**,** 4591-5.

RESNICK, N., YAHAV, H., SHAY-SALIT, A., SHUSHY, M., SCHUBERT, S., ZILBERMAN, L. C. & WOFOVITZ, E. (2003) Fluid shear stress and the vascular endothelium: for better and for worse. *Prog Biophys Mol Biol,* 81**,** 177-99.

RIDLEY, A. J. (2006) Rho GTPases and actin dynamics in membrane protrusions and vesicle trafficking. *Trends Cell Biol,* 16**,** 522-9.

RIZZO, V. (2007) Lights, camera, actin! The cytoskeleton takes center stage in mechanotransduction. Focus on "Mapping the dynamics of shear stress-induced structural changes in endothelial cells." *Am J Physiol Cell Physiol,* 293**,** C1771-2.

ROOF, R. W., HASKELL, M. D., DUKES, B. D., SHERMAN, N., KINTER, M. & PARSONS, S. J. (1998) Phosphotyrosine (p-Tyr)-dependent and -independent mechanisms of p190 RhoGAP-p120 RasGAP interaction: Tyr 1105 of p190, a substrate for c-Src, is the sole p-Tyr mediator of complex formation. *Mol Cell Biol,* 18**,** 7052-63.

ROSENBERG, G. A., ESTRADA, E., KELLEY, R. O. & KORNFELD, M. (1993) Bacterial collagenase disrupts extracellular matrix and opens blood-brain barrier in rat. *Neurosci Lett,* 160**,** 117-9.

RUBIN, L. L. & STADDON, J. M. (1999) The cell biology of the blood-brain barrier. *Annu Rev Neurosci,* 22**,** 11-28.

SAITOU, M., ANDO-AKATSUKA, Y., ITOH, M., FURUSE, M., INAZAWA, J., FUJIMOTO, K. & TSUKITA, S. (1997) Mammalian occludin in epithelial cells: its expression and subcellular distribution. *Eur J Cell Biol,* 73**,** 222-31.

SAITOU, M., FUJIMOTO, K., DOI, Y., ITOH, M., FUJIMOTO, T., FURUSE, M., TAKANO, H., NODA, T. & TSUKITA, S. (1998) Occludin-deficient embryonic stem cells can differentiate into polarized epithelial cells bearing tight junctions. *J Cell Biol,* 141**,** 397-408.

SAKAKIBARA, A., FURUSE, M., SAITOU, M., ANDO-AKATSUKA, Y. & TSUKITA, S. (1997) Possible involvement of phosphorylation of occludin in tight junction formation. *J Cell Biol,* 137**,** 1393-401.

SAKURAI, A., FUKUHARA, S., YAMAGISHI, A., SAKO, K., KAMIOKA, Y., MASUDA, M., NAKAOKA, Y. & MOCHIZUKI, N. (2006) MAGI-1 is required for Rap1 activation upon cell-cell contact and for enhancement of vascular endothelial cadherin-mediated cell adhesion. *Mol Biol Cell,* 17**,** 966-76.

SALLEE, J. L. & BURRIDGE, K. (2009) Density-enhanced phosphatase 1 regulates phosphorylation of tight junction proteins and enhances barrier function of epithelial cells. *J Biol Chem,* 284**,** 14997-5006.

SANDER, E. E., TEN KLOOSTER, J. P., VAN DELFT, S., VAN DER KAMMEN, R. A. & COLLARD, J. G. (1999) Rac downregulates Rho activity: reciprocal balance between both GTPases determines cellular morphology and migratory behavior. *J Cell Biol,* 147**,** 1009-22.

SANTAGUIDA, S., JANIGRO, D., HOSSAIN, M., OBY, E., RAPP, E. & CUCULLO, L. (2006) Side by side comparison between dynamic versus static models of blood-brain barrier in vitro: a permeability study. *Brain Res,* 1109**,** 1-13.

SASTRY, S. K. & HORWITZ, A. F. (1993) Integrin cytoplasmic domains: mediators of cytoskeletal linkages and extra- and intracellular initiated transmembrane signaling. *Curr Opin Cell Biol,* 5**,** 819-31.

SATOH, H., ZHONG, Y., ISOMURA, H., SAITOH, M., ENOMOTO, K., SAWADA, N. & MORI, M. (1996) Localization of 7H6 tight junction-associated antigen along the cell border of vascular endothelial cells correlates with paracellular barrier function against ions, large molecules, and cancer cells. *Exp Cell Res,* 222**,** 269-74.

SAVETTIERI, G., DI LIEGRO, I., CATANIA, C., LICATA, L., PITARRESI, G. L., D'AGOSTINO, S., SCHIERA, G., DE CARO, V., GIANDALIA, G., GIANNOLA, L. I. & CESTELLI, A. (2000) Neurons and ECM regulate occludin localization in brain endothelial cells. *Neuroreport,* 11**,** 1081-4.

SCHILLER, M. R. (2006) Coupling receptor tyrosine kinases to Rho GTPases--GEFs what's the link. *Cell Signal,* 18**,** 1834-43.

SCHINKEL, A. H. (1999) P-Glycoprotein, a gatekeeper in the blood-brain barrier. *Adv Drug Deliv Rev,* 36**,** 179-194.

SCHLAGETER, K. E., MOLNAR, P., LAPIN, G. D. & GROOTHUIS, D. R. (1999) Microvessel organization and structure in experimental brain tumors: microvessel populations with distinctive structural and functional properties. *Microvasc Res,* 58**,** 312-28.

SCHLEGEL, N., BAUMER, Y., DRENCKHAHN, D. & WASCHKE, J. (2009) Lipopolysaccharide-induced endothelial barrier breakdown is cyclic adenosine monophosphate dependent in vivo and in vitro. *Crit Care Med,* 37**,** 1735-43.

SCHNITTLER, H. J., PUSCHEL, B. & DRENCKHAHN, D. (1997) Role of cadherins and plakoglobin in interendothelial adhesion under resting conditions and shear stress. *Am J Physiol,* 273**,** H2396-405.

SCHNITTLER, H. J. (1998) Structural and functional aspects of intercellular junctions in vascular endothelium. *Basic Res Cardiol,* 93 Suppl 3**,** 30-9.

SCHULZE, C. & FIRTH, J. A. (1993) Immunohistochemical localization of adherens junction components in blood-brain barrier microvessels of the rat. *J Cell Sci,* 104 (Pt 3)**,** 773-82.

SCHULZE, C., SMALES, C., RUBIN, L. L. & STADDON, J. M. (1997) Lysophosphatidic acid increases tight junction permeability in cultured brain endothelial cells. *J Neurochem,* 68**,** 991-1000.

SCUDAMORE, C. L., JEPSON, M. A., HIRST, B. H. & MILLER, H. R. (1998) The rat mucosal mast cell chymase, RMCP-II, alters epithelial cell monolayer permeability in association with altered distribution of the tight junction proteins ZO-1 and occludin. *Eur J Cell Biol,* 75**,** 321-30.

SERVITJA, J. M., MARINISSEN, M. J., SODHI, A., BUSTELO, X. R. & GUTKIND, J. S. (2003) Rac1 function is required for Src-induced transformation. Evidence of a role for Tiam1 and Vav2 in Rac activation by Src. *J Biol Chem,* 278**,** 34339-46.

SIDDHARTHAN, V., KIM, Y. V., LIU, S. & KIM, K. S. (2007) Human astrocytes/astrocyte-conditioned medium and shear stress enhance the barrier properties of human brain microvascular endothelial cells. *Brain Res,* 1147**,** 39-50.

SIDEROVSKI, D. P. & WILLARD, F. S. (2005) The GAPs, GEFs, and GDIs of heterotrimeric G-protein alpha subunits. *Int J Biol Sci,* 1**,** 51-66.

SIMIONESCU, M., SIMIONESCU, N. & PALADE, G. E. (1975) Segmental differentiations of cell junctions in the vascular endothelium. The microvasculature. *J Cell Biol,* 67**,** 863-85.

SIMIONESCU, M., SIMIONESCU, N. & PALADE, G. E. (1976) Segmental differentiations of cell junctions in the vascular endothelium. Arteries and veins. *J Cell Biol,* 68**,** 705-23.

SINGER, K. L., STEVENSON, B. R., WOO, P. L. & FIRESTONE, G. L. (1994) Relationship of serine/threonine phosphorylation/dephosphorylation signaling to glucocorticoid regulation of tight junction permeability and ZO-1 distribution in nontransformed mammary epithelial cells. *J Biol Chem,* 269**,** 16108-15.

SOLODUSHKO, V., PARKER, J. C. & FOUTY, B. (2008) Pulmonary microvascular endothelial cells form a tighter monolayer when grown in chronic hypoxia. *Am J Respir Cell Mol Biol,* 38**,** 491-7.

SPINDLER, V., SCHLEGEL, N. & WASCHKE, J. (2010) Role of GTPases in control of microvascular permeability. *Cardiovasc Res,* [Epub ahead of print].

SPRAGUE, E. A., LUO, J. & PALMAZ, J. C. (1997) Human aortic endothelial cell migration onto stent surfaces under static and flow conditions. *J Vasc Interv Radiol,* 8**,** 83-92.

STADDON, J. M., HERRENKNECHT, K., SMALES, C. & RUBIN, L. L. (1995) Evidence that tyrosine phosphorylation may increase tight junction permeability. *J Cell Sci,* 108 (Pt 2)**,** 609-19.

STAMATOVIC, S. M., DIMITRIJEVIC, O. B., KEEP, R. F. & ANDJELKOVIC, A. V. (2006) Protein kinase Calpha-RhoA cross-talk in CCL2-induced alterations in brain endothelial permeability. *J Biol Chem,* 281**,** 8379-88.

STANNESS, K. A., WESTRUM, L. E., FORNACIARI, E., MASCAGNI, P., NELSON, J. A., STENGLEIN, S. G., MYERS, T. & JANIGRO, D. (1997) Morphological and functional characterization of an in vitro blood-brain barrier model. *Brain Res,* 771**,** 329-42.

STANNESS, K. A., NEUMAIER, J. F., SEXTON, T. J., GRANT, G. A., EMMI, A., MARIS, D. O. & JANIGRO, D. (1999) A new model of the blood--brain barrier: co-culture of neuronal, endothelial and glial cells under dynamic conditions. *Neuroreport,* 10**,** 3725-31.

STEVENSON, B. R., SILICIANO, J. D., MOOSEKER, M. S. & GOODENOUGH, D. A. (1986) Identification of ZO-1: a high molecular weight polypeptide associated with the tight junction (zonula occludens) in a variety of epithelia. *J Cell Biol,* 103**,** 755-66.

STOFEGA, M., DERMARDIROSSIAN, C. & BOKOCH, G. M. (2006) Affinity-based assay of Rho guanosine triphosphatase activation. *Methods Mol Biol,* 332**,** 269-79.

SU, Z. J., HAHN, C. N., GOODALL, G. J., RECK, N. M., LESKE, A. F., DAVY, A., KREMMIDIOTIS, G., VADAS, M. A. & GAMBLE, J. R. (2004) A vascular cell-restricted RhoGAP, p73RhoGAP, is a key regulator of angiogenesis. *Proc Natl Acad Sci U S A,* 101**,** 12212-7.

SUI, X. F., KISER, T. D., HYUN, S. W., ANGELINI, D. J., DEL VECCHIO, R. L., YOUNG, B. A., HASDAY, J. D., ROMER, L. H., PASSANITI, A., TONKS, N. K. & GOLDBLUM, S. E. (2005) Receptor protein tyrosine phosphatase micro regulates the paracellular pathway in human lung microvascular endothelia. *Am J Pathol,* 166**,** 1247-58.

SUN, H., BRESLIN, J. W., ZHU, J., YUAN, S. Y. & WU, M. H. (2006) Rho and ROCK signaling in VEGF-induced microvascular endothelial hyperpermeability. *Microcirculation,* 13**,** 237-47.

SUZUKI, S., SANO, K. & TANIHARA, H. (1991) Diversity of the cadherin family: evidence for eight new cadherins in nervous tissue. *Cell Regul,* 2**,** 261-70.

SWEET, D. T. & TZIMA, E. (2009) Spatial signaling networks converge at the adaptor protein Shc. *Cell Cycle,* 8**,** 231-5.

TADDEI, A., GIAMPIETRO, C., CONTI, A., ORSENIGO, F., BREVIARIO, F., PIRAZZOLI, V., POTENTE, M., DALY, C., DIMMELER, S. & DEJANA, E. (2008) Endothelial adherens junctions control tight junctions by VE-cadherin-mediated upregulation of claudin-5. *Nat Cell Biol,* 10**,** 923-34.

TAKAHASHI, K., NAKANISHI, H., MIYAHARA, M., MANDAI, K., SATOH, K., SATOH, A., NISHIOKA, H., AOKI, J., NOMOTO, A., MIZOGUCHI, A. & TAKAI, Y. (1999) Nectin/PRR: an immunoglobulin-like cell adhesion molecule recruited to cadherin-based adherens junctions through interaction with Afadin, a PDZ domain-containing protein. *J Cell Biol,* 145**,** 539-49.

TAKAHASHI, K., SASAKI, T., MAMMOTO, A., TAKAISHI, K., KAMEYAMA, T., TSUKITA, S. & TAKAI, Y. (1997) Direct interaction of the Rho GDP dissociation inhibitor with ezrin/radixin/moesin initiates the activation of the Rho small G protein. *J Biol Chem,* 272**,** 23371-5.

TAKAHASHI, M. & BERK, B. C. (1996) Mitogen-activated protein kinase (ERK1/2) activation by shear stress and adhesion in endothelial cells. Essential role for a herbimycin-sensitive kinase. *J Clin Invest,* 98**,** 2623-31.

TAKAI, Y., SASAKI, T. & MATOZAKI, T. (2001) Small GTP-binding proteins. *Physiol Rev,* 81**,** 153-208.

TAKEDA, H. & TSUKITA, S. (1995) Effects of tyrosine phosphorylation on tight junctions in temperature-sensitive v-src-transfected MDCK cells. *Cell Struct Funct,* 20**,** 387-93.

TAKENAGA, Y., TAKAGI, N., MUROTOMI, K., TANONAKA, K. & TAKEO, S. (2009) Inhibition of Src activity decreases tyrosine phosphorylation of occludin in brain capillaries and attenuates increase in permeability of the blood-brain barrier after transient focal cerebral ischemia. *J Cereb Blood Flow Metab,* 29**,** 1099-108.

TANAKA, M., KAMATA, R. & SAKAI, R. (2005) EphA2 phosphorylates the cytoplasmic tail of Claudin-4 and mediates paracellular permeability. *J Biol Chem,* 280**,** 42375-82.

TCHERKEZIAN, J. & LAMARCHE-VANE, N. (2007) Current knowledge of the large RhoGAP family of proteins. *Biol Cell,* 99**,** 67-86.

TOBIN, N. P., HENEHAN, G. T., MURPHY, R. P., ATHERTON, J. C., GUINAN, A. F., KERRIGAN, S. W., COX, D., CAHILL, P. A. & CUMMINS, P. M. (2008) Helicobacter pylori-induced inhibition of vascular endothelial cell functions: a role for VacA-dependent nitric oxide reduction. *Am J Physiol Heart Circ Physiol,* 295**,** H1403-13.

TONG, X. K. & HAMEL, E. (1999) Regional cholinergic denervation of cortical microvessels and nitric oxide synthase-containing neurons in Alzheimer's disease. *Neuroscience,* 92**,** 163-75.

TOWBIN, H., STAEHELIN, T. & GORDON, J. (1979) Electrophoretic transfer of proteins from polyacrylamide gels to nitrocellulose sheets: procedure and some applications. *Proc Natl Acad Sci U S A,* 76**,** 4350-4.

TSUJI, T., ISHIZAKI, T., OKAMOTO, M., HIGASHIDA, C., KIMURA, K., FURUYASHIKI, T., ARAKAWA, Y., BIRGE, R. B., NAKAMOTO, T., HIRAI, H. & NARUMIYA, S. (2002) ROCK and mDia1 antagonize in Rho-dependent Rac activation in Swiss 3T3 fibroblasts. *J Cell Biol,* 157**,** 819-30.

TSUKAMOTO, T. & NIGAM, S. K. (1999) Role of tyrosine phosphorylation in the reassembly of occludin and other tight junction proteins. *Am J Physiol,* 276**,** F737-50.

TURKSEN, K. & TROY, T. C. (2004) Barriers built on claudins. *J Cell Sci,* 117**,** 2435-47.

TUROWSKI, P., MARTINELLI, R., CRAWFORD, R., WATERIDGE, D., PAPAGEORGIOU, A. P., LAMPUGNANI, M. G., GAMP, A. C., VESTWEBER, D., ADAMSON, P., DEJANA, E. & GREENWOOD, J. (2008) Phosphorylation of vascular endothelial cadherin controls lymphocyte emigration. *J Cell Sci,* 121**,** 29-37.

TZIMA, E., DEL POZO, M. A., SHATTIL, S. J., CHIEN, S. & SCHWARTZ, M. A. (2001) Activation of integrins in endothelial cells by fluid shear stress mediates Rho-dependent cytoskeletal alignment. *EMBO J,* 20**,** 4639-47.

TZIMA, E., DEL POZO, M. A., KIOSSES, W. B., MOHAMED, S. A., LI, S., CHIEN, S. & SCHWARTZ, M. A. (2002) Activation of Rac1 by shear stress in endothelial cells mediates both cytoskeletal reorganization and effects on gene expression. *EMBO J,* 21**,** 6791-800.

TZIMA, E., IRANI-TEHRANI, M., KIOSSES, W. B., DEJANA, E., SCHULTZ, D. A., ENGELHARDT, B., CAO, G., DELISSER, H. & SCHWARTZ, M. A. (2005) A mechanosensory complex that mediates the endothelial cell response to fluid shear stress. *Nature,* 437**,** 426-31.

TZIMA, E. (2006) Role of small GTPases in endothelial cytoskeletal dynamics and the shear stress response. *Circ Res,* 98**,** 176-85.

UEMATSU, M., OHARA, Y., NAVAS, J. P., NISHIDA, K., MURPHY, T. J., ALEXANDER, R. W., NEREM, R. M. & HARRISON, D. G. (1995) Regulation of endothelial cell nitric oxide synthase mRNA expression by shear stress. *Am J Physiol,* 269**,** C1371-8.

UKROPEC, J. A., HOLLINGER, M. K., SALVA, S. M. & WOOLKALIS, M. J. (2000) SHP2 association with VE-cadherin complexes in human endothelial cells is regulated by thrombin. *J Biol Chem,* 275**,** 5983-6.

UMEDA, K., IKENOUCHI, J., KATAHIRA-TAYAMA, S., FURUSE, K., SASAKI, H., NAKAYAMA, M., MATSUI, T., TSUKITA, S., FURUSE, M. & TSUKITA, S. (2006) ZO-1 and ZO-2 independently determine where claudins are polymerized in tight-junction strand formation. *Cell,* 126**,** 741-54.

VAN ITALLIE, C. M., GAMBLING, T. M., CARSON, J. L. & ANDERSON, J. M. (2005) Palmitoylation of claudins is required for efficient tight-junction localization. *J Cell Sci,* 118**,** 1427-36.

VAN ITALLIE, C. M., FANNING, A. S., BRIDGES, A. & ANDERSON, J. M. (2009) ZO-1 stabilizes the tight junction solute barrier through coupling to the perijunctional cytoskeleton. *Mol Biol Cell,* 20**,** 3930-40.

VAN NIEUW AMERONGEN, G. P., BECKERS, C. M., ACHEKAR, I. D., ZEEMAN, S., MUSTERS, R. J. & VAN HINSBERGH, V. W. (2007) Involvement of Rho kinase in endothelial barrier maintenance. *Arterioscler Thromb Vasc Biol,* 27**,** 2332-9.

VANHOUTTE, P. M., BOULANGER, C. M. & MOMBOULI, J. V. (1995) Endothelium-derived relaxing factors and converting enzyme inhibition. *Am J Cardiol,* 76**,** 3E-12E.

VAPORCIYAN, A. A., DELISSER, H. M., YAN, H. C., MENDIGUREN, II, THOM, S. R., JONES, M. L., WARD, P. A. & ALBELDA, S. M. (1993) Involvement of platelet-endothelial cell adhesion molecule-1 in neutrophil recruitment in vivo. *Science,* 262**,** 1580-2.

VENKITESWAREN K., XIAO K., SUMMERS S., CALKINS C. C., VINCENT P. A., PUMIGLIA K. and KOWALCZYK A. P. (2002) Regulation of endothelial barrier function and growth by VE-cadherin, plakoglobin, and beta-catenin. *Am J Physiol Cell Physiol* **283,** C811-821.

VESTWEBER, D. (2008) VE-cadherin: the major endothelial adhesion molecule controlling cellular junctions and blood vessel formation. *Arterioscler Thromb Vasc Biol,* 28**,** 223-32.

VON OFFENBERG SWEENEY, N., CUMMINS, P. M., COTTER, E. J., FITZPATRICK, P. A., BIRNEY, Y. A., REDMOND, E. M. & CAHILL, P. A. (2005) Cyclic strain-mediated regulation of vascular endothelial cell migration and tube formation. *Biochem Biophys Res Commun,* 329**,** 573-82.

VORBRODT, A. W. & DOBROGOWSKA, D. H. (2003) Molecular anatomy of intercellular junctions in brain endothelial and epithelial barriers: electron microscopist's view. *Brain Res Brain Res Rev,* 42**,** 221-42.

WACHTEL, M., FREI, K., EHLER, E., FONTANA, A., WINTERHALTER, K. & GLOOR, S. M. (1999) Occludin proteolysis and increased permeability in endothelial cells through tyrosine phosphatase inhibition. *J Cell Sci,* 112 (Pt 23)**,** 4347-56.

WALLEZ, Y. & HUBER, P. (2008) Endothelial adherens and tight junctions in vascular homeostasis, inflammation and angiogenesis. *Biochim Biophys Acta,* 1778**,** 794-809.

WALLEZ, Y., CAND, F., CRUZALEGUI, F., WERNSTEDT, C., SOUCHELNYTSKYI, S., VILGRAIN, I. & HUBER, P. (2007) Src kinase phosphorylates vascular endothelial-cadherin in response to vascular endothelial growth factor: identification of tyrosine 685 as the unique target site. *Oncogene,* 26**,** 1067-77.

WALPOLA, P. L., GOTLIEB, A. I., CYBULSKY, M. I. & LANGILLE, B. L. (1995) Expression of ICAM-1 and VCAM-1 and monocyte adherence in arteries exposed to altered shear stress. *Arterioscler Thromb Vasc Biol,* 15**,** 2-10.

WANG, L. & DUDEK, S. M. (2009) Regulation of vascular permeability by sphingosine 1-phosphate. *Microvasc Res,* 77**,** 39-45.

WANG, Y., MIAO, H., LI, S., CHEN, K. D., LI, Y. S., YUAN, S., SHYY, J. Y. & CHIEN, S. (2002) Interplay between integrins and FLK-1 in shear stress-induced signaling. *Am J Physiol Cell Physiol,* 283**,** C1540-7.

WARD, P. D., KLEIN, R. R., TROUTMAN, M. D., DESAI, S. & THAKKER, D. R. (2002) Phospholipase C-gamma modulates epithelial tight junction permeability through hyperphosphorylation of tight junction proteins. *J Biol Chem,* 277**,** 35760-5.

WASCHKE, J., DRENCKHAHN, D., ADAMSON, R. H., BARTH, H. & CURRY, F. E. (2004) cAMP protects endothelial barrier functions by preventing Rac-1 inhibition. *Am J Physiol Heart Circ Physiol,* 287**,** H2427-33.

WASCHKE, J., BURGER, S., CURRY, F. R., DRENCKHAHN, D. & ADAMSON, R. H. (2006) Activation of Rac-1 and Cdc42 stabilizes the microvascular endothelial barrier. *Histochem Cell Biol,* 125**,** 397-406.

WEINBAUM, S., TARBELL, J. M. & DAMIANO, E. R. (2007) The structure and function of the endothelial glycocalyx layer. *Annu Rev Biomed Eng,* 9**,** 121-67.

WEIS, W. I. & NELSON, W. J. (2006) Re-solving the cadherin-catenin-actin conundrum. *J Biol Chem,* 281**,** 35593-7.

WEISS, N., MILLER, F., CAZAUBON, S. & COURAUD, P. O. (2008) The blood-brain barrier in brain homeostasis and neurological diseases. *Biochim Biophys Acta*.

WELCH, H. C., COADWELL, W. J., STEPHENS, L. R. & HAWKINS, P. T. (2003) Phosphoinositide 3-kinase-dependent activation of Rac. *FEBS Lett,* 546**,** 93-7.

WELLS, C. D., FAWCETT, J. P., TRAWEGER, A., YAMANAKA, Y., GOUDREAULT, M., ELDER, K., KULKARNI, S., GISH, G., VIRAG, C., LIM, C., COLWILL, K., STAROSTINE, A., METALNIKOV, P. & PAWSON, T. (2006) A Rich1/Amot complex regulates the Cdc42 GTPase and apical-polarity proteins in epithelial cells. *Cell,* 125**,** 535-48.

WENNERBERG, K., ROSSMAN, K. L. & DER, C. J. (2005) The Ras superfamily at a glance. *J Cell Sci,* 118**,** 843-6.

WHITE, C. R. & FRANGOS, J. A. (2007) The shear stress of it all: the cell membrane and mechanochemical transduction. *Philos Trans R Soc Lond B Biol Sci,* 362**,** 1459-67.

WIELAND, T. & MITTMANN, C. (2003) Regulators of G-protein signalling: multifunctional proteins with impact on signalling in the cardiovascular system. *Pharmacol Ther,* 97**,** 95-115.

WILCOX, J. N., SUBRAMANIAN, R. R., SUNDELL, C. L., TRACEY, W. R., POLLOCK, J. S., HARRISON, D. G. & MARSDEN, P. A. (1997) Expression of multiple isoforms of nitric oxide synthase in normal and atherosclerotic vessels. *Arterioscler Thromb Vasc Biol,* 17**,** 2479-88.

WILDENBERG, G. A., DOHN, M. R., CARNAHAN, R. H., DAVIS, M. A., LOBDELL, N. A., SETTLEMAN, J. & REYNOLDS, A. B. (2006) p120-catenin and p190RhoGAP regulate cell-cell adhesion by coordinating antagonism between Rac and Rho. *Cell,* 127**,** 1027-39.

WILLIS, C. L., LEACH, L., CLARKE, G. J., NOLAN, C. C. & RAY, D. E. (2004a) Reversible disruption of tight junction complexes in the rat blood-brain barrier, following transitory focal astrocyte loss. *Glia,* 48**,** 1-13.

WILLIS, C. L., NOLAN, C. C., REITH, S. N., LISTER, T., PRIOR, M. J., GUERIN, C. J., MAVROUDIS, G. & RAY, D. E. (2004b) Focal astrocyte loss is followed by microvascular damage, with subsequent repair of the blood-brain barrier in the apparent absence of direct astrocytic contact. *Glia,* 45**,** 325-37.

WILLOTT, E., BALDA, M. S., FANNING, A. S., JAMESON, B., VAN ITALLIE, C. & ANDERSON, J. M. (1993) The tight junction protein ZO-1 is homologous to the

Drosophila discs-large tumor suppressor protein of septate junctions. *Proc Natl Acad Sci U S A,* 90**,** 7834-8.

WILLOTT, E., BALDA, M. S., HEINTZELMAN, M., JAMESON, B. & ANDERSON, J. M. (1992) Localization and differential expression of two isoforms of the tight junction protein ZO-1. *Am J Physiol,* 262**,** C1119-24.

WOJCIAK-STOTHARD, B., ENTWISTLE, A., GARG, R. & RIDLEY, A. J. (1998) Regulation of TNF-alpha-induced reorganization of the actin cytoskeleton and cell-cell junctions by Rho, Rac, and Cdc42 in human endothelial cells. *J Cell Physiol,* 176**,** 150-65.

WOJCIAK-STOTHARD, B., POTEMPA, S., EICHHOLTZ, T. & RIDLEY, A. J. (2001) Rho and Rac but not Cdc42 regulate endothelial cell permeability. *J Cell Sci,* 114**,** 1343-55.

WOJCIAK-STOTHARD, B. & RIDLEY, A. J. (2002) Rho GTPases and the regulation of endothelial permeability. *Vascul Pharmacol,* 39**,** 187-99.

WOJCIAK-STOTHARD, B. & RIDLEY, A. J. (2003) Shear stress-induced endothelial cell polarization is mediated by Rho and Rac but not Cdc42 or PI 3-kinases. *J Cell Biol,* 161**,** 429-39.

WOJCIAK-STOTHARD, B., TSANG, L. Y. & HAWORTH, S. G. (2005) Rac and Rho play opposing roles in the regulation of hypoxia/reoxygenation-induced permeability changes in pulmonary artery endothelial cells. *Am J Physiol Lung Cell Mol Physiol,* 288**,** L749-60.

WOLBURG, H., NEUHAUS, J., KNIESEL, U., KRAUSS, B., SCHMID, E. M., OCALAN, M., FARRELL, C. & RISAU, W. (1994) Modulation of tight junction structure in blood-brain barrier endothelial cells. Effects of tissue culture, second messengers and cocultured astrocytes. *J Cell Sci,* 107 (Pt 5)**,** 1347-57.

WOLBURG, H. & LIPPOLDT, A. (2002) Tight junctions of the blood-brain barrier: development, composition and regulation. *Vascul Pharmacol,* 38**,** 323-37.

WOLBURG, H., WOLBURG-BUCHHOLZ, K., KRAUS, J., RASCHER-EGGSTEIN, G., LIEBNER, S., HAMM, S., DUFFNER, F., GROTE, E. H., RISAU, W. & ENGELHARDT, B. (2003) Localization of claudin-3 in tight junctions of the blood-brain barrier is selectively lost during experimental autoimmune encephalomyelitis and human glioblastoma multiforme. *Acta Neuropathol,* 105**,** 586-92.

WONG, V. & GUMBINER, B. M. (1997) A synthetic peptide corresponding to the extracellular domain of occludin perturbs the tight junction permeability barrier. *J Cell Biol,* 136**,** 399-409.

XIAO, K., ALLISON, D. F., BUCKLEY, K. M., KOTTKE, M. D., VINCENT, P. A., FAUNDEZ, V. & KOWALCZYK, A. P. (2003) Cellular levels of p120 catenin function as a set point for cadherin expression levels in microvascular endothelial cells. *J Cell Biol,* 163**,** 535-45.

XIAO, K., GARNER, J., BUCKLEY, K. M., VINCENT, P. A., CHIASSON, C. M., DEJANA, E., FAUNDEZ, V. & KOWALCZYK, A. P. (2005) p120-Catenin regulates clathrin-dependent endocytosis of VE-cadherin. *Mol Biol Cell,* 16**,** 5141-51.

YAMAMOTO, K., SOKABE, T., MATSUMOTO, T., YOSHIMURA, K., SHIBATA, M., OHURA, N., FUKUDA, T., SATO, T., SEKINE, K., KATO, S., ISSHIKI, M., FUJITA, T., KOBAYASHI, M., KAWAMURA, K., MASUDA, H., KAMIYA, A. & ANDO, J. (2006) Impaired flow-dependent control of vascular tone and remodeling in P2X4-deficient mice. *Nat Med,* 12**,** 133-7.

YAMAMOTO, M., RAMIREZ, S. H., SATO, S., KIYOTA, T., CERNY, R. L., KAIBUCHI, K., PERSIDSKY, Y. & IKEZU, T. (2008) Phosphorylation of claudin-5 and occludin by rho kinase in brain endothelial cells. *Am J Pathol,* 172**,** 521-33.

YAMAMOTO, T., HARADA, N., KANO, K., TAYA, S., CANAANI, E., MATSUURA, Y., MIZOGUCHI, A., IDE, C. & KAIBUCHI, K. (1997) The Ras target AF-6 interacts with ZO-1 and serves as a peripheral component of tight junctions in epithelial cells. *J Cell Biol,* 139**,** 785-95.

YAMAUCHI, K., RAI, T., KOBAYASHI, K., SOHARA, E., SUZUKI, T., ITOH, T., SUDA, S., HAYAMA, A., SASAKI, S. & UCHIDA, S. (2004) Disease-causing mutant WNK4 increases paracellular chloride permeability and phosphorylates claudins. *Proc Natl Acad Sci U S A,* 101**,** 4690-4.

YAO, Y., RABODZEY, A. & DEWEY, C. F., JR. (2007) Glycocalyx modulates the motility and proliferative response of vascular endothelium to fluid shear stress. *Am J Physiol Heart Circ Physiol,* 293**,** H1023-30.

ZHANG, S., ZHANG, D. & SUN, B. (2007) Vasculogenic mimicry: current status and future prospects. *Cancer Lett,* 254**,** 157-64.

ZHOU, S. F. (2008) Structure, function and regulation of P-glycoprotein and its clinical relevance in drug disposition. *Xenobiotica,* 38**,** 802-32.

ZONDAG, G. C., EVERS, E. E., TEN KLOOSTER, J. P., JANSSEN, L., VAN DER KAMMEN, R. A. & COLLARD, J. G. (2000) Oncogenic Ras downregulates Rac activity, which leads to increased Rho activity and epithelial-mesenchymal transition. *J Cell Biol,* 149**,** 775-82.

ZWICK, E., BANGE, J. & ULLRICH, A. (2001) Receptor tyrosine kinase signalling as a target for cancer intervention strategies. *Endocr Relat Cancer,* 8**,** 161-73.